MEDITERRANEAN ACTION PLAN

UNITED NATIONS ENVIRONMENT PROGRAMME

WORLD METEOROLOGICAL ORGANIZATION

METEOROLOGICAL AND CLIMATOLOGICAL DATA FROM SURFACE AND UPPER AIR MEASUREMENTS FOR THE ASSESSMENT OF ATMOSPHERIC TRANSPORT AND DEPOSITION OF POLLUTANTS IN THE MEDITERRANEAN BASIN: A REVIEW

PART A
by Uri Dayan and John M. Miller

PART B
Seasonal Distribution of the Planetary Boundary Layer Depths over the Mediterranean Basin
by Uri Dayan, Jerome L. Heffter and John M. Miller

MAP Technical Reports Series No 30

UNEP
Athens, 1989

This volume is the thirtieth issue of the Mediterranean Action Plan Technical Report Series.

This series contains selected reports resulting from the various activities performed within the framework of the components of the Mediterranean Action Plan: Pollution Monitoring and Research Programme (MED POL), Blue Plan, Priority Actions Programme, Specially Protected Areas and Regional Oil Combating Centre.

Preface

The United Nations Environment Programme (UNEP) convened an Intergovernmental Meeting on the Protection of the Mediterranean (Barcelona, 28 January - 4 February 1975), which was attended by representatives of 16 States bordering on the Mediterranean Sea. The meeting discussed the various measures necessary for the prevention and control of pollution of the Mediterranean Sea, and concluded by adopting an Action Plan consisting of three substantive components:

- Integrated planning of the development and management of the resources of the Mediterranean Basin (management component);

- Co-ordinated programme for research, monitoring and exchange of information and assessment of the state of pollution and of protection measures (assessment component);

- Framework convention and related protocols with their technical annexes for the protection of the Mediterranean environment (legal component).

All components of the Action Plan are interdependent and provide a framework for comprehensive action to promote both the protection and the continued development of the Mediterranean ecoregion. No component is an end in itself. The Action Plan is intended to assist the Mediterranean Governments in formulating their national policies related to the continuous development and protection of the Mediterranean area and to improve their ability to identify various options for alternative patterns of development and to make choices and appropriate allocations of resources.

MED POL - Phase I (1976-1980)

The Co-ordinated Mediterranean Research and Monitoring Programme (MED POL) was approved as the assessment (scientific/technical) component of the Action Plan.

The general objectives of its pilot phase (MED POL - Phase I), which evolved through a series of expert and intergovernmental meetings, were:

- to formulate and carry out a co-ordinated pollution monitoring and research programme taking into account the goals of the Mediterranean Action Plan and the capabilities of the Mediterranean research centres to participate in it;

- to assist national research centres in developing their capabilities to participate in the programme;

- to analyse the sources, amounts, levels, pathways, trends and effects of pollutants relevant to the Mediterranean Sea;

- to provide the scientific/technical information needed by the Governments of the Mediterranean States and the EEC for the negotiation and implementation of the Convention for the Protection of the Mediterranean Sea against Pollution and its related protocols;

- to build up consistent time-series of data on the sources, pathways, levels and effects of pollutants in the Mediterranean Sea and thus to contribute to the scientific knowledge of the Mediterranean Sea.

MED POL - Phase I initially consisted of seven pilot projects (MED POL I - VII), which were later expanded by additional six pilot projects (MED POL VIII-XIII), some of which remained in a conceptual stage only.

MED POL - Phase I was implemented in the period from 1975 to 1980. The large number of national research centres designated by their Governments to participate in MED POL (83 research centres from 15 Mediterranean States and the EEC), the diversity of the programme and its geographic coverage, the impressive number of Mediterranean scientists and technicians (about 200) and the number of co-operating agencies and supporting organizations involved in it qualifies MED POL as certainly one of the largest and most complex co-operative scientific programmes with a specific and well-defined aim ever undertaken in the Mediterranean basin.

The overall co-ordination and guidance for MED POL - Phase I was provided by UNEP, acting as the secretariat of the Mediterranean Action Plan (MAP). Co-operating specialized United Nations Agencies (ECE, UNIDO, FAO, UNESCO, WHO, WMO, IAEA IOC) were responsible for the technical implementation and day-to-day co-ordination of the work of national research centres participating in the pilot projects.

MED POL - Phase II (1981-1990)

The intergovernmental Review Meeting of Mediterranean Coastal States and First Meeting of the Contracting Parties to the Convention for the Protection of the Mediterranean Sea against Pollution, and its related protocols (Geneva, 5-10 February 1979), having examined the status of MED POL - Phase I, recommended that during the 1979/80 biennium a Long-term pollution monitoring and research programme should be formulated.

Based on the recommendations made at various expert and intergovernmental meetings, a draft Long-term (1981-1990) Programme for pollution Monitoring and Research in the Mediterranean (MED POL-Phase II) was formulated by the Secretariat of the Barcelona Convention (UNEP), in co-operation with the United Nations Agencies which were responsible for the technical implementation of MED POL-Phase I, and it was formally approved by the Second Meeting of the Contracting Parties of the Mediterranean Sea against pollution and its related protocols and Intergovernmental Review Meeting of Mediterranean Coastal States of the Action Plan held in Cannes, 2-7 March 1981.

The general long-term objectives of MED POL - Phase II were to further the goals of the Barcelona Convention by assisting the Parties to prevent, abate and combat pollution of the Mediterranean Sea Area and to protect and enhance the marine environment of the Area. The specific objectives were designed to provide, on a continuous basis, the Parties to the Barcelona Convention and its related protocols with:

- information required for the implementation of the Convention and the protocols;

- indicators and evaluation of the effectiveness of the pollution prevention measures taken under the Convention and the protocols;

- scientific information which may lead to eventual revisions and amendments of the relevant provisions of the Convention and the protocols and for the formulation of additional protocols;

- information which could be used in formulating environmentally sound national, bilateral and multilateral management decisions essential for the continuous socio-economic development of the Mediterranean region on a sustainable basis;

- periodic assessment of the state of pollution of the Mediterranean Sea.

The monitoring of, and research on, pollutants affecting the Mediterranean marine environment reflects primarily the immediate and long-term requirements of the Barcelona Convention and its protocols, but also takes into account factors needed for the understanding of the relationship between the socio-economic development of the region and the pollution of the Mediterranean Sea.

For this purpose, monitoring was organized on several levels:

- monitoring of sources of pollution providing information on the type and amount of pollutants released directly into the environment;

- monitoring of nearshore areas, including estuaries, under the direct influence of pollutants from identifiable primary (outfalls, discharge and coastal dumping points) or secondary (rivers) sources;

- monitoring of offshore areas (reference areas) providing information on the general trends in the level of pollution in the Mediterranean;

- monitoring of the transport of pollutants to the Mediterranean through the atmosphere, providing additional information on the pollution load reaching the Mediterranean Sea.

Research and study topics included initially in the MED POL-Phase II were:

- development of sampling and analytical techniques for monitoring the sources and levels of pollutants. Testing and harmonization of these methods at the Mediterranean scale and their formulation as reference methods. Priority will be given to the substances listed in the annexes of the Protocol for the prevention of pollution of the Mediterranean Sea by dumping from ships and aircraft and the Protocol for the protection of the Mediterranean Sea against pollution from land-based sources (activity A);

- development of reporting formats required according to the Dumping, Emergency and Land-Based Sources Protocols (activity B);

- formulation of the scientific rationale for the environmental quality criteria to be used in the development of emission standards, standards of use or guidelines for substances listed in annexes I and II of the Land-Based Sources Protocol in accordance with Articles 5, 6 and 7 of that Protocol (activity C);

- epidemiological studies related to the confirmation (or eventual revision) of the proposed environmental quality criteria (standards of use) for bathing waters, shellfish-growing waters and edible marine organisms (activity D);

- development of proposals for guidelines and criteria governing the application of the Land-Based Sources Protocol, as requested in Article 7 of that Protocol (activity E);

- research on oceanographic processes, with particular emphasis on surface circulation and vertical transport. Needed for the understanding of the distribution of pollutants through the Mediterranean and for the development of contingency plans for cases of emergency (activity F);

- research on the toxicity, persistence, bioaccumulation, carcinogenicity and mutagenicity of selected substances listed in annexes of the Land-Based Sources Protocol and the Dumping Protocol (activity G);

- research on eutrophication and concomitant plankton blooms. Needed to assess the feasibility of alleviating the consequences and damage from such recurring blooms (activity H);

- study of ecosystem modifications in areas influenced by pollutants, and in areas where ecosystem modifications are caused by large-scale coastal or inland engineering activity (activity I);

- effects of thermal discharges on marine and coastal ecosystems, including the study of associated effects (activity J);

- biogeochemical cycle of specific pollutants, particularly those relevant to human health (mercury, lead, survival of pathogens in the Mediterranean Sea, etc.) (activity K);

- study of pollutant-transfer processes (i) at river/sea and air/sea interface, (ii) by sedimentation and (iii) through the straits linking the Mediterranean with other seas (activity L);

As in MED POL - Phase I, the overall co-ordination and guidance for MED POL - Phase II is provided by UNEP as the secretariat of the Mediterranean Action Plan (MAP). Co-operating specialized United Nations Agencies (FAO, UNESCO, WHO, WMO, IAEA, IOC) are responsible for the technical implementation and day-to-day co-ordination of the work of national centres participating in monitoring and research.

The first eight volumes of the MAP Technical Reports Series present the collection of final reports of the principal Investigators who participated in the relevant pilot projects (MED POL I - MED POL VIII). The ninth volume of the MAP Technical Reports Series is the final report on the implementation of MED POL - Phase I, prepared, primarily on the basis of individual final reports of the principal investigators with the co-operation of relevant United Nations Agencies (FAO, UNESCO, WHO, WMO IAEA, IOC).

From the tenth volume onwards, the MAP Technical Report Series contains final reports on research projects assessment documents, and other reports on activities performed within the framework of MED POL Phase II as well as documentation originating from other components of the Mediterranean Action Plan.

This thirtieth volume of the MAP Technical Reports Series contains review on meteorological and climatological data for the assessment of atmospheric transport and deposition of pollutants into the Mediterranean basin which was prepared in 1986-1988 under a research project within the MED POL Research Activity "L" on pollutant-transfer processes at air/sea interface and airborne pollution of the sea co-ordinated by the World Meteorological Organization.

Some results of this research were presented at the WMO/UNEP Workshop on Airborne Pollution of the Mediterranean Sea (Belgrade, Yugoslavia, 10-13 November 1987). The proceedings of the workshop containing all papers presented are being published as the MAP Technical Reports Series No 31. Taking into account the great amount of data collected for the present review and presented in the form of tables and figures convenient for their further modelling application, the above Workshop recommended that the review should be published as a separate issue in the MAP Technical Reports Series. This publication is believed to be a useful reference book for those who deal with modelling atmospheric transport and deposition of pollutants into the Mediterranean Sea and with the interpretation of corresponding measurement results.

TABLE OF CONTENTS

PART A

ABSTRACT

An overview is presented of the meteorological measurements that are pertinent in describing the transport and deposition of pollutants into the Mediterranean region. Procedures such as an innovative statistical method for mapping trajectory flow climatology are applied. For evaluations of convection processes in the Mediterranean region, long-range transport model outputs of boundary layer heights are analyzed along with Heffter's independent method. Routinely measured meteorological parameters also provide information to determine the relative importance of the dry and wet deposition processes. They include monthly average precipitation amounts, duration and intensities of precipitation, cloud amounts, etc. Suggestions are made for further analyses of meteorological data that would help in understanding pollution of the Mediterranean via the atmosphere.

1.0 INTRODUCTION

The oceans, in spite of their great size and depth, are vulnerable to hazardous pollutants through either inputs from rivers or deposition from the atmosphere. This vulnerability is even more accentuated when one deals with inland water bodies such as the Mediterranean Sea. Initially scientists believed that the main source of contamination to inland seas was through direct discharge of waste into coastal waters, but now they realize that the atmospheric path may be equally or more important for certain pollutants. The main question is what meteorological factors control atmospheric transport and deposition of potentially harmful substances. To answer this question, this report summarizes the essential meteorological parameters required to understand transport of pollutants to the Mediterranean. This constitutes a contribution to the activities of the Joint Group of Experts on the Scientific Aspects of Marine Pollution (GESAMP) Working Group on the Interchange of Pollutants between the Atmosphere and the Oceans.

Meteorological data that are used in describing long-range transport and deposition of pollutants can be obtained from two sources. The first and obvious is the surface and upper air measurements made on a routine basis around the region. A second source is a derived data set from numerical weather forecasting models, which supply horizontal and vertical winds with other pertinent fields (Klug, 1984). In this paper, only data from the first source are used.

To assess the contribution of different source areas to the pollutant concentrations and their deposition in the region, the meteorological data must not only be analyzed but must also be input into models whose calculations can be used for a more sophisticated evaluation.

1.1 Geographical Features

The Mediterranean Sea lies between 30°N and 46°N, and between 5.5°W and 36°E as shown in Fig. 1. Its east-west extent is approximately 4000 km, and its average north-south extent is only about 800 km. The western outlet to the Atlantic through the Strait of Gibraltar is less than 15 km wide at its narrowest point. The sea is enclosed by mountains except along the North African Coast east of Tunisia; the whole coastline is very irregular, having many indentations. It is commonly divided into two major geographical areas:

(1) the western basin--from Gibraltar to Italy, and
(2) the eastern basin--from Italy to the Syrian Coast. These divisions will be used in discussing the flow climatology of the region.

The topography behind the coastline of the Mediterranean is complex; it provides both barriers to and channels for air flow that bring at times extremely different air masses to the region. Strong winds, which are funnelled through gaps in the mountain ranges that surround the Mediterranean Basin, are among the best known meteorological features of the region: (1) the north-westerly mistral through the Alps-Pyrenees gap; (2) the northeasterly bora through the Trieste gap; (3) the easterly levanter and the westerly vendaval through the Strait of Gibraltar; and (4) the warm southeasterly to southwesterly scirocco, ghibli, or Khamsin from Africa (Air Ministry, Meteorological Office, 1962; Reiter, 1975).

In the vertical, mixing heights are usually at an elevation of about 1000 m above the sea surface. In general, this is what would be expected over a large body of water and is further documented in this report by calculations made at more than 100 radiosonde stations along the Mediterranean Sea coast and within the basin. However, the frictional drag of air along the rough surface of the hills surrounding the coast causes a pronounced inflow across the isobars towards the lower pressure and may affect the mixing heights. This departure from the geostrophic wind may force an ageostrophic flow over the orographic obstacles surrounding the basin and promote vertical mixing.

Thus, the topographic features shown in Fig. 1 may interact with large-scale atmospheric flow within the boundary layer by influencing both the horizontal transport and the vertical mixing of the pollutants in very complex ways. These factors must be taken into account in describing the atmospheric input into the Mediterranean, especially on the scales of hundreds of kilometers.

1.2 Synoptic Weather Patterns

European meteorologists have been very successful in classifying individual large-scale synoptic patterns or Grosswetterlagen (Hess and Brezowski, 1969). These can be used as analogs against which day-to-day weather can be compared. The statistics of occurrence of a given type and its evolution are very useful in understanding the overall flow configurations. This analog type of approach has been frequently applied and cited in the literature (e.g., Air Ministry, Meteorological Office, 1962; Topol et al., 1986). Although this classification of synoptic situations into distinct patterns cannot be applied in all cases, it enables us to describe in general terms the more prevalent and therefore important situations.

A modified Grosswetterlagen classification is applied to the Mediterranean Basin using Hess and Brezowski, 1969 as a guide. It is based mainly on the positions of the anticyclones and their influence on the development and positions of major low-pressure systems surrounding the area. Brief descriptions of the five main synoptic weather patterns are the following:

Type A: An anticyclone or ridge of high pressure lies over the northeastern Atlantic or the British Isles. During the presence of this blocking anticyclone, a quasi-permanent low-pressure trough in the mid-troposphere (about 500 hPa) extends along the axis of the Mediterranean Basin. The trough line leads to cyclogenesis when vorticity maxima move into its region of influence. This cyclogenesis in the Bay of Genova and the subsequent cyclone's movement eastward especially during the winter period constitute a major synoptic pattern (Miller et al., 1987) (Fig. 2).

Type B: Northern Europe is dominated by an anticyclone. Pressure is relatively low over the Mediterranean (Fig. 3).

Type C: Westerly type. A deep depression (or a sequence of depressions) dominates the middle latitudes of Europe, and westerly winds prevail over most of the Mediterranean (Fig. 4).

Type D: Easterly type. An anticyclone dominates central and southern Europe, giving easterly winds over most of the Mediterranean. Pressure is relatively low over northern Europe (Fig. 5).

Type E: Anticyclonic type. An anticyclone or ridge of high pressure covers the greater part of the Mediterranean area, giving generally light winds, mainly westerly in the north, easterly in the south, and northerly in the east. Pressure is relatively low over central or northern Europe (Fig. 6).

Types A, B, and C are the most common types during winter in the Mediterranean Basin. Types D and E, which are the most frequent during summer in the Mediterranean, are classified as a short-fetch, northwesterly type in the eastern Mediterranean Basin (Dayan, 1986). When types D or E prevail, the high pressure over the Mediterranean decreases toward the east, the prevailing wind is northwesterly, and the weather is warm. These easterly patterns are almost continuous in July and August, but very infrequent from November to April.

Although the Grosswetterlagen classifications are very useful to form the overall picture, each individual weather system has its own unique characteristics and may greatly influence the transport of pollutants to the region. Thus other more specific methods must be applied. Some of these are described in Section 2.0.

2.0 TRANSPORT AND DISPERSION

2.1 Horizontal Transport and Dispersion

One of the problems encountered with long-range transport and dispersion calculations is that not only must the physical movement of the materials be accounted for but also the chemical transformations must be described. Fortunately, in the case of the Mediterranean Basin, the pollutants of interest such as heavy metals, and chlorofluoromethane and other anthropogenic organic substances behave more or less as inert substances. For example, the pilot substance that was chosen for initial study by the GESAMP working group is cadmium. This material is transported by the atmosphere with no chemical reactions expected to take place during transit. Thus, the observed concentration patterns of cadmium and other materials of interest should be solely due to the influence of the winds and mixing as well as to precipitation scavenging and/or dry deposition.

2.1.1 Monthly averaged winds over the sea surface

To give the simplest picture of the flow in the basin, the charts shown in Figs. 7-18 depict the general air movement at 10 meters above sea level (a.s.l.) The arrows in each 1° square are the mean vector of all observed winds. Length and thickness of the arrows represent the relative constancy of the general wind pattern in four intervals. Relative constancy means the ratio of the force of the mean resultant wind to the mean wind force regardless of direction, that is, the ratio of the vectorial mean to the scalar mean.

In regions where the wind has about the same direction, the ratio will be near 100%, but when constancy is small, the direction of the wind arrow depends on variable winds. Noteworthy is the strong stability of the wind in summer (Figs. 12-14) in the eastern part of the Mediterranean (KNMI, 1957).

2.1.2 Monthly horizontal flow patterns at the 850 hPa level

Another method of viewing the transport is to look directly at the data from the upper air soundings. The 850 hPa (approximately 1500 m) standard level was chosen as the most representative of the top of the transport layer. This level is taken as the approximate boundary between the surface wind regime and the regime of the upper winds relatively free from local surface effects.

One of the most obvious features of upper air data is the small number of observations that are available compared with surface data. It is essential therefore that all the available data be used, especially in areas such as the Mediterranean where there are so few soundings. For this reason we used the following two different data bases to construct the monthly horizontal flow patterns at 850 hPa, expressed as averaged $\bar{u}$ and $\bar{v}$ values, the zonal and meridional components respectively: (1) radiosonde data collected for the period 1957-1964 (Newell et al., 1972); and (2) radiosonde data collected for the period 1946-1950 (Air Ministry, Meteorological Office, 1962).

The ū component is the major one in these latitudes, and it is the seasonal and spatial distribution of this value as influenced by large weather patterns at this altitude that is important to understand (Figs. 19-30). During winter and spring months (Figs. 19a-23a), a low-pressure region or trough is located over the western Mediterranean Basin, yielding relatively high positive values in the ū component. During summer months (Figs. 24a-27a), anticyclonic flow prevails over the western Mediterranean and a weak trough over the eastern basin. The extension of this anticyclonic high pressure from the Azores into Central Europe and North Africa and the low-pressure region located over the eastern Mediterranean produce high positive values for ū in the central Mediterranean region and weak or even negative values in the eastern basin.

2.1.3 Single back-trajectory analysis

Since the wind field is known to be the most important factor affecting the transport of pollutants (over distances on the order of 500 km), flow climatologies based on a one-layer backward trajectory model were constructed to represent the seasonal transport paths in the eastern and western parts of the region. Studies of Lagrangian models for long-range transport of pollutants are numerous in the scientific literature (Eliassen, 1984). The gridded trajectory model of the Air Resources Laboratory (ARL) (Harris, 1982) was used to develop these climatologies for the Mediterranean. Such flow studies have been constructed in the past for remote sites such as the island of Bermuda; Barrow, Alaska; and Mauna Loa, Hawaii (Miller, 1981a,b; Miller and Harris, 1985) and for some receptor locations within the Mediterranean region (Dayan, 1986; Miller, et al. 1987). The ARL operational model uses wind data acquired from the National Meteorological Center. These data consist of gridded wind components at standard pressure levels from 1000 hPA to 100 hPa, twice a day over the whole globe. The 850 hPa standard level was chosen as the transport layer. Though the 925 hPa level would have been preferred, in these studies only the standard levels were available. The 850 hPa level can be thought of as the approximate boundary between the surface sea-level regime and the regime of upper winds relatively free from local surface effects. At that level, the surrounding complex topography would begin to lose its influence especially during strong synoptic flow.

The ARL model was designed specifically for the forward and backward trajectory calculations that can be used in understanding atmospheric transport. It employs the average observed 850 hPA winds and applies an inverse-distance-squared wind weighting with the modified Euler advection technique (Heffter and Taylor, 1975). This technique calculates the center-line trajectory for the trajectory's duration (40 individually computed 3-hour trajectory segments placed end to end) using the modified Euler advection technique for each segment (Carnahan et al., 1969). First the latitude and longitude coordinates of the endpoint of the previous trajectory segment are converted to grid units (x,y). Bilinear interpolation is used to calculate the winds at (x,y) from the winds at the four grid points surrounding (x,y). A first-guess trajectory segment is then computed assuming that this wind persists from 3 hours before to 3 hours after observation time. At the midpoint of the first-guess segment (xm, ym), the winds are again calculated by bilinear interpolation. These latter winds are then used to compute the final trajectory segment beginning at (x,y), because they are assumed to be more representative of winds for the 3-hour segment. The model has been used for many applications since its completion over a decade ago (Miller, 1987).

For the western Mediterranean, trajectories of 5-10 days' duration were calculated at 40°N, 6°E for January 1975 to December 1984 (Miller et al., 1987). The eastern Mediterranean region was represented by trajectories to a receptor site located in Israel (33°N, 35°E) for January 1978 to December 1982.

The most interesting feature of frequency distributions of air parcel trajectories to both the western and eastern sites is the relatively high frequency of trajectories arriving from the west during the winter months and trajectories arriving from the north-northwest during the summer season. This feature is more accentuated in the eastern part of the Mediterranean Basin.

2.1.3.1 Flow climatology of the eastern Mediterranean

The classification for the eastern Mediterranean (Israel) trajectory (33°N, 35°E) is shown in Fig. 31 (Dayan, 1986). The trajectory direction was divided into five distinctive categories: (1) NW, the long fetch of maritime air masses from northwestern Europe crossing the Mediterranean Sea, evenly distributed throughout the whole year; (2) NE, northeastern continental flow originating in eastern Europe, most frequent during the summer season; (3) SE, southeastern flow from the Arabian Peninsula, infrequently observed and occurring mainly during the fall; (4) SW, southwestern flow along the North African coast, most frequent during late winter and spring; and (5) SSW, south-southwestern flow from inland North Africa, most frequent during winter and spring. These five air flow patterns were evaluated in conjunction with seasonal weather types featuring the Mediterranean Basin. From the aspect of pollution transport within this region, the flow pattern that exerted a rather long fetch transport (mostly from northwestern Europe along the Mediterranean) was the most frequent trajectory path, and predominated in the winter; the northeast continental flow crossing Asia Minor and reaching the eastern Mediterranean was the second most frequent trajectory path, and predominated during the summer season. These features are displayed in Section 2.1.4.

2.1.3.2 Flow climatology of the western Mediterranean

Trajectories for the 10-year period were calculated from a point in the western Mediterranean (Med Pol, 40°N, 6°E) and were visually categorized according to the scheme shown in Fig. 31 (Miller et al., 1987). There were six different categories: (1) N--trajectories coming from the north would conceivably bring the most pollution with them; (2) E--trajectories rarely come from the east; (3) S--the flow pattern from the south brings air from the Sahara with accompanying desert dust; (4) W--trajectories from the west could be expected to be the cleanest; (5) Misc--the miscellaneous category includes both the times when the trajectories show strong cyclonic motions and the times during very weak flow when categorization is impossible; and (6) Miss--missing. A summary of the frequency expressed in percents for each category is shown in Fig. 31. One can see the prevailing westerly and northerly flow.

2.1.4 Statistical flow climatology of single back trajectories in the Mediterranean Basin

Although the visual classification method for single back trajectories is common and has been used among the atmospheric scientific community for over the last decade (Pack et al., 1978; Miller, 1981a,b; Miller and Harris, 1985; Billman-Stunder et al., 1986; Dayan et al., 1985; Dayan, 1986), this categorization method is rather slow and complicated for long data records. Miller et al. (1987) describe in their study a comparison between two categorization methods: the visual conventional classification method and an automatic analysis scheme for a concurrent time (10 years) at the same location using two different long-range transport models. These two models show similar results, which gives us confidence in the use of automatic categorization methods.

For the present study, the authors used a program developed by Heffter (personal communication) to analyze the trajectory positions statistically in time and space for climatological use. The program takes into account both the trajectory position and horizontal diffusion about that position using a puff radius R, in meters, defined (Heffter, 1965) as:

$$R = 0.5\ t$$

where t is the transit time in seconds. The results of these calculations are shown in Figs. 32 to 35.

In Figure 33b, using the trajectory statistics for December as an example, the depiction shows the percentage of the boundary layer (1000 to 850 hPa) at the receptor R (Israel) that had traversed a location on the map. About 70% of the boundary layer air at Israel traversed Cyprus, about 20% of the air traversed northern Italy, but less than 1% traversed Spain. These percentages were determined as follows. Constant-level backward-in-time trajectories from the two Mediterranean receptor sites were computed between 1000 and 850 hPa using archived gridded wind fields (Harris, 1982) for the 5-year period (1978-1982) at these two sites. Then each trajectory of 5 days' duration, was identified by segment and end-point positions (40 3-h positions per 5-day trajectory).

Heffter's (1986) program also determines the first time of arrival at the receptor (in days) from any location on the map. Maps shown in Figs. 34 and 35 depict the first time of arrival at a receptor. They are valuable for emergency planning following an accidental release of pollutants in the atmosphere above the Mediterranean Basin or for general planning for source-receptor relationships in this region. Again using December as an example (Fig. 35b), one can see that the first time of arrival at Israel from Cyprus is about half a day, from Greece less than 2 days, and from Spain about 5 days.

2.2 Convective Processes--The Effect of Thermal Stratification on Vertical Transport in the Lower Atmosphere

For the calculation of long-range transport of pollutants during a given episode in the Mediterranean region, the daily and even hourly mixing-height values would be very useful (Maul, 1982; Bhumralkar et al., 1981; Eliassen, 1984). However, due to lack of data, we could calculate only selected monthly climatological mixing height values. To obtain these values, data from more than 100 radiosonde stations around the Mediterranean area were processed on a yearly basis according to Heffter's method (1983). The lowest stable layer was defined as the lid of the mixing height. Its magnitude at local noon time was calculated using the 100 radiosonde soundings within and around the Mediterranean Basin. The criteria for defining the inversion are

(1) $\Delta\theta/\Delta Z \geqslant 0.005^{\circ}K/m$

(2) $\theta_T - \theta_B \geqslant 2^{\circ}K$

where $\Delta\theta/\Delta Z$ is the change of potential temperature (θ) with height (Z) and θ_T and θ_B are defined at the top and base of the inversion. A default value of 3000 m is assumed when no critical inversion is detected.

Examples of the average estimated mixing height for the winter season (January 1984) and for a typical summer month (July 1984) are presented in Figs. 36 and 37, respectively. As one might expect, the mixing height was found to be generally larger over land and probably at its minimum thickness above the Mediterranean Sea. It is noteworthy to mention that all sites that had less than 31 soundings (one per day) were excluded in the calculation of these mixing height values.

3.0 DEPOSITION

Many organic compounds and heavy metals entering the Mediterranean area, such as cadmium, and chlorinated and petroleum hydrocarbons, are currently of greatest concern (Duce et al., 1976; GESAMP, 1985; Pacyna, 1985; Dulac, 1986). After these trace constituents are mixed into the atmosphere and transported by the winds, there is the final stage of removal or deposition. This process can be broken down into two types: dry deposition and wet deposition. Wet deposition includes both the rainout (within-cloud scavenging) and washout (below-cloud scavenging). The routinely measured meteorological parameters that can help in understanding deposition include distribution of cloud types and their amounts, plus duration and amount of precipitation.

3.1 Clouds of the Mediterranean and Their Associated Air Masses

One of the most notable features of the Mediterranean cloud cover is that the area is nearly cloudless during the summer and about 50% overcast during the winter. From November to February, the central regions, including Italy, Greece, and the Aegean Sea, are 50-60% covered and eastern Spain and Egypt are 35% covered. In spring, the cloud area gradually retreats northward, and in May a mean cloudiness of 50% is found only over northern Italy and north of northern Greece. During the summer, northern Italy retains a 40% cloud cover, while all other sections enjoy nearly cloudless skies. In September, the overcast begins to increase again, but is not appreciable until October. In that month, a 50% cover will be found over Italy and Sicily, while eastern Spain and Egypt are still nearly clear. The wedge of cloudiness, which has spread south, then extends itself east and west in returning to winter conditions. The distribution of mountain ranges, the changes of air-mass stability and moisture content, and the original air-mass characteristics determine which cloud types will form. Air moving over the Mediterranean from North Africa is warmer than the sea at all seasons, especially in winter, whereas air reaching it from the northeastern Atlantic is cooler at all seasons, but especially in the summer. Continental air reaching the Mediterranean from Europe is heated from below in the winter, but cooled in the summer (Air Ministry, Meteorological Office, 1962; Biel, 1944; Conrad, 1973).

3.1.1 Clouds in the winter

In mPa air, which is the most common air mass using the Bergeron classification scheme (Table 1), the same cloud sequences are found behind cold fronts as in the Atlantic: cumulonimbus slowly decreasing, becoming broken usually 160 km to the rear of each front, but often persisting for days in the mPa air due to the steep lapse rates and persistent cyclonic curvature of isobars behind the fronts. As the air becomes stagnant mPm, fog or low stratus is frequently found over land in the mornings, whereas scattered cumulonimbus is still reported in the afternoon. The cPe air arriving from Europe with a north-west to northeast trajectory is shallow, 2-3 km in depth; an extensive overcast altostratus or altocumulus forms in mPm air, which is underrun by the cPe air. Low stratus found over the Balkans during an advance of cPe air from the east or northeast dissipates along the Dalmatian coast, as the cPe air descends about 700-900 m to the Mediterranean. The cPs air is cloudless over Africa, but develops low stratus while passing over the Mediterranean. The amount of stratus depends upon the period of time the cPs air has spent over the water as well as upon the surface temperatures of the air mass as it leaves the North African coast. When the stratus lifts along the mountain ranges bordering the northern Mediterranean, especially the Dalmatian coast, middle clouds and rain remain (Brady and Nestor, 1980; KNMI, 1968).

3.1.2 Clouds in the summer

The mTm air (Table 1), which is most commonly present, is characterized by instability in the lower levels, but moderate stability in upper levels. This fair-weather cumulus is observed over the sea, but cumulonimbus is rarely observed except during occasional frontal passages. Greater frequency of cumulus clouds is found over the land, especially in the mountainous regions. High and middle clouds appear to be almost absent. The mPa air occasionally reaches the Mediterranean in summer behind a cold front. Behind the front, low stratocumulus is soon followed by cumulonimbus, the instability resulting from the fact that the Mediterranean is about 3-4°C warmer than the Atlantic in summer. The cTe air reaches the Mediterranean only with northerly flow. Since its lower part is cooled over the sea, and daytime heating is negligible over the water, only scattered cumulus clouds with high bases and lacking of vertical development are observed.

The appearance of altostratus and cirrostratus is associated with mTa air arriving from the southwest and preceding a cold front from the Atlantic. When mTa air reaches the surface of the Mediterranean, it picks up moisture from below, resulting in low stratocumulus. The cTs air mass is cooled from below, during this season, and acquires moisture in passing northward. Altocumulus clouds are fairly common in this air mass moving north, because of the excessive instability aloft.

3.2 Monthly Data of the Mean Cloud Amount over the Mediterranean Sea

Monthly mean cloud amounts are given in Figs. 38-49 using oktas or eights (8 = overcast). The first striking feature of this representation is the relative clearness of the skies throughout the Mediterranean in summer as compared with winter. The Ionian Sea, in particular, should be noted for clear skies in summer. Also, in the Mediterranean the amount of cloud at a given station varies considerably and often irregularly in the course of a day; days of persistent overcast skies are rare.

In many places ashore, the diurnal variation of clouds in winter gives a maximum in the early morning because of low stratus, which usually dissolves after sunrise. There is a second maximum in the afternoon caused by the development of cumulus. The modeler should however keep in mind when simulating transport and diffusion of pollutants on a diurnal basis, that the clearest time is the evening.

Coastal waters are commonly affected by the diurnal changes of cloud amount over the neighboring coast. However, convection is often suppressed and the sky clears completely over the offshore waters up to about 15-25 km from the coast, when cumulus development grows over the land. This fact should be taken into consideration in parameterization of wet deposition of pollutants along the Mediterranean coast by scavenging efforts in convective cloud atmosphere (KNMI, 1957).

3.3 Monthly Precipitation Amounts

The monthly average amount of precipitation is difficult to determine, since direct measurement of precipitation is monitored by ships only. As a part of the meteorological data, distribution of precipitation intensities are displayed in Figs. 50 and 51, and monthly amounts and duration of precipitation are given in Tables 2 and 3. The summer dry season and the wet season from late autumn to early spring are noticeable features nearly everywhere in this basin except in the northern part of the Adriatic and Ligurian seas where summer thunderstorms are quite frequent, amounting to about 25% of the total annual rainfall. Elsewhere in the northern Mediterranean, summer rainfall is only about 10% of the annual total. South of about 40°N, the summer precipitation amounts represent barely 5% of the total annual amount. In the southeast and south-central Mediterranean there is practically no rain during these summer months (Air Ministry, Meteorological Office, 1962).

3.3.1 Geographical distribution of precipitation

As one goes southward, the month of greatest precipitation occurs later in the year, in general, because of the progressive penetration of polar air masses southward into the Mediterranean. Therefore, north of a line from north-east Spain through the center of the western basin, the center of Italy, northern Greece, and north of the Aegean Sea, the month with maximum rainfall is October. Between this region and a line from the Strait of Gibraltar through Sardinia, the south of Italy, and the central Aegean, the month of greatest rainfall is November. South of this second line, the month of greatest rainfall is usually December and sometimes January. The general pattern can be seen in the rainfall intensity maps (Figs. 50 and 51) and in Table 3. There are, of course, many local exceptions to this general pattern (Air Ministry, Meteorological Office, 1962).

3.4 Indirect Methods for Evaluation of Precipitation Amounts and Rates

There are several indirect methods to evaluate precipitation amounts and occurrence. For example, one method uses radar reflectivity data to assess intensity rates and integral rain amounts. Another method, suggested by Goossens (1985), uses a principal component analysis followed by a cluster analysis technique (Fig. 52).

Goossens' method allows the classification of Mediterranean rainfall sites into homogeneous regional groups. These climatic regions may be characterized as follows: Group 1: Northwestern Spain, northern Portugal, northern Italy, eastern Mediterranean coast of France; characterized by a west European rather than a Mediterranean coastal climate with a yearly rainfall distribution exceeding 700 mm over much of the region. Group 2: Northeastern and southern Spain, southern Portugal, western Mediterranean coast of France; characterized by rainfall in winter and very little rain in summer months. Group 3: Balearic Islands, central and southern Italy, northwest Africa, northern Greece, part of Yugoslavia; most of the rainfall occurs during the winter half year, but summer is not rainless; the amount and duration of rain, however, decrease progressively towards the south. Group 4: Yugoslavia, Albania, and southeastern Italy; characterized by a single maximum of rain in winter, summer being almost but not quite rainless. Group 5: Southern Greece; characterized by considerably less precipitation, and dry and dusty lands throughout the long summer months. All these features can be seen by reviewing Figs. 50-52 and Tables 2 and 3.

4.0 SUMMARY

This report reviews the needed parameters for understanding the atmospheric transport of pollutants to the Mediterranean Basin. The main goal of the report is to answer one of the questions raised by the GESAMP Working Group (GESAMP, 1985); that is, what are the major atmospheric pathways for contaminants reaching the Mediterranean?

Beginning with a description of well-known geographical and synoptical features of the Mediterranean climate, special studies are presented that use the meteorological data in models for a more sophisticated analysis. The use of trajectory climatologies and statistical studies are examples of such approaches.

To assess the effect of thermal stratification on vertical transport, temperature profiles were extracted from a global, upper-air data base for the Mediterranean region from which average values of boundary layer heights were mapped. The authors also describe some important parameters affecting two possible types of deposition: dry deposition and wet deposition (consisting of within cloud scavenging and below-cloud scavenging). The routinely measured meteorological parameters necessary for such processes include distribution of cloud types and their amounts as well as duration and amount of precipitation. These data are displayed in the most practical way for a potential user on a 1° square resolution. An extensive reference list is provided.

5.0 BIBLIOGRAPHY AND REFERENCES

This section presents a selected bibliography arranged by topic, and references for this paper. The bibliography is not intended to be a complete listing of publications but a selection of particularly useful publications for the reader. It is hoped that it will provide a practical guide to obtaining background knowledge in the important meteorological factors directly influencing the transport phenomena in the Mediterranean area.

5.1 Selected Bibliography

5.1.1 General features of the Mediterranean Basin

Alpert, P., 1984: An Early Winter Subtropical Cyclone in the Eastern Mediterranean. Isr. J. Earth Sci., 33, 150-156.

Biel, E.R., 1944: Climatology of the Mediterranean Area. Misc. Report No. 13, University of Chicago, Inst. of Meteorology, Chicago, IL, 180 pp.

Brady, L.R., and J.R. Nestor, 1980: Regional Forecasting Aids for the Mediterranean Basin. Tech. Rep. TR 80-10, U.S. Naval Environmental Prediction Research Facility, Monterey, CA, 94 pp.

Conrad, V., 1973: The Climate of the Mediterranean Region. Bull. Amer. Meteorol. Soc., 24, 127.

Fleet Weather Central, 1966: Forecasting Aids for the Mediterranean Sea. Rota, Spain, 67 pp.

Frank, S.R., and R.D. Elliott, 1953: Operational Weather of the Mediterranean Area, Area 1. AROWA 09-1053-097, Navy, Applied Research Operation. Weather Analysis, Monterey, CA.

Hess, P., and H. Brezowsky, 1969: Catalog of European Large Scale Weather Patterns. Deutscher Wetterdienst Berichte, 15 (113), 56 pp.

KNMI (Koninklijk Nederlands Meteorologisch Instituut), 1957: The Mediterranean, Oceanographic and Meteorological Data. De Bilt, The Netherlands, 91 pp.

KNMI (Koninklijk Nederlands Meteorologisch Instituut), 1968: Marine Climatological Summaries for the Mediterranean and the South Indian Ocean, Vol. 8. De Bilt, The Netherlands, 476 pp.

National Climatic Center, 1975: A Climatic Resume of the Mediterranean Sea. Asheville, North Carolina (available NTIS, U.S. Department of Commerce, AD-A 023 929).

NAVWEARSCHFAC (Navy Weather Research Facility), 1958: An Aid to Forecasting Weather in the Mediterranean Sea. Norfolk, VA, 42 pp.

Petterssen, S., 1956: Weather Analysis and Forecasting, Volume 1, McGraw-Hill Book Co., New York, 428 pp.

Reiter, E.R., 1971: Digest of Selected Weather Problems of the Mediterranean. NAVWEARSCHFAC Tech. Paper No. 9-71, Navy Weather Research Facility, Norfolk, VA.

Sutcliffe, R.C., 1960a: The Mediterranean in Relation to the General Circulation. UNESCO/WMO Seminar on Mediterranean Synoptic Meteorology, Rome, 1958. Meteorologishe Abhandlungen, Band IX, Heft 1, Institut fur Meteorologie und Geophysik der Freien Universitat Berlin, 125-133.

Sutcliffe, R.C., 1960b: Depressions, Fronts and Air Mass Modifications in the Mediterranean. UNESCO/WMO Seminar on Mediterranean Synoptic Meteorology, Rome, 1958, Meteorologische Abhandlungen, Band IX, Heft 1, Institut fur Meteorologie und Geophysik der Freien Universitat Berlin, 135-143.

Trewartha, G.T., 1961: Mediterranean Lands. In The Earth's Problem Climates. The Univ. of Wisconsin Press, 223-247.

University of Chicago, Institute of Meteorology: A Report on the Synoptic Conditions in the Mediterranean Area. Chicago, IL.

U.S. Naval Weather Service Command, 1970: Summary of Synoptic Meteorological Observations for the Mediterranean Marine Areas. (Available U.S. Dept. of Commerce, NTIS, AD-712 761.)

5.1.2 Transport and dispersion

Arnold, M., 1985: Géochimie et transport des aérosols métalliques au dessus de la Méditerranee Occidentale. Thèse d'Etat., Univ. Paris 7.

Bleeker, W.: A Climatological Analysis of the Fields of Flow and Temperature in the Mediterranean Area. Scientific Report No. 11, Dept. of Meteorology, Florida State University.

Butzer, K.W., 1960: Dynamic Climatology of Large Scale European Circulation Patterns in the Mediterranean Area. Meteorologishe Rundschau, 13,(4), 97-105.

Defaut, F., 1951: Local Winds. In Compendium of Meteorology. American Meteorological Society, Boston, 655-672.

Dobbins, A., 1979: Atmospheric Motion and Air Pollution. John Wiley and Sons, New York.

Dulac, F. 1986: Dynamique du Transport et des Retombées d'Aérosols Métalliques en Méditerranee Occidentale. Thèse de doctorat, Univ. Paris 7.

Dulac, F., P. Buat-Menard, M. Arnold, U. Ezat, and D. Martin, 1987: Atmospheric Impact of Trace Metals to the Western Mediterranean Sea: 1. Factors Controlling the Variability of Atmospheric Concentrations. J. Geophys. Res., 92(D7), 8437-8453.

Estoque, M.A., 1962: The Sea Breeze as a Function of the Prevailing Synoptic Situation. J. Atmos. Sci., 19(3), 244-250.

GESAMP (Joint Group of Experts on the Scientific Aspects of Marine Pollution), 1985: Atmospheric Transport of Contaminants into the Mediterranean Region. Reports and Studies GESAMP No. 26, IMO/FAO/UNESCO/WMO/WHO/IAEA/UN/UNEP, Geneva, Switzerland.

Levi, M., 1965: Local Winds Around the Mediterranean Sea. Series C, No. 13, Israel Meteorological Service, Tel Aviv, Israel.

Mahrer, Y., 1985: A Numerical Study of the Effects of Sea-Surface Temperature on the Sea and Land Breeze Circulation. Isr. J. Earth Sci., 34, 91-95.

Mahrer, Y., and R.A. Pielke, 1977: A Numerical Study of the Airflow over Irregular Terrain. Beitraege Z. Physik Atmosphaere, 50, 98-113.

Martin, D., C. Mithieux, and B. Strauss, 1987: On the Use of the Synoptic Vertical Wind Component in a Transport Trajectory Model. Atmos. Environ., 21(1), 45-52.

Maring, H., D.M. Settle, P. Buat-Menard, F. Dulac, and C. Patterson, 1987: Stable Lead Isotope Tracers of Air Mass Trajectories in the Mediterranean Region. Nature, 330(12), 154-156.

Neumann, J., and Y. Mahrer, 1971: A Theoretical Study of the Land and Sea Breeze Circulation. J. Atmos. Sci., 28(4), 532-542.

Pacyna, J.M., A. Samb, and J.E. Hanssen, 1984: Emission and Long-Range Transport of Trace Elements in Europe. Tellus, 36B, 163-178.

Papas, G., 1983: Sea Breeze Circulation and Photochemical Pollution in Athens, Greece. Atmos. Environ., 17(9), 1621-1632.

Piexoto, J.P., 1980: Atmospheric Moisture Transport and the Water Balance of the Mediterranean Sea. Water Resources Res., 18(1), 83-90.

Reiter, E.R., 1969: Atmospheric Transport Processes, Part 1: Energy Transfers and Transformations. AEC Critical Review Series, USAEC Report TID-24868, U.S. Atomic Energy Commission, Washington, DC.

Reiter, E.R., 1972: Atmospheric Transport Processes, Part 3: Hydrodynamic Tracers. AEC Critical Review Series, USAEC Report TID-25731, U.S. Atomic Energy Commission, Washington, DC.

Segal, M., R.A. Pielke, and Y. Mahrer, 1982: Evaluations of Onshore Pollutant Recirculation Over the Mediterranean Coastal Area of Central Israel. Isr. J. Earth Sci., 31, 39-46.

Skibin, D., and A. Hod, 1979: Subjective Analysis of Mesoscale Flow Patterns in North Israel. J. Appl. Meteorol., 18, 329-338.

WMO (World Meteorological Organization), 1979: WMO Symposium on the Long-Range Transport of Pollutants and its Relation to General Circulation Including Stratospheric/Tropospheric Exchange Processes. WMO No. 538, Geneva, Switzerland.

5.1.3 Deposition processes in the Mediterranean Basin

Arnold, M., A. Seghaier, D. Martin, P. Buat Menard, and R. Chesselet, 1982: Géochimie de l'Aérosol Marin au-dessus de la Méditerranée Occidentale. Workshop on Pollution of the Mediterranean, Cannes, December 2-4, CIESM, 27-37.

Berger, W.R., and W.D. Garrett, 1976: Surface Active Organic Material in Air over the Mediterranean and over the Eastern Equatorial Pacific. J. Geophys. Res., 81, 3151-3157.

Bidleman, T.F., and C.E. Olney, 1974: Chlorinated Hydrocarbons in the Saragasso Sea Atmosphere and Surface Water. Science, 183, 516-518.

Buat-Menard, P., and R. Chesselet, 1979: Variable Influence of the Atmospheric Flux on the Trace Metal Chemistry of Oceanic Suspended Matter. Earth Planet. Sci. Lett., 42, 399-411.

Burns, K.A., and J.P. Villeneuve, 1983: Biogeochemical Processes Affecting the Distribution and Vertical Transport of Hydrocarbon Residues in the Coastal Mediterranean. Geoch. Cosmochim. Acta, 47, 995-1006.

Chester, R., A.C. Saydam, and E.J. Sharples, 1981: An Approach to the Assessment of Local Tracer Metal Pollution in the Mediterranean Marine Atmosphere. Mar. Poll. Bull., 12, 426-431.

Druyan, L.M., 1984: A Simple Algorithm for the Probability of Precipitation. Isr. J. Earth Sci., 33, 72-75.

Ho, R., J.C. Marty, and A. Saliot, 1982: Les Hydrocarbures à l'interface Air-Mer en Méditerranée Occidentale, VI. J. Etud. Poll., 39-45.

Levich, E., and E. Tzvetkov, 1985: A Hydrodynamical Model for a Single Rain Situation in Eastern Mediterranean. Isr. J. Earth Sci., 34, 86-90.

Seghaier, A., 1984: Abondance et Origine de quelques Métaux (Al, Fe, Zn, Cu, Cd, Pb) dans l'aérosol Marin de la Méditerranée Occidentale. Thèse 3e cycle, Univ. Paris 7.

Tomadin, L., R. Lenaz, V. Lauduzzi, A. Mazzucotelli, and P. Vanucci, 1984: On Wind-Blown Dusts Over the Central Mediterranean. Oceanol. Acta, 7, 13-23.

Tr'etkov, E., G. Assaf, and A. Manes, 1985: Synoptics and Cloud Fields Connected with Rain Situations in Israel. Isr. J. Earth Sci., 34, 102-109.

UNEP (United Nations Environmental Program), 1984: Pollutants from Land-Based Sources in the Mediterranean. UNEP Regional Seas Reports and Studies No. 32, UNEP/ECE/UNIDO/FAO/UNESCO/WHO/IAEA, Nairobi, Kenya.

Viala, A., F. Gouezo, B. Mallet, J. Fondarai, J.P. Cano, J.M. Sauve, F. Grimaldi, and E. Deturmeny, 1981: Mesure de Quatre Métaux-Traces (Plomb, Cadmium, Chrome et Zinc) dans les Poussières Atmosphériques à Marseille de 1977 a 1979. Poll. Atmos., 91, 207-222.

5.2 References

Air Ministry, Meteorological Office, 1962: Weather in the Mediterranean. Vol. I (second edition). Her Majesty's Stationery Office, London, 362 pp.

Bergeron, T., 1928: Uber die Dreidimensional Verknupfende Wetteranalyse. Geof. Publ.,V, Oslo.

Bhumralkar, C.M., R.L. Mancuso, D.E. Wolf, W.B. Johnson, and J. Pankrath, 1981: Regional Air Pollution Model for Calculating Short-Term (Daily) Patterns and Transfontier Exchanges of Airborne Sulphur in Europe. Tellus, 33, 142-161.

Biel, E.R., 1944: Climatology of the Mediterranean Area. Misc. Report No. 13, University of Chicago, Inst. of Meteorology, 180 pp.

Billman-Stunder, B.J., J.L. Heffter, and U. Dayan, 1986: Trajectory Analysis of Wet Deposition at Whiteface Mountain: A Sensitivity Study. Atmos. Environ., 20(9), 1691-1695.

Brady, L.R., and J.R. Nestor, 1980: Regional Forecasting Aids for the Mediterranean Basin. Tech. Rep. TR-80-10, U.S. Naval Environmental Prediction Research Facility, Monterey, CA., 94 pp.

Carnahan, B., H.A. Luther, and J.O. Wilkes, 1969: Applied Numerical Methods. John Wiley and Sons, New York, 362 pp.

Conrad, V., 1973: The Climate of the Mediterranean Region. Bull. Amer. Meteorol. Soc., 24, 127-138.

Dayan, U., 1979: Synoptic Meteorology of the Mediterranean Region. Hebrew University Press, Jerusalem, Israel, 120 pp.

Dayan, U., 1986: Climatology of Back Trajectories from Israel Based on Synoptic Analysis. J. Clim. Appl. Meteorol., 25, 591-595.

Dayan, U., and M. Graber, 1981: Analysis of Synoptic Conditions in the Eastern Mediterranean that Led to Elevated Air Pollution Concentration in Israel. In Developments in Arid Zone Ecology and Environmental Quality, Balaban International Science Service, Philadelphia, PA, 383-391.

Dayan, U., J.M. Miller, W.C. Keene, and J.N. Galloway, 1985. An Analysis of Precipitation Chemistry Data from Alaska. Atmos. Environ., 19, 651-657.

Duce, R.A., G.L. Hoffman, B.J. Ray, I.S. Fletcher, G.T. Wallace, J.L. Fashing, S.R. Piotrowicz, P.R. Walsh, E.J. Hoffman, J.M. Miller, and J.L. Heffter, 1976: Trace Metals in the Marine Atmosphere: Sources and Fluxes. In Marine Pollutant Transfer, edited by H.L. Windom and R.A. Duce, D.C. Heath, Lexington, MA, 77-119.

Dulac, F., 1986: Dynamique du Transport et des Retombées d'Aérosols Métalliques en Méditerranée Occidentale. Thèse de Doctorat, Univ. Paris 7.

Eliassen, A., 1984: Aspects of Lagrangian Air Pollution Modelling. In: Air Pollution Modeling and its Application, III, edited by C. De Wispelaere, Plenum, New York.

Eliassen, A., and J. Saltbones, 1983: Modelling of Long-Range Transport of Sulphur over Europe: A Two-Year Model Run and Some Model Experiments. Atmos. Environ., 17, 1457-1474.

GESAMP (Joint Group of Experts on the Scientific Aspects of Marine Pollution), 1985: Atmospheric Transport of Contaminants into the Mediterranean Region. Reports and Studies GESAMP No. 26, IMO/FAO/UNESCO/WMO/WHO/IAEA/UN/UNEP, Geneva, Switzerland, 53 pp.

Goossens, C., 1985: Principal Component Analysis of Mediterranean Rainfall. J. Climatol., 5, 379-388.

Harris, J.M., 1982: The GMCC Atmospheric Trajectory Program. NOAA. Tech. Memo. ERL-ARL-116, Air Resources Laboratory, Boulder, CO, 30 pp.

Heffter, J.L., 1965: The Variation of Horizontal Diffusion Parameters with Time for Travel Periods of One Hour or Longer. J. Appl. Meteorol., 4(1), 153-156.

Heffter, J.L., 1983: Branching Atmospheric Trajectory (BAT) Model. NOAA Tech. Memo. ERL-ARL-121, Air Resources Laboratory, Rockville, MD, 16 pp.

Heffter, J.L., and A.D. Taylor, 1975: Trajectory Model - Part 1. A Regional Continental Scale Transport, Diffusion, and Deposition Model. NOAA Tech. Memo. ERL-ARL-50, Air Resources Laboratory, Rockville, MD, 28 pp.

Hess, P., and H. Brezowsky, 1969: Catalog of European Large Scale Weather Patterns. Deutscher Wetterdienst Berichte, 15 (113), 56 pp.

Klug, W., 1984: Suggestions for the Development of a Mesoscale Transport and Diffusion Model for the Mediterranean Area. Report prepared for the World Meteorological Organization.

KNMI (Koninklijk Nederlands Meteorologisch Instituut), 1957: The Mediterranean, Oceanographic and Meteorological Data. De Bilt, The Netherlands, 91 pp.

KNMI (Koninklijk Nederlands Meteorologisch Instituut), 1968: Marine Climatological Summaries for the Mediterranean and the South Indian Ocean, Vol. 8. De Bilt, The Netherlands, 476 pp.

Maul, P.R., 1982: A Time-Dependent Model for the Atmospheric Transport of Sulphur Compound Pollutants. Environ. Poll., B3, 159-179; B4, 11-25.

Miller, J.M., 1981a: A Five-Year Climatology of Five-Day Back Trajectories from Barrow, Alaska. Atmos. Environ., 15, 1401-1405.

Miller, J.M., 1981b: A Five-Year Climatology of Back-Trajectories from the Mauna Loa Observatory, Hawaii. Atmos. Environ., 15, 1553-1558.

Miller, J.M., 1987: The Use of Back Air Trajectories in Interpreting Atmospheric Chemistry Data: A Review and Bibliography. NOAA Tech. Memo. ERL ARL-155, Air Resources Laboratory, Silver Spring, MD, 32 pp.

Miller, J.M., and J. Harris, 1985: The Flow Climatology to Bermuda and its Implications for Long-Range Transport. Atmos. Environ., 19, 409-414.

Miller, J.M., D. Martin, and B. Strauss, 1987: A Comparison of Results from Two Trajectory Models Used to Produce Flow Climatologies to the Western Mediterranean. NOAA Tech. Memo. ERL ARL-151, Air Resources Laboratory, Silver Spring, MD, 11 pp.

Newell, R.E., J.W. Kidson, D.G. Vincent, and G.J. Boer, 1972: The General Circulation of the Tropical Atmosphere, Vol. 1. The MIT Press, Boston, MA.

Pack, D.H., G.J. Ferber, J.L. Heffter, K. Telegadas, J.K. Angell, W.H. Hoecker, and L. Machta, 1978: Meteorology of Long-Range Transport. Atmos. Environ., 12, 425-441.

Pacyna, J.M., 1985: Spatial Distributions of the As, Cd, Cu, Pb, V, and Zn Emissions in Europe Within a 1.5° Grid net. Tech. Rept., NILU OR60/85, Ref. 0-8551, Norwegian Inst. for Air Res., Lillestrom, Norway.

Reiter, E.R., 1975: Handbook for Forecasters in the Mediterranean, Weather Phenomena of the Mediterranean Basin, Part 1: General Description of the Meteorological Processes. ENVPREDRSCHFAC Tech. Paper No. 5-75, Naval Environmental Prediction Research Facility, 344 pp.

Topol, L.E., R. Vyayakumar, C.M. McKinley, and T.L. Warren, 1986: The Effect of Seasonal and Storm Type on Precipitation Chemistry. J. Air Pollut. Control Assoc., 36, 393-398.

6.0 ACKNOWLEDGMENTS

The authors would like to thank the following people for helping in the preparation of this report: J. Harris, J. Heffter, S. Sheridan, A. Taylor, and B. Wells.

Table 1

Bergeron classification of air masses over the Mediterranean (Bergeron, 1928)

Identifier	Definition
Winter	
cTs	Continental Tropical Saharan
cPs	Continental Polar Saharan
cPe	Continental Polar European
mPa	Maritime Polar Atlantic
mPm	Maritime Polar Mediterranean
Summer	
cTs	Continental Tropical Saharan
cTe	Continental Tropical European
mTa	Maritime Tropical Atlantic
mTm	Maritime Tropical Mediterranean

Table 2. Monthly precipitation amounts (mm) and duration (average number of rainy days) for selected sites along and within the Mediterranean.

Station Name	Lat	Long	Jan *	Jan **	Feb		Mar		Apr		May		Jun		Jul		Aug		Sep		Oct		Nov		Dec		Total	
C. Spartel	35°47'N	5°55'W	101	10	85	11	104	12	55	8	43	7	13	3	2	0.5	2	0.5	27	4	77	7	140	11	121	11	770	85
Oran	35°42'N	0°39'W	71	9	49	7	51	7	31	7	21	5	6	3	0.6	0.9	2	1	13	4	33	6	51	8	50	8	377	64
Gilbraltar	36°6'N	5°21'W	117	10	114	11	119	12	69	9	41	6	13	2	-	0.4	3	0.8	33	4	84	8	163	11	137	11	892	85
Algiers	36°48'N	3°2'E	100	15	62	13	81	13	53	11	46	9	17	5	4	2	4	2	28	7	79	11	87	13	95	15	656	117
Bizerte	37°17'N	9°50'E	143	15	77	12	59	11	41	9	25	6	15	3	4	2	3	2	21	5	65	9	86	12	115	15	654	100
Malaga	36°43'N	4°27'W	76	5	50	4	84	7	68	7	28	4	13	2	3	0.8	5	0.8	27	2	64	5	87	5	102	6	607	49
Cartagena	37°36'N	0°47'W	45	5	36	4	41	6	27	4	26	3	20	2	2	1	6	1	35	3	42	4	48	5	52	5	379	43
Barcelona	41°23'N	2°8'E	36	5	37	5	45	6	49	8	42	7	37	6	26	3	0.3	4	77	6	78	8	45	6	36	5	543	70
Palma	39°34'N	2°37'E	43	8	35	7	39	7	37	7	40	6	19	3	11	1.5	8	2	55	6	77	9	55	9	55	8	484	73
Mahon	39°53'N	4°21'E	61	9	44	7	54	8	49	6	36	7	24	4	14	2	15	3	55	5	104	10	97	11	76	9	628	80
Ajaccio	41°55'N	8°44'E	75	8	52	6	61	10	52	8	41	7	28	4	4	1	21	3	50	5	91	9	118	11	72	9	665	80
Cagliari	39°13'N	9°6'E	47	10	35	9	50	10	42	10	29	7	19	4	2	1	4	1	31	5	60	8	75	10	55	11	449	86
Marseilles	43°18'N	5°23'E	49	7	36	9	41	10	43	8	48	9	26	6	14	5	24	4	60	6	102	14	79	11	52	10	574	99
Nice	43°43'N	7°18'E	70	6	56	7	69	8	89	9	81	8	45	7	10	5	26	5	66	8	160	10	113	10	72	8	857	91
Cannes	43°30'N	7°E	75	6.6	56	5.6	73	6.7	74	6.9	61	5.9	30	4.1	14	2.2	23	2.2	59	4.3	137	7.3	114	7.7	81	6.8	796	66.3

* monthly amounts in (mm)

** average number of rainy days

Table 2. (con't)

Station Name	Lat	Long	Jan		Feb		Mar		Apr		May		Jun		Jul		Aug		Sep		Oct		Nov		Dec		Total	
			*	**																								
Genoa	44°25'N	8°55'E	104	10	108	9	107	11	100	11	87	12	71	9	63	6	61	7	124	9	200	13	180	12	126	11	1311	120
Leghorn	43°33'N	10°18'E	68	10	62	9	77	7	61	10	60	9	50	6	26	3	36	4	84	7	140	12	119	12	100	12	883	111
Rome	41°54'N	12°29'E	83	11	65	9	73	11	65	10	55	8	39	6	19	3	26	4	64	7	127	10	114	12	98	11	828	102
Naples	40°52'N	14°15'E	94	12	76	11	72	12	65	11	50	9	35	6	16	3	27	4	73	7	116	11	114	13	112	13	848	112
Messina	38°12'N	15°33'E	94	14	83	13	73	12	67	11	39	7	22	5	12	2	26	4	52	7	98	12	122	14	110	16	798	117
Palermo	38°7'N	13°21'E	86	15	70	13	69	13	49	10	29	6	16	4	6	2	11	2	46	6	81	11	85	13	95	16	643	111
Siracusa	37°03'N	15°18'E	93	11	60	9	40	7	36	6	19	4	5	2	6	1	8	2	51	5	83	8	127	10	98	11	626	76
Tunis	36°48'N	10°10'E	54	11	51	10	46	9	38	8	24	5	13	3	3	1	5	1	26	4	49	8	52	9	62	9	425	79
Malta	35°54'N	14°31'E	82	13	56	10	38	8	22	5	10	3	2	1	1	0.2	3	0.7	32	3	73	7	91	11	94	14	504	77
Galipoli	40°4'N	18°1'E	60	8	48	6	31	6	39	6	27	4	14	3	6	1	13	2	46	4	65	6	71	7	69	8	489	61
Corfu	39°37'N	19°57'E	164	13	139	12	98	9	77	9	48	6	25	5	6	2	22	2	78	5	172	11	191	11	218	13	1238	98
Argostolion	38°10'N	20°30'E	107	10	106	11	67	8	40	5	28	4	21	2	6	1	24	1	34	3	105	6	133	10	178	12	861	72
Mesolongion	38°22'N	21°27'E	87	13	75	12	70	11	50	11	47	9	20	6	7	2	5	2	22	6	81	9	131	13	128	14	725	107
Patros	38°15'N	21°44'E	101	14	77	12	63	10	56	11	36	8	18	6	4	1	6	2	30	5	93	11	115	13	123	13	720	106
Vostitza	38°14'N	22°0'E	86	10	62	10	57	9	34	8	32	7	8	3	2	1	7	2	17	3	70	8	114	12	86	10	575	83

* monthly amounts in (mm)
** average number of rainy days

Table 2. (con't)

Station Name	Lat	Long	Jan *	Jan **	Feb *	Feb **	Mar *	Mar **	Apr *	Apr **	May *	May **	Jun *	Jun **	Jul *	Jul **	Aug *	Aug **	Sep *	Sep **	Oct *	Oct **	Nov *	Nov **	Dec *	Dec **	Total *	Total **
Zante	37°47'N	20°55'E	187	13	139	13	84	10	56	8	29	6	9	4	3	1	13	2	30	4	128	10	218	13	224	16	1119	100
Tripoli	32°54'N	13°11'E	94	11	53	6	25	5	15	3	7	2	1	0.3	1	0.3	2	0.2	12	1	39	4	59	6	114	11	422	49
Benghazi	32°7'N	20°2'E	65	11	39	8	17	6	4	2	3	1	-	-	-	-	-	-	3	2	15	4	47	7	62	13	255	54
Venice	45°26'N	12°20'E	41	6	40	7	51	9	60	11	74	9	75	10	58	6	63	7	71	8	91	9	68	8	48	7	740	97
Trieste	45°39'N	13°45'E	61	8	59	7	72	9	76	10	94	11	102	11	81	8	93	8	120	9	152	11	104	10	78	9	1092	111
Split	43°31'N	16°26'E	75	8	62	11	76	10	85	10	68	6	55	7	30	5	42	4	74	7	112	10	106	11	92	14	877	102
Huar	43°10'N	16°26'E	77	10	64	9	72	10	59	9	40	7	38	6	21	3	39	4	63	6	97	9	111	11	105	12	786	97
Pelagosa	42°23'N	16°15'E	46	8	30	8	43	8	40	7	35	5	20	4	10	2	16	2	23	4	53	7	51	8	53	9	420	73
Ostri Point	42°27'N	18°34'E	104	12	105	12	116	12	95	12	60	9	42	7	21	4	33	4	65	6	102	12	107	12	124	13	974	115
Durazzo	41°19'N	19°28'E	75	10	83	9	102	12	56	8	41	7	49	5	12	2	48	4	44	4	168	10	214	14	187	12	1079	97
Ancona	43°37'N	13°32'E	63	9	46	8	50	9	56	9	48	9	48	7	32	5	40	5	71	7	98	10	76	11	60	10	688	99
Bari	41°9'N	16°51'E	65	12	51	10	40	10	44	10	50	9	29	5	14	3	27	4	55	7	61	9	65	11	64	12	565	103
Brindisi	40°38'N	17°57'E	98	10	63	10	55	6	58	7	41	5	24	3	13	2	27	2	53	4	83	8	82	7	93	10	690	72
Siros	37°27'N	24°56'E	101	13	65	10	52	8	26	4	21	4	7	1	1	0.4	5	0.6	14	2	37	4	74	9	92	11	495	67
Santoraro	36°25'N	25°26'E	71	13	38	9	35	8	22	6	19	5	1	1	0	0.1	0	0	6	1	19	4	69	9	82	14	362	70
Cergio	36°10'N	23°0'E	113	7	86	6	50	5	20	2	14	2	5	0.7	1	0.2	3	0.3	12	0.8	55	4	112	7	148	10	619	45

* monthly amounts in (mm)

** average number of rainy days

Table 2. (con't)

Station Name	Lat	Long	Jan *	Jan **	Feb		Mar		Apr		May		Jun		Jul		Aug		Sep		Oct		Nov		Dec		Total	
Candia	35°20'N	25°8'E	88	13.5	74	11	37	7	21	4	19	3	2	1	0.8	0.1	4	0.5	13	1	36	5	76	9	96	12	467	70
Athens	37°58'N	23°43'E	55	13	39	11	33	10	22	9	22	8	15	5	7	3	10	3	15	4	42	8	72	12	65	13	397	99
Voloe	39°24'N	22°58'E	43	7	49	8	44	8	33	7	29	6	22	6	16	3	34	3	33	4	44	6	71	9	55	8	473	75
Solonica	40°39'N	22°57'E	37	7	34	8	41	8	49	8	58	8	44	6	27	4	31	3	43	5	55	8	70	8	58	9	547	82
Smyrna	38°26'N	27°9'E	98	10	71	9	79	8	37	6	31	5	14	2	4	1	6	1	18	2	49	5	91	9	108	11	606	69
Sidi Barrani	31°38'N	25°58'E	34	6	42	6	11	2.5	3	1	3	0.6	-	-	-	-	-	-	-	-	24	2.2	19	3.6	36	6.6	172	29
Alexandria	31°12'N	29°53'E	54	11	23	6	14	5	3	1	1	1	-	-	-	-	0.1	0.1	1	0.2	6	1	35	7	66	10	204	42
Port Said	31°16'N	32°19'E	22	4	11	3	10	2	6	1	2	1	1	0.1	-	-	-	-	-	-	2	0.5	12	2.5	17	3.8	83	18
El'Arish	31°7'N	33°46'E	20	5.7	24	5.9	14	3	9	2	2	1	-	-	-	-	-	-	-	-	2	0.7	18	3.6	13	4.5	102	26.3
Gaza	31°30'N	34°27'E	110	9	50	6	37	5	7	1.5	8	1.5	1	0.1	-	-	-	-	1	0.2	21	2.7	80	6.9	105	7.6	420	40.6
Hefa	32°48'N	34°59'E	156	13	90	10	54	8	25	3	7	2	1	0.1	-	-	-	-	2	0.1	21	3	92	9	162	13	610	62
Beirut	33°54'N	35°28'E	191	16	151	14	98	11	56	6	21	3	4	0.8	0.5	0.2	0.5	0.2	7	1	53	3	135	10	191	13	908	79
Kyrenia	35°20'N	33°19'E	116	11	82	9	61	8	21	3	25	3	5	1	-	-	0.5	0.1	5	1	34	3	97	8	124	10	570	57
Famagusta	35°7'N	33°57'E	75	11	60	10	47	8	27	5	15	4	1	1	-	-	-	-	9	1	43	4	57	7	129	10	462	61
Limasol	34°31'N	33°3'E	95	14	89	10	47	7	21	4	17	3	10	0.7	-	-	0.2	0.2	6	1	36	3	55	7	119	12	494	62
Adana	36°57'N	35°15'E	127	8	84	6	77	6	41	5	54	6	13	1	9	0.7	5	0.5	18	1	55	4	49	3	113	7	646	50

* monthly amounts in (mm)

** average number of rainy days

Table 3. Maximum fall in 24 hrs for selected sites in the Mediterranean region.

Station Name	Lat	Long	Jan *	Feb	Mar	Apr	May	Jun	Jul	Aug	Sep	Oct	Nov	Dec
C. Spartel	35°47'N	5°55'W	82	61	56	68	39	36	21	20	42	50	114	84
Oran	35°42'N	0°39'W	63	81	25	30	33	20	5	23	27	43	70	52
Gilbraltar	36°6'N	5°21'W	198	109	198	165	56	53	10	43	145	137	165	175
Algiers	36°48'N	3°2'E	57	29	73	57	61	39	14	12	47	134	81	64
Bizerte	37°17'N	9°50'E	55	83	39	43	30	60	17	11	28	133	57	89
Cartagena	37°36'N	0°47'W	72	64	41	50	69	84	10	23	106	96	68	66
Barcelona	41°23'N	2°8'E	58	52	47	50	67	52	98	68	114	134	71	70
Palma	39°34'N	2°37'E	57	33	60	43	57	52	31	118	64	60	55	54
Mahon	39°53'N	4°21'E	69	51	81	57	65	65	86	40	125	100	81	54
Marseilles	43°18'N	5°23'E	46	58	50	49	73	45	104	73	101	221	150	91
Rome	41°54'N	12°29'E	129	51	60	66	85	67	47	77	105	142	158	64
Messina	38°12'N	15°33'E	56	57	39	71	66	32	45	57	37	90	94	34
Palermo	38°7'N	13°21'E	58	60	44	46	50	38	18	39	61	67	92	98
Siracusa	37°03'N	15°18'E	132	108	68	54	35	26	91	22	120	198	94	58
Tunis	36°48'N	10°10'E	43	23	40	24	16	28	2	0.2	39	47	87	37
Malta	35°54'N	14°31'E	69	79	73	43	39	19	16	31	123	294	184	197
Corfu	39°37'N	19°57'E	139	205	63	98	83	66	30	85	155	169	129	173
Vostitza	38°14'N	22°0'E	50	50	38	37	38	16	6	21	53	77	74	57

* values are in mm

Table 3. (con't)

Station Name	Lat	Long	Jan *	Feb	Mar	Apr	May	Jun	Jul	Aug	Sep	Oct	Nov	Dec
Tripoli	32°54'N	13°11'E	50	125	31	50	20	11	4	28	78	65	130	72
Venice	45°26'N	12°20'E	66	47	42	70	83	50	51	63	128	82	73	79
Split	43°31'N	16°26'E	19	17	53	29	47	89	34	26	103	35	30	39
Durazzo	41°19'N	19°28'E	44	35	36	39	33	42	25	64	72	72	110	96
Ancona	43°37'N	13°32'E	47	80	31	30	36	51	40	36	120	63	59	31
Brindisi	40°38'N	17°57'E	99	71	74	99	122	81	72	133	122	80	99	104
Siros	37°27'N	24°56'E	65	62	31	29	58	32	20	43	46	95	71	49
Cergio	36°10'N	23°0'E	55	45	46	30	25	25	15	35	31	55	120	78
Candia	35°20'N	25°8'E	44	57	33	23	41	9	13	33	75	59	66	113
Solonica	40°39'N	22°57'E	39	37	43	74	74	58	54	50	49	77	86	59
Sidi Barrani	31°38'N	25°58'E	23	28	16	11	11	0	0	drops	2	76	20	25
Alexandria	31°12'N	29°53'E	47	32	18	30	10	1	0	2	14	27	46	80
Port Said	31°16'N	32°19'E	37	58	20	35	7	33	0	0	6	17	25	53
El'Arish	31°7'N	33°46'E	14	21	21	18	5	0	0	0	0	6	21	11
Beirut	33°54'N	35°28'E	90	90	50	72	35	60	10	7	53	139	95	78
Kyrenia	35°20'N	33°19'E	213	232	150	77	81	27	1	5	38	154	250	273
Limaosol	34°31'N	33°3'E	44	51	34	38	44	104	drops	2	37	51	42	67
Adana	36°57'N	35°15'E	107	69	81	67	65	43	36	28	63	59	95	60

* values are in mm

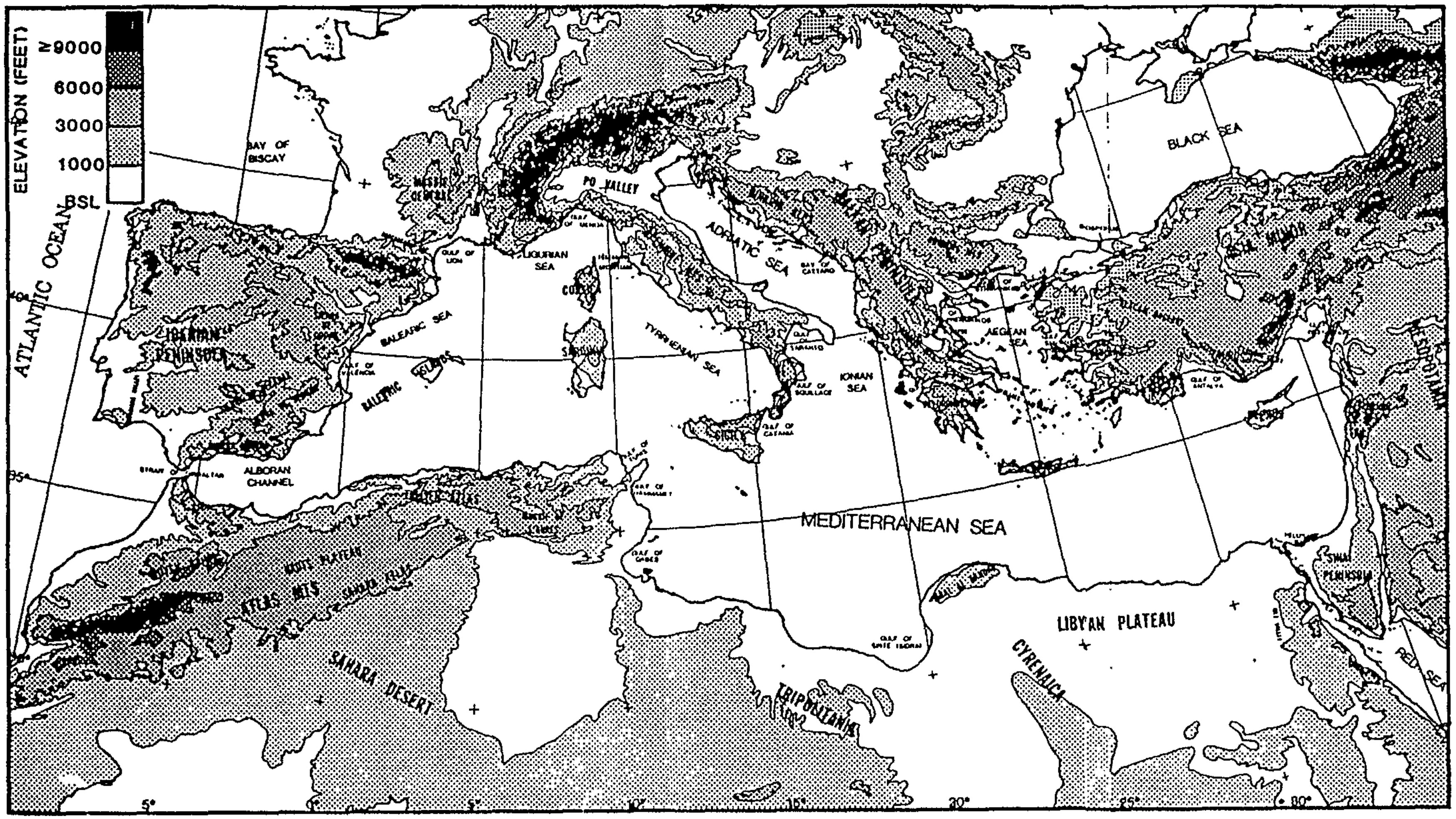

Fig. 1 - Topographical map of the Mediterranean area

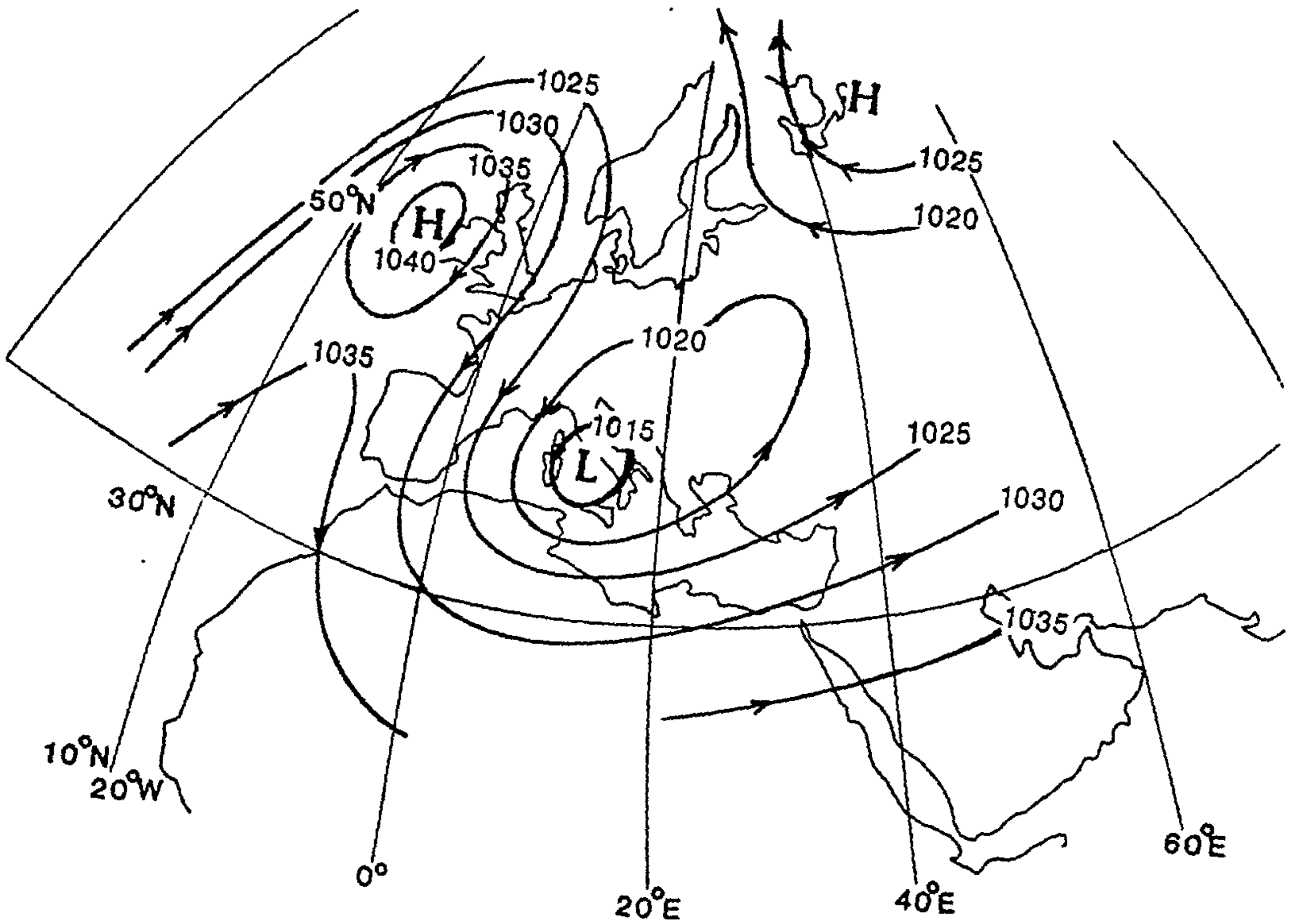

Fig 2 - Synoptic weather pattern type A

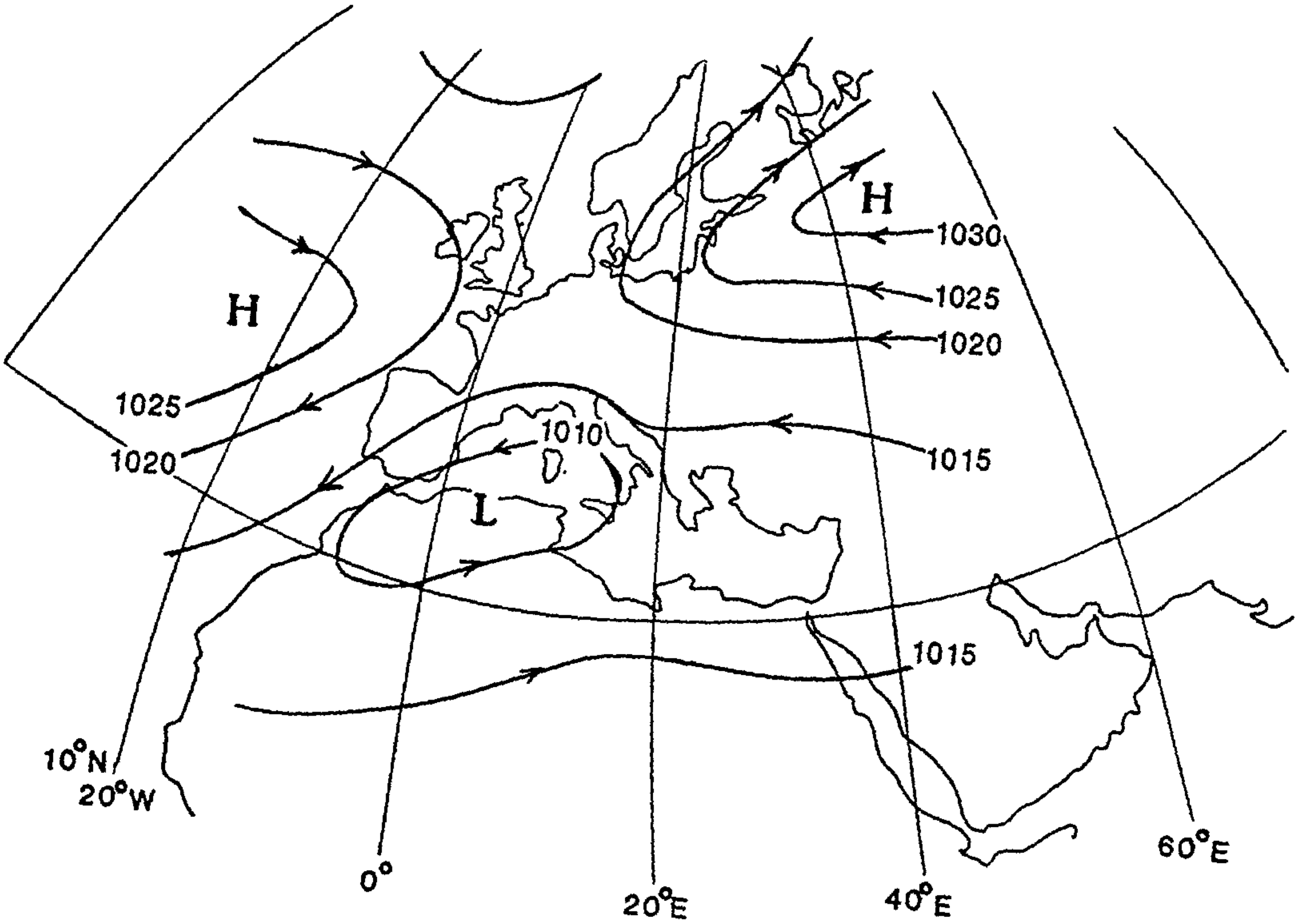

Fig. 3 - Syroptic weather pattern type ß

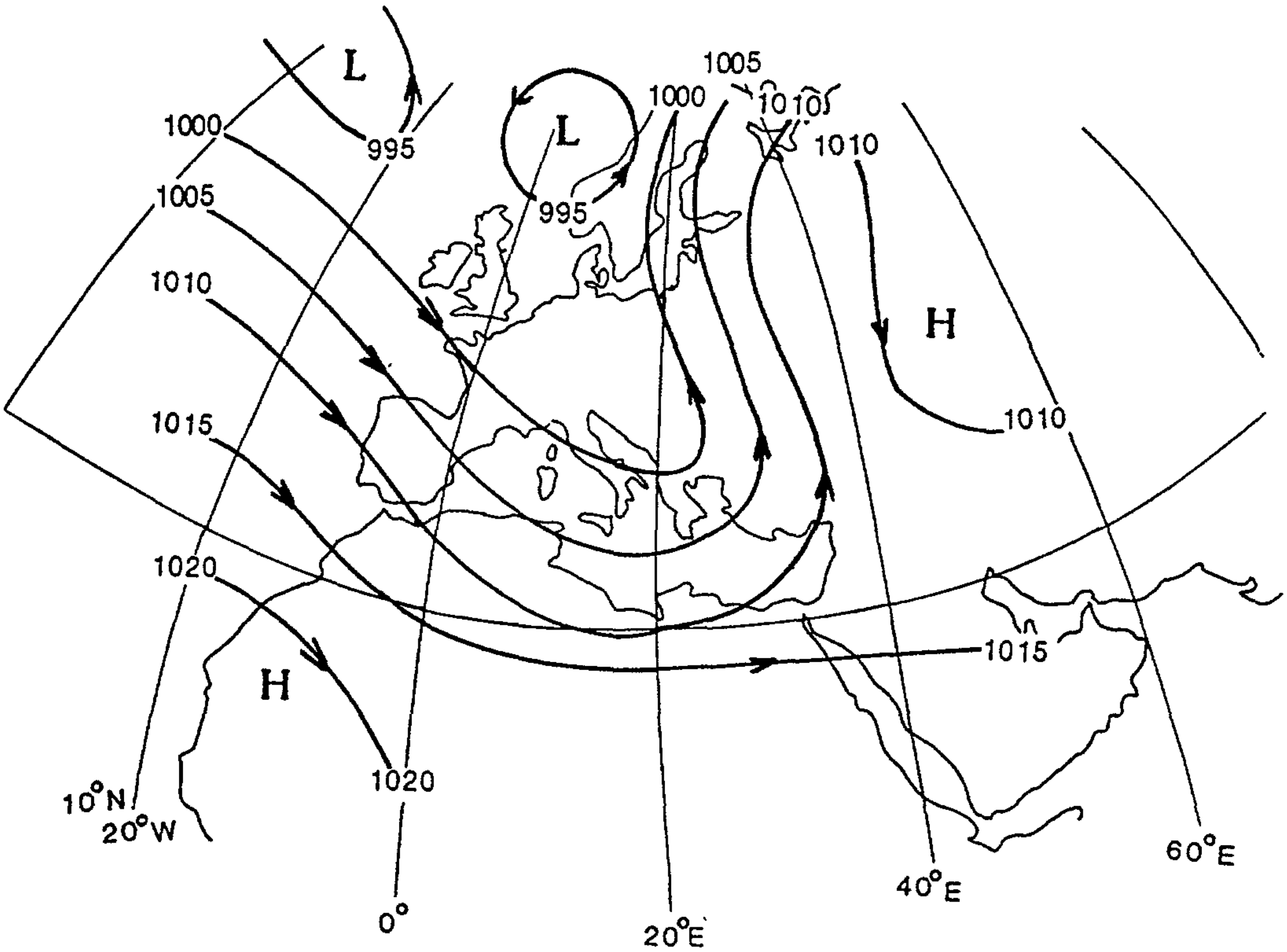

Fig. 4 - Synoptic weather pattern type C

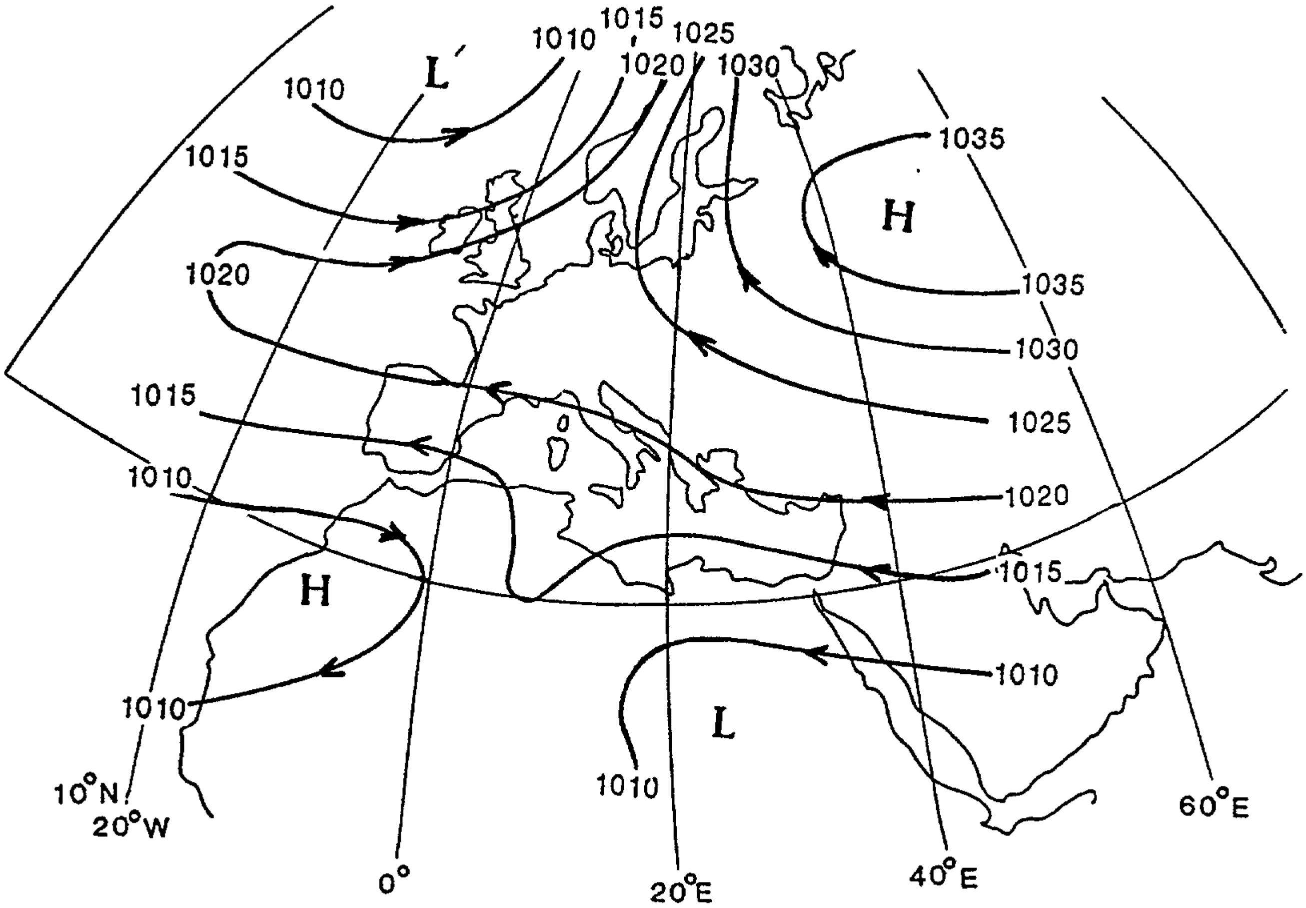

Fig. 5 - Synoptic weather pattern type *D*

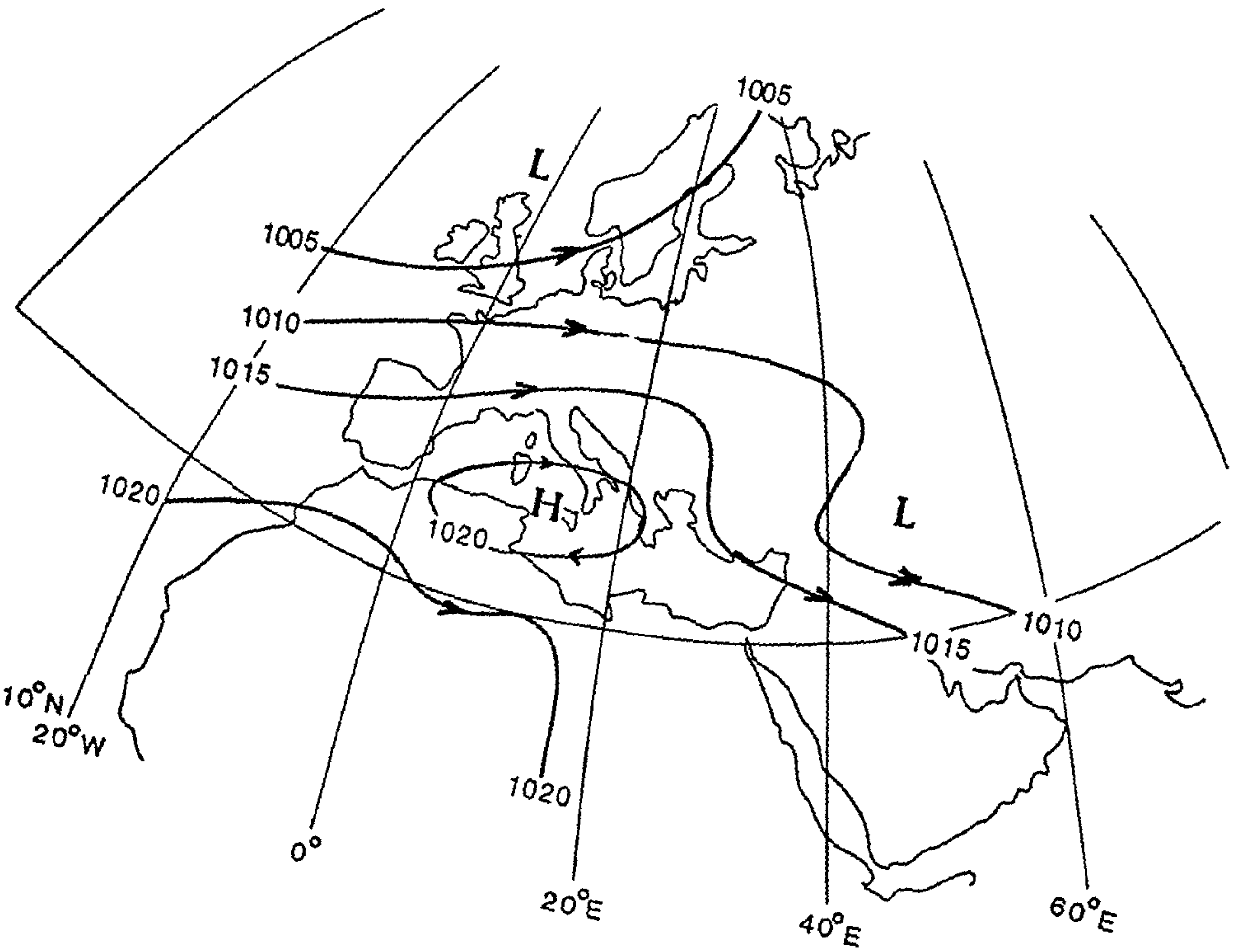

Fig. 6 - Synoptic weather pattern type E

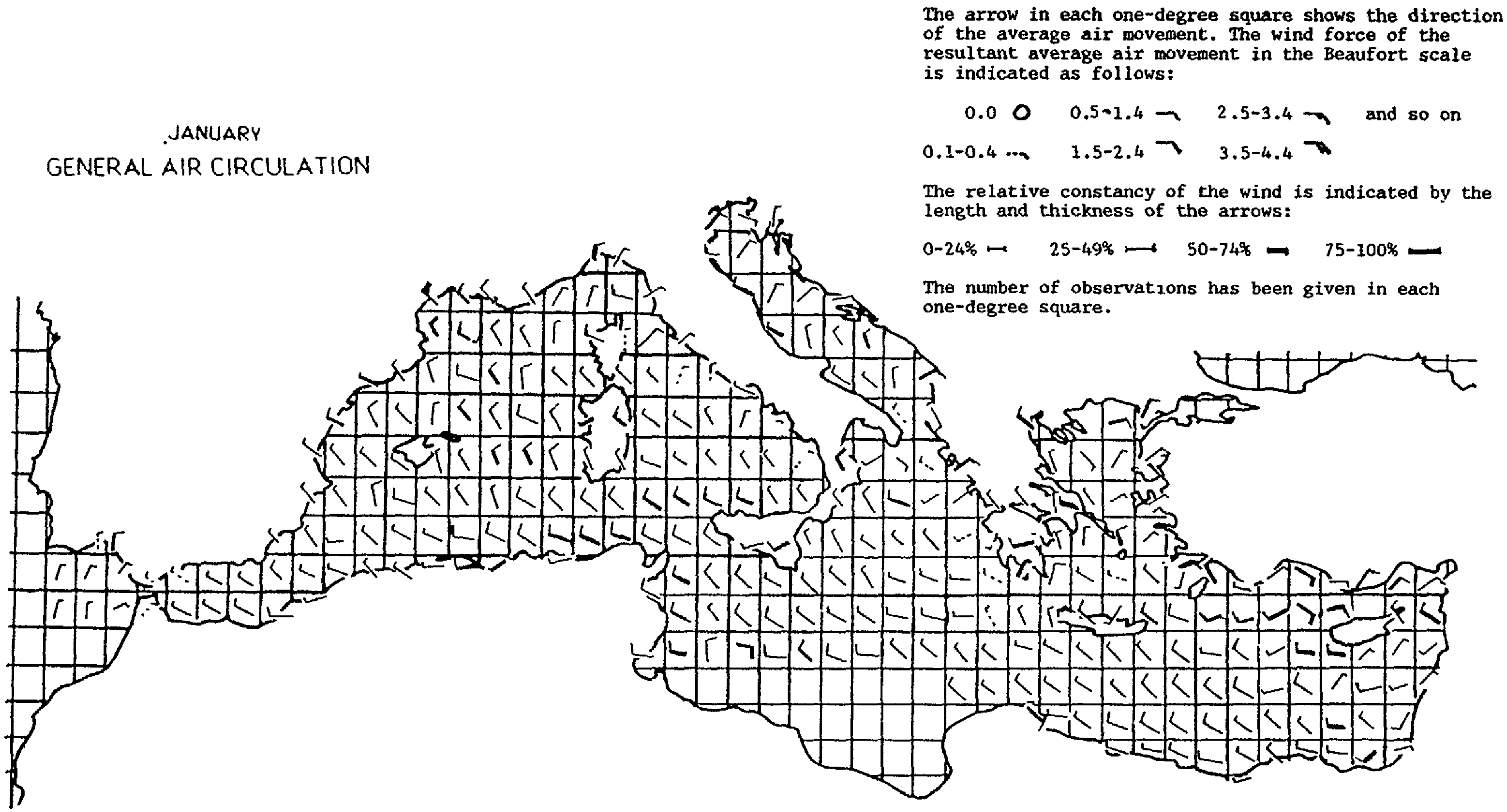

Fig. 7 - Vectorial monthly surface winds (10 m a.s.l.) January

FEBRUARY

GENERAL AIR CIRCULATION

The arrow in each one-degree square shows the direction of the average air movement. The wind force of the resultant average air movement in the Beaufort scale is indicated as follows:

0.0 O   0.5-1.4   2.5-3.4   and so on

0.1-0.4   1.5-2.4   3.5-4.4

The relative constancy of the wind is indicated by the length and thickness of the arrows:

0-24%   25-49%   50-74%   75-100%

The number of observations has been given in each one-degree square.

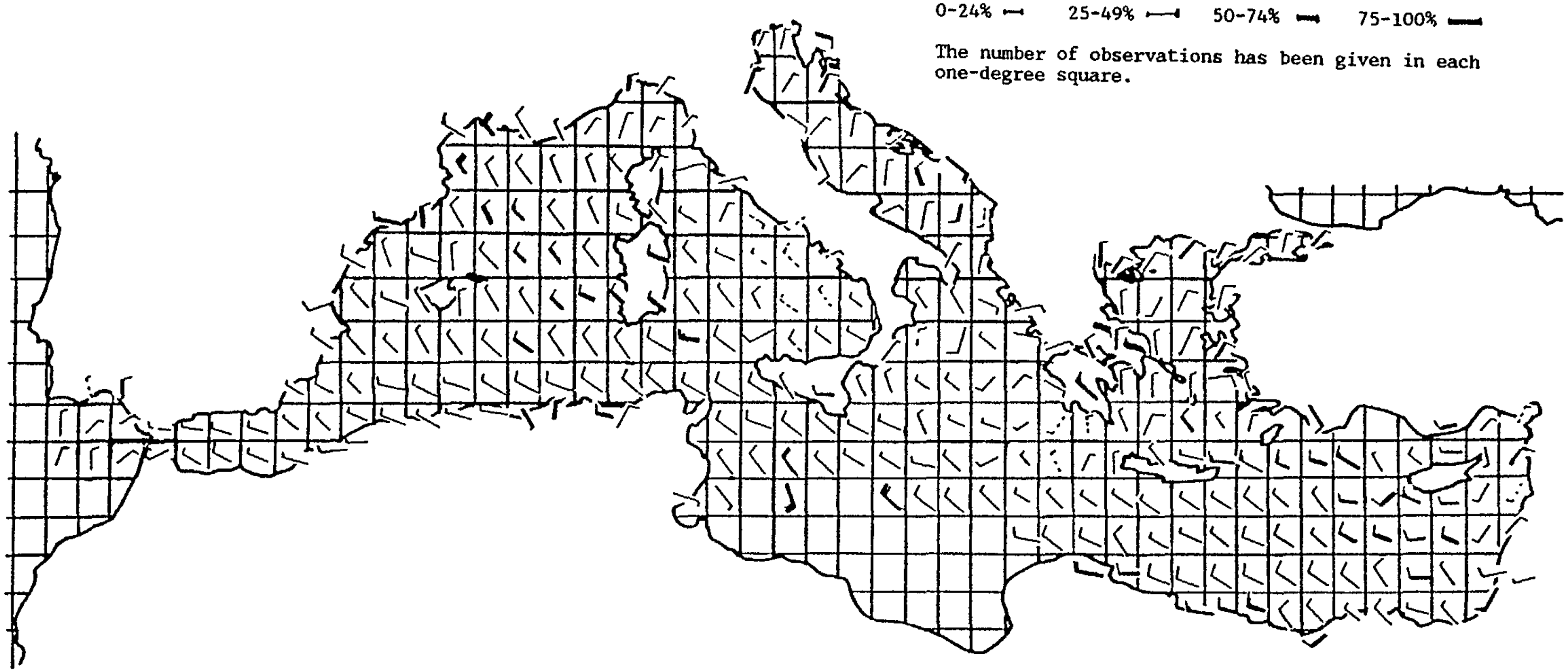

Fig. 8 - Vectorial monthly surface winds (10 m a.s.l) February

MARCH

GENERAL AIR CIRCULATION

The arrow in each one-degree square shows the direction of the average air movement. The wind force of the resultant average air movement in the Beaufort scale is indicated as follows:

0.0 ○ 0.5-1.4 2.5-3.4 and so on

0.1-0.4 1.5-2.4 3.5-4.4

The relative constancy of the wind is indicated by the length and thickness of the arrows:

0-24% 25-49% 50-74% 75-100%

The number of observations has been given in each one-degree square.

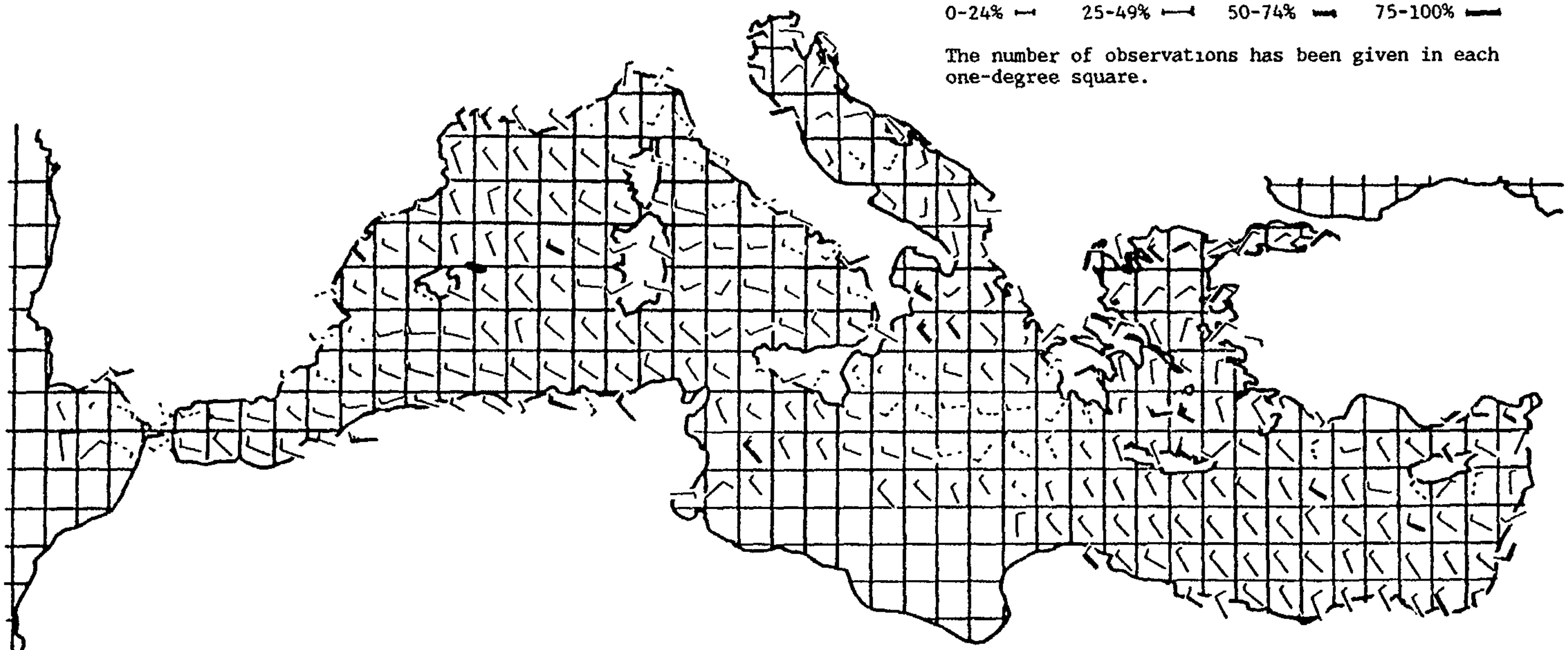

Fig. 9 - Vectorial monthly surface winds (10 m a.s.l) March

APRIL
GENERAL AIR CIRCULATION

The arrow in each one-degree square shows the direction of the average air movement. The wind force of the resultant average air movement in the Beaufort scale is indicated as follows:

0.0 ○ 0.5-1.4 ⌐ 2.5-3.4 ⌐ and so on

0.1-0.4 ⌐ 1.5-2.4 ⌐ 3.5-4.4 ⌐

The relative constancy of the wind is indicated by the length and thickness of the arrows:

0-24% ⟝ 25-49% ⟝ 50-74% ⟝ 75-100% ⟝

The number of observations has been given in each one-degree square.

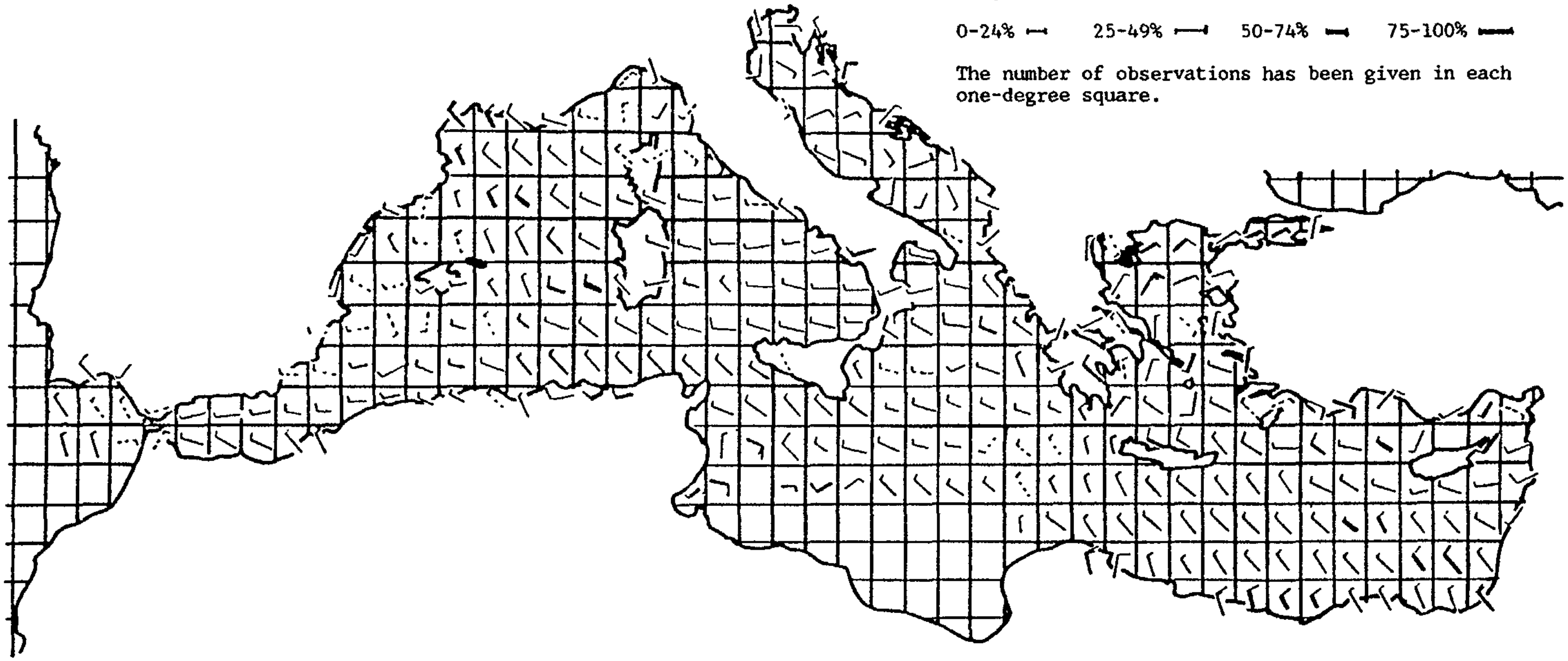

Fig. 10 - Vectorial monthly surface winds (10 m a.s.l) April

MAY
GENERAL AIR CIRCULATION

The arrow in each one-degree square shows the direction of the average air movement. The wind force of the resultant average air movement in the Beaufort scale is indicated as follows:

0.0 ○ 0.5-1.4 2.5-3.4 and so on

0.1-0.4 1.5-2.4 3.5-4.4

The relative constancy of the wind is indicated by the length and thickness of the arrows:

0-24% 25-49% 50-74% 75-100%

The number of observations has been given in each one-degree square.

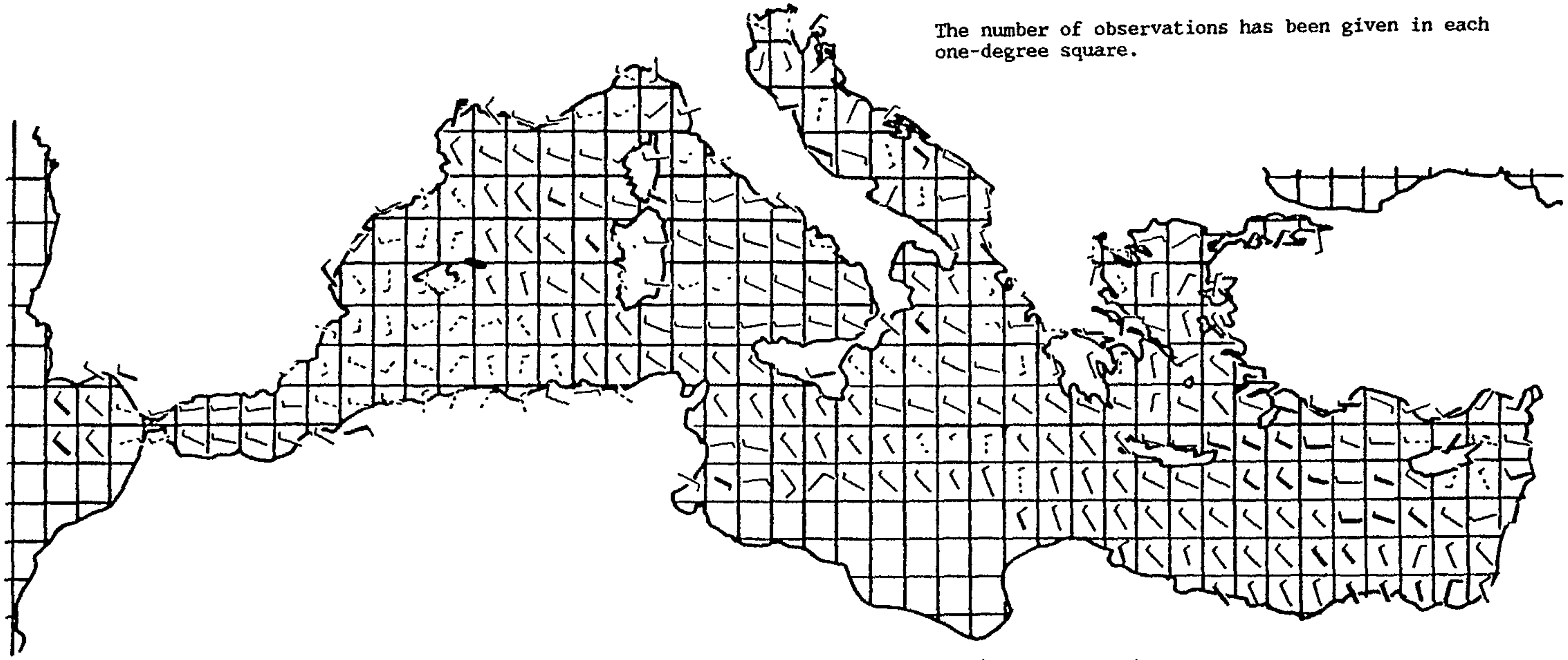

Fig. 11 - Vectorial monthly surface winds (10 m a.s.l) May

JUNE
GENERAL AIR CIRCULATION

The arrow in each one-degree square shows the direction of the average air movement. The wind force of the resultant average air movement in the Beaufort scale is indicated as follows:

0.0 O   0.5-1.4   2.5-3.4   and so on

0.1-0.4   1.5-2.4   3.5-4.4

The relative constancy of the wind is indicated by the length and thickness of the arrows:

0-24%   25-49%   50-74%   75-100%

The number of observations has been given in each one-degree square.

Fig. 12 - Vectorial monthly surface winds (10 m a.s.l) June

JULY
GENERAL AIR CIRCULATION

The arrow in each one-degree square shows the direction of the average air movement. The wind force of the resultant average air movement in the Beaufort scale is indicated as follows:

0.0 O   0.5-1.4   2.5-3.4   and so on

0.1-0.4   1.5-2.4   3.5-4.4

The relative constancy of the wind is indicated by the length and thickness of the arrows:

0-24%   25-49%   50-74%   75-100%

The number of observations has been given in each one-degree square.

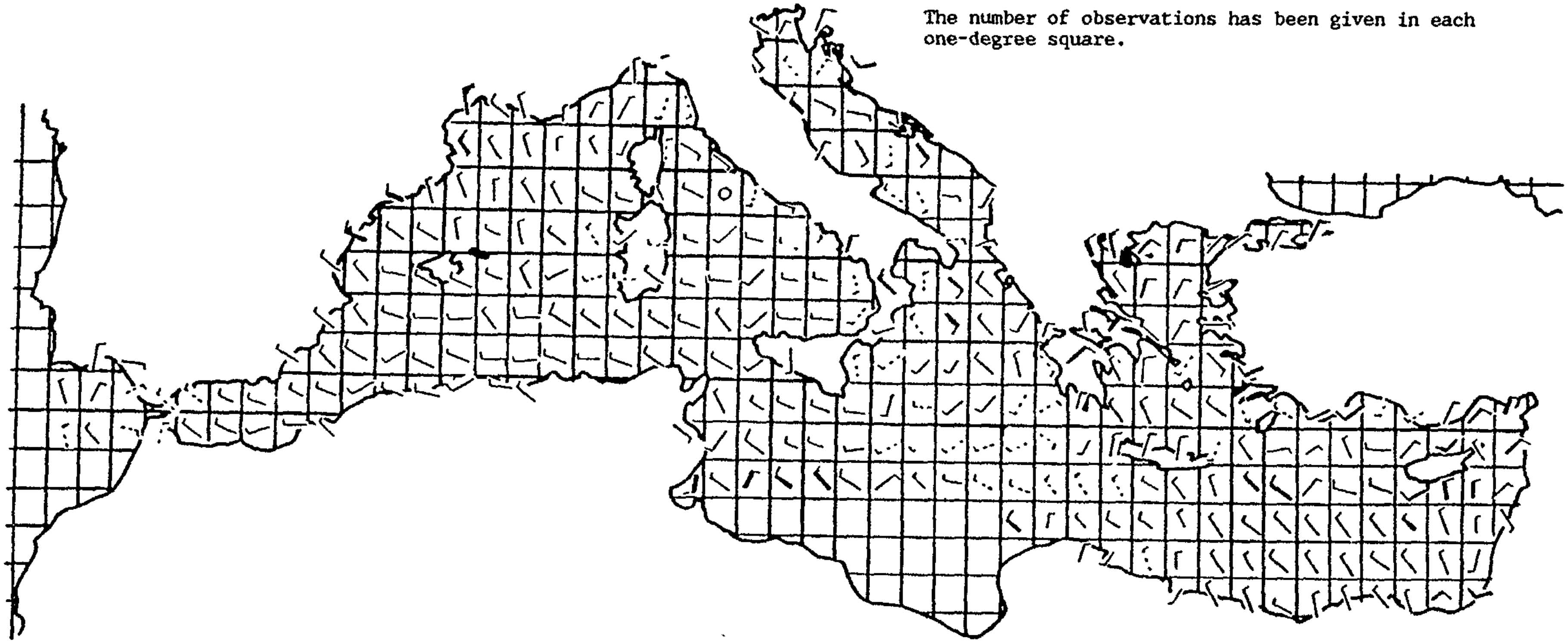

Fig. 13 - Vectorial monthly surface winds (10 m a.s.l) July

AUGUST
GENERAL AIR CIRCULATION

The arrow in each one-degree square shows the direction of the average air movement. The wind force of the resultant average air movement in the Beaufort scale is indicated as follows:

0.0   0.5-1.4   2.5-3.4   and so on

0.1-0.4   1.5-2.4   3.5-4.4

The relative constancy of the wind is indicated by the length and thickness of the arrows:

0-24%   25-49%   50-74%   75-100%

The number of observations has been given in each one-degree square.

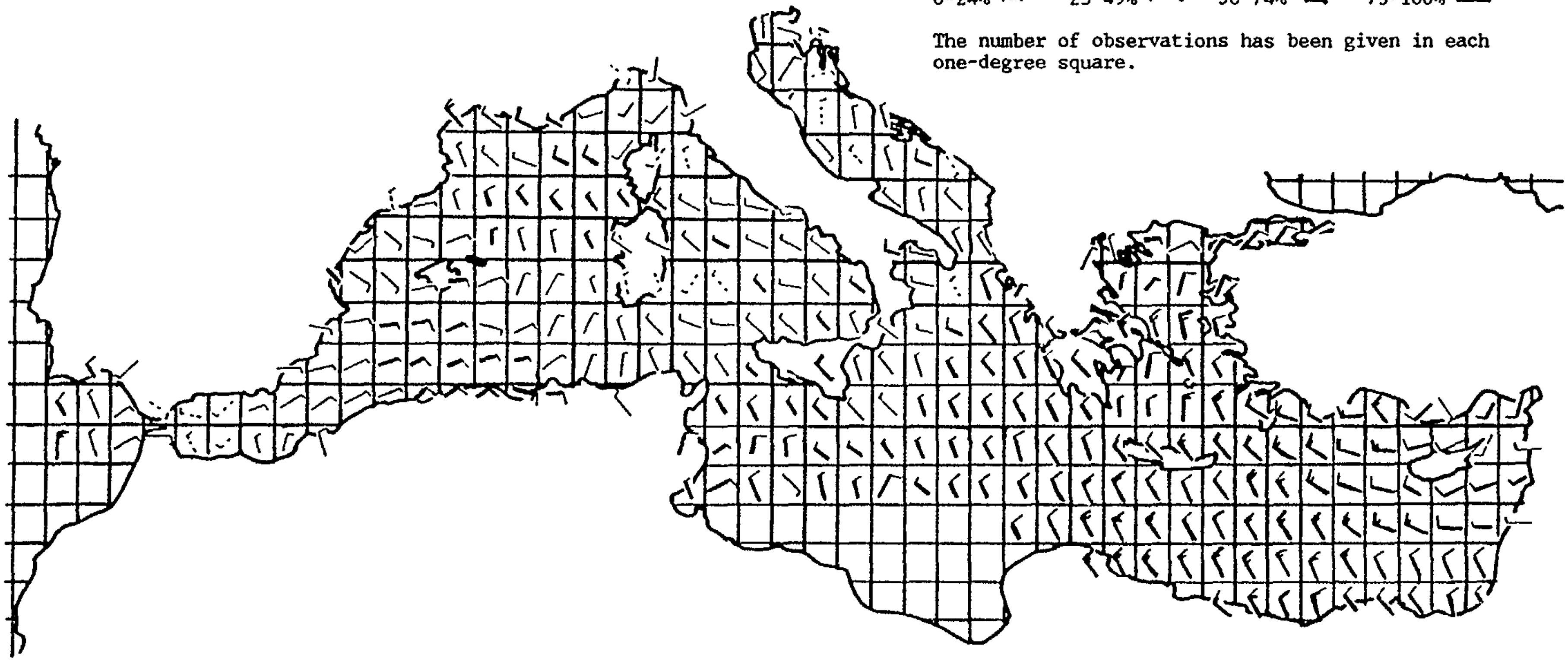

Fig. 14 - Vectorial montnly surface winds (10 m a.s.1 August

SEPTEMBER
GENERAL AIR CIRCULATION

The arrow in each one-degree square shows the direction of the average air movement. The wind force of the resultant average air movement in the Beaufort scale is indicated as follows:

0.0 O 0.5-1.4 2.5-3.4 and so on

0.1-0.4 1.5-2.4 3.5-4.4

The relative constancy of the wind is indicated by the length and thickness of the arrows:

0-24% 25-49% 50-74% 75-100%

The number of observations has been given in each one-degree square.

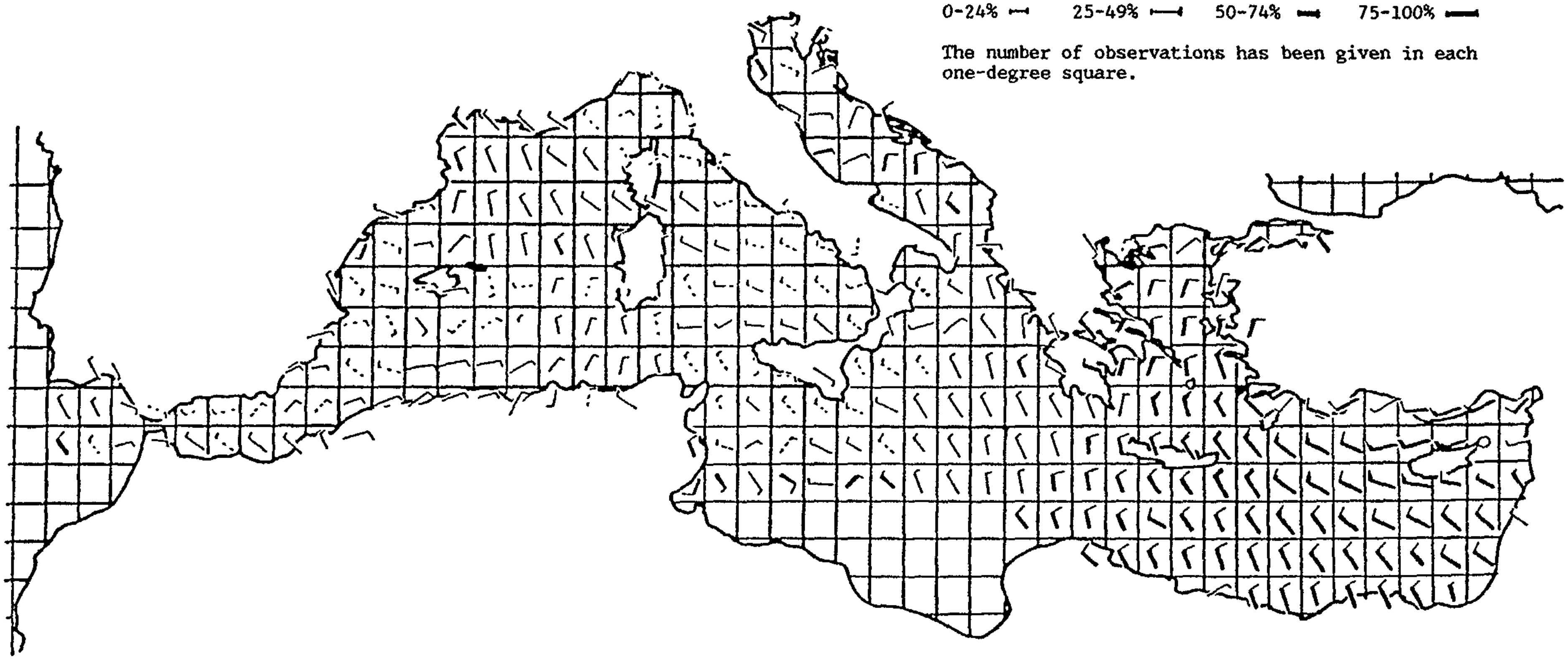

Fig. 15 - Vectorial monthly surface winds (10 m a.s.l) Septemoer

OCTOBER
GENERAL AIR CIRCULATION

The arrow in each one-degree square shows the direction of the average air movement. The wind force of the resultant average air movement in the Beaufort scale is indicated as follows:

0.0 O 0.5-1.4 2.5-3.4 and so on

0.1-0.4 1.5-2.4 3.5-4.4

The relative constancy of the wind is indicated by the length and thickness of the arrows:

0-24% 25-49% 50-74% 75-100%

The number of observations has been given in each one-degree square.

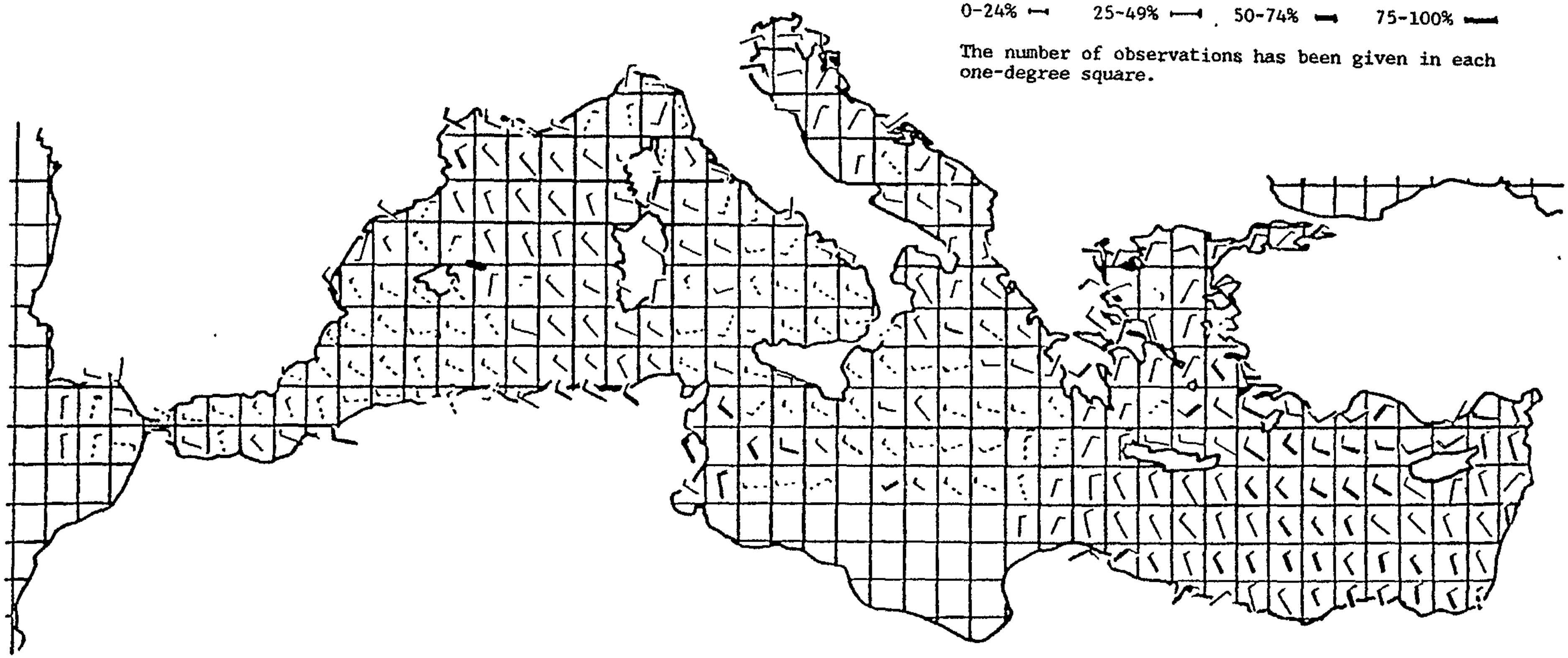

Fig. 16 - Vectorial monthly surface winds (10 m a.s.l) October

NOVEMBER
GENERAL AIR CIRCULATION

The arrow in each one-degree square shows the direction of the average air movement. The wind force of the resultant average air movement in the Beaufort scale is indicated as follows:

0.0 ○ 0.5-1.4 2.5-3.4 and so on

0.1-0.4 1.5-2.4 3.5-4.4

The relative constancy of the wind is indicated by the length and thickness of the arrows:

0-24% 25-49% 50-74% 75-100%

The number of observations has been given in each one-degree square.

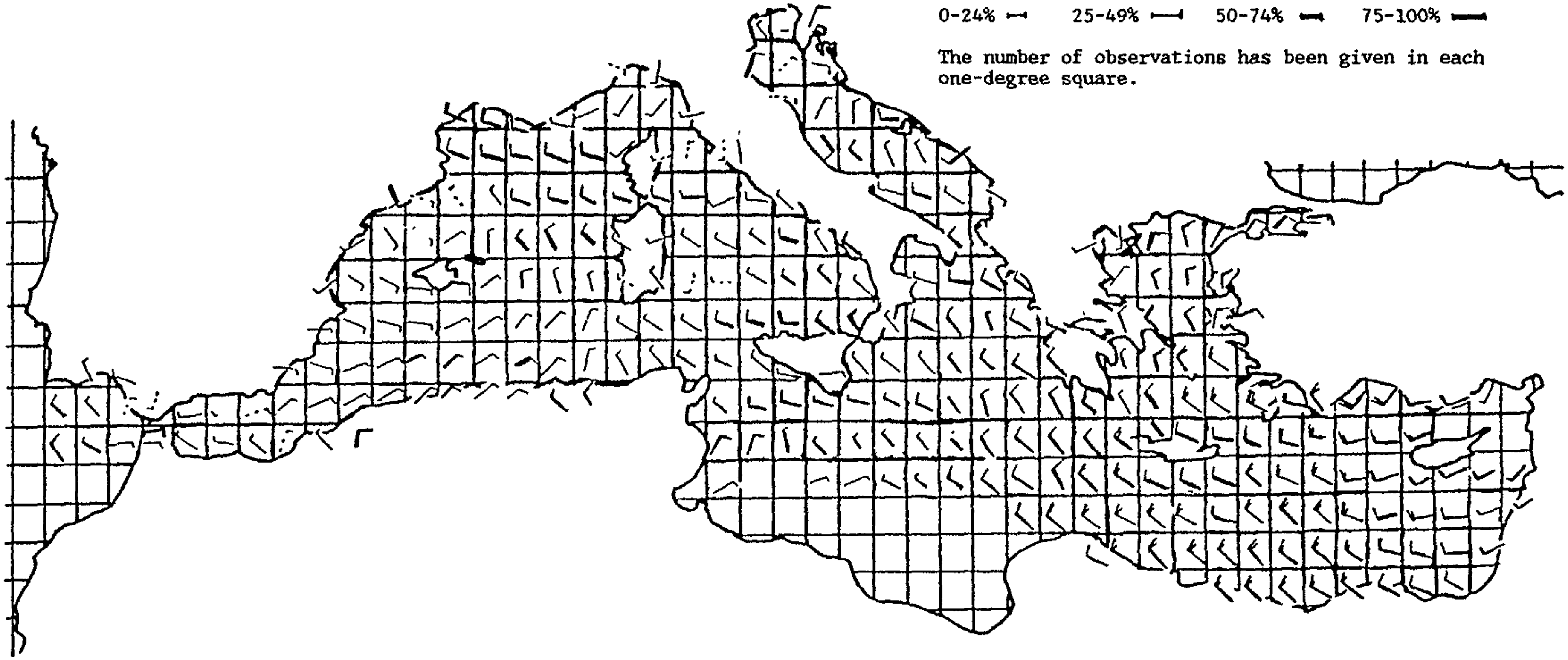

Fig. 17 - Vectorial monthly surface winds (10 m a.s.l) November

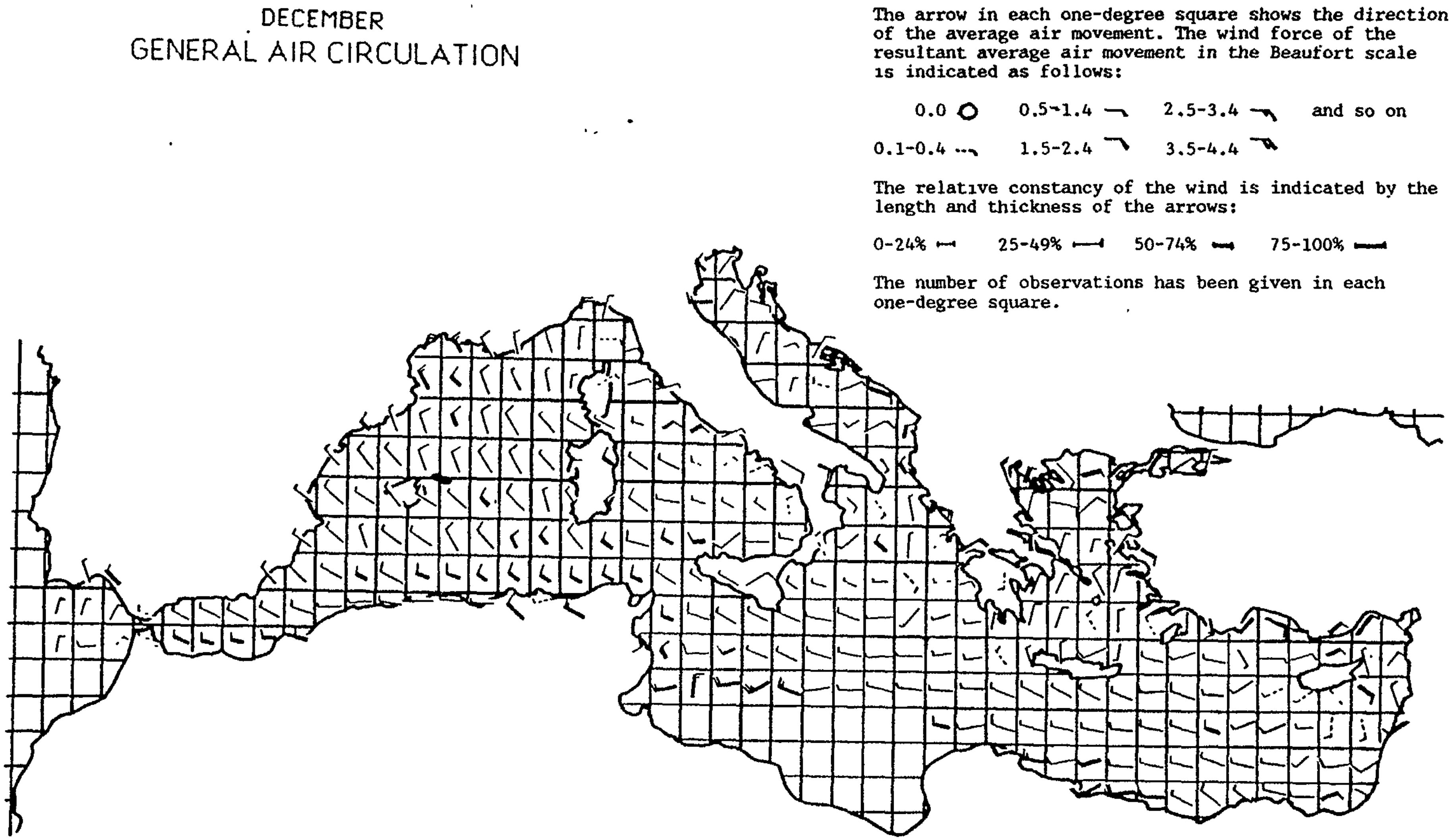

Fig. 18 - Vertical monthly surface winds (10 m a.s.l) December

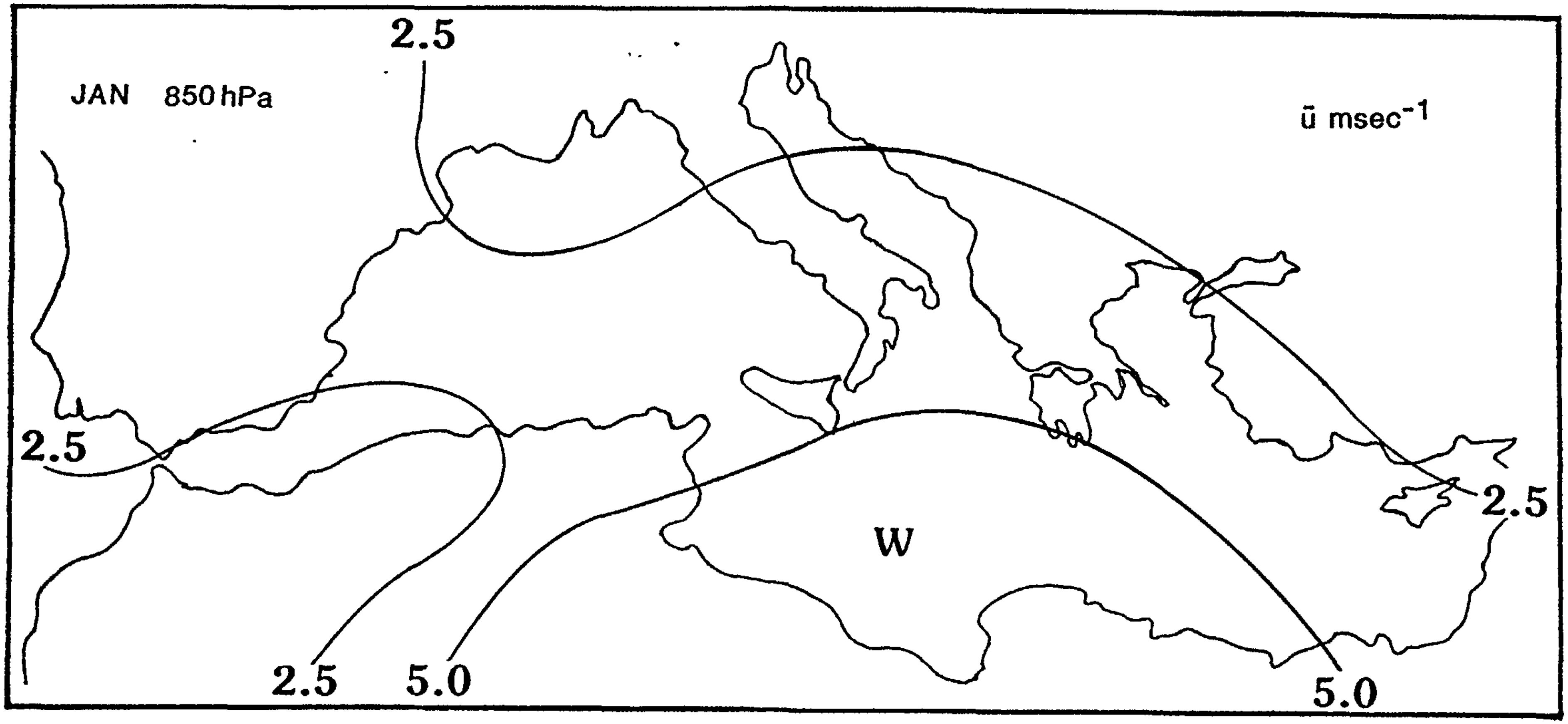

Fig. 19(a) - Mean zonal ($\bar{u}$) winds (m s^{-1}) at the 850 hPa level for January

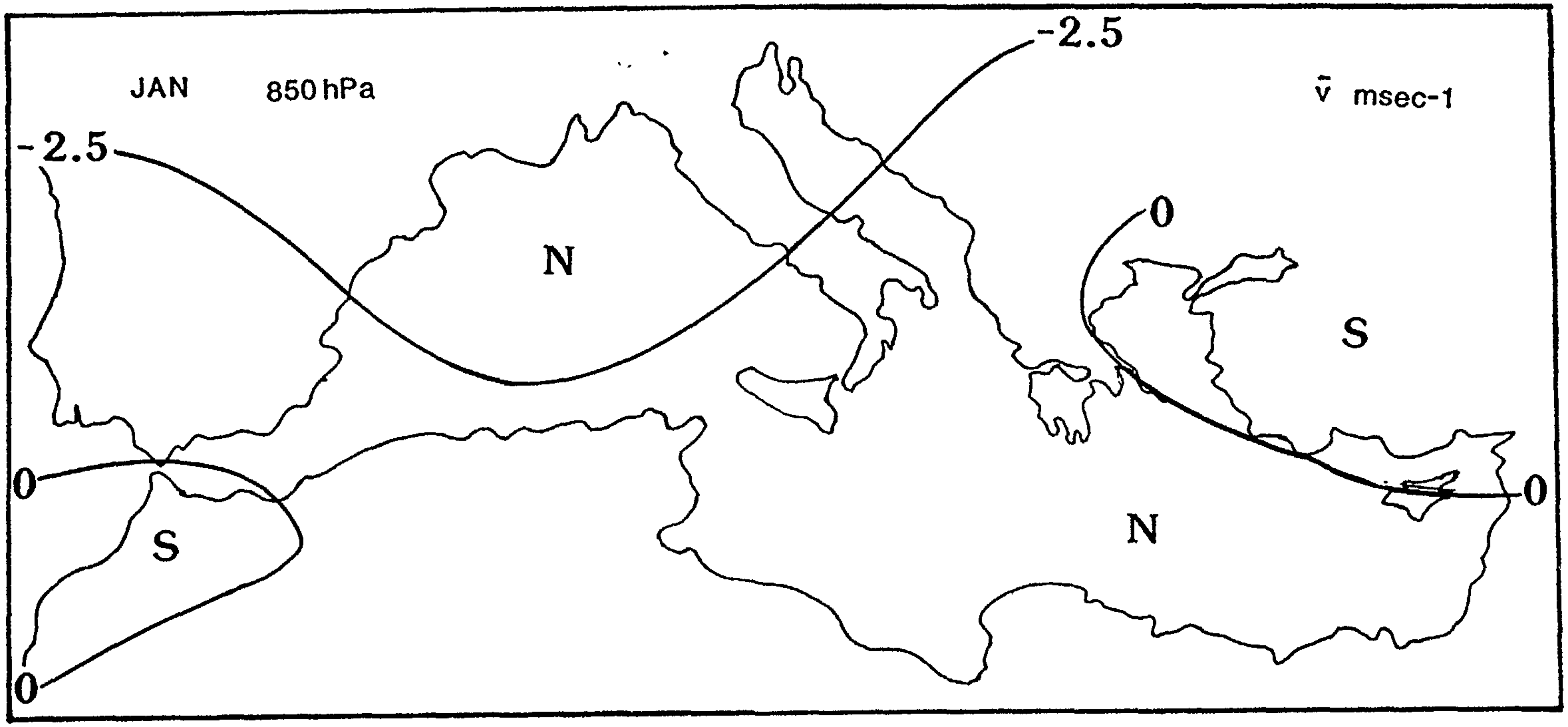

Fig. 19(b) - Mean meridional ($\acute{v}$) winds ($m\ s^{-1}$) at the 850 hPa level for January

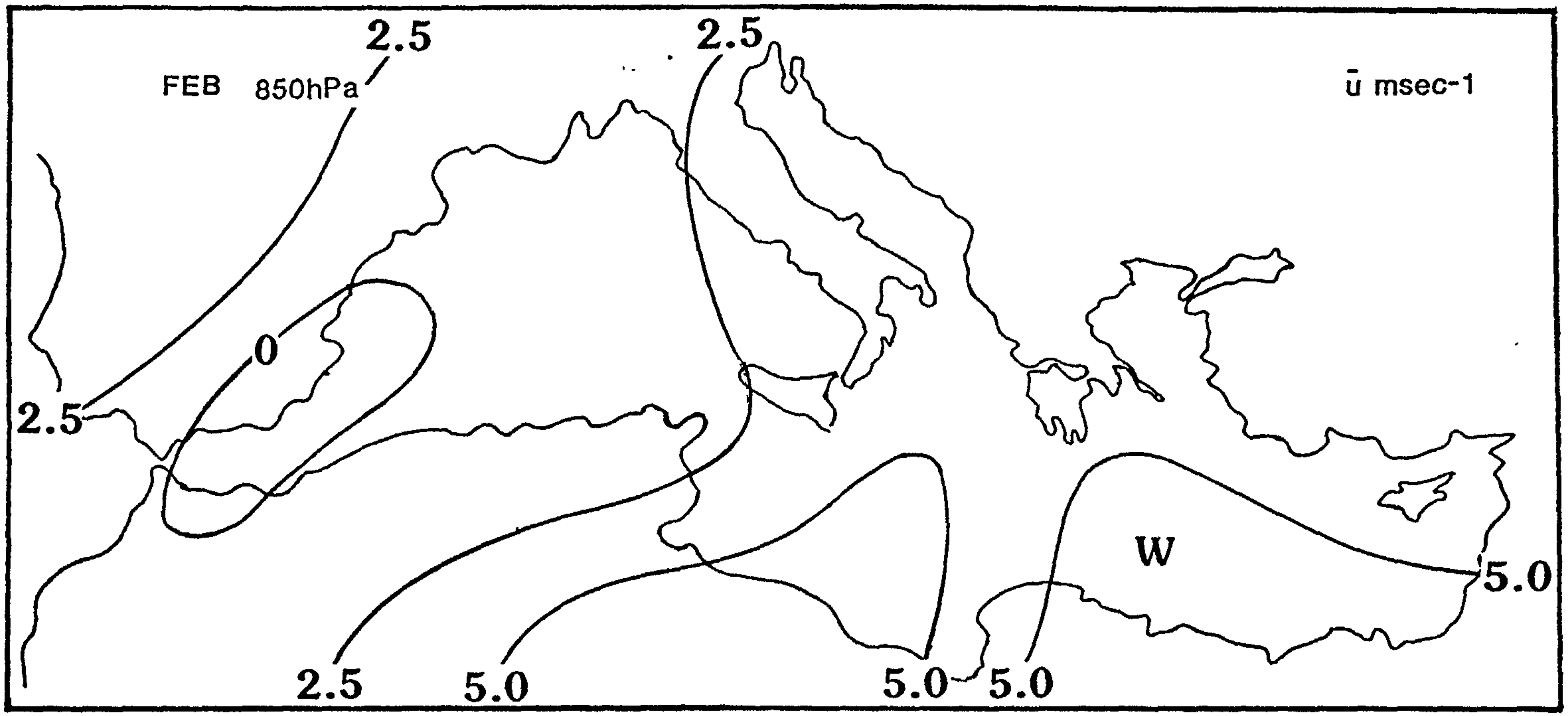

Fig. 20(a) - Mean zonal ($\bar{u}$) winds (m s^{-1}) at the 850 hPa level for February

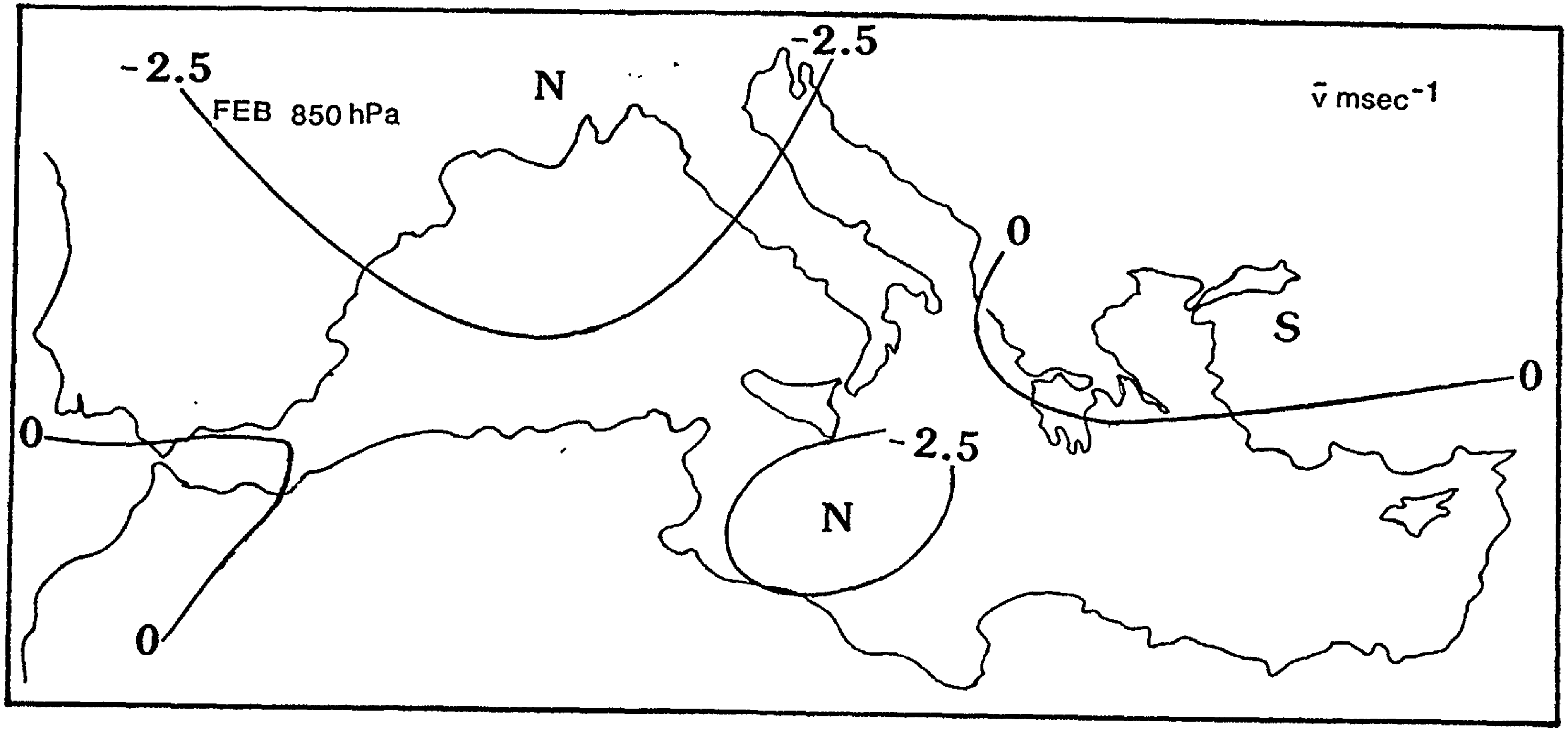

Fig. 20(b) - Mean meridional ($\bar{v}$) winds (m s^{-1}) at the 850 hPa level for February

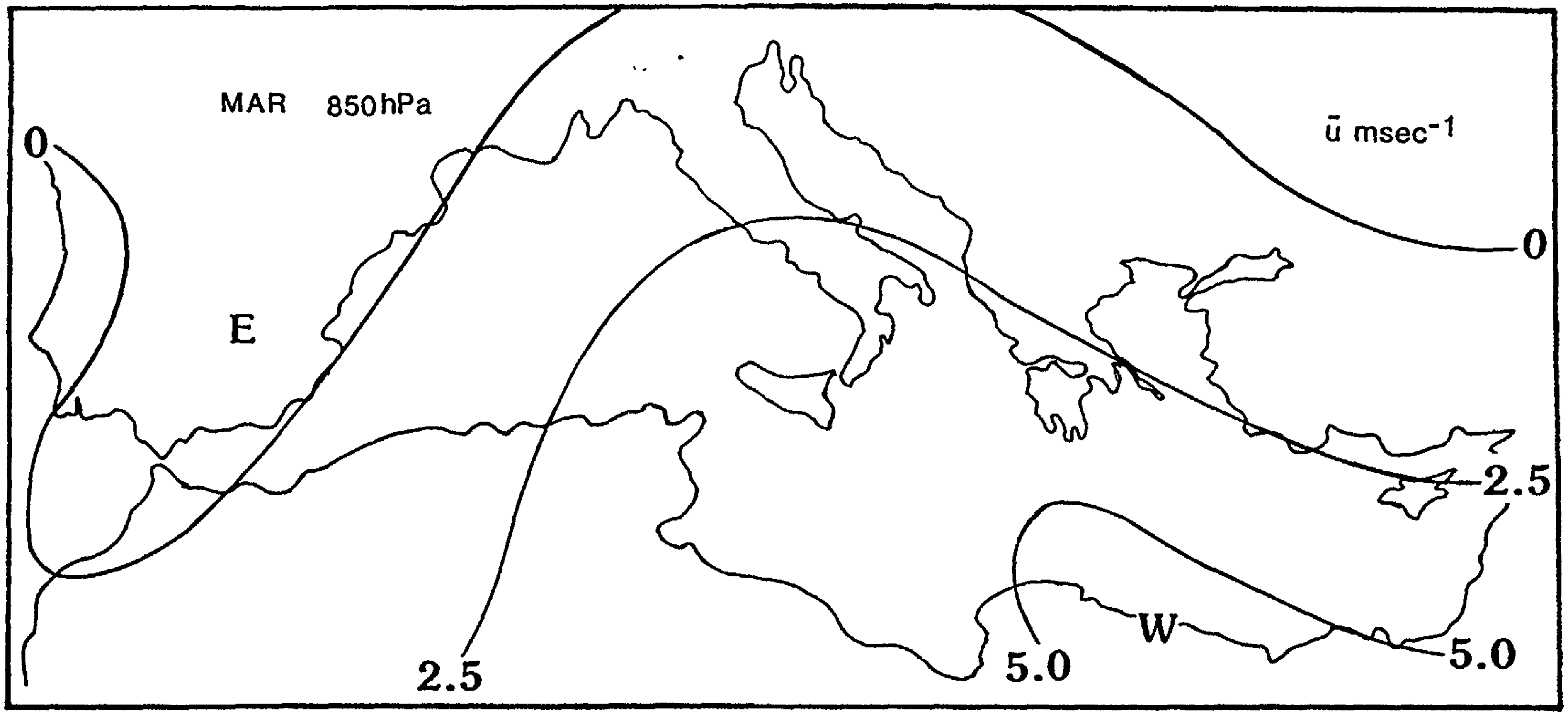

Fig. 21(a) - Mean zonal ($\bar{u}$) winds (m s^{-1}) at the 850 hPa level for March

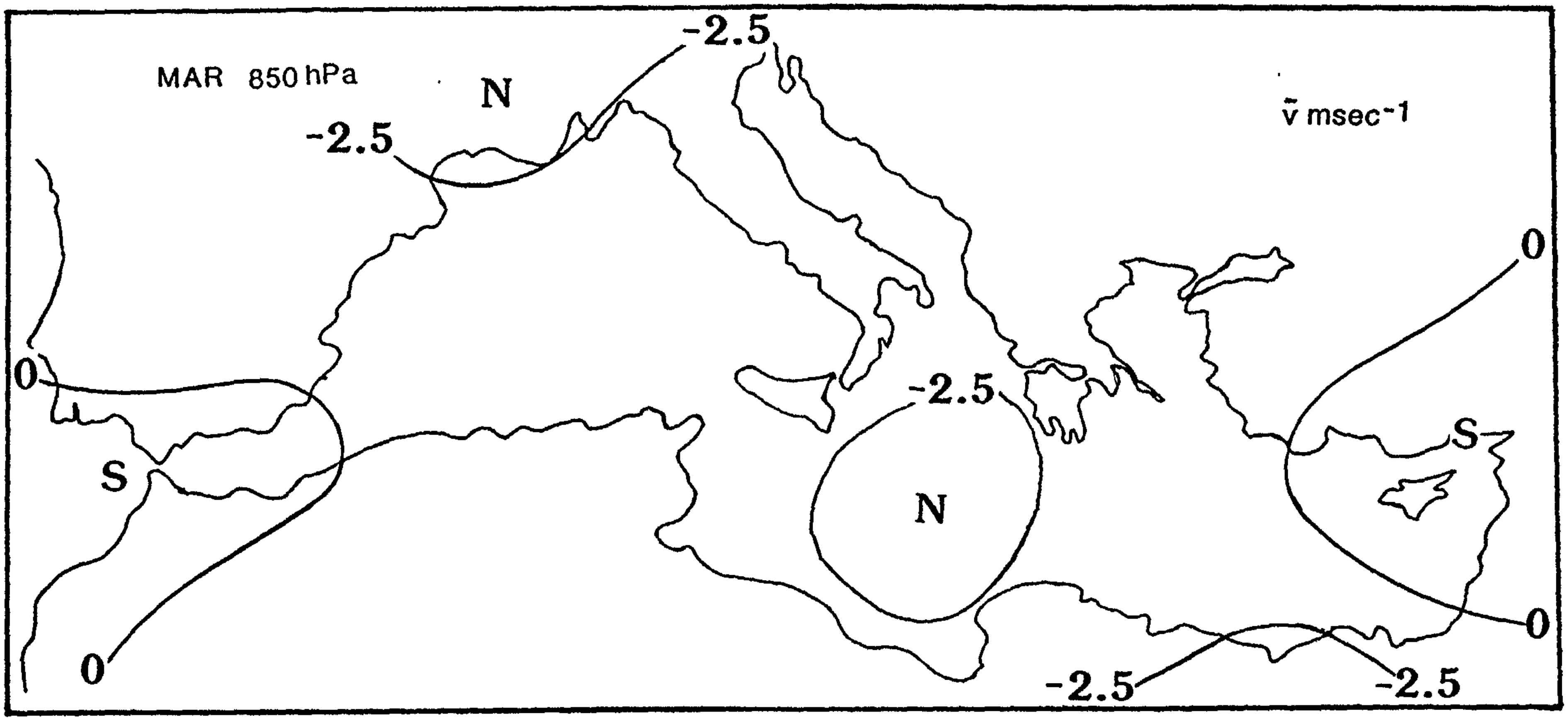

Fig. 21(b) - Mean meridional ($\bar{v}$) winds ($m\ s^{-1}$) at the 850 hPa level for March

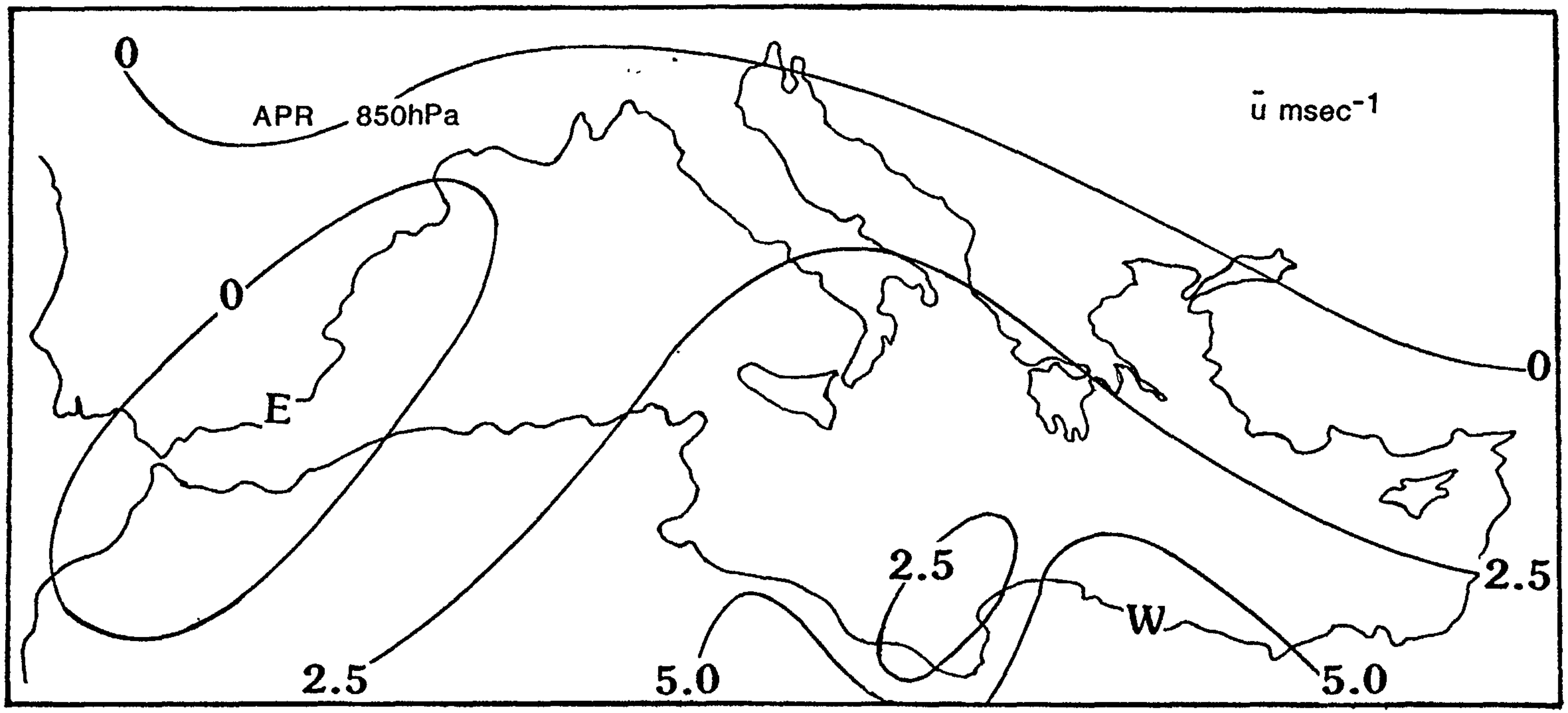

Fig. 22(a) - Mean zonal ($\bar{u}$) winds (m s^{-1}) at the 850 hPa level for April

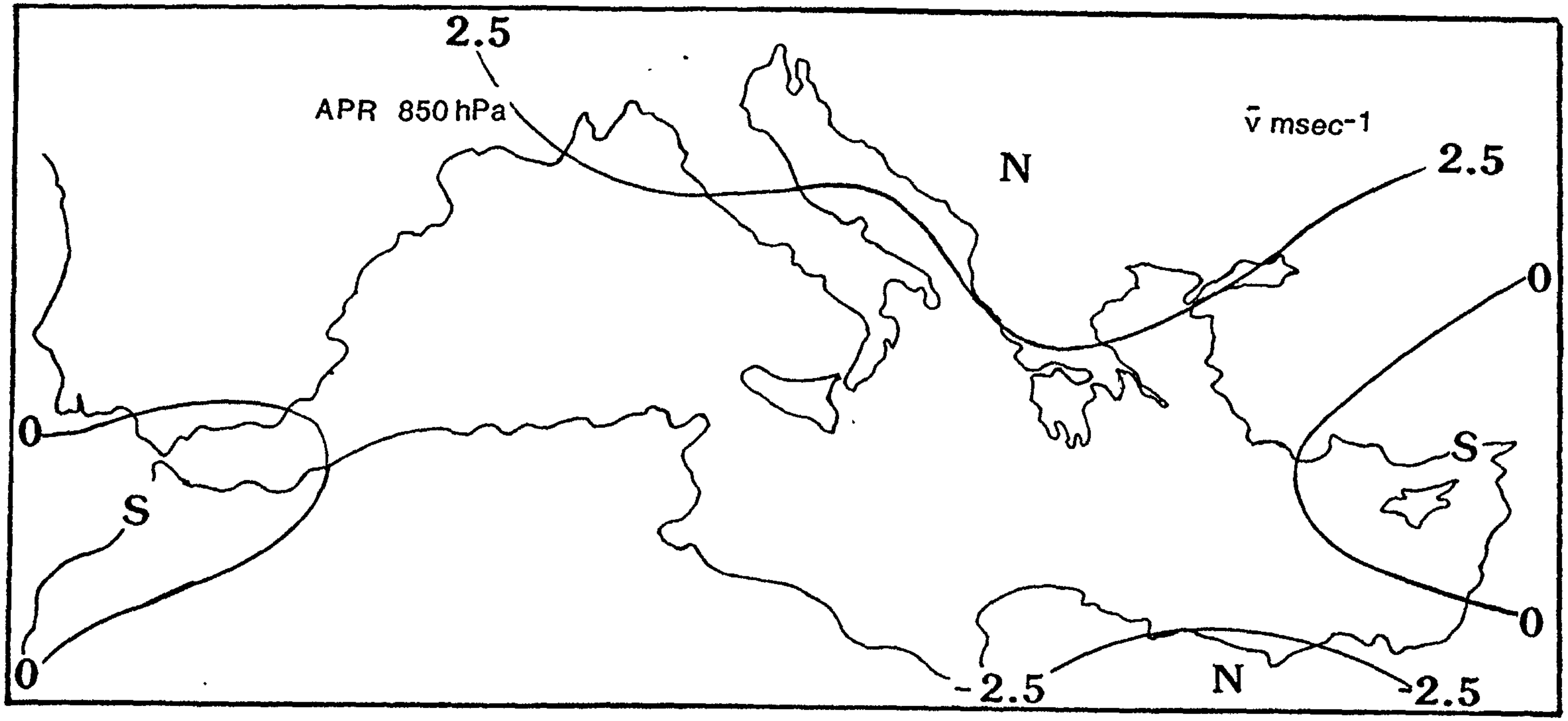

Fig. 22(b) - Mean meridional ($\bar{v}$) winds (m s^{-1}) at the 850 hPa level for April

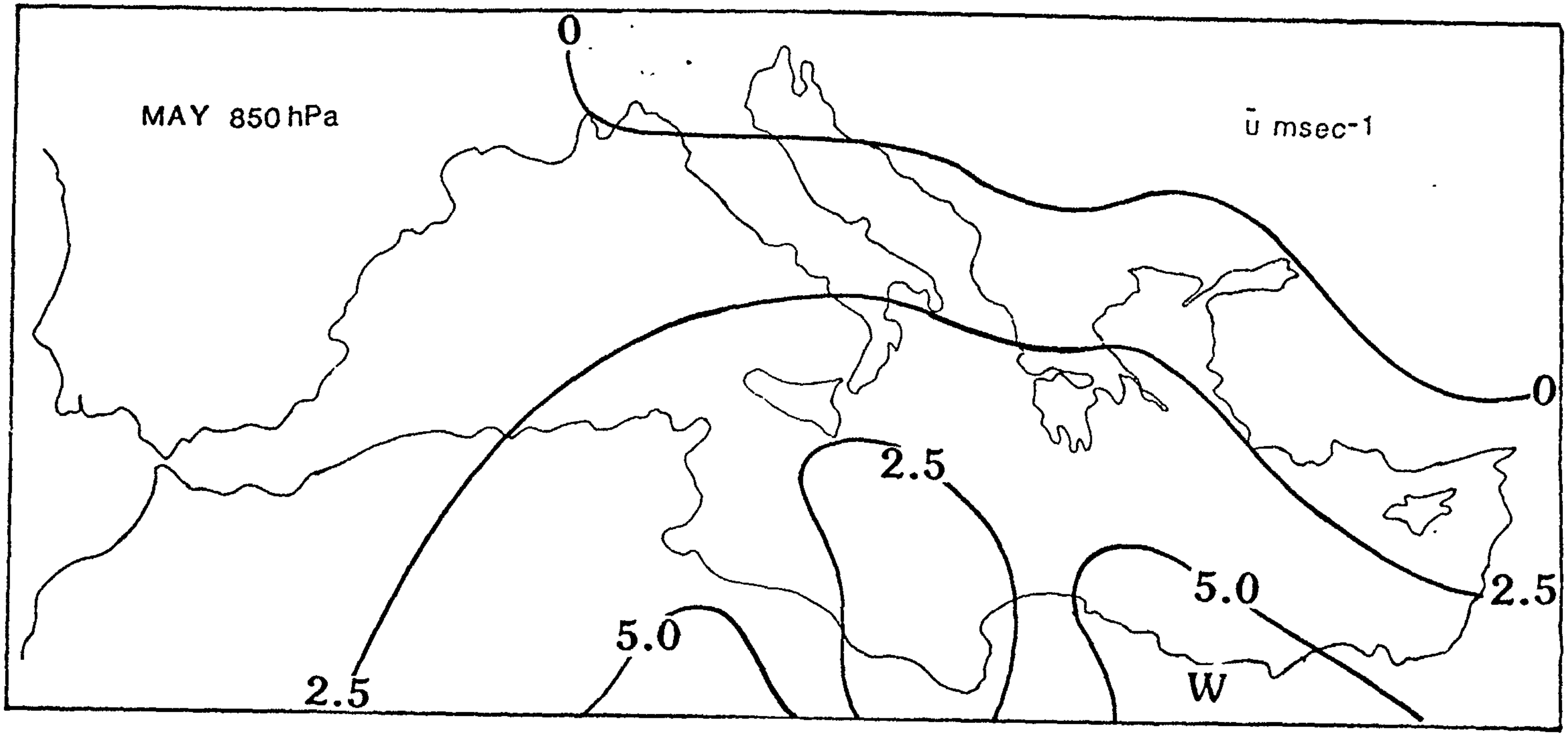

Fig. 23(a) - Mean zonal ($\bar{u}$) winds ($m\ s^{-1}$) at the 850 hPa level for May

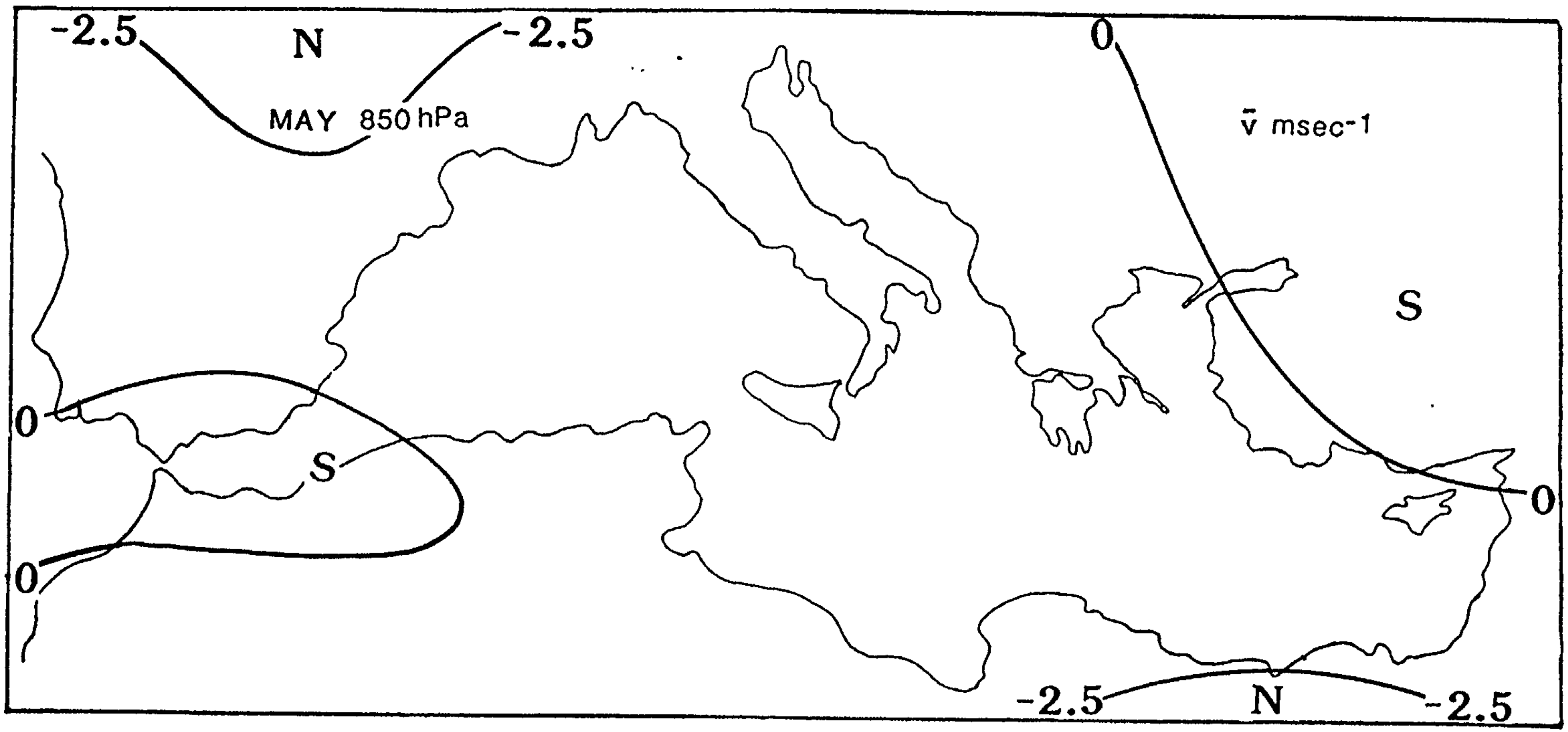

Fig. 23(b) - Mean meridional ($\bar{v}$) winds (m s^{-1}) at the 850 hPa level for May

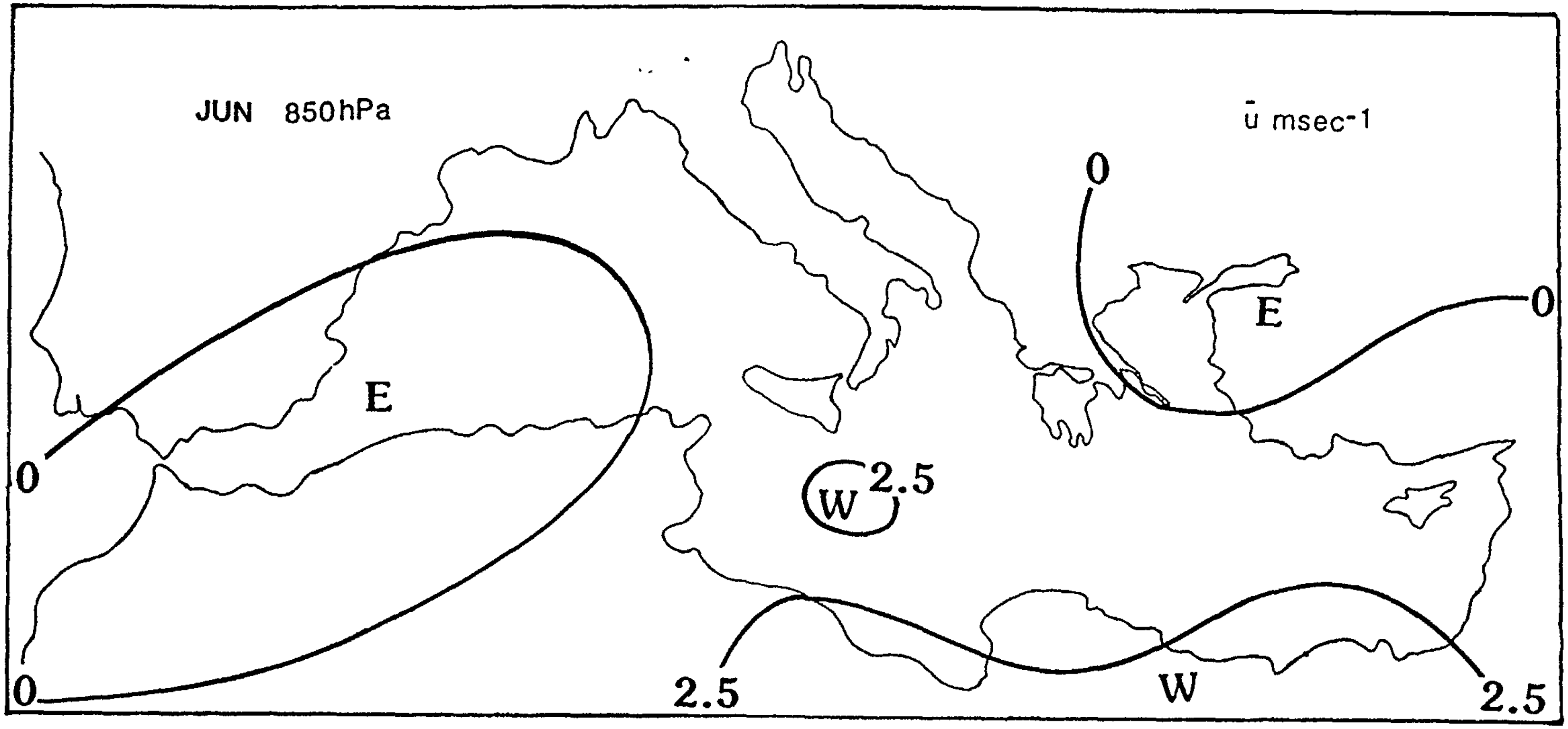

Fig. 24(a) - Mean zonal ($\bar{u}$) winds ($m\ s^{-1}$) at the 850 hPa level for June

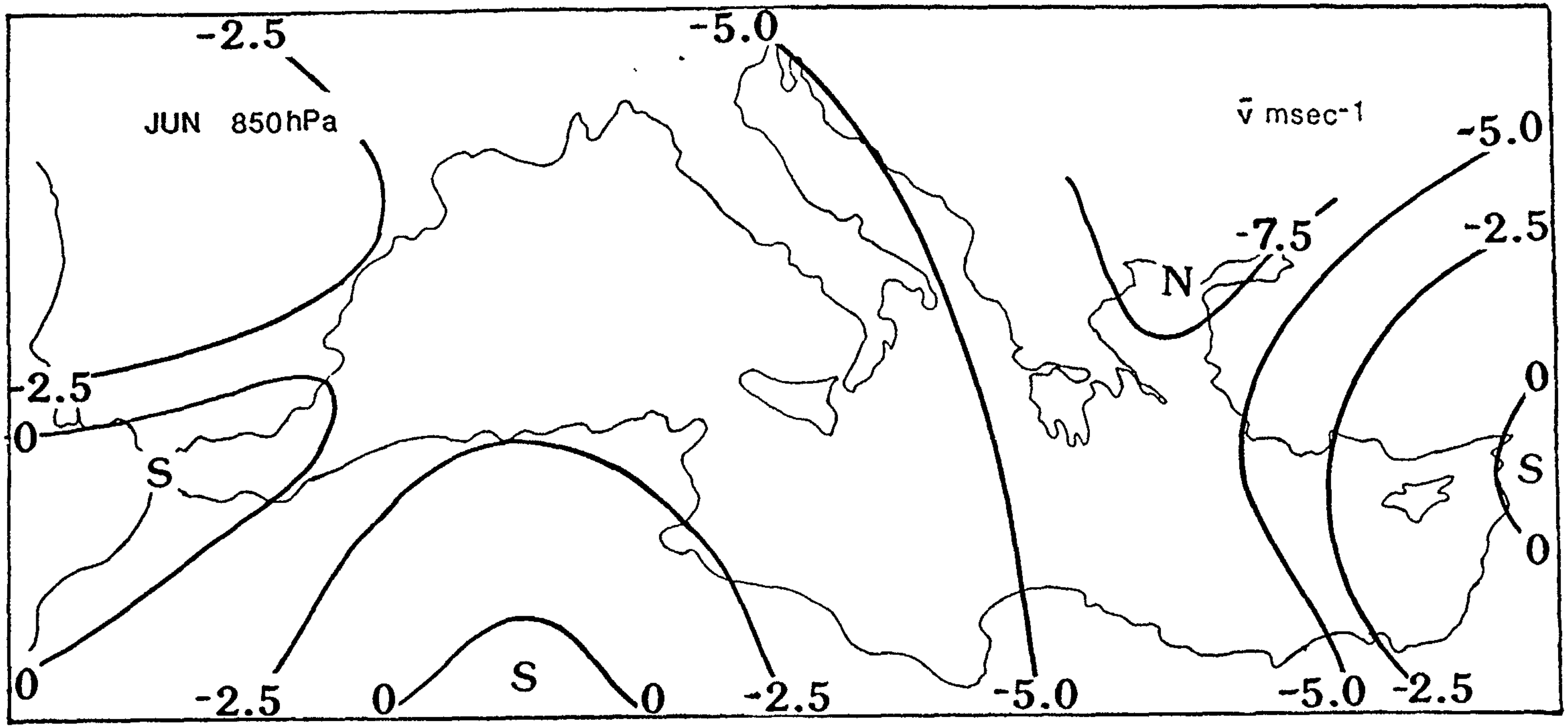

Fig. 24(b) - Mean meridional ($\bar{v}$) winds (m s^{-1}) at the 850 hPa level for June

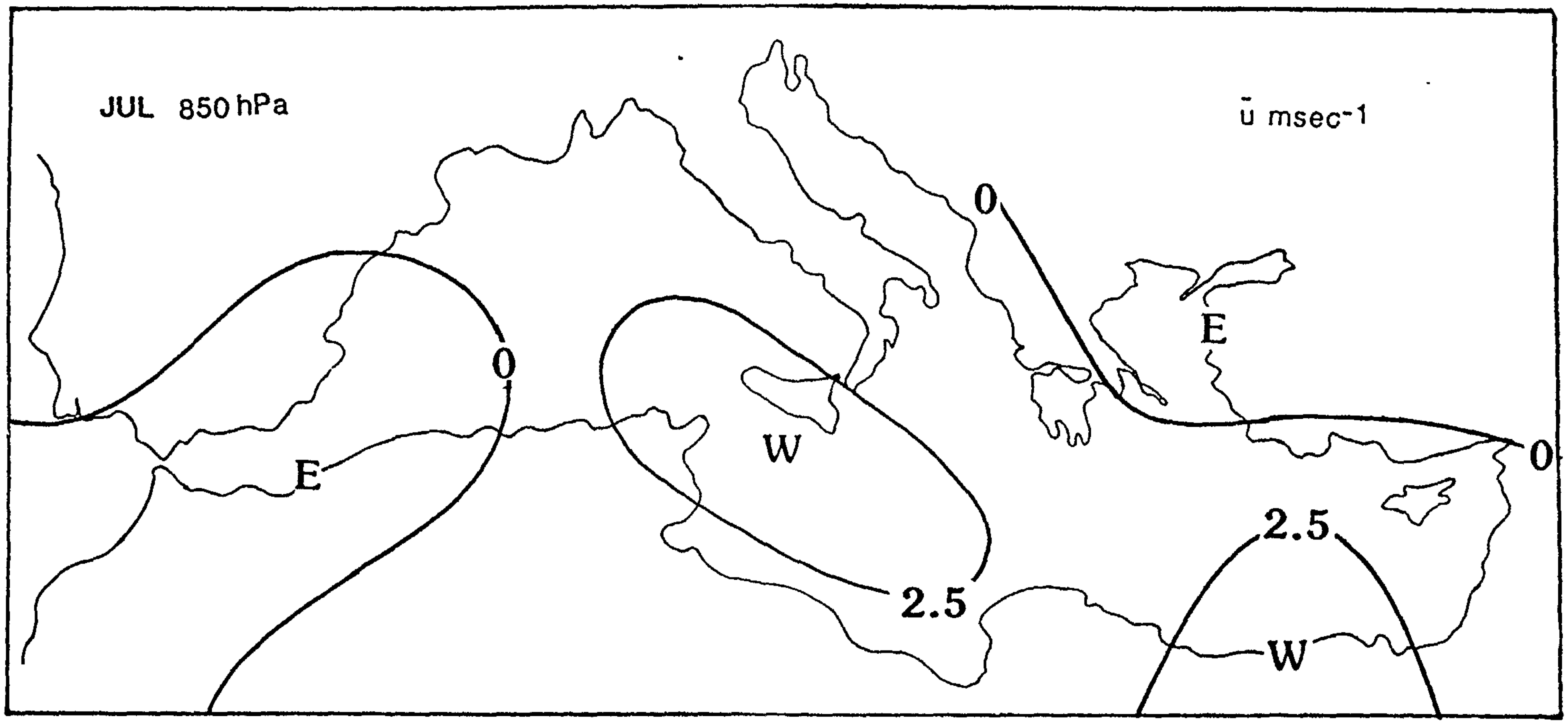

Fig. 25(a) - Mean zonal ($\bar{u}$) winds ($m\ s^{-1}$) at the 850 hPa level for July

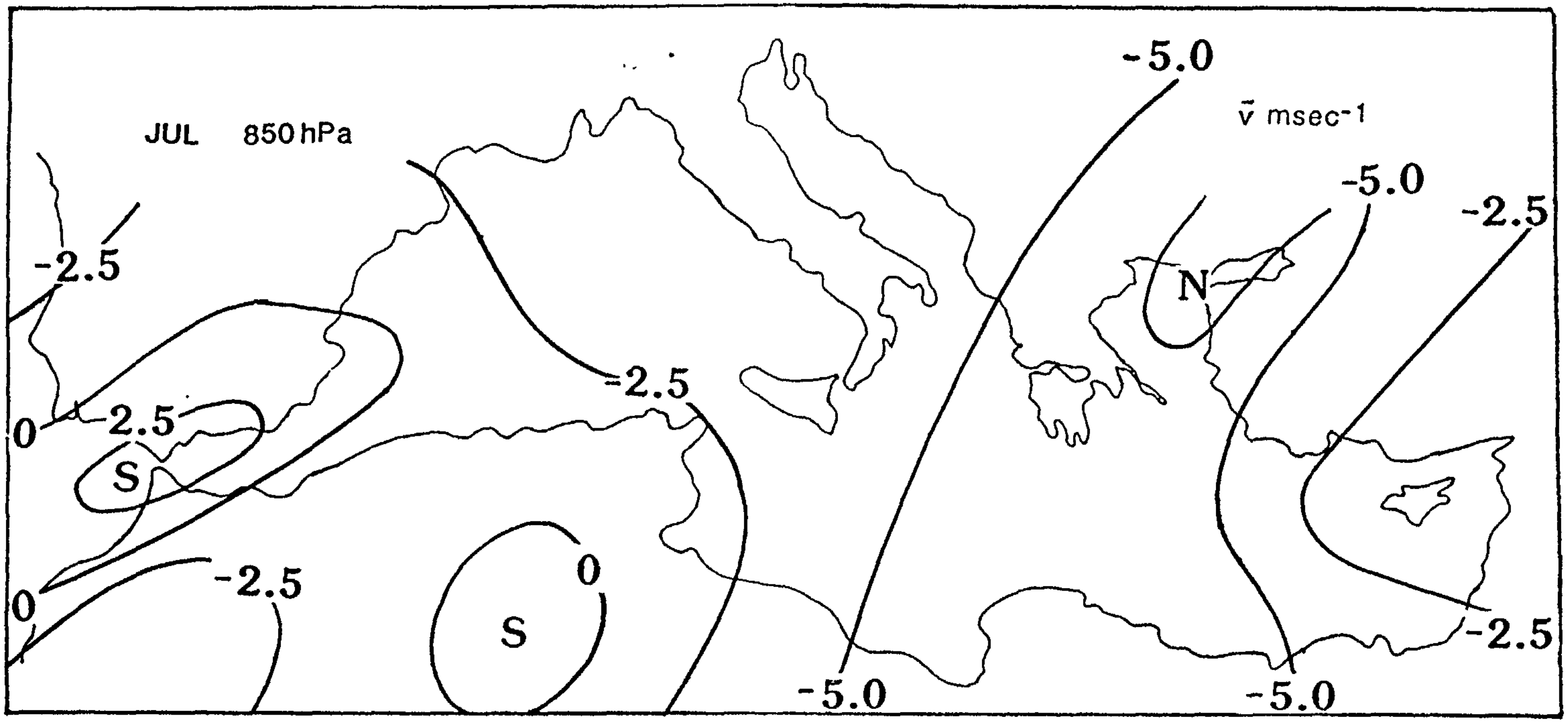

Fig. 25(b) - Mean meridional ($\bar{v}$) winds (m s^{-1}) at the 850 hPa level for July

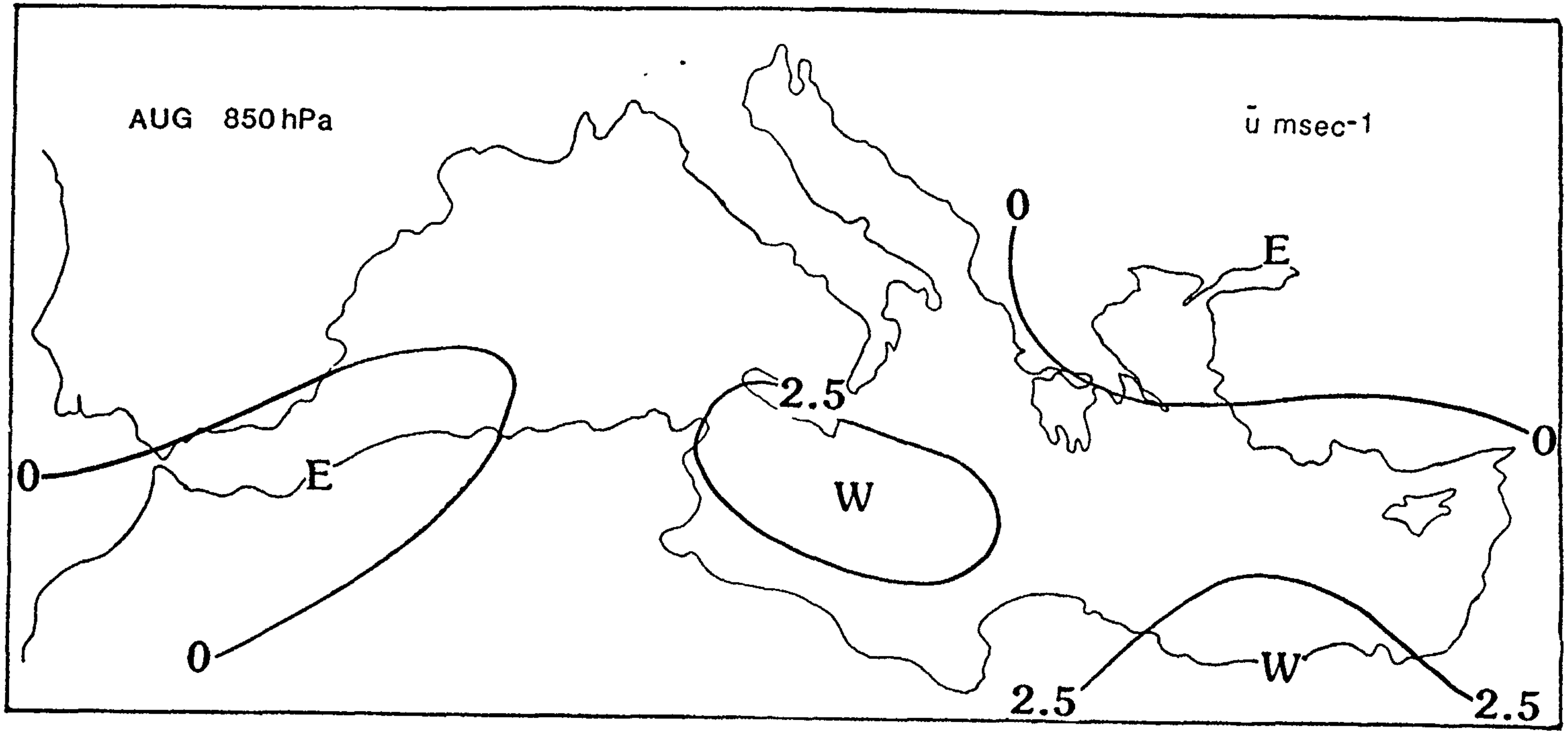

Fig. 26(a) - Mean zonal ($\bar{u}$) winds ($m\ s^{-1}$) at the 850 hPa level for August

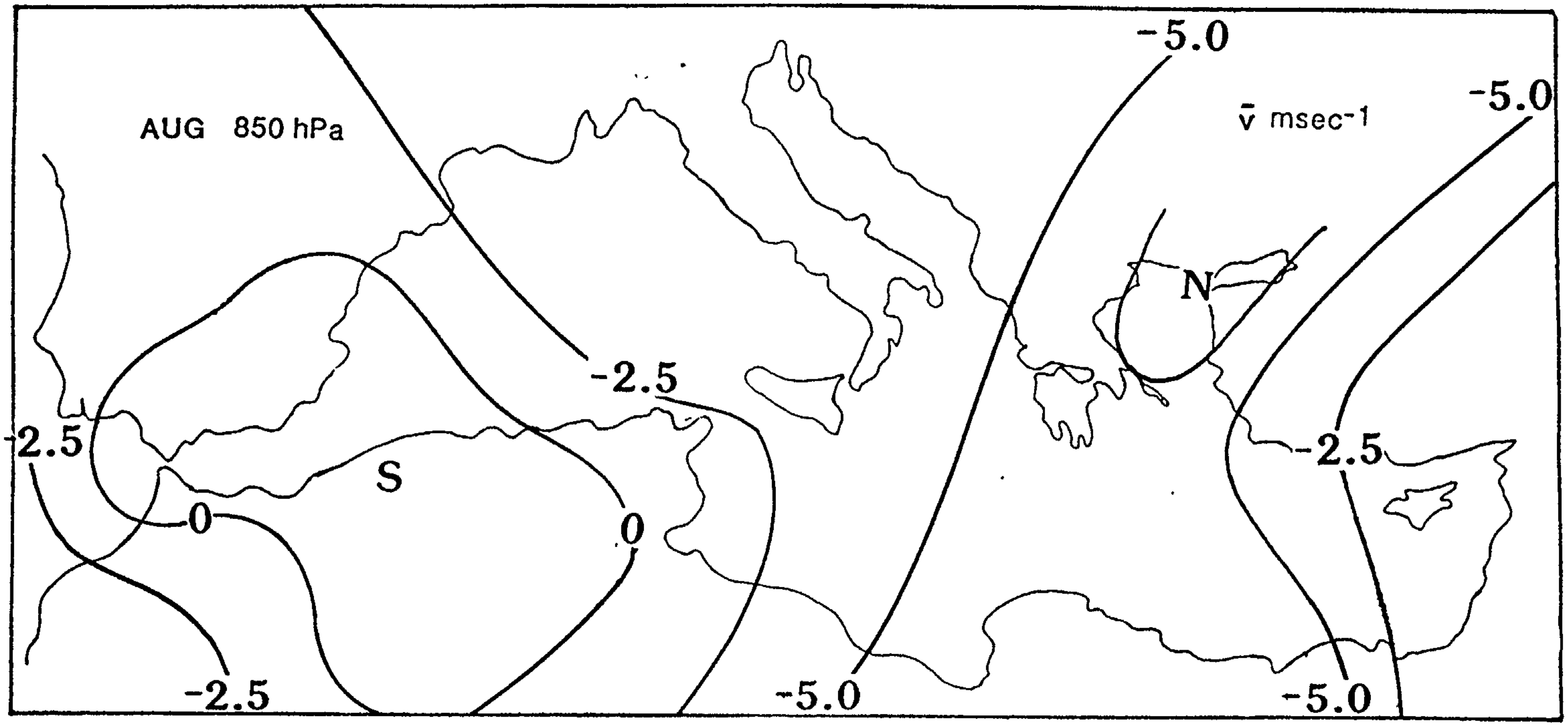

Fig. 26(b) - Mean meridional ($\bar{v}$) winds (m s^{-1}) at the 850 hPa level for August

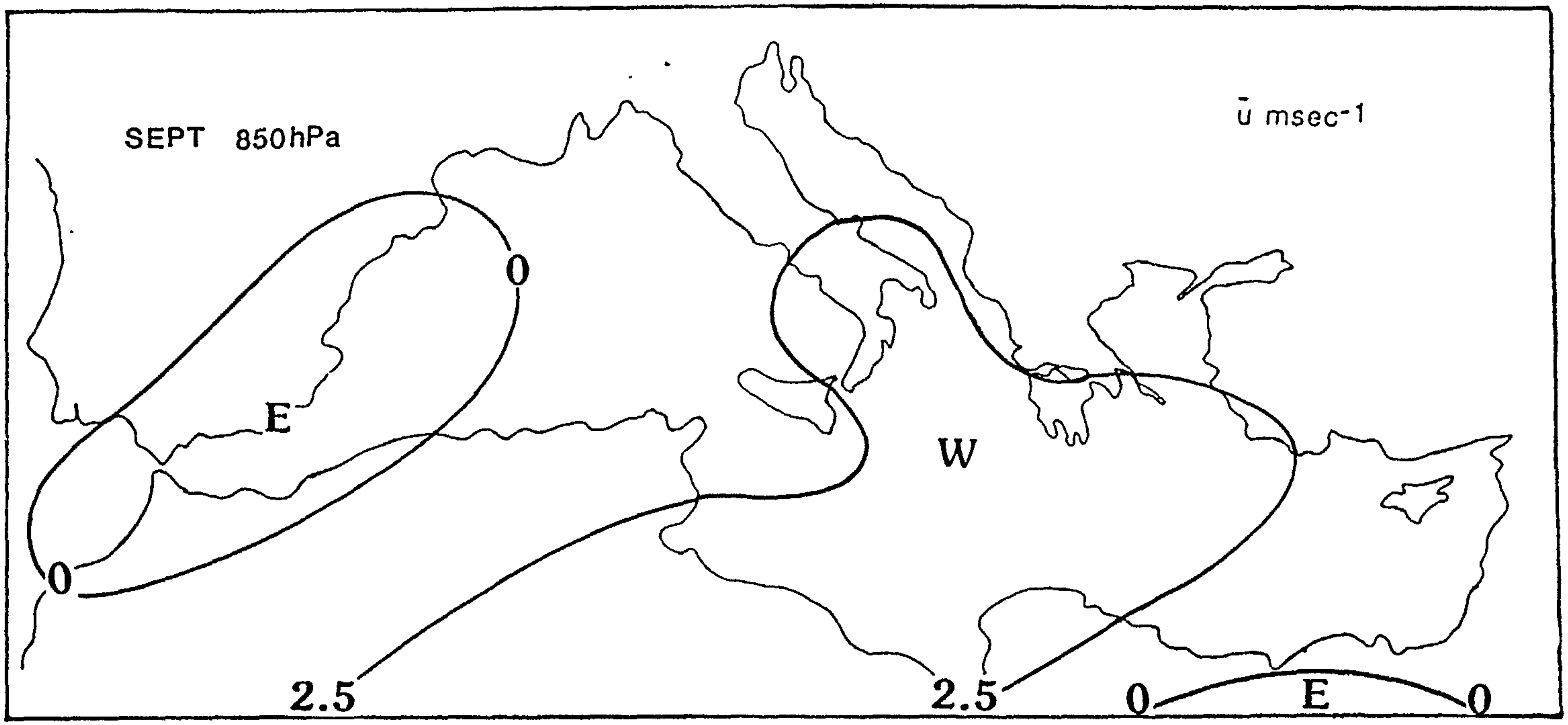

Fig. 27(a) - Mean zonal ($\bar{u}$) winds (m s^{-1}) at the 850 hPa level for September

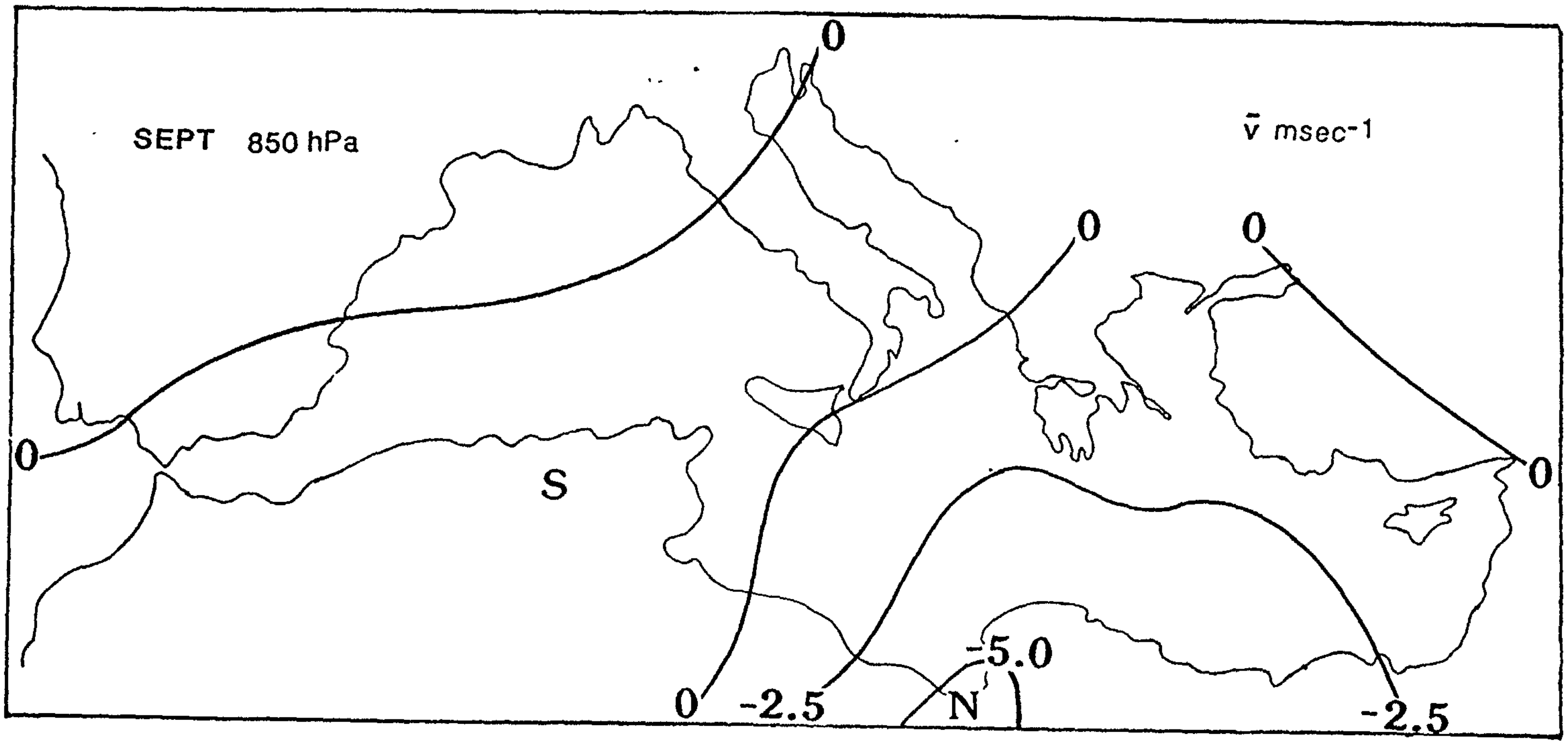

Fig. 27(b) - Mean meridional ($\bar{v}$) winds (m s^{-1}) at the 850 hPa level for September

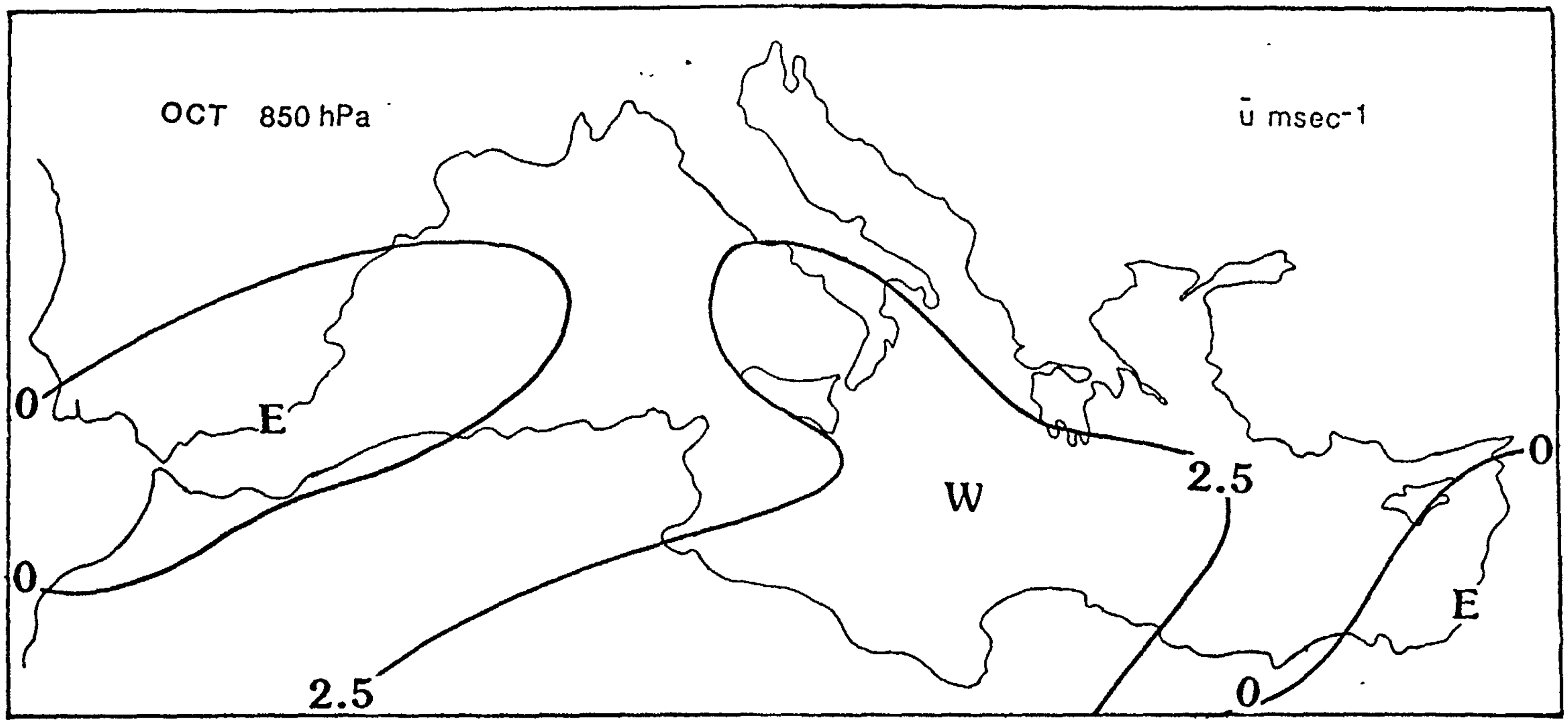

Fig. 28(a) - Mean zonal ($\bar{u}$) winds ($m\ s^{-1}$) at the 850 hPa level for October

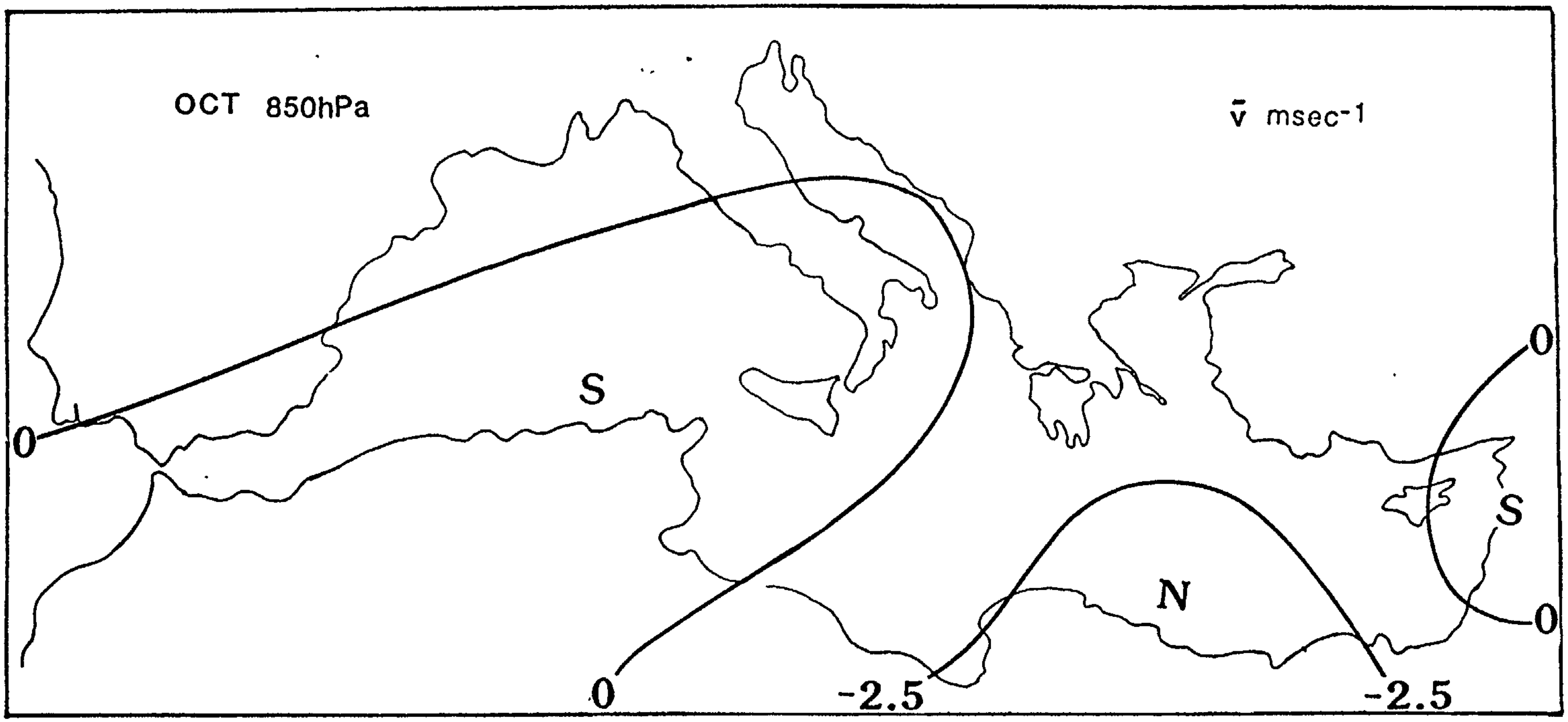

Fig. 28(b) - Mean meridional ($\bar{v}$) winds (m s^{-1}) at the 850 hPa level for October

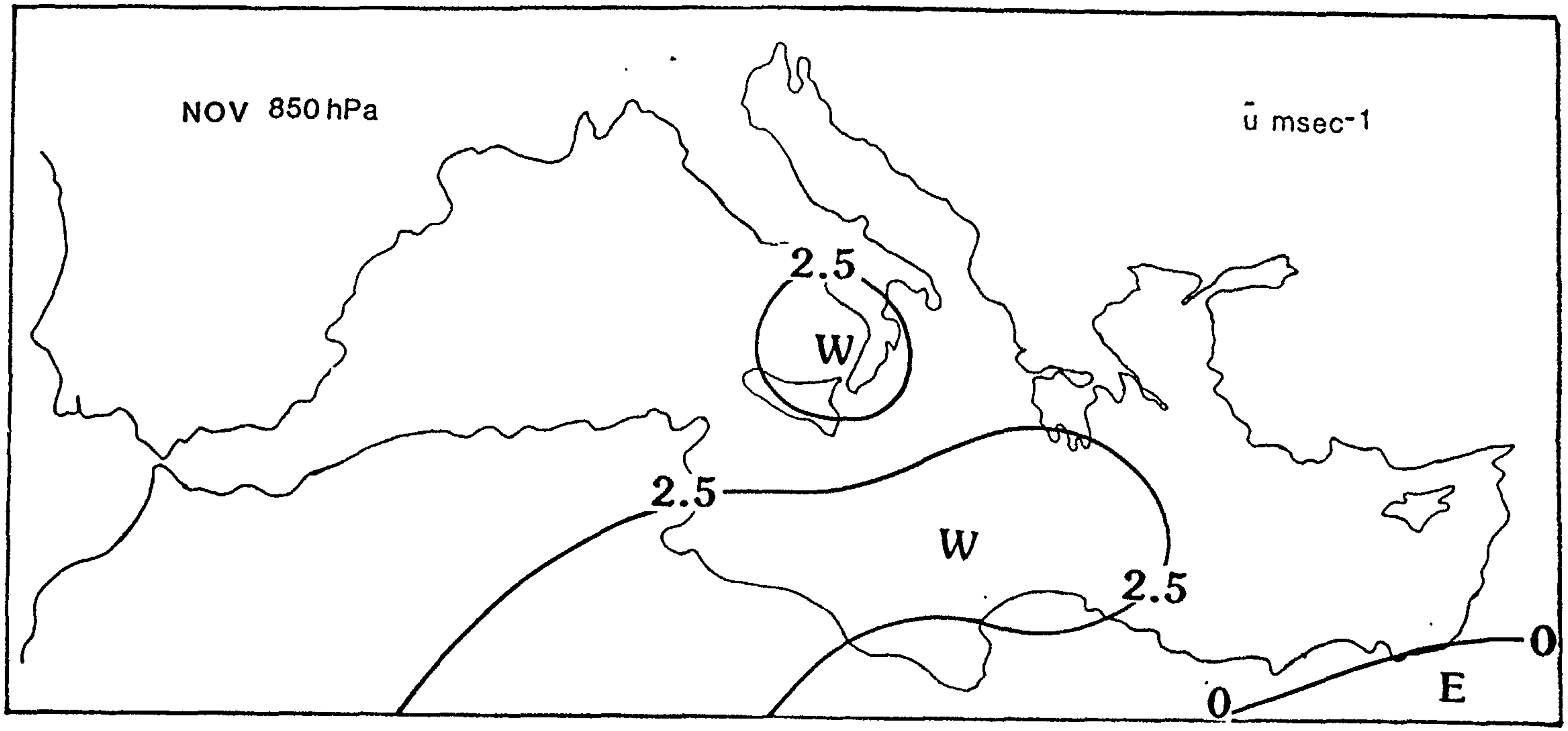

Fig. 29(a) - Mean zonal ($\bar{u}$) winds (m s^{-1}) at the 850 hPa level for November

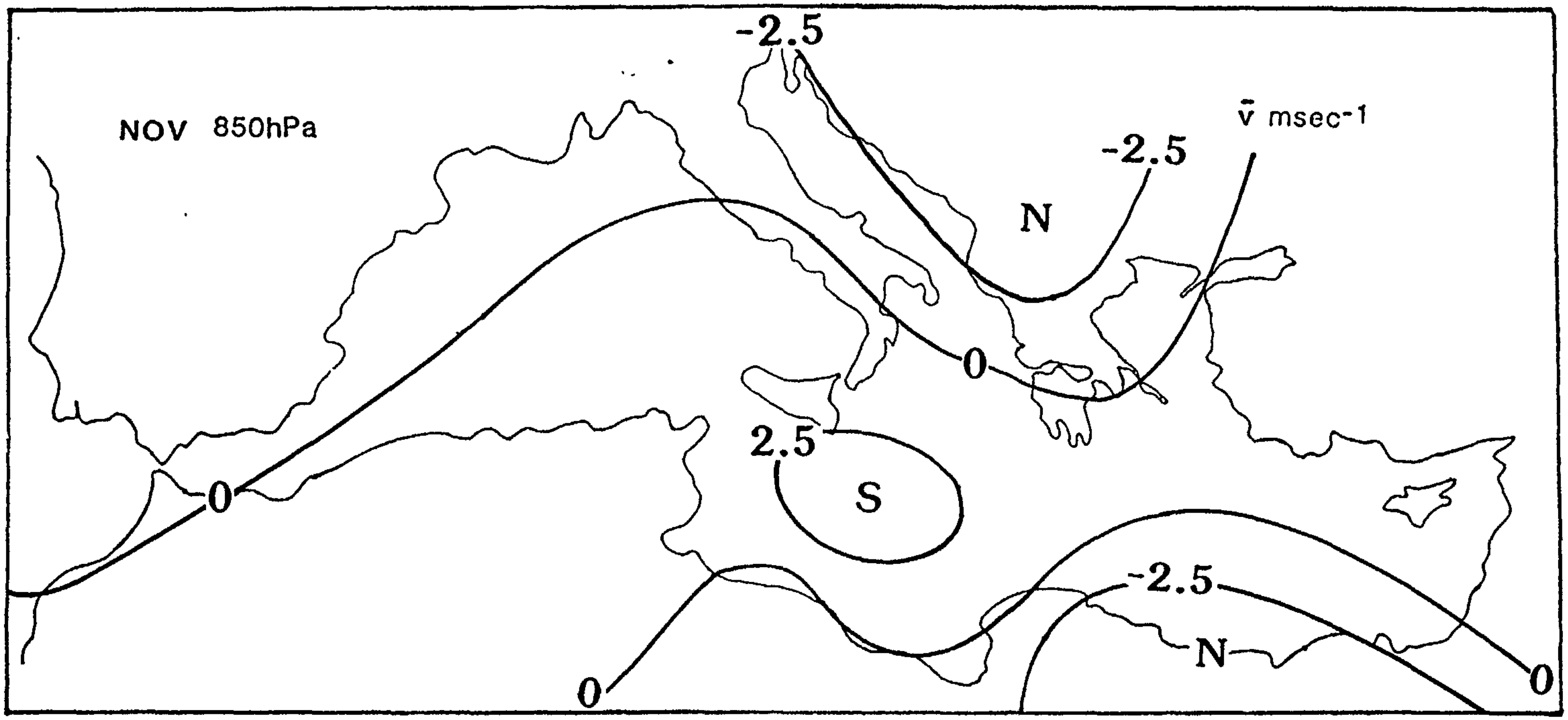

Fig. 29(b) - Mean meridional ($\bar{v}$) winds ($m\ s^{-1}$) at the 850 hPa level for November

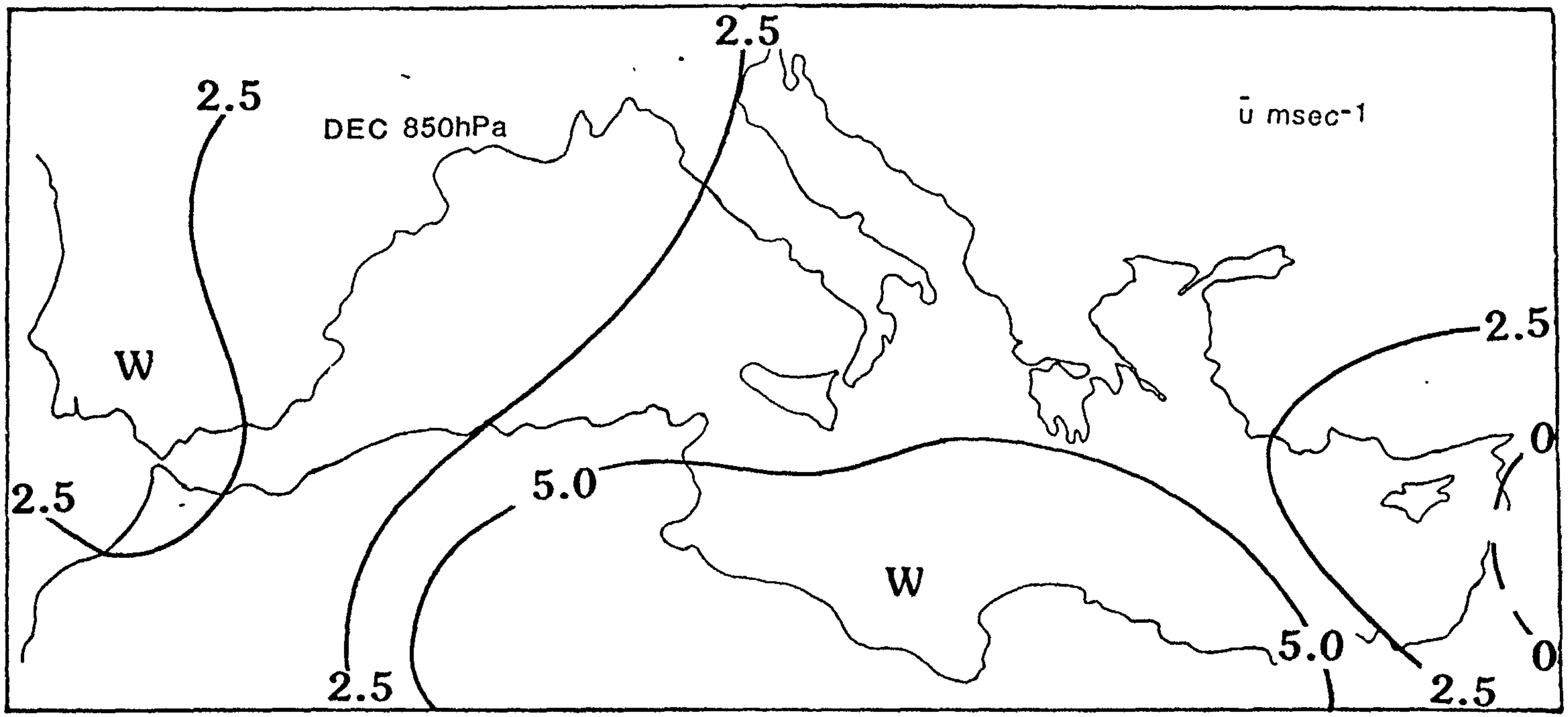

Fig. 30(a) - Mean zonal ($\bar{u}$) winds ($m\ s^{-1}$) at the 850 hPa level for December

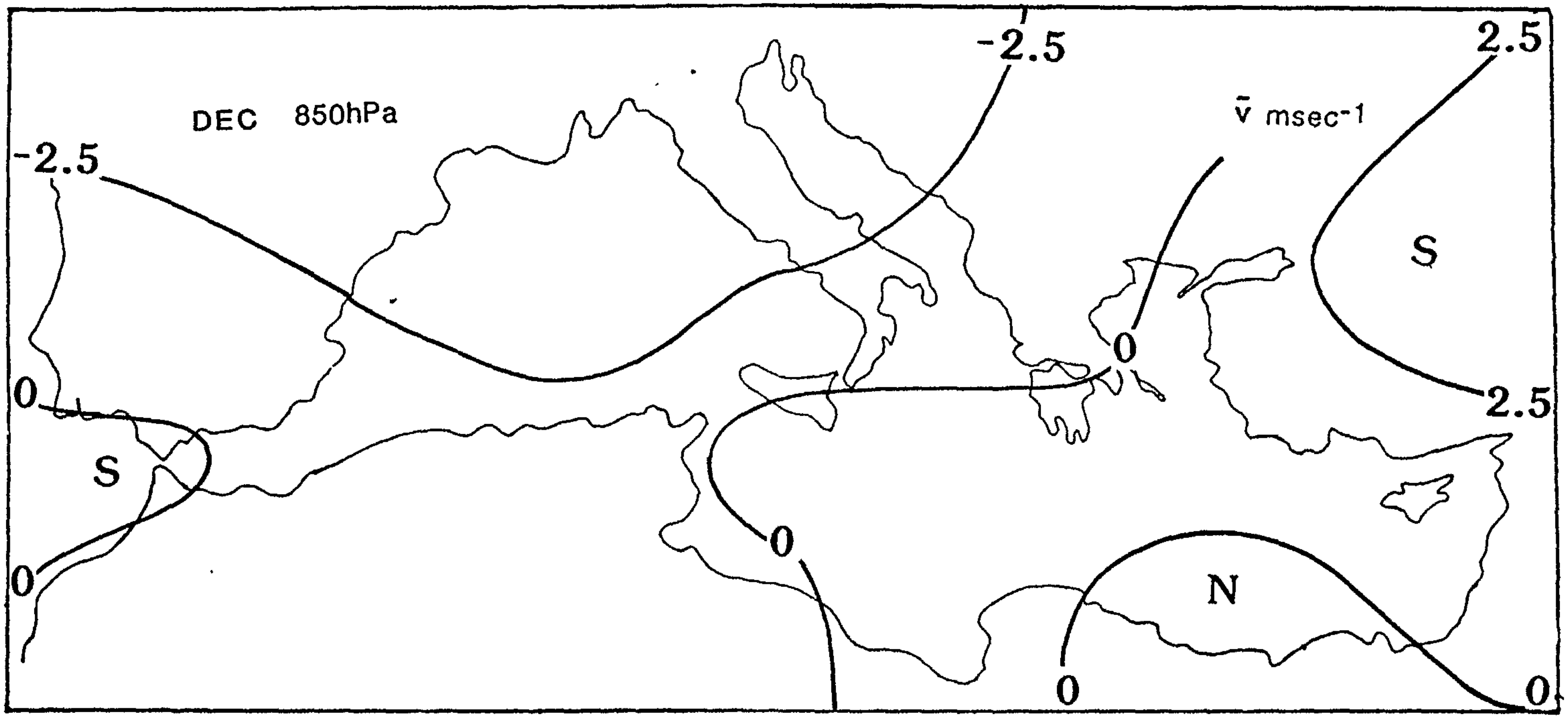

Fig. 30(b) - Mean meridional ($\bar{v}$) winds (m s^{-1}) at the 850 hPa level for December

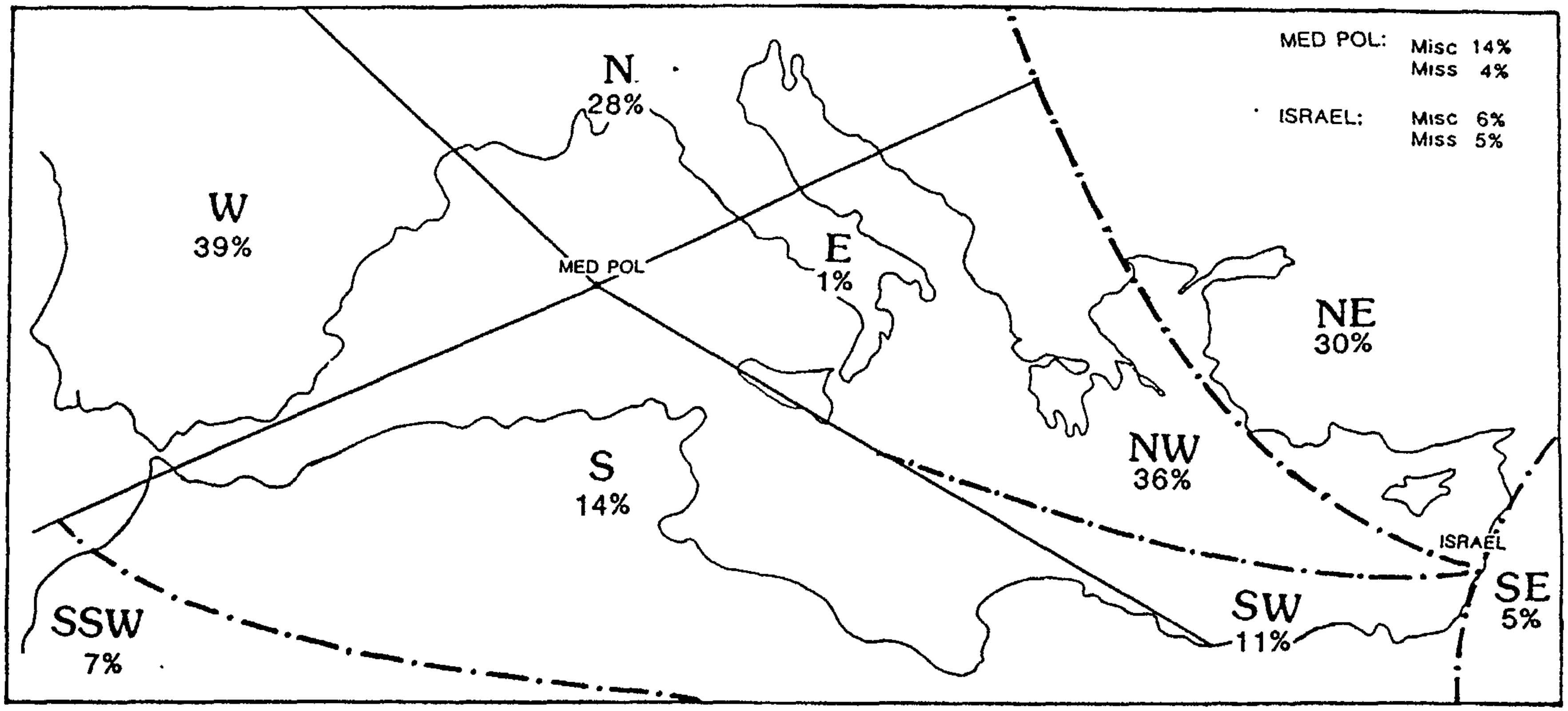

Fig. 31 - Locations of the western (Med Pol) and easter (Israel) receptors in the Mediterranean Basin. Sectors NW, NE, SE, SW and SSW, separated by broken lines, are trajectory directions for the western Mediterranean: sectors N, E, S and W, separated by solid lines, are trajectory directions for the eastern Mediterranean. The percentage of flow from each sector is indicated. The percentages of miscellaneous and missing data are also given.

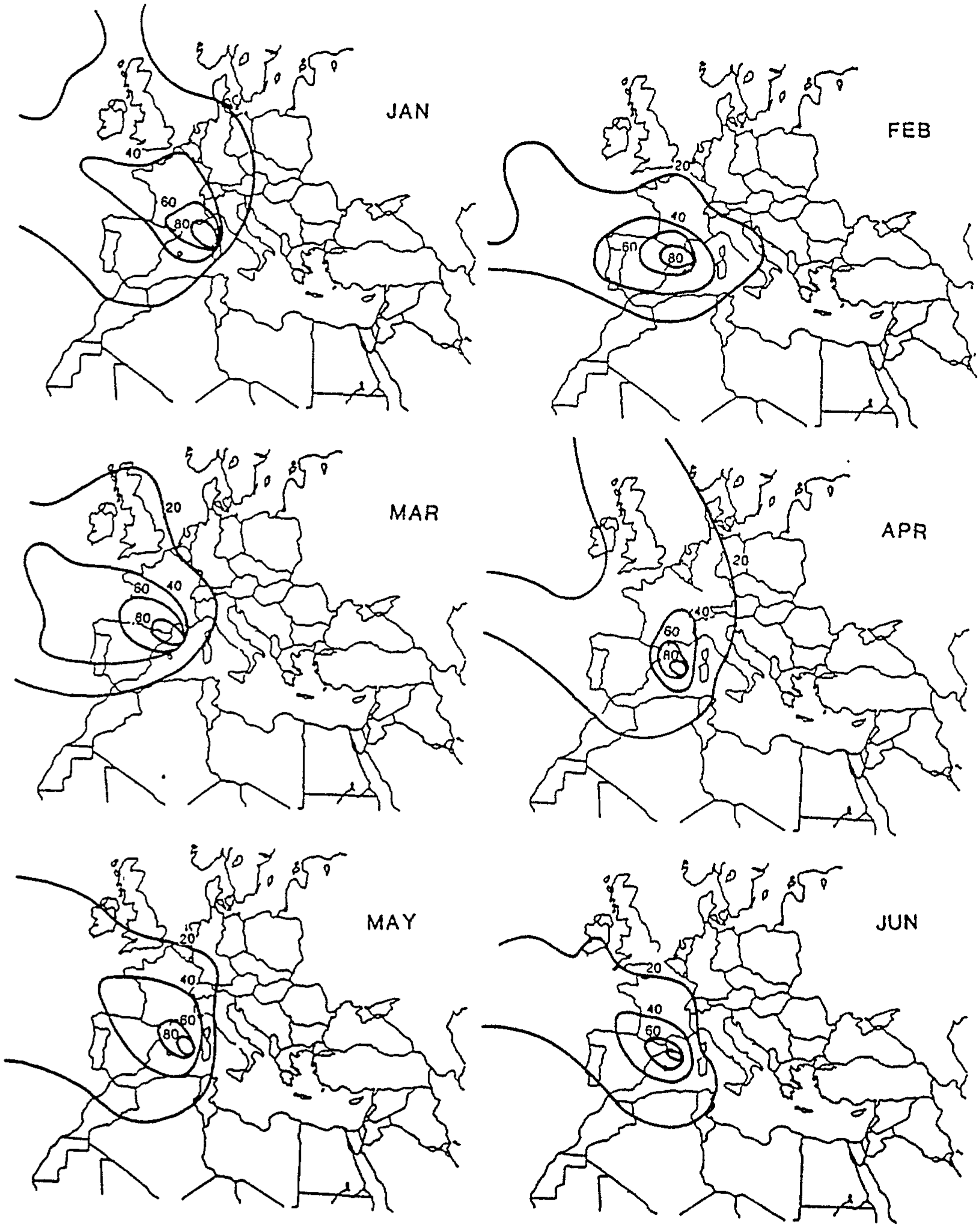

Fig. 32(a) - Trajectory statistics at the western Mediterranean (Med Pol) point for January-June, 1975-1984. The values shown are the percentages of boundary layer trajectories (1000-850 hPa) that had arrived at Med Pol and had traversed a given location on the map.

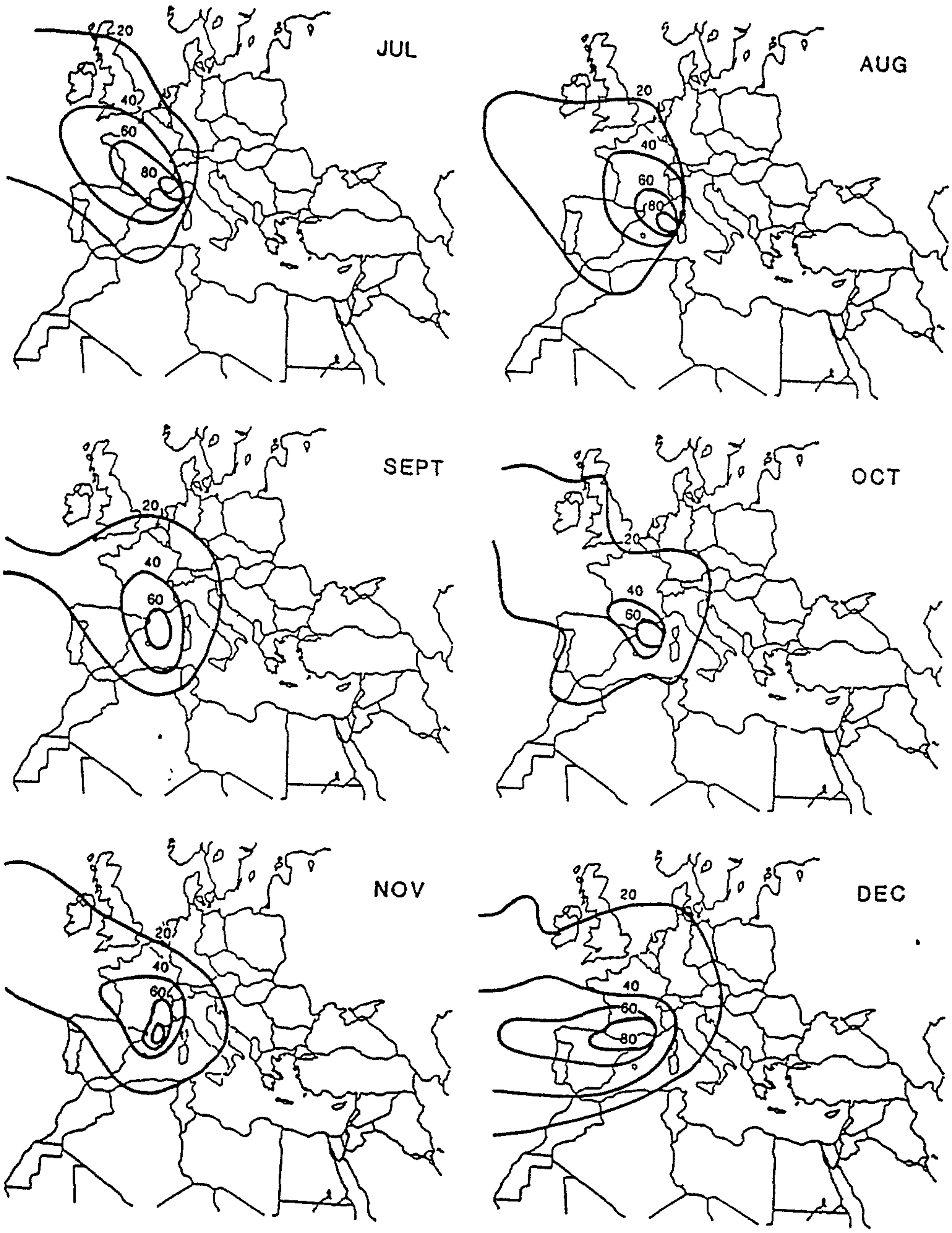

Fig. 32(b) - Trajectory statistics at the western Mediterranean (Med Pol) point for July-December, 1975-1984. The values shown are the percentages of boundary layer trajectories (1000-850 hPa) that had arrived at Med Pol and had traversed a given location on the map.

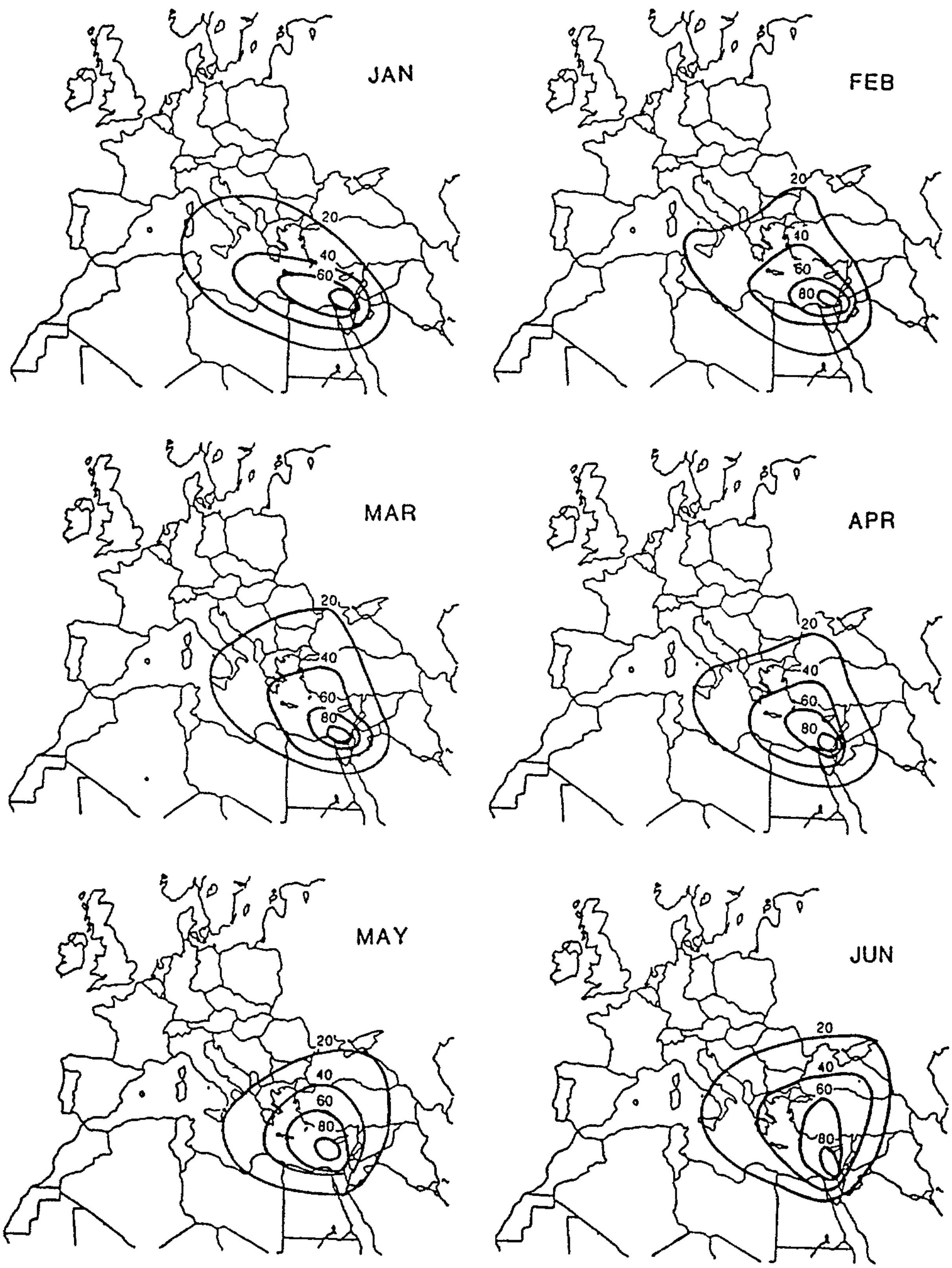

Fig. 33(a) - Trajectory statistics at the eastern Mediterranean (Israel) point for January-June, 1978-1987. The values shown are the percentages of boundary layer trajectories (1000-850 hPa) that had arrived at Israel and had traversed a given location on the map.

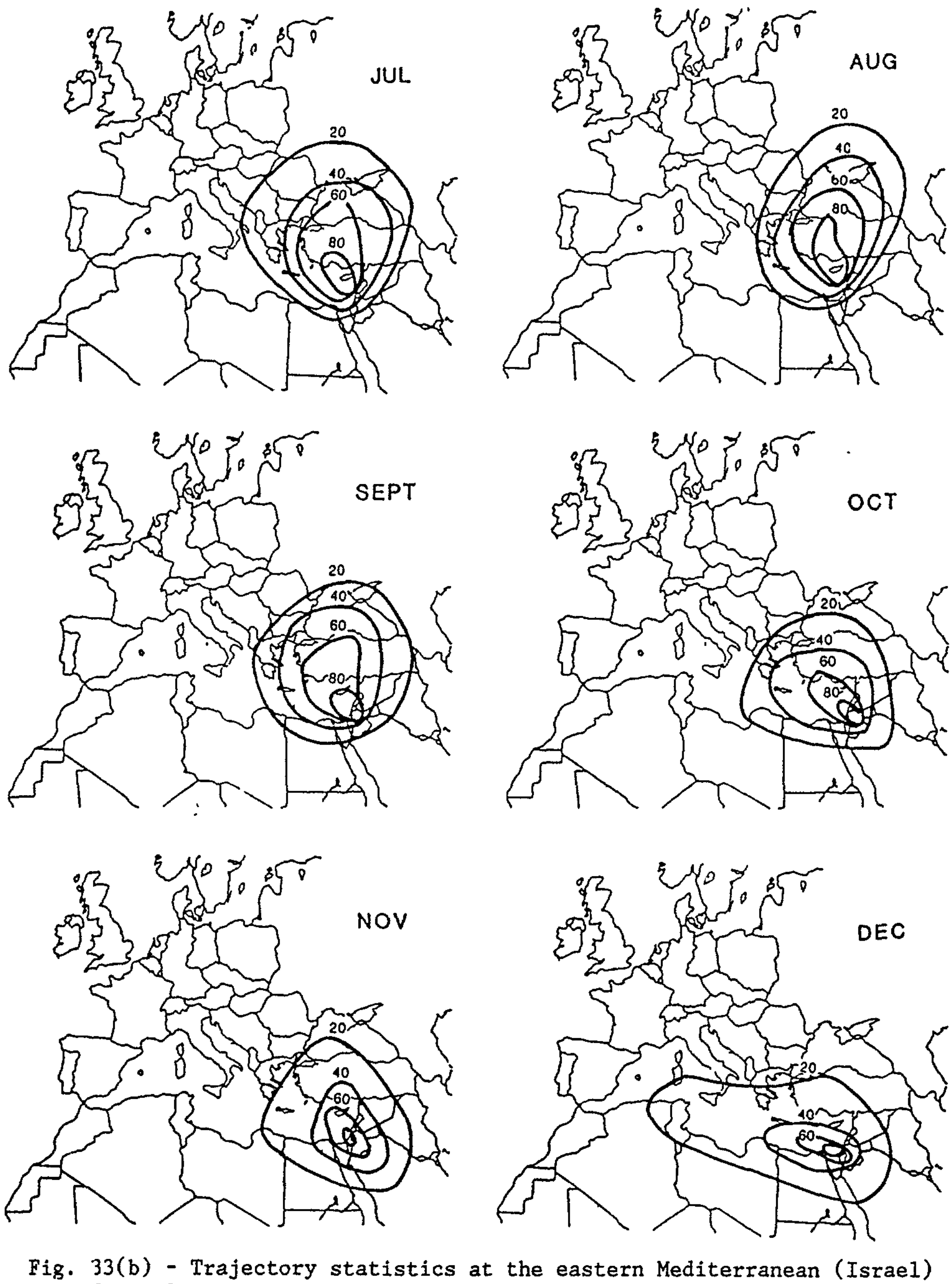

Fig. 33(b) - Trajectory statistics at the eastern Mediterranean (Israel) point for July-December, 1978-1987. The values shown are the percentages of boundary layer trajectories (1000-850 hPa) that had arrived at Israel and had traversed a given location on the map.

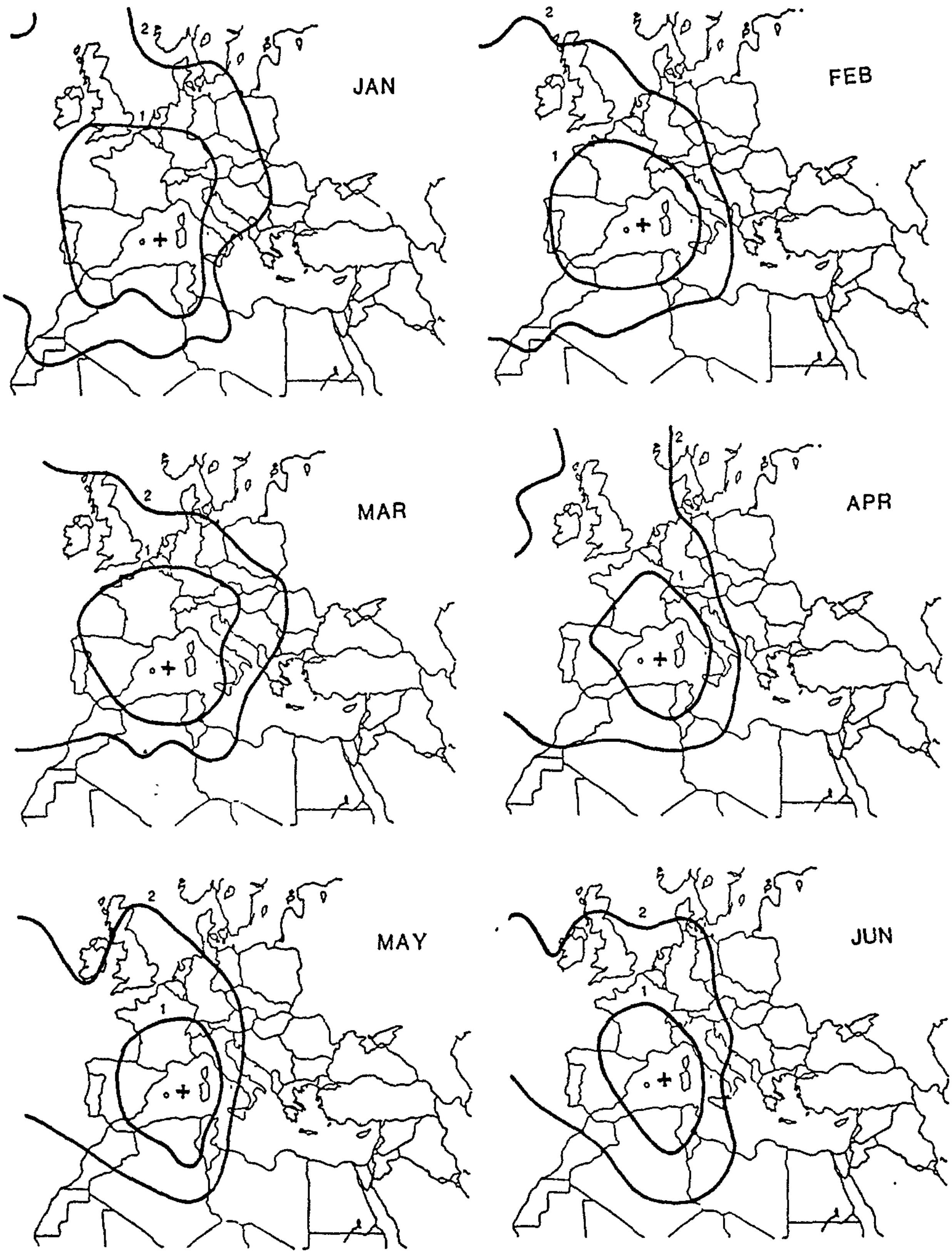

Fig. 34(a) - Arrival time (days) to the western site for January-June, 1975-1984.

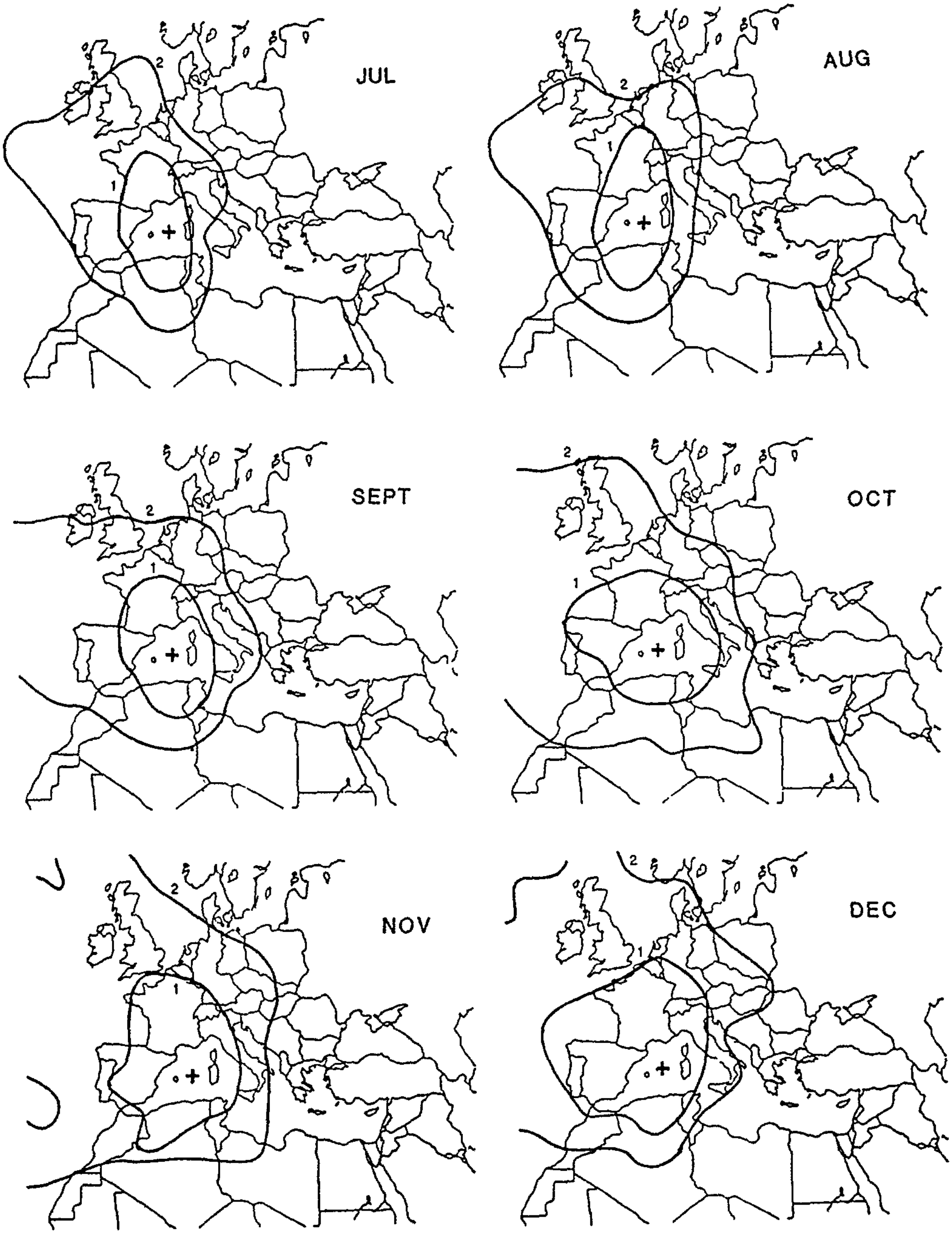

Fig. 34(b) - Arrival time (days) to the western site for July-August, 1975-1984.

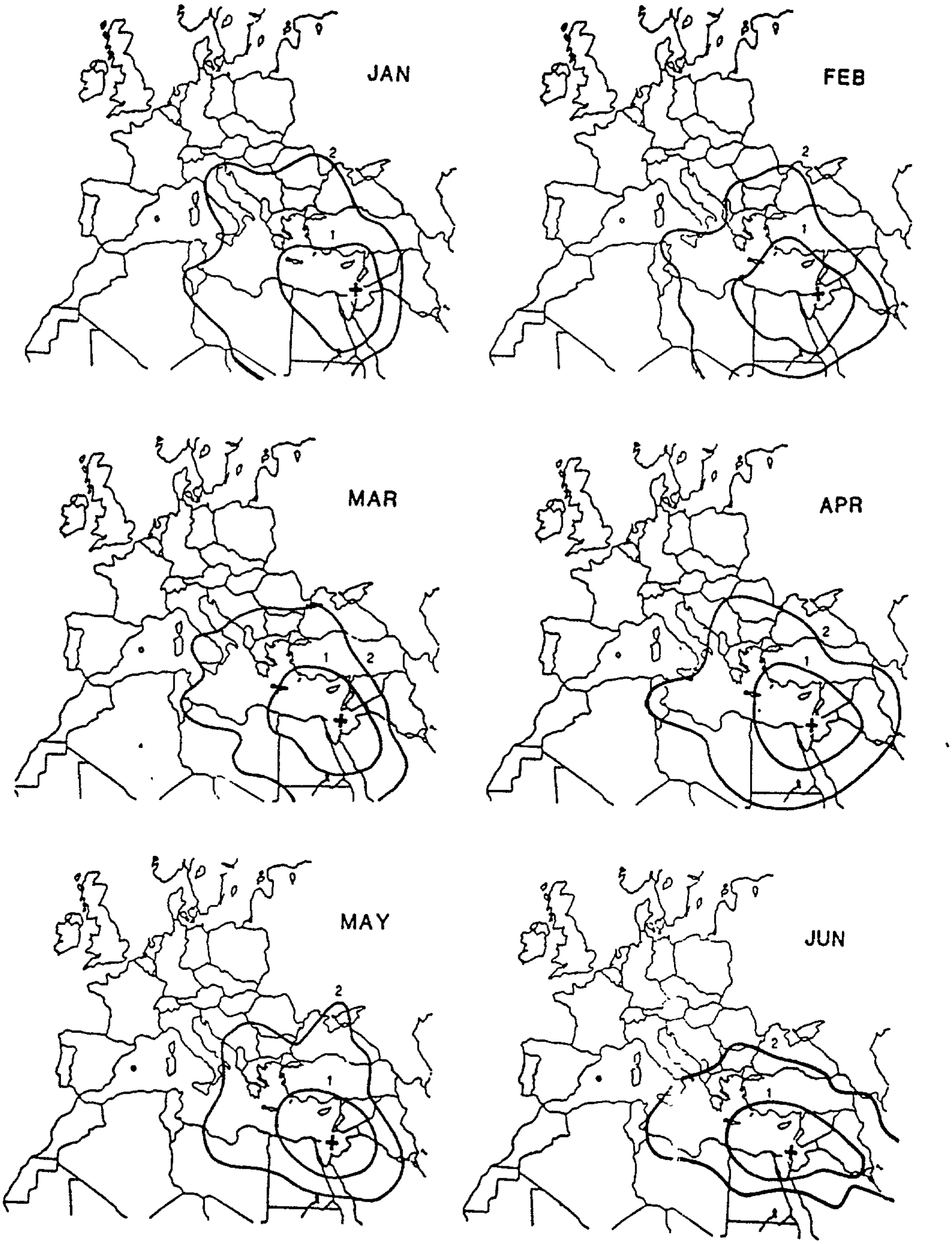

Fig. 35(a) - Arrival time (days) to the eastern site for January-June, 1978-1982

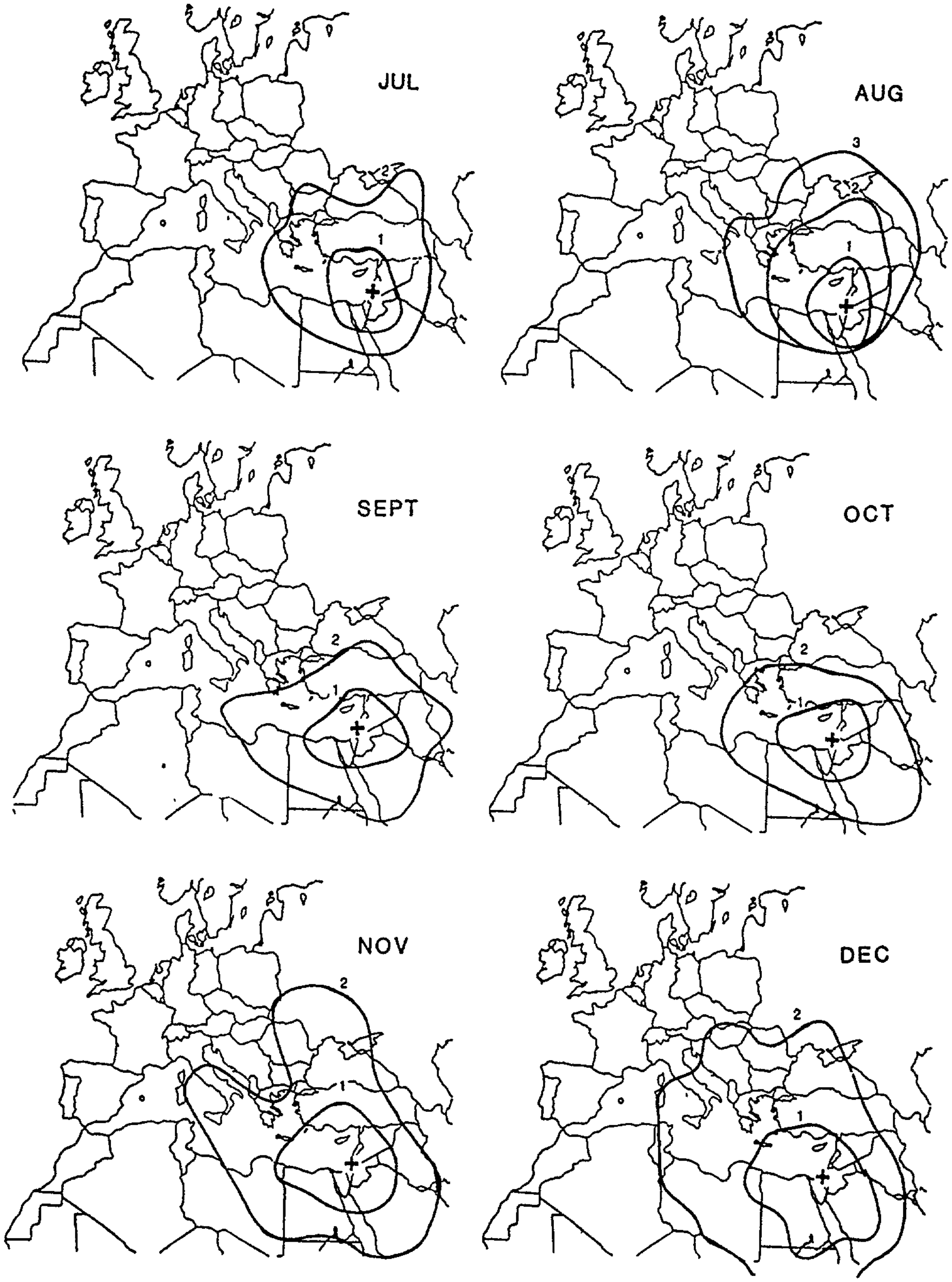

Fig. 35(b) - Arrival time (days) to the eastern site for July-December, 1978-1982.

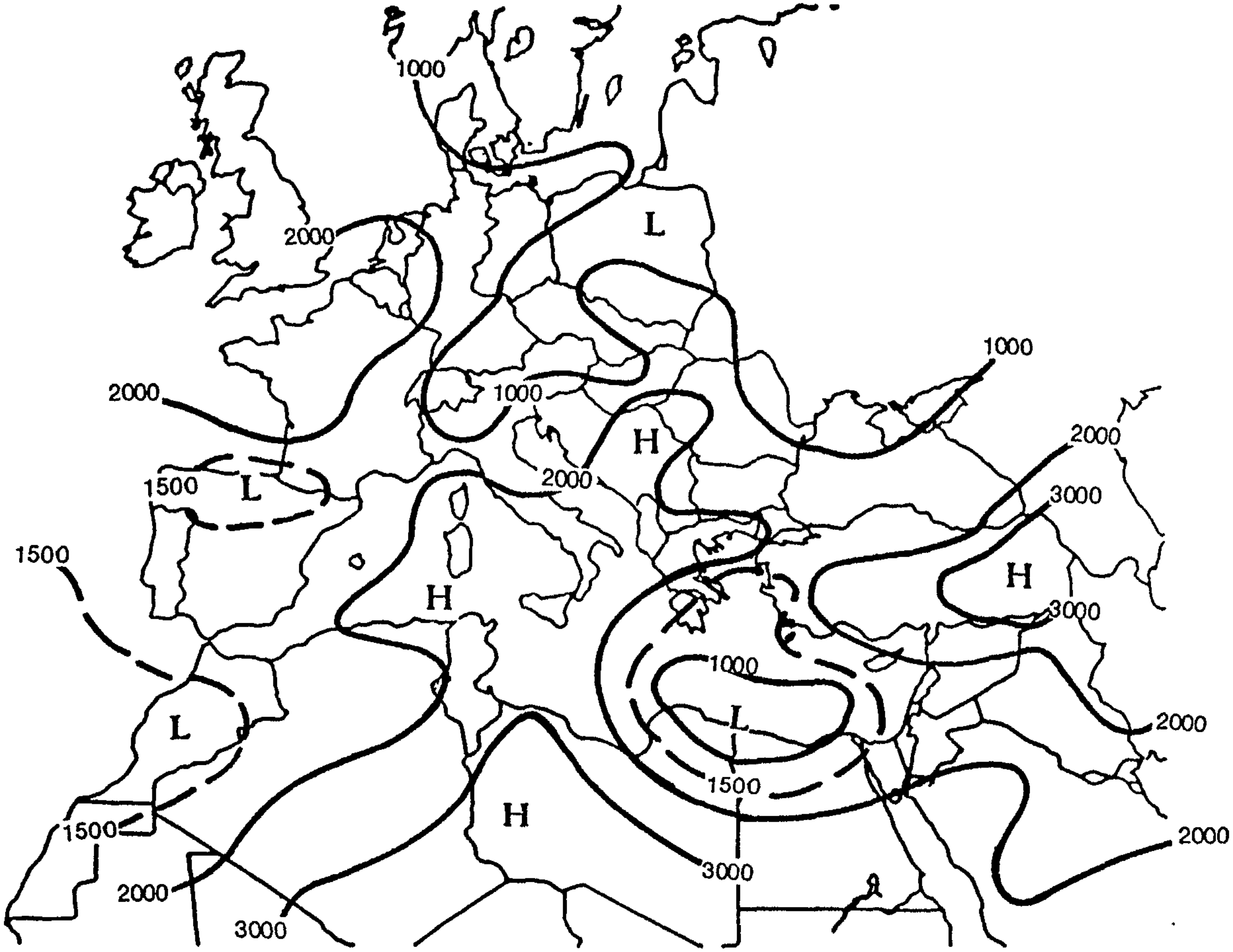

Fig.36 - Average calculated mixing height (m) for winter exemplified by January 1984.

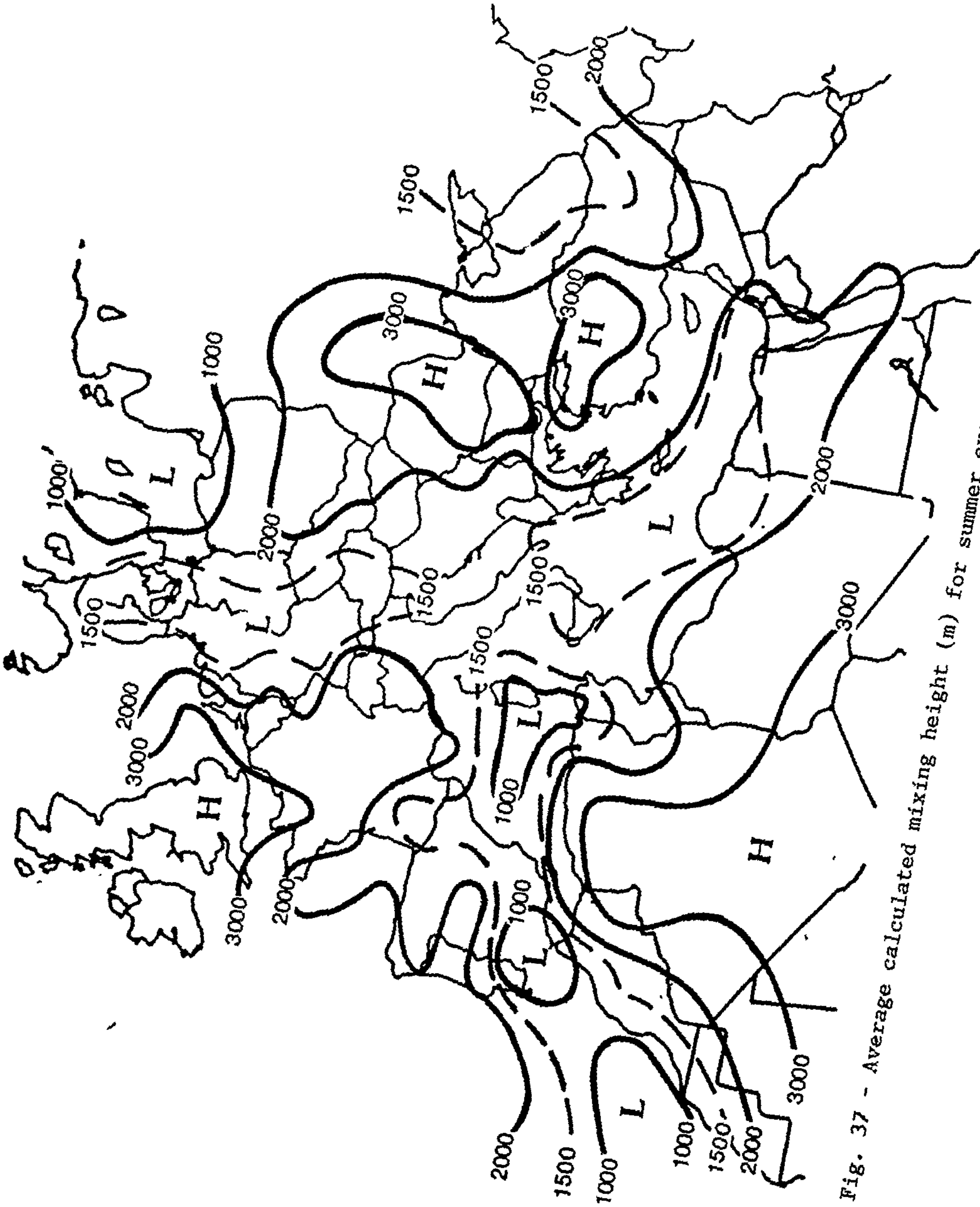

Fig. 37 - Average calculated mixing height (m) for summer exemplified by July 1984.

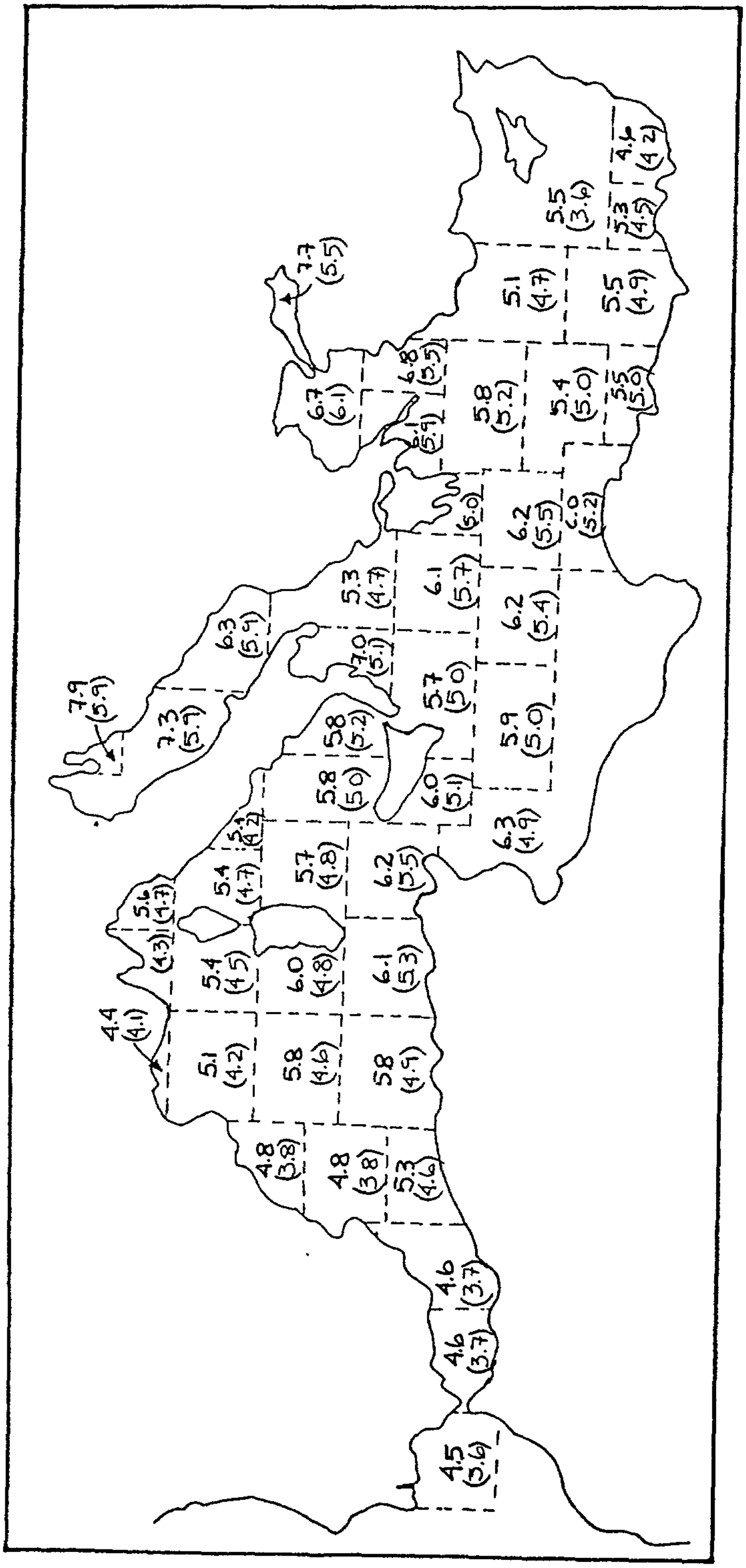

Fig. 38 - Monthly mean cloud amounts (oktas) for day and night - January

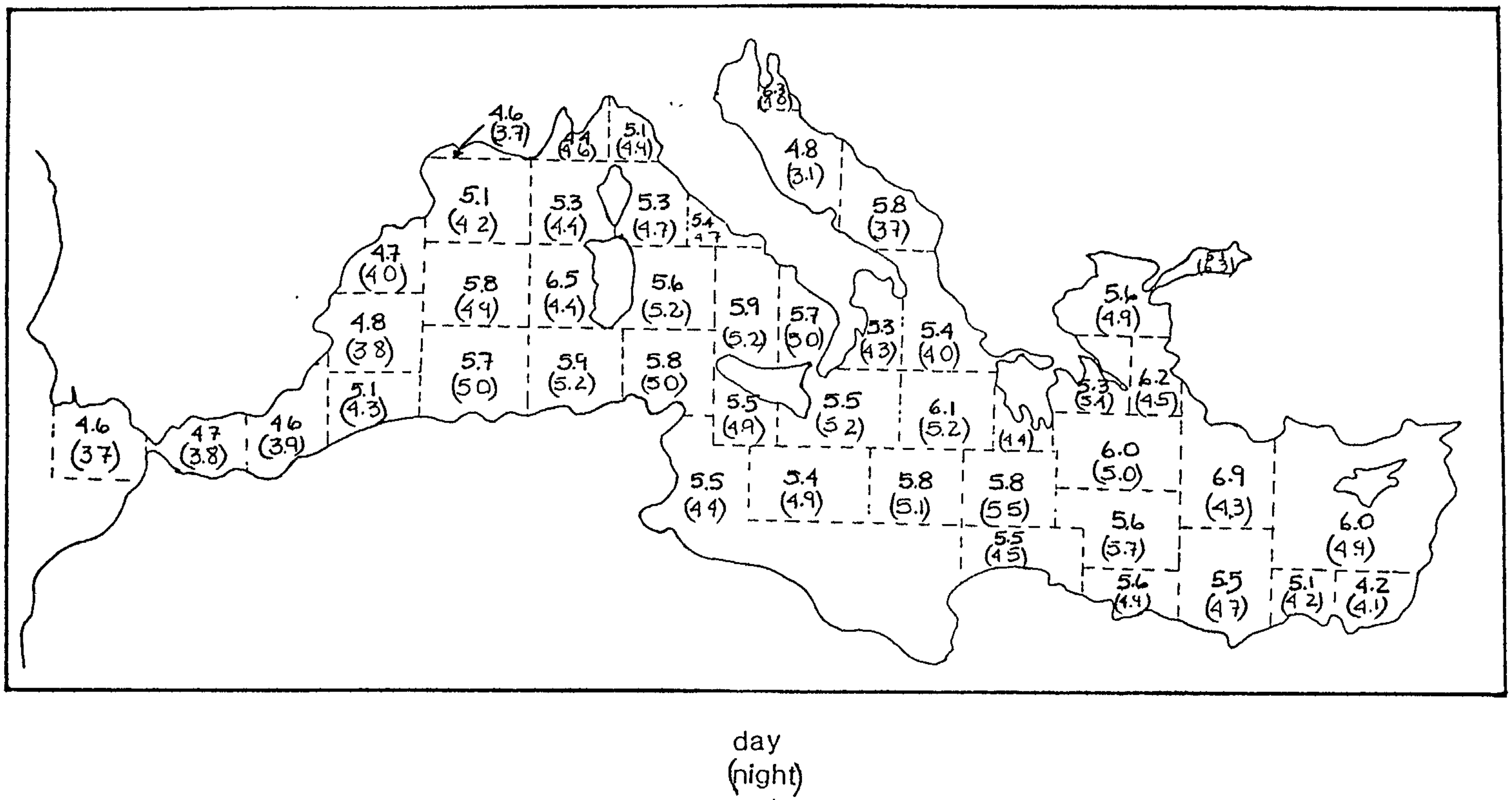

Fig. 39 - Monthly mean cloud amounts (oktas) for day and night - February

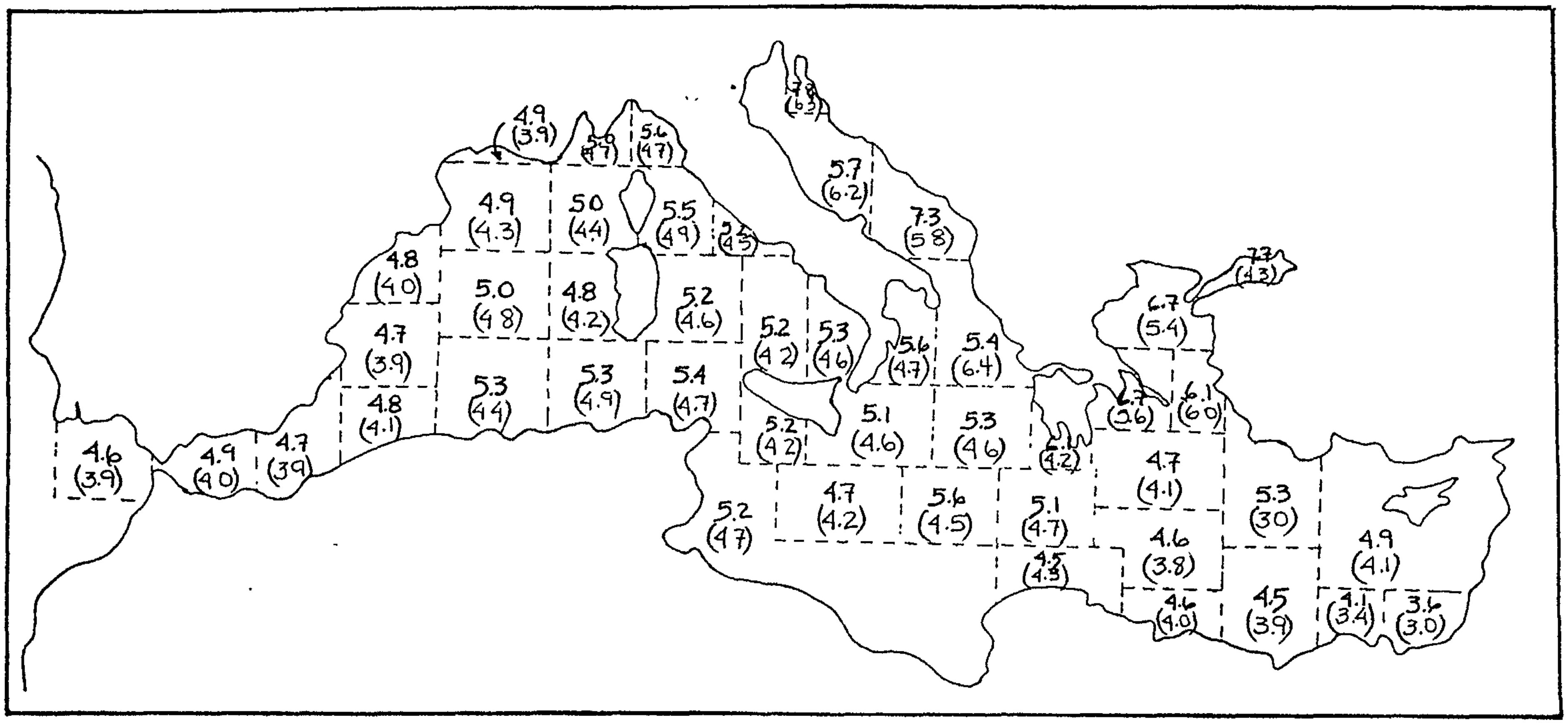

day
(night)

Fig. 40 - Monthly mean cloud amounts (oktas) for day and night - March

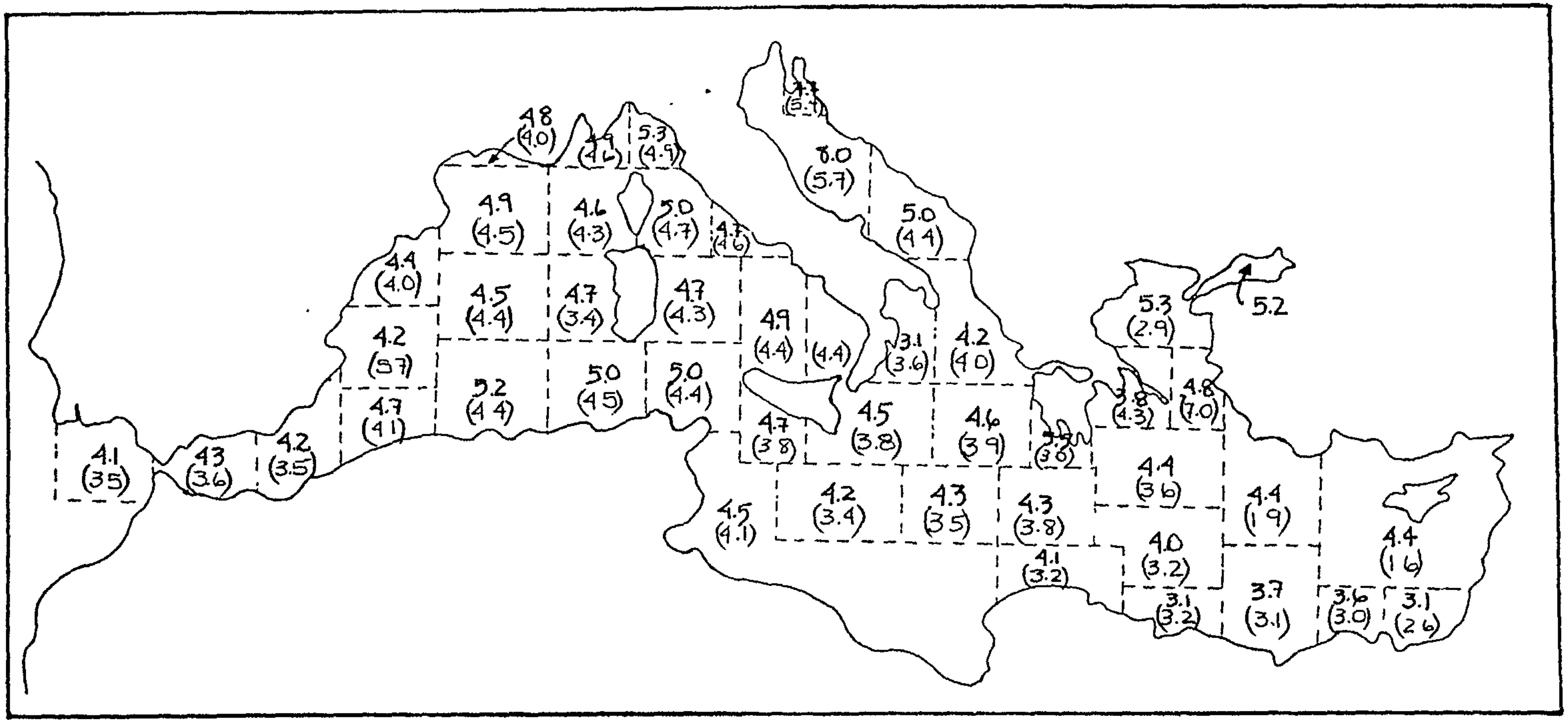

day
(night)

Fig. 41 - Monthly mean cloud amounts (oktas) for day and night - April

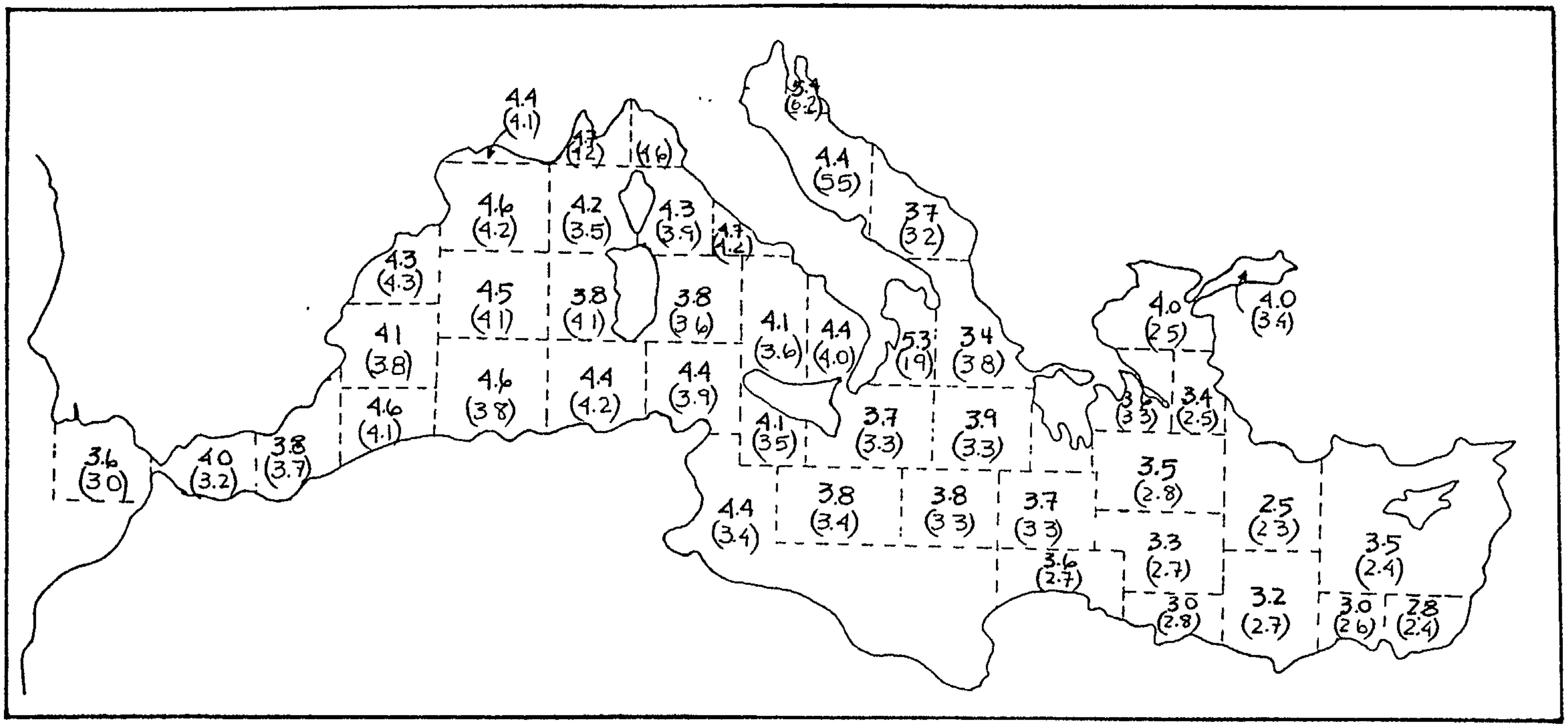

Fig. 42 - Monthly mean cloud amounts (oktas) for day and night - May

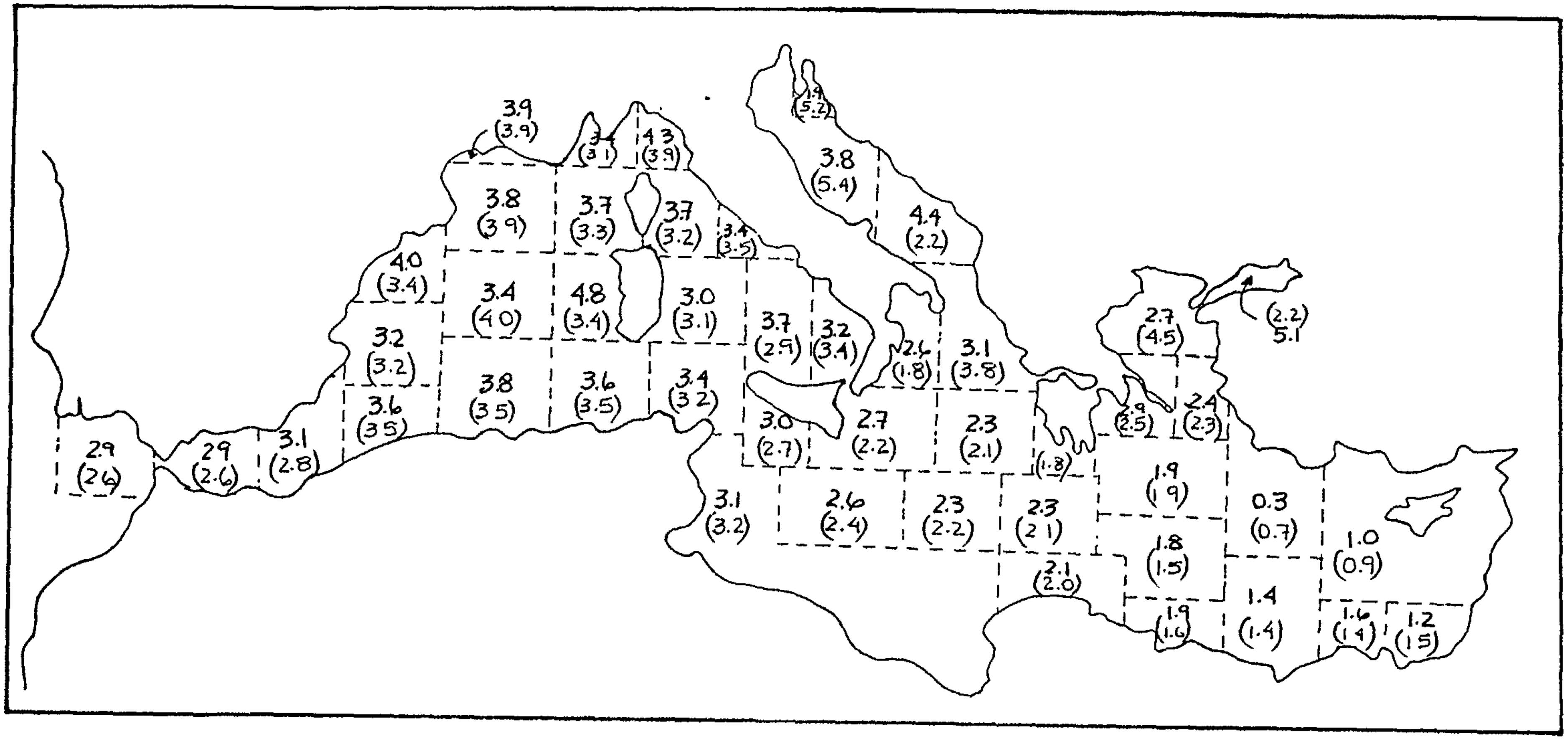

day
(night)

Fig. 43 - Monthly mean cloud amounts (oktas) for day and night - June

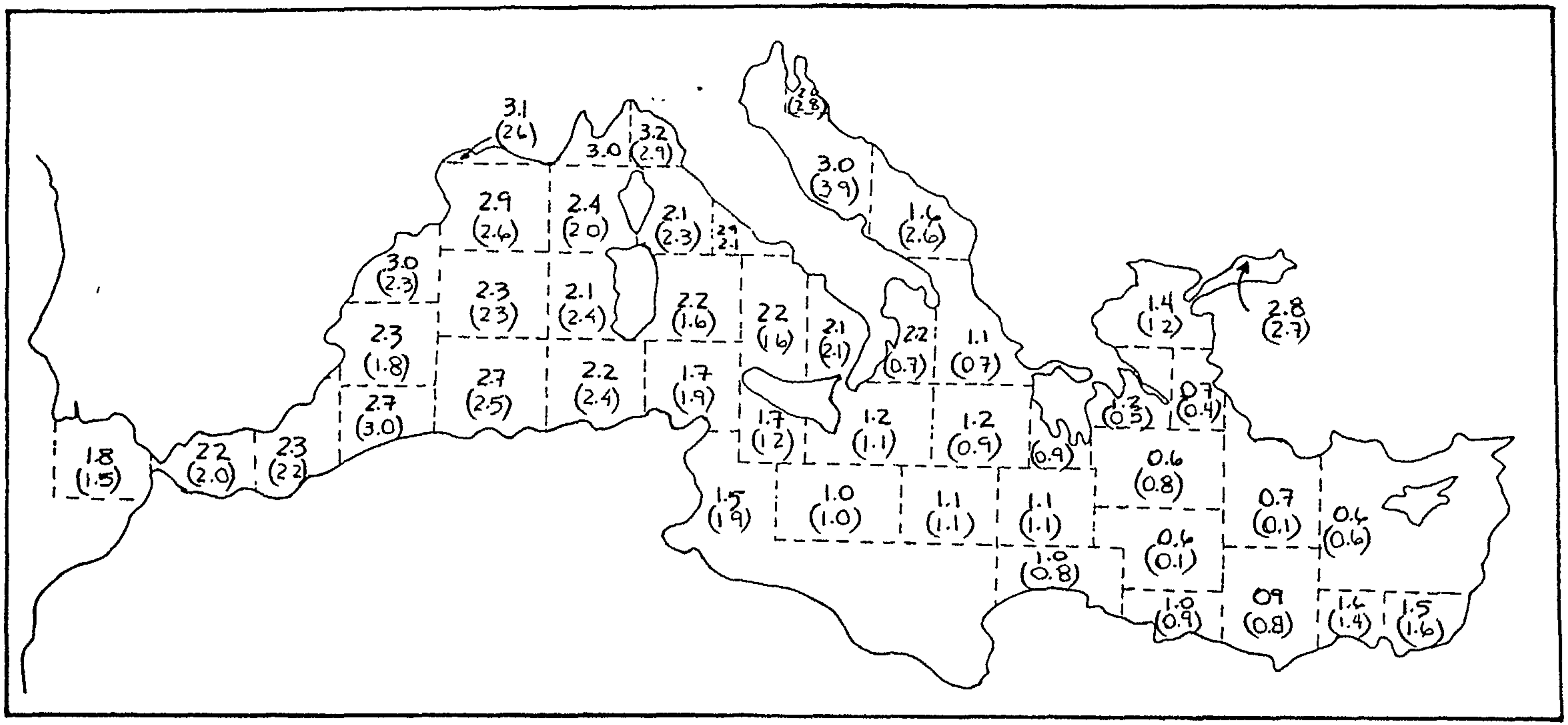

day
(night)

Fig. 44 - Monthly mean cloud amounts (oktas) for day and night - July

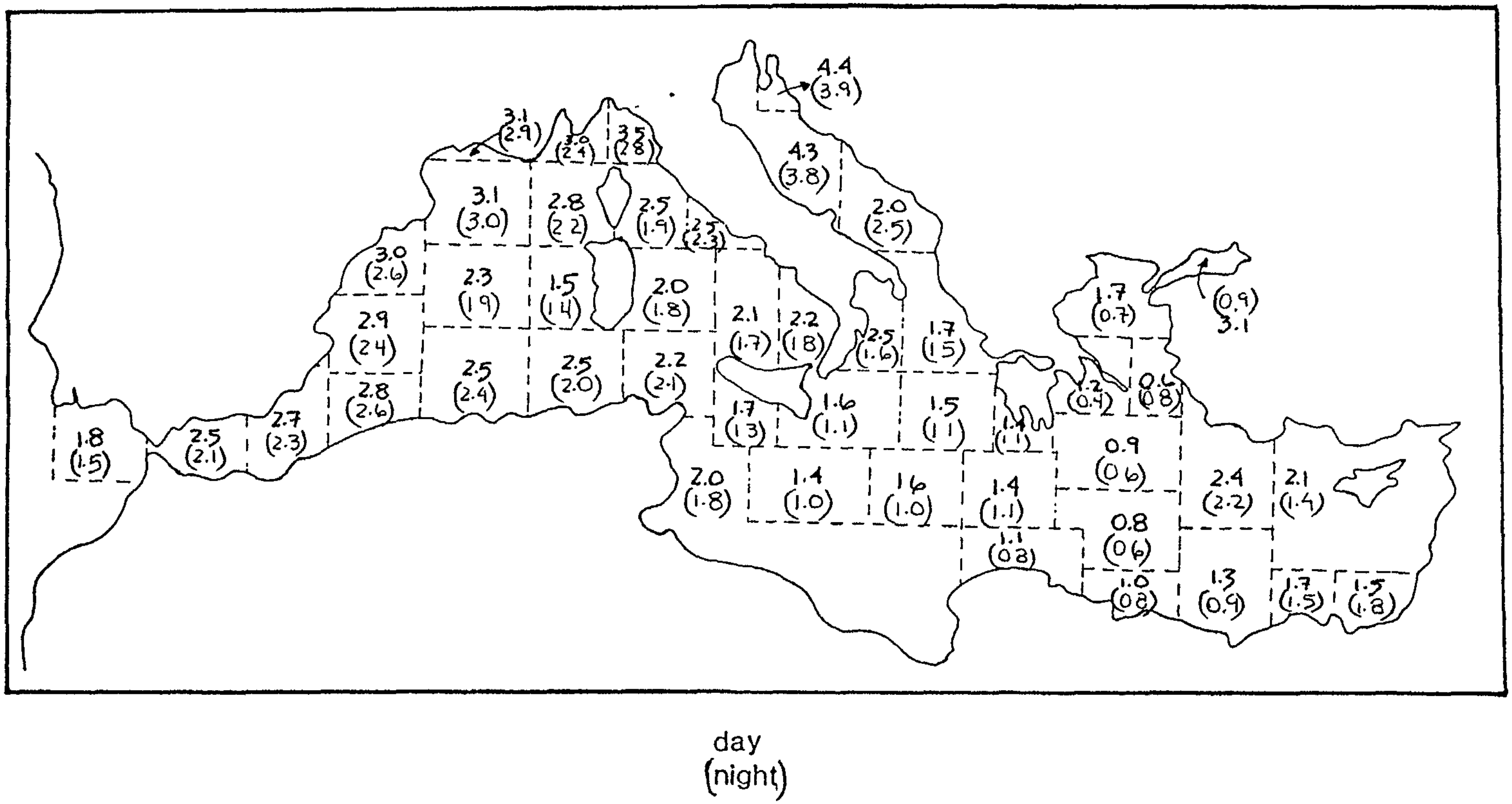

Fig. 45 - Monthly mean cloud amounts (oktas) for day and night - August

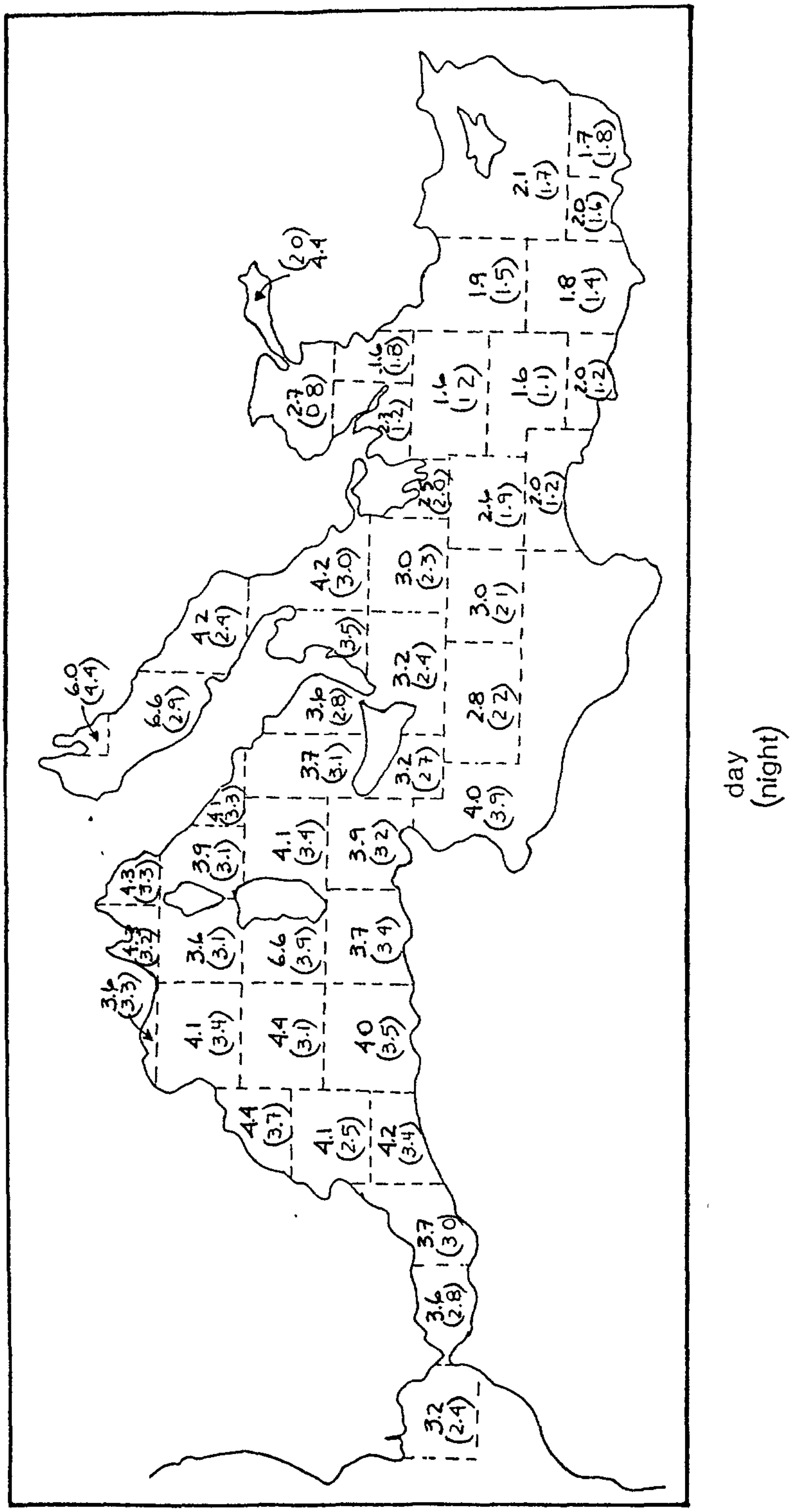

Fig. 46 - Monthly mean cloud amounts (oktas) for day and night - September

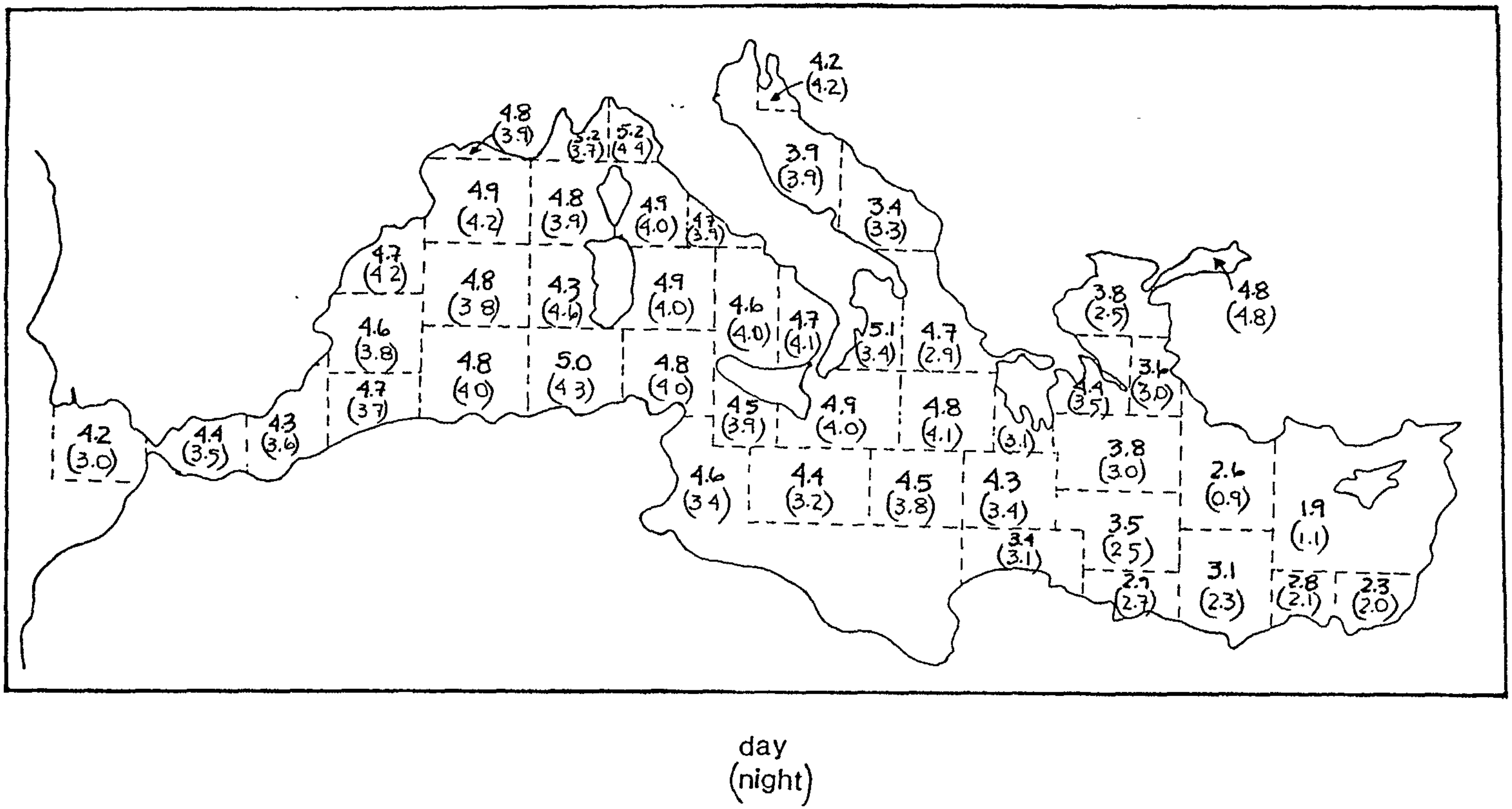

Fig. 47 - Monthly mean cloud amounts (oktas) for day and night - October

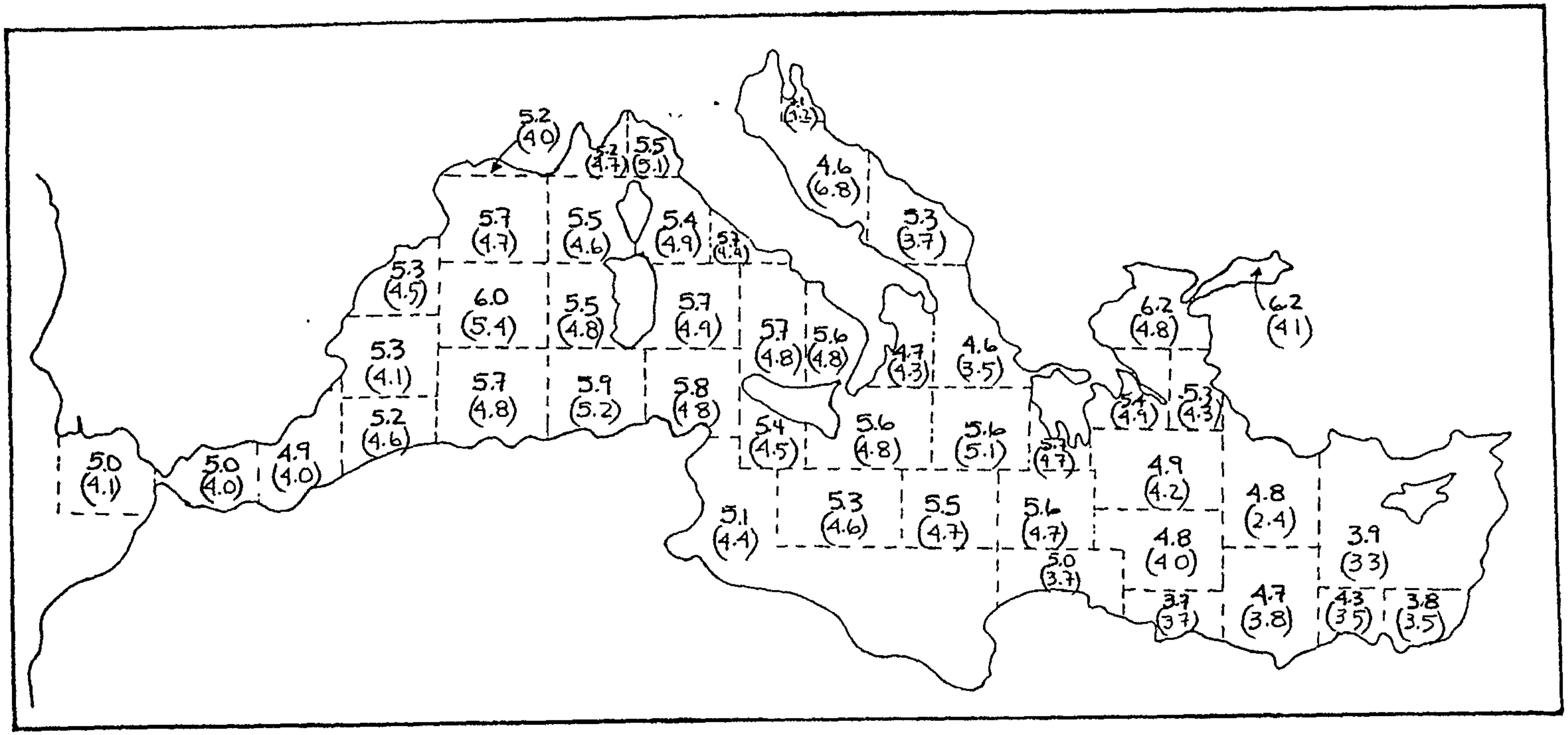

day
(night)

Fig. 48 - Monthly mean cloud amounts (oktas) for day and night - November

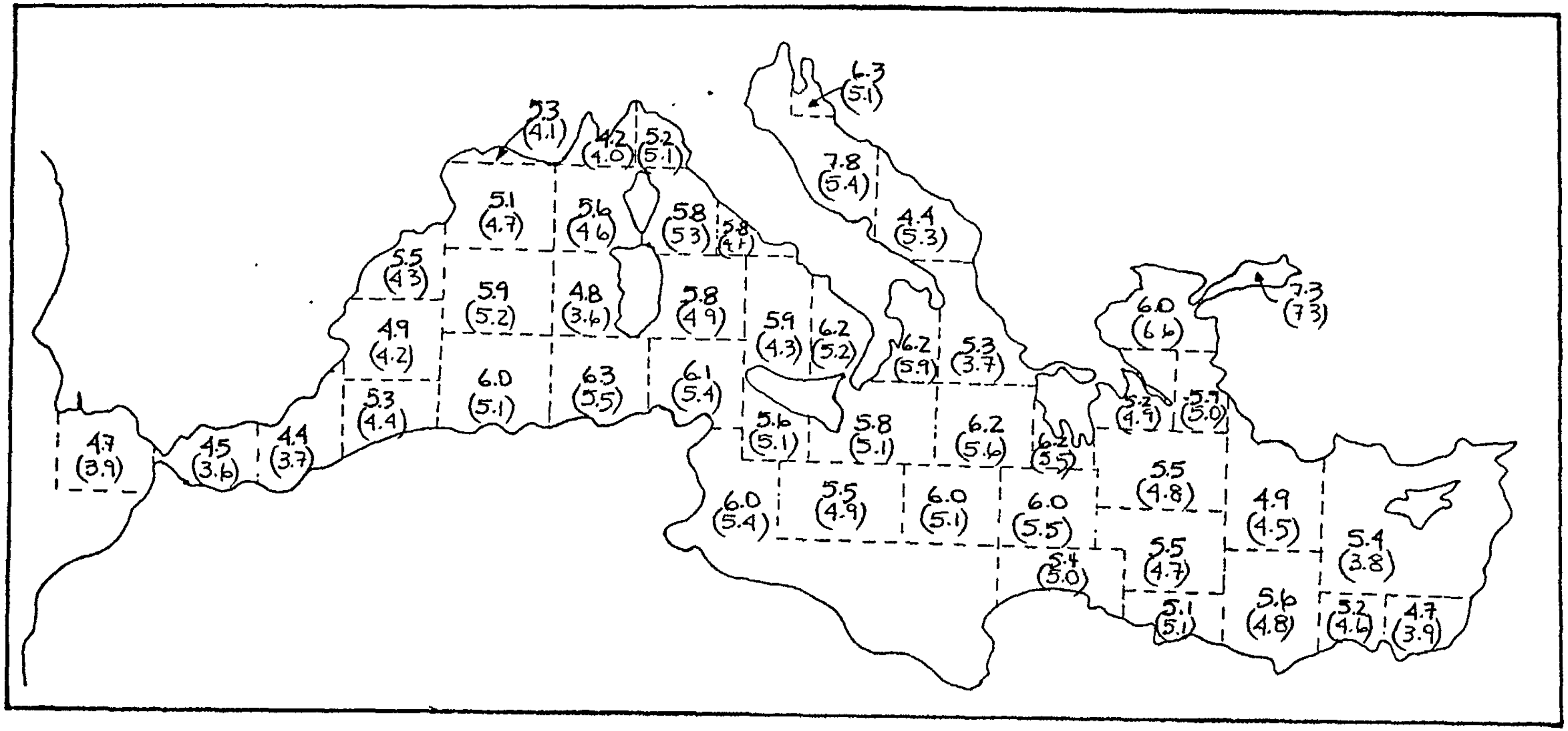

day
(night)

Fig. 49 - Monthly mean cloud amounts (oktas) for day and night - December

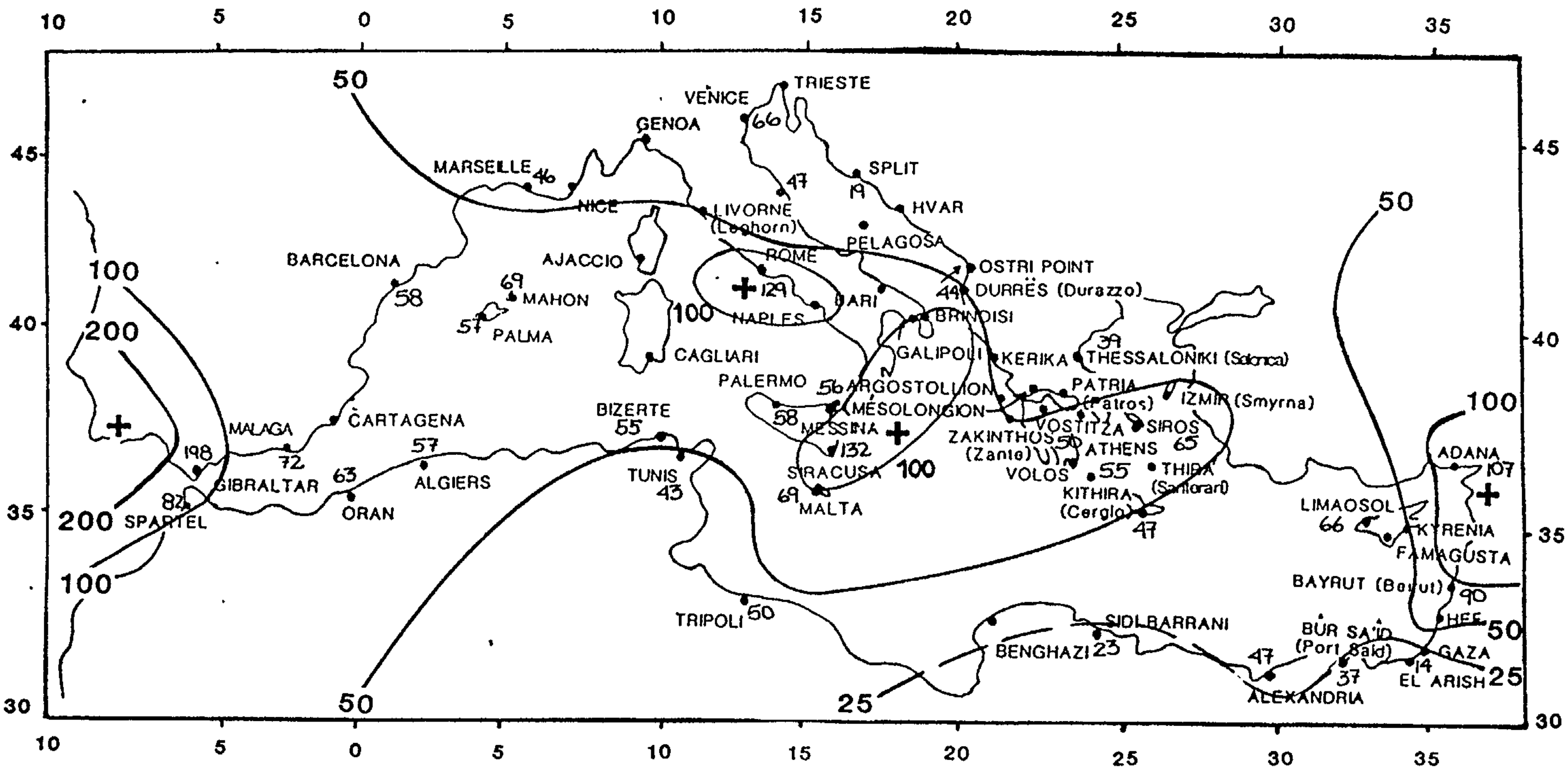

Fig. 50 - D'stribution of maxımum ɑaıly precipitation mm) for January.

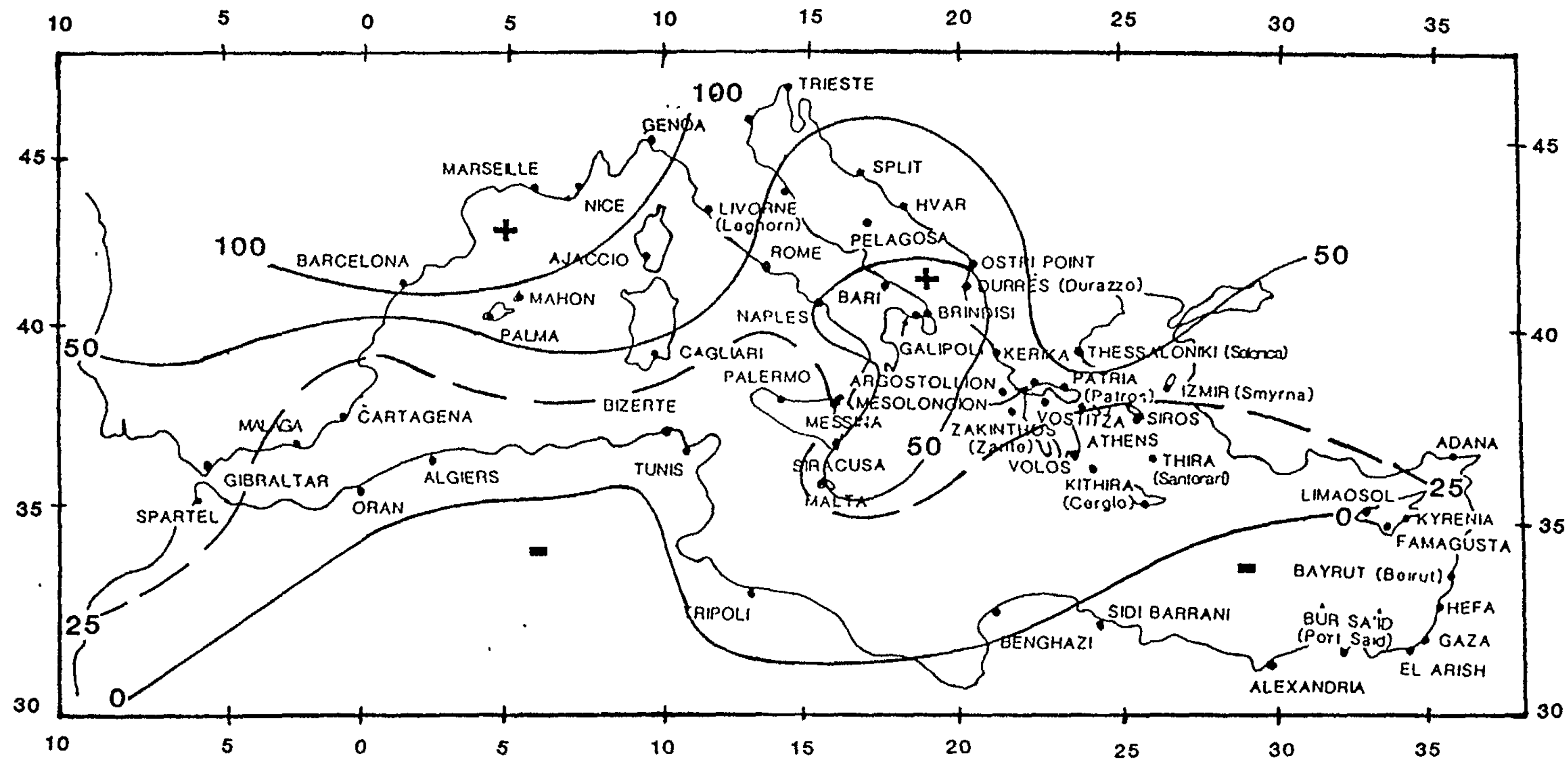

Fig. 51 - Discribution oı maximum daı.y precıpitatıon (mm) for Juıv.

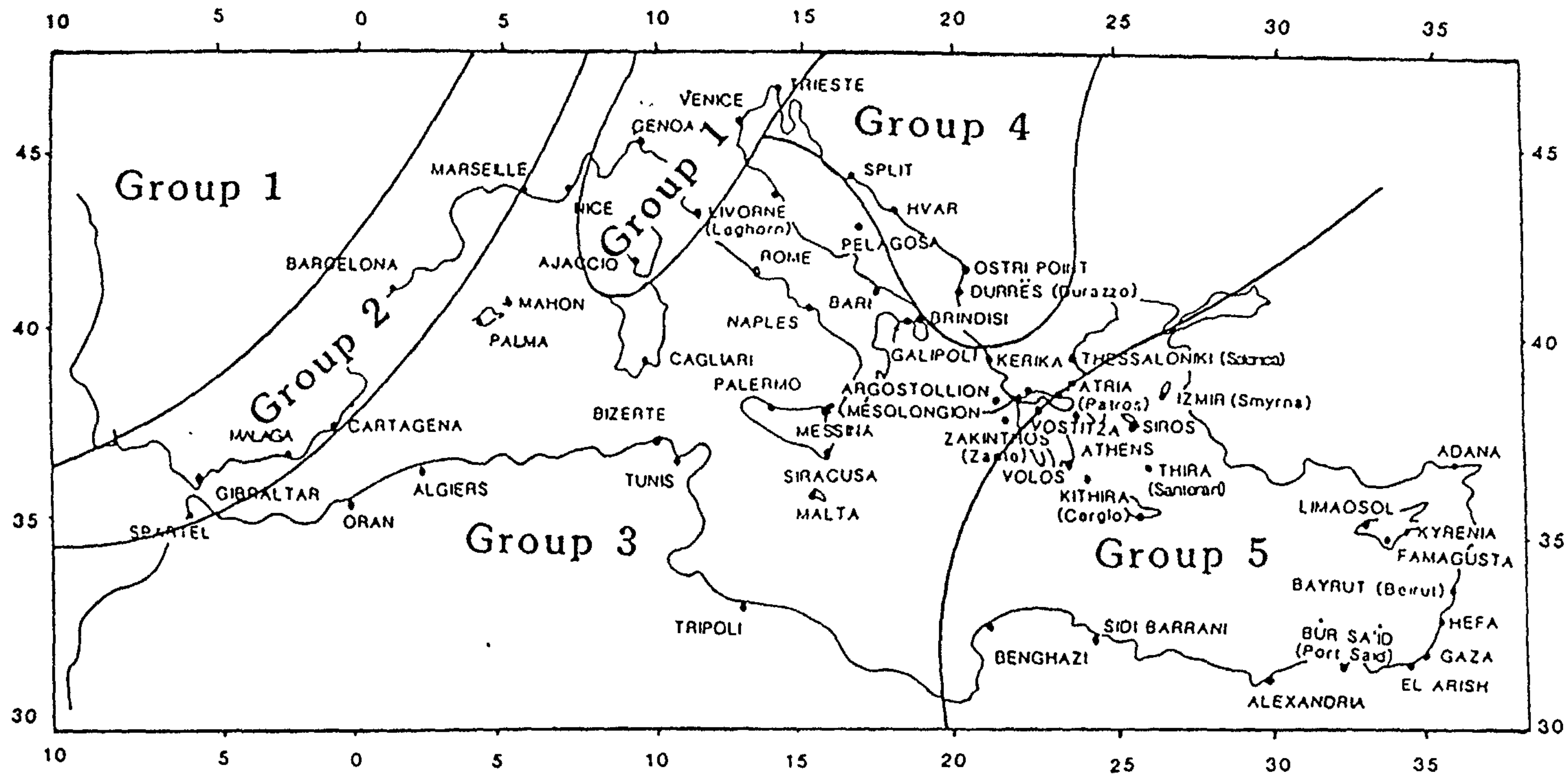

Fig. 52 - Regional groups of precipitation (Goossens, 1985)

PART B

ABSTRACT

Results are given of a detailed study to determine the spatial and temporal (seasonal) distributions of the planetary boundary layer depths* (PBLD) over the Mediterranean Basin. More than 65,000 upper-air measurements from 45 rawinsonde stations in the basin were compiled and analyzed for two consecutive years from spring 1986 through winter 1988. A methodology using both tested and newly developed criteria was applied to determine PBLD values. As expected, the values prove to be generally higher over land and are probably minimum over the eastern and western ends of the Mediterranean Sea. Factors influencing this spatial distribution are mainly topographic, the distance from the shoreline, and to a lesser extent, synoptic weather systems. The most striking temporal effect on PBLD distribution over the Mediterranean Basin is caused by larger scale synoptic weather systems; secondary is the diurnal cycle, which has its largest effects mainly for the summer months.

The PBLD values are displayed as analyzed seasonal maps; typical values were extracted from these maps and are presented in tabular form. The main purpose of this paper is to make available seasonal input values for dynamical meteorological models so that transport and dispersion over the Mediterranean Basin can be better assessed.

* Planetary boundary layer = Atmospheric layer extending from the earth's surface and of depth about 600 to 800 m, within which air motion is affected significantly by surface friction (WMO, 1966).

1.0 INTRODUCTION

In Part A an overview of the meteorological measurements appropriate for the description of transport and dispersion of pollutants in the Mediterranean region is presented. In the conclusion section suggestions are made for further analyses of meteorological data that would help in understanding pollution of the Mediterranean area via the atmosphere.

One of the most important meteorological parameters affecting the dispersion of primary, secondary, and radioactive pollutants in the atmospheric boundary layer is the vertical thermal structure of air from the ground up to about 1500 m (Benarie, 1980). In the Mediterranean Basin, reliable data regarding the vertical thermal structure along the Mediterranean shoreline and the inland variations are required for various purposes such as the following:

(1) Input to atmospheric flow pattern simulation models such as sea and land breeze circulations (Neumann, 1977; Mahrer, 1985).

(2) Input to pollution dispersion simulation models for the coastal plain surrounding the Mediterranean Basin (Segal et al., 1982; Graber et al., 1984).

(3) Determination of the height of power plant stacks sited along the Mediterranean shoreline (Graber et al., 1984) or inland (Dayan et al., 1988).

(4) Studies and assessments of air pollution potential (Rindsberger, 1976; Tadmor and Manes, 1973; Dayan and Koch, 1988).

For these reasons, and Van Dop's (1986) finding that air pollution simulation models are most sensitive to changes in the mixing depth parameter, the object of this second part of the review is to develop a methodology to analyze the daily routine upper-air data measured above the Mediterranean Basin and along the shoreline in order to establish the spatial and temporal behavior of the mixed layer over the whole water body.

2.0 EFFECT OF VARIATIONS IN MIXING HEIGHT ON ATMOSPHERIC DISPERION CALCULATIONS

The height of atmospheric temperature inversions is well correlated with the depth of the mixed layer above an enclosed water body such as the Mediterranean Sea, the latter being usually governed by large-scale synoptic patterns (Holzworth, 1967; Dayan et al., 1988). Also, as discussed below, changes in the depth of the marine mixed layer are related to the formation, duration, and destruction of temperature inversions.

The problem of the stability of the atmosphere near the seashore, over the water body has been discussed by McRae et al. (1981) and Hanna et al. (1984; 1985). Since the summer daytime water temperature is generally lower than the adjacent land temperature, the mixed layer over the water is much thinner than over the land (Hanna et al., 1984). On the other hand, since thermal conditions as well as the sea breeze wind direction are reversed at night (Neumann, 1977), ne can expect a mirror image of the daytime situation for the mixed layer at night, that is, a developed mixed layer over the water and a thinner mixed layer over the land (McRae et al., 1981).

The practical impact of finite mixing depth above the Mediterranean can be seen in "fumigation" and "trapping" of a plume above this basin. In fumigation, the plume is initially emitted above the boundary layer (from a coastal high stack at night, say) and travels above the water undispersed until the late-evening mixing layer grows above water to sufficient depth. Thereafter, rapid downward mixing can lead to high sea-surface-level concentrations at appreciable distances offshore downwind of the coastal source.

The term trapping is applied to the more general situation in which vertical mixing is impeded because of the finite depth of the mixing layer above the sea, which is formed by the distinct interface between the inflow and the outflow layers (Fig. 1). This maintains sea-level pollutant concentrations that are higher than those that would prevail under conditions of unlimited vertical mixing. Beyond some distance offshore, in the open sea, the transported pollutant can be considered to be spread uniformly throughout the mixing layer.

The above discussion on the effect of variations in the mixing layer on atmospheric dispersion above the Mediterranean Sea is very idealized and glosses over many complexities and uncertainties because data on the temperature profiles over the open sea are not yet available. Therefore, no attempt is made in this part of the review to quantify precisely the changes of the mixed layer over the transition area from the open sea to the coastal surroundings of the Mediterranean Basin; rather, the mixed layer is characterized on a seasonal basis over the whole water body, as analyzed from synoptic radiosonde data.

3.0 CHARACTERISTICS OF TRANSPORT AND DISPERSION OVER WATER BODIES AND ALONG THE MEDITERRANEAN LITTORAL REGIONS

No distinction is made here between different forms of industrial pollutants emitted from the Mediterranean coastal environments, because, from the point of view of over-water and coastal dispersion, no distinction is necessary between the emissions of nuclear, chemical or other industries.

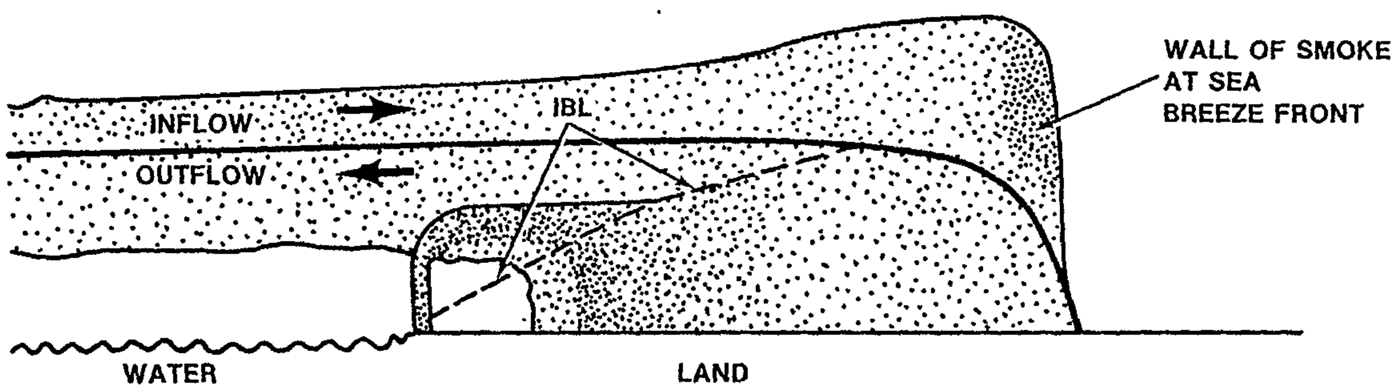

Fig. 1: General smoke pattern observed by Lyons and Olsson (1973) (adapted from their paper) in a well-developed lake breeze. Intensity of shading represents smoke intensity. The heavy line represents the interface between the inflow and outflow layers; the dotted line represents the internal boundary layer.

3.1 Specific Features of Over-Water Dispersion and Transport

The over-water meteorological data necessary for characterizing offshore dispersion are different from over-land meteorological data. For example, categories of over-land turbulence levels, which have been successfully parameterized as a function of solar radiation and wind speed only, can be used without considering surface temperature or humidity. This is not the case for the boundary layer over water surfaces where diurnal temperature changes are quite small but response times make turbulence heat fluxes important. Over-water turbulence levels are largely governed by the air-water temperature difference, over-water wind speed, and specific humidity.

The data compiled and analyzed in part A of this review lead to the general conclusion that dispersion over water is less than that over land around the Mediterranean Sea. This is primarily because of the reduction in mechanical turbulence due to the smoother water surface. The actual magnitude of over-water diffusion is influenced by the thermal stratification of layers above the sea-surface. For example, in the spring, relatively warm air is advected offshore from the North Africa Coast to the Mediterranean cooler waters; the resulting inversion conditions act to reduce any mechanically generated turbulence and therefore to minimize dispersion. In the early morning hours of the fall, if relatively cool air is advected over warmer shallow Mediterranean waters, the situation is reversed. Nevertheless, most studies indicate that for the same atmospheric stability condition, as specified by the thermal lapse rate, dispersion over-water is generally less than that over land, because of the smoother water surface.

A further consequence of the smoother water surface is that the wind speed is usually greater. Such intensification above the sea was observed in Section 2.1.1 of Part A of this review, in which monthly averaged winds over the sea-surface were displayed as arrows in each 1° square representing the mean vector of all observed winds. The reduced surface frictional effect reduces the wind speed shear and so increases the low-level wind speed. Noteworthy is the corresponding change in wind direction shear, as displayed in Figs. 12-14, Part A, resulting in a wind direction shift as air traverses the Mediterranean coastline.

3.2 Dependence of Over-Water Diffusion on the Over-Water Temperature Profile

The dependence of over-water diffusion on the over-water temperature profile has been demonstrated by Prophet (1961). He computed vertical eddy diffusivities from a number of experiments reported in the literature, as a function of the water-air temperature difference. In Fig. 2, the strong dependence of vertical diffusion rates over water on the temperature difference can be seen. The Mediterranean Sea, being a small and almost enclosed water body, is relatively warm; therefore the water-air temperature difference is expected to be small, not more than 3°-5°C, the positive value indicating that water is warmer than air. This is true even in the spring, when the sea reaches its coldest water temperature. This small temperature difference assures usually reduced values of vertical eddy diffusivity. Hence, marked convective turbulence is not expected over the Mediterranean Sea. It is clear that under these weak turbulent conditions, dispersion would be quite reduced, although as mentioned in Part A, no data exist to allow this to be quantified above the Mediterranean Basin.

In conclusion, therefore, transport over water seems to be characterized by increased wind speeds and reduced dispersion, when compared with over-land transport. The quantitative nature of these effects is governed by the over-water temperature profile; therefore an analysis of radiosonde profiles above the Basin is given here in Part B in order to calculate noontime monthly climatological values of the mixing depth for the whole Mediterranean region.

4.0 DESCRIPTION OF THE UPPER-AIR DATA BASE

The planetary boundary layer depth (PBLD) values in the present study are derived from observed upper-air rawinsonde data in the Mediterranean Basin. The source for this data base is a NOAA Air Resources Laboratory upper-air observation archive for the Mediterranean Basin.

Station location with respect to the sea shore, and station elevation have an important role in determining thermal stratification of the atmosphere above the Mediterranean Sea. Fig. 3 gives the station locations for this study; Fig. 4 presents station elevations.

There were 45 rawinsonde stations included in this data base. Synoptic rawinsonde measurements are taken according to WMO protocols each 6 hours for some western stations along the Mediterranean Basin and at least every 12 hours (at 0000 and 1200 GMT) for all sites. Therefore, the PBLDs were calculated for these two latter observation times (i.e., midnight and midday). PBLD values were calculated and are displayed as seasonal maps for two consecutive years from spring 1986 through winter 1988.

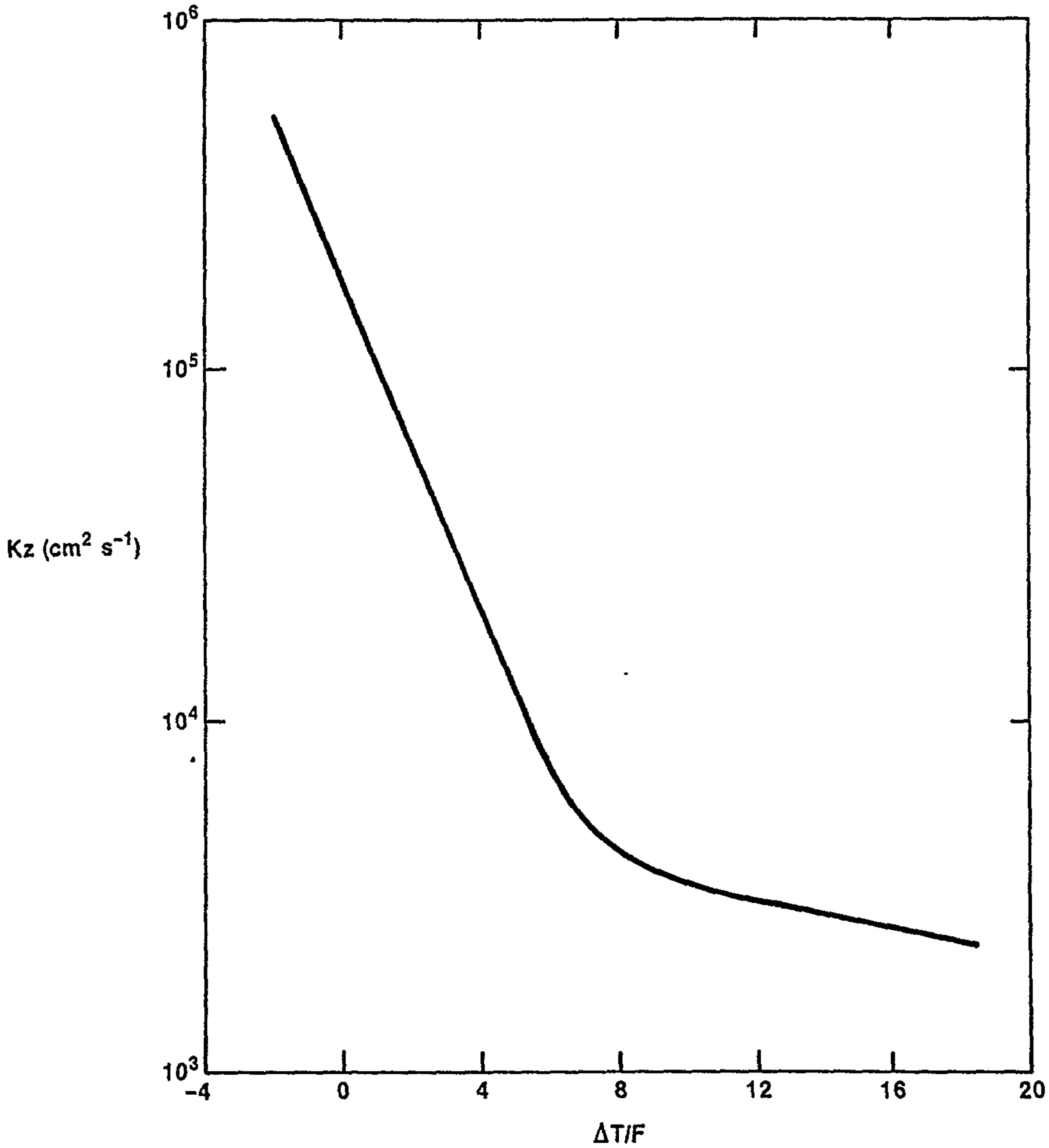

Fig. 2: Vertical eddy diffusivity for over-water flow (Kz) as a function of the over-water temperature difference (ΔT), as computed by Prophet (1961).

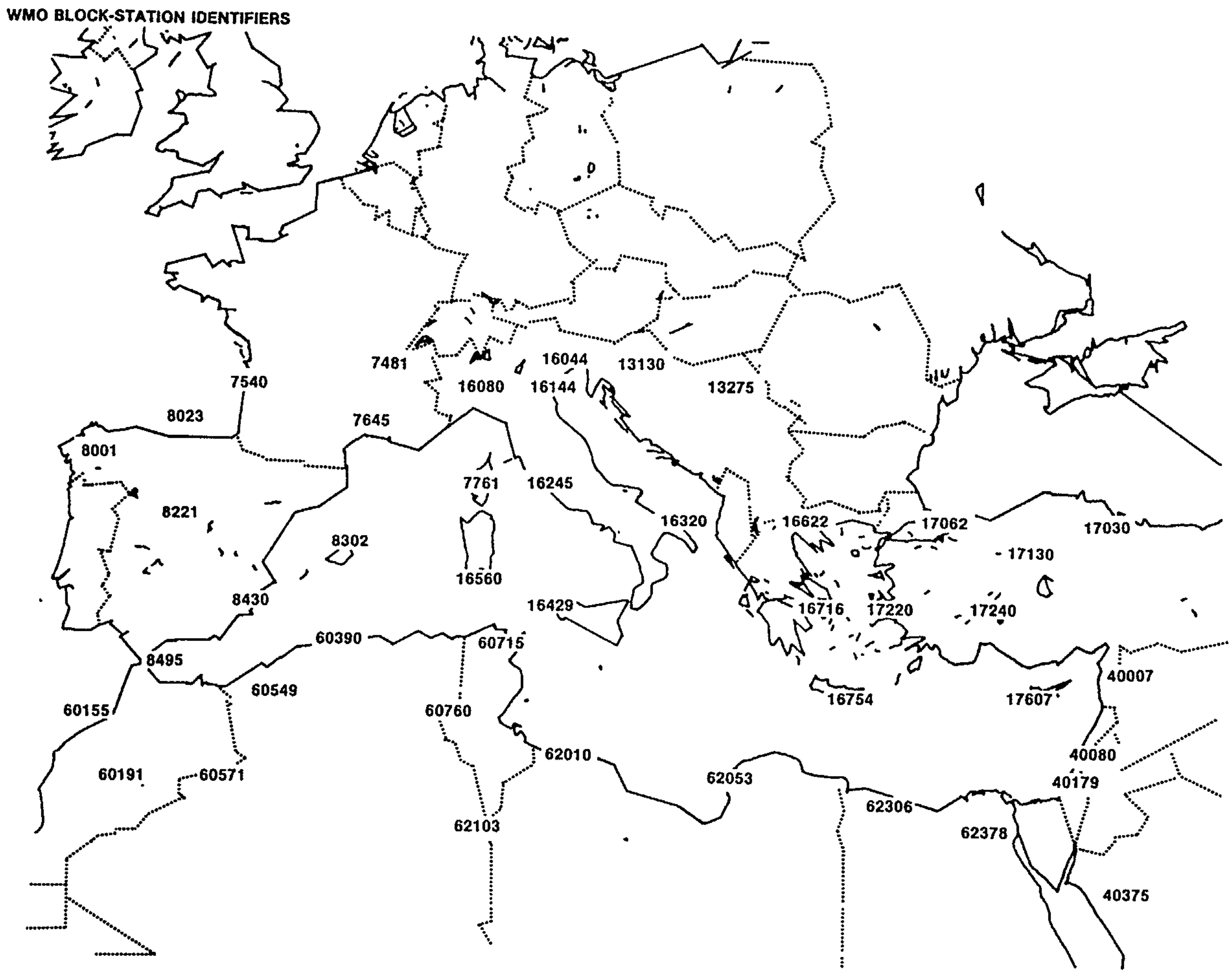

Fig. 3: Locations of rawinsonde stations, designated by WMO block-station identifiers.

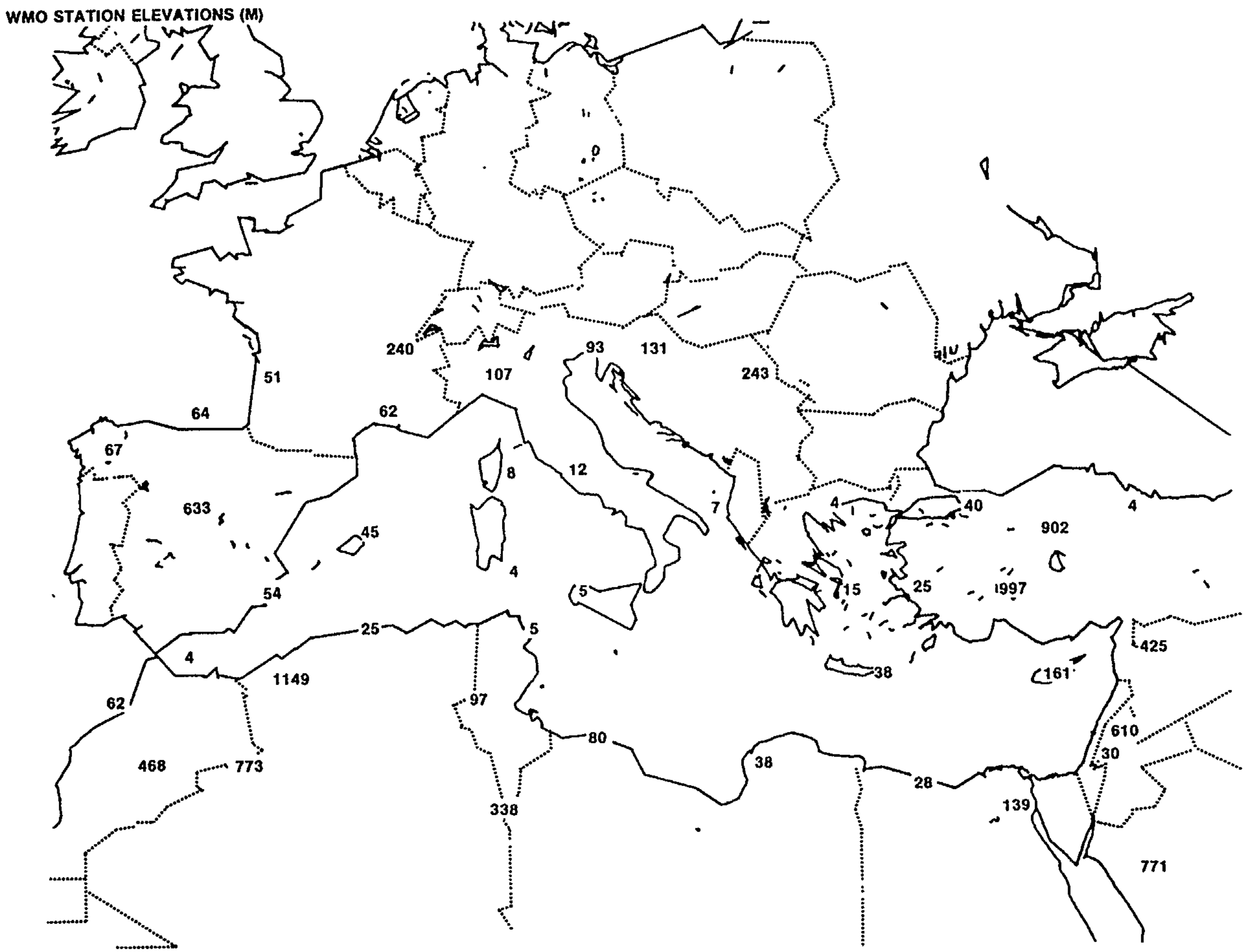

Fig. 4: Elevations (m) of the WMO rawinsonde stations shown in Fig. 3.

5.0 DETERMINATION OF PLANETARY BOUNDARY LAYER DEPTH (PBLD)

The vertical extent of mixing for long-range transport and dispersion models is not necessarily confined to the depth of the boundary layer. Furthermore, numerous methods for estimating mixing depths with application to diffusion are cited in the literature (Hanna, 1969; Holzworth, 1967; Nieuwstadt, 1980; Nieuwstadt and Van Ulden, 1978; Van Ulden and Holtslag, 1985). This diversity of methods is especially emphasized when the nature of dispersion is nonbuoyant or momentum driven, such as dispersion of passive contaminants released from a continuous and wide area source in the atmospheric surface layer above the Mediterranean Basin. Therefore we thought it most appropriate here to use the PBLD as determined for rawinsonde temperature profiles around and within the Mediterranean Sea. This PBLD value was calculated by a methodology in which two criteria were used (Fig. 5):

1) The lapse rate: $\Delta\theta/\Delta Z \geqslant 0.005^{\circ}K/m$.

2) The temperature change in the inversion: $\theta_{Top} - \theta_{Bottom} \geqslant 2^{\circ}K$.

Here θ = potential temperature and Z = height. The maximum PBLD value was set to a default of 3000 m whenever both criteria could not be met. Since vertical resolution for transport in most models is equal to or greater than 300 m, this value was adopted as the minimum PBLD value.

To assure reliable PBLD comparisons within the Mediterranean Basin, the PBLD climatological averages were incorporated in the analyses only if at least 45 soundings were available during each season.

6.0 MAPS OF SEASONAL DISTRIBUTIONS OF THE PBLD

Seasonal maps of the planetary boundary layer depths (m) follow for spring 1986 through winter 1988 over the Mediterranean Basin at 0000 GMT and 1200 GMT where SPRG = March, April, May; SUMR = June, July, August; FALL = September, October, November; and WNTR = December, January, February.

Each map is identified at upper left.

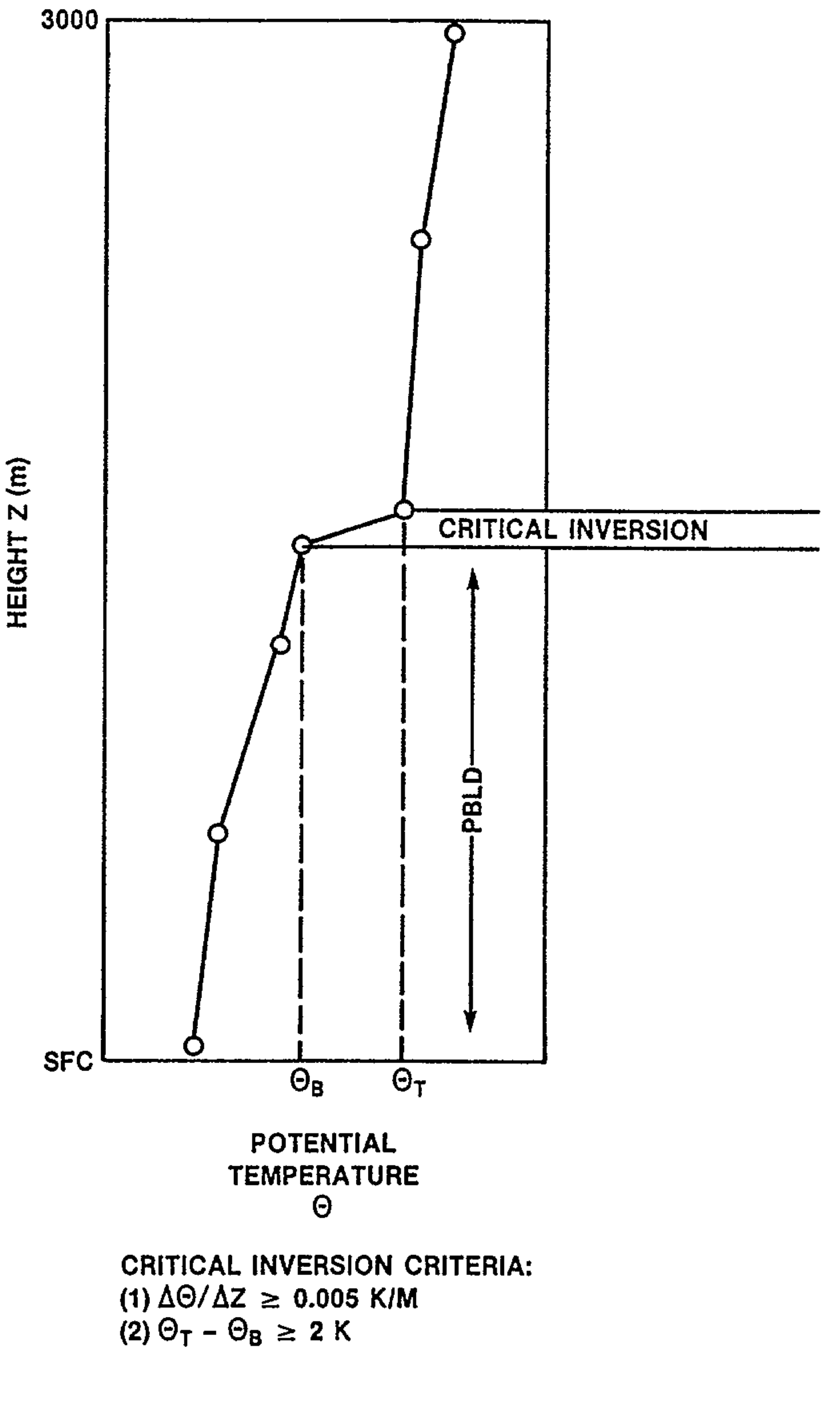

Fig. 5: Method used for determining PBLD values from rawinsonde data.

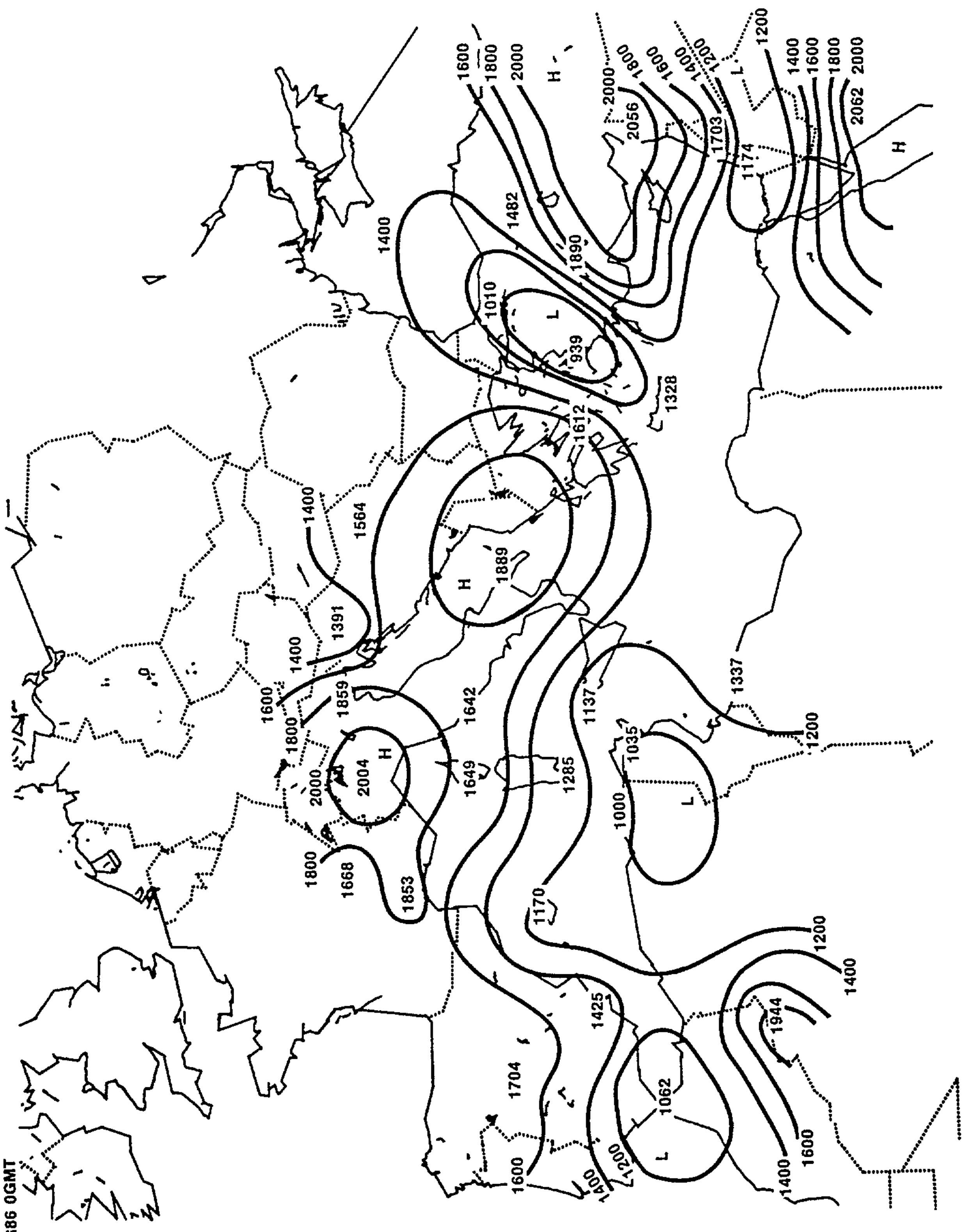

Map 1
SPRG86 0GMT

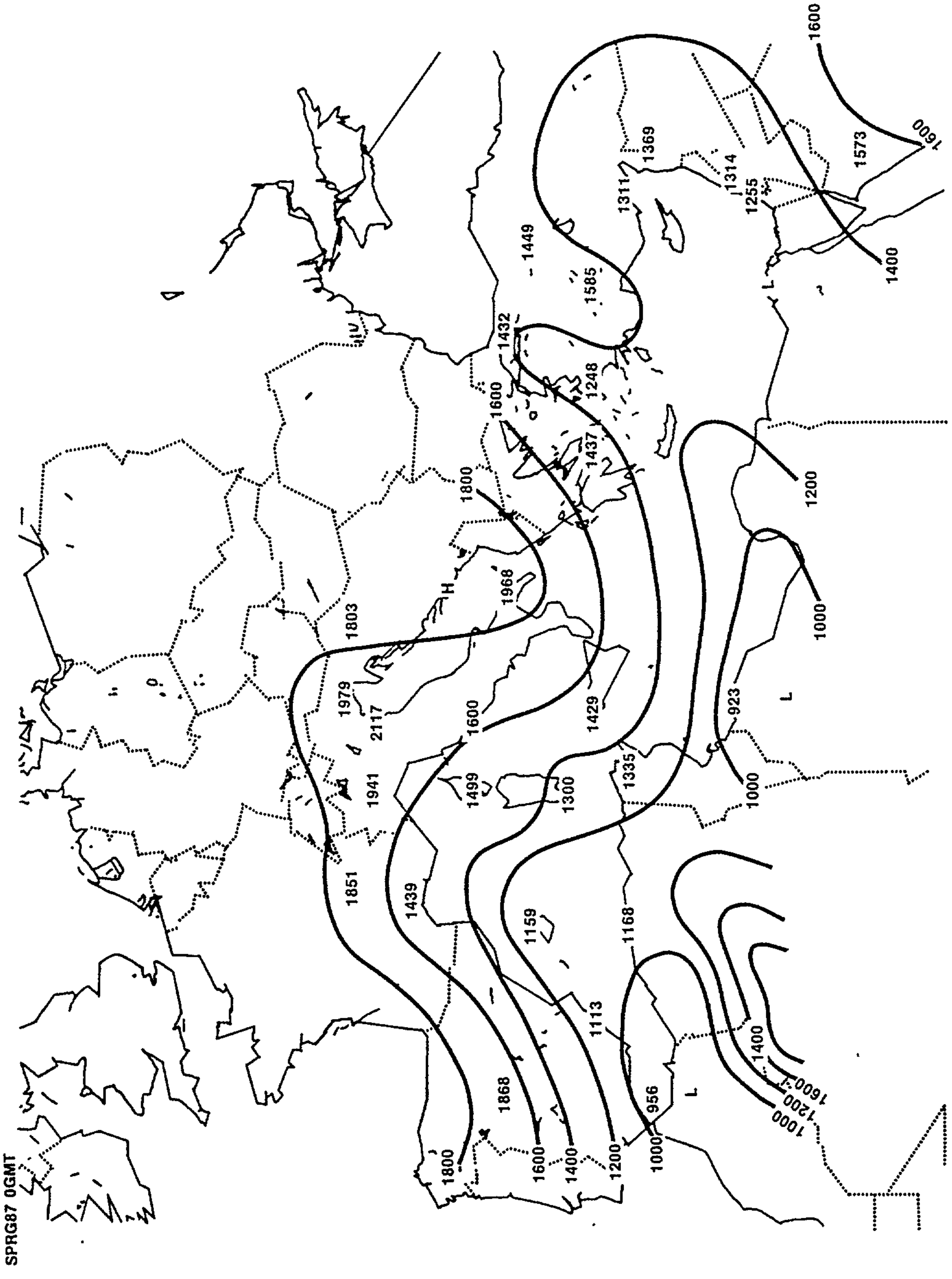

Map 2
SPRG87 0GMT

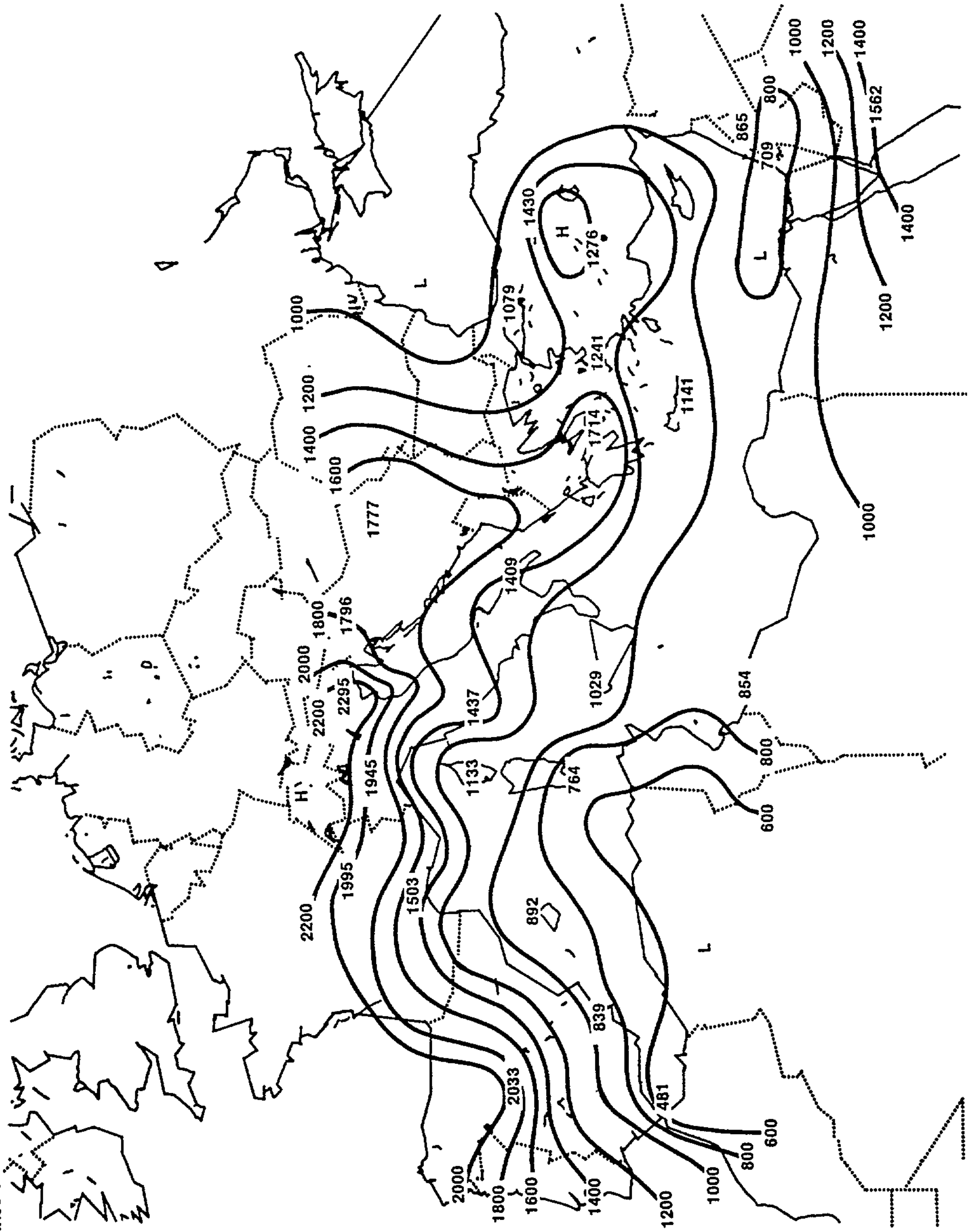

Map 3
SUMR86 0GMT

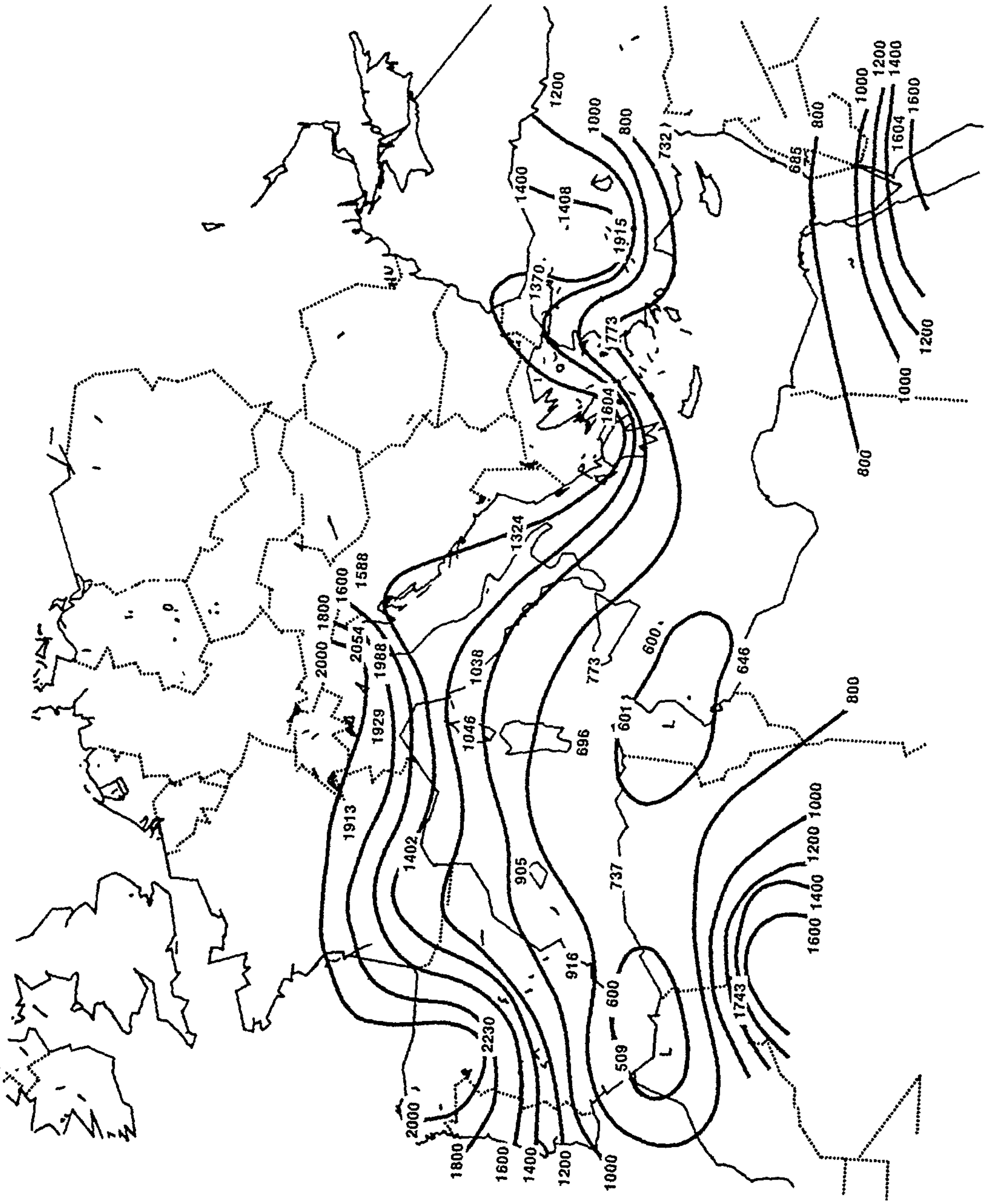

Map 4
SUMR87 0GMT

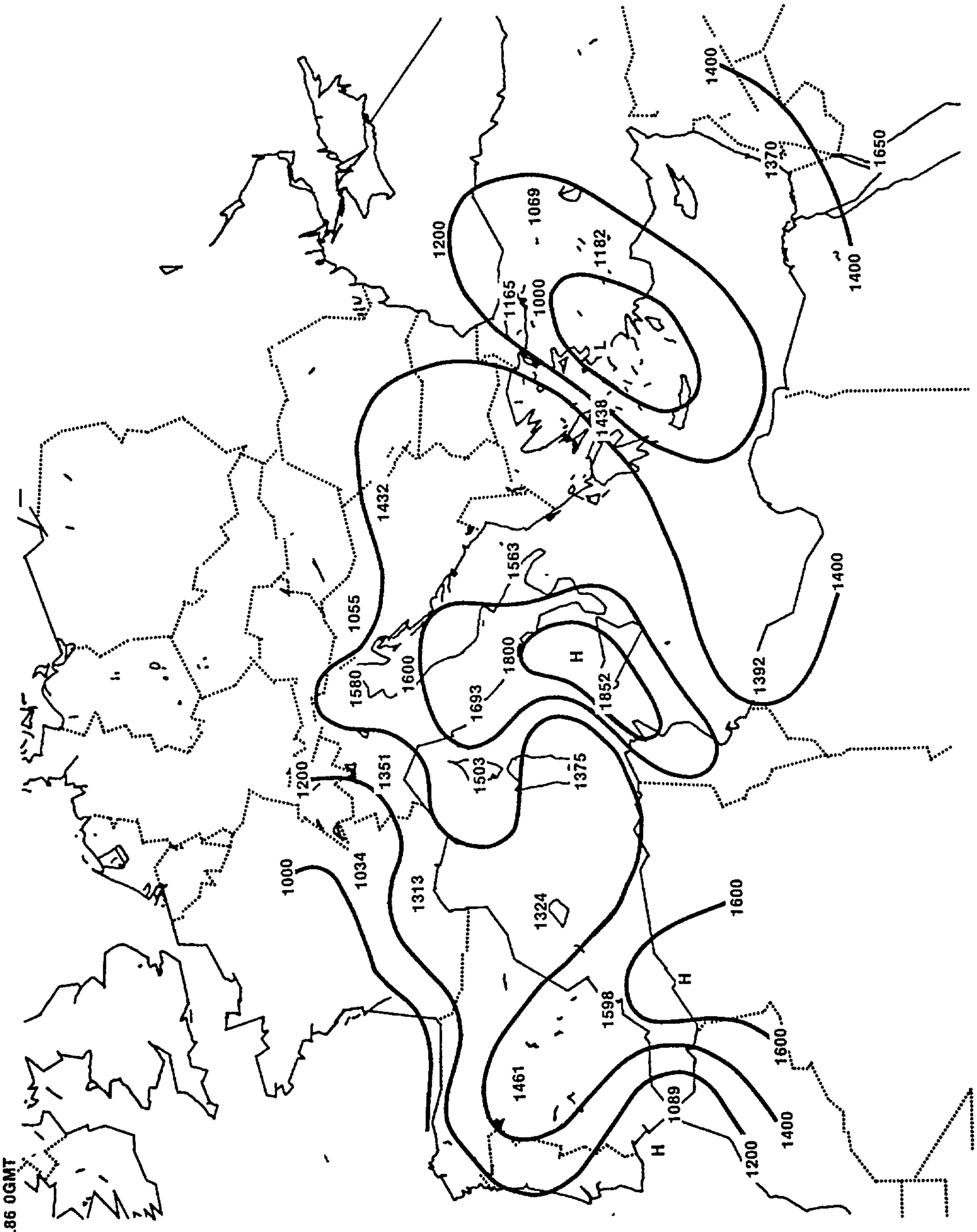

Map 5
FALL86 0GMT

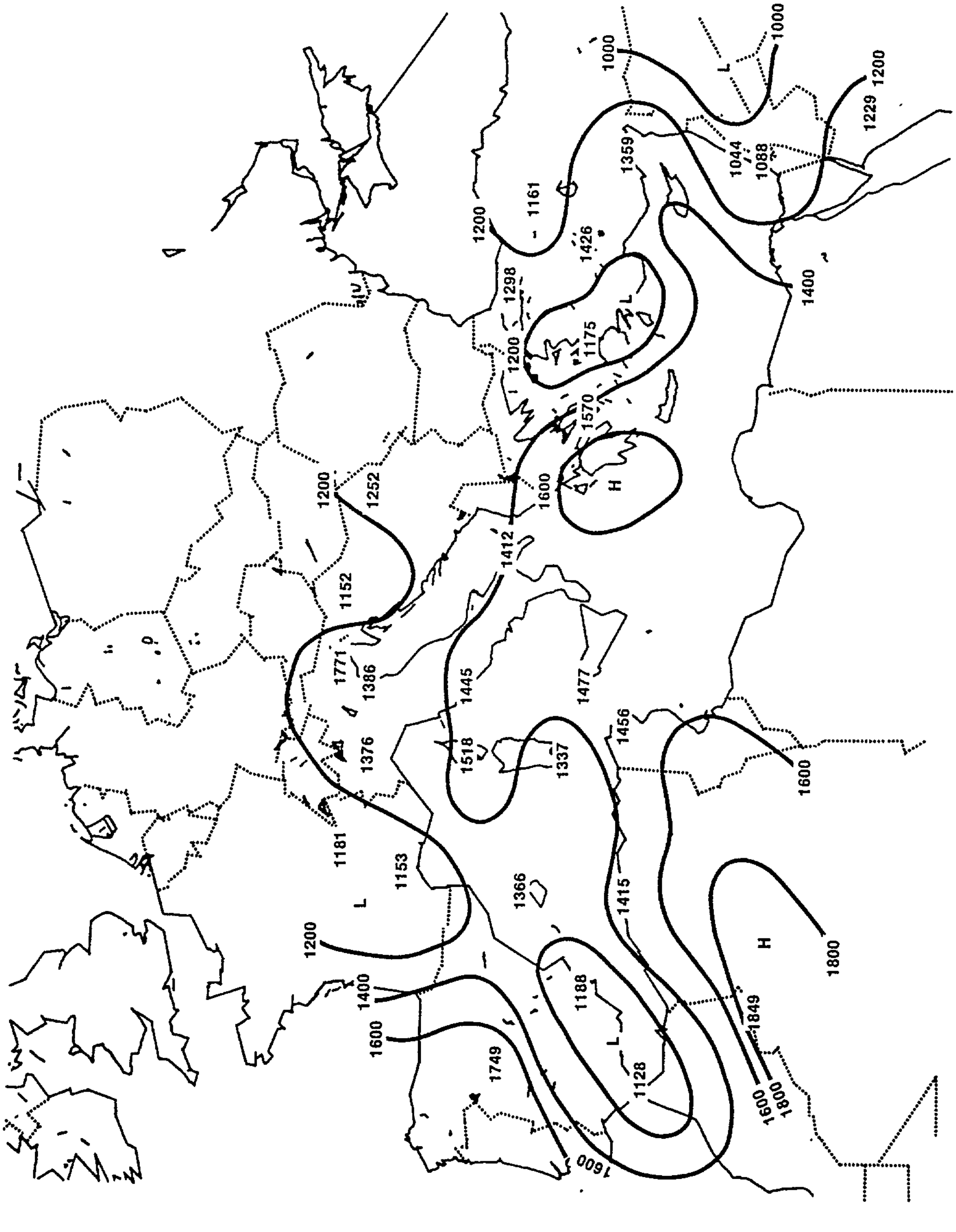

Map 6
FALL87 0GMT

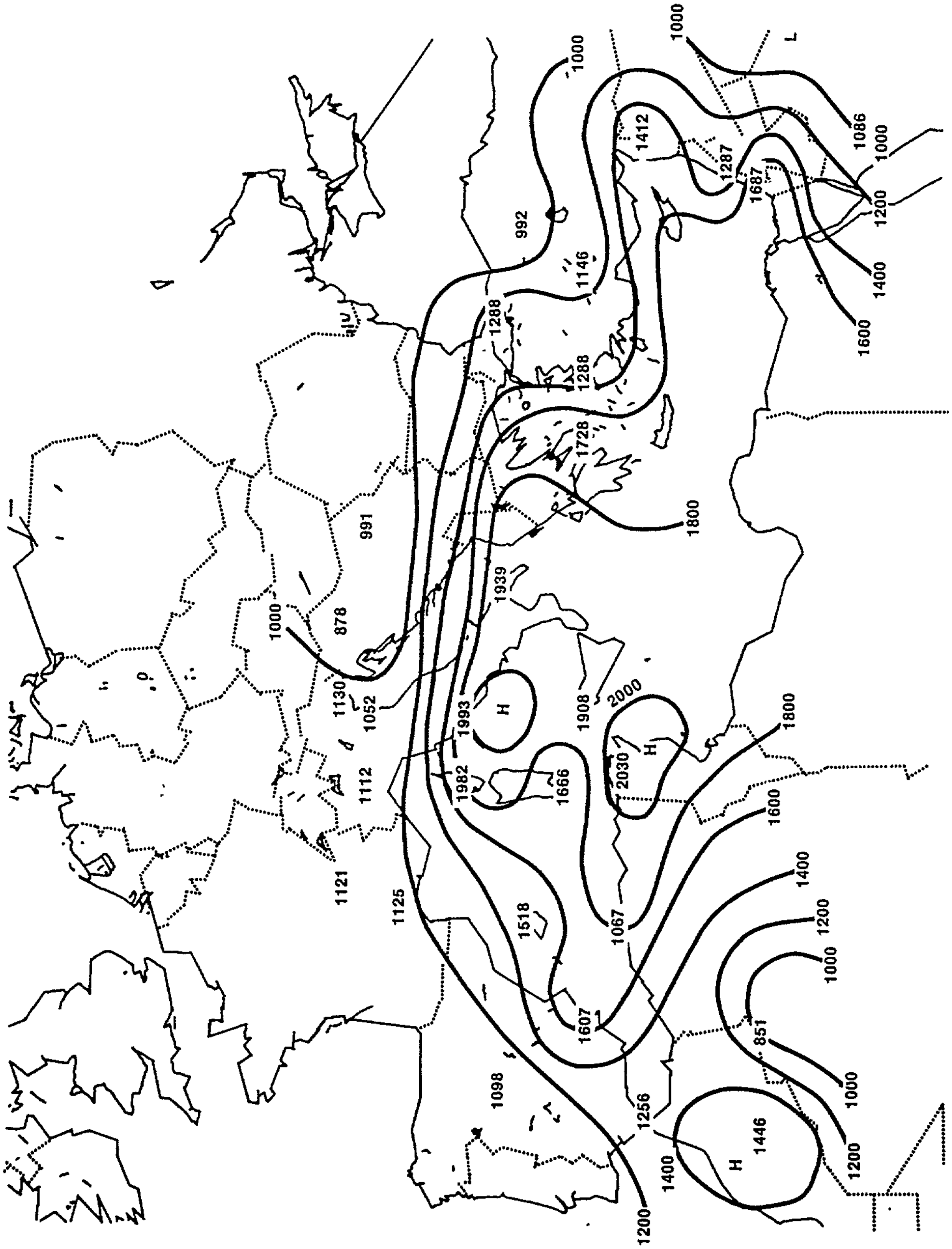

Map 7
WNTR87 0GMT

Map 8
WNTR88 0GMT

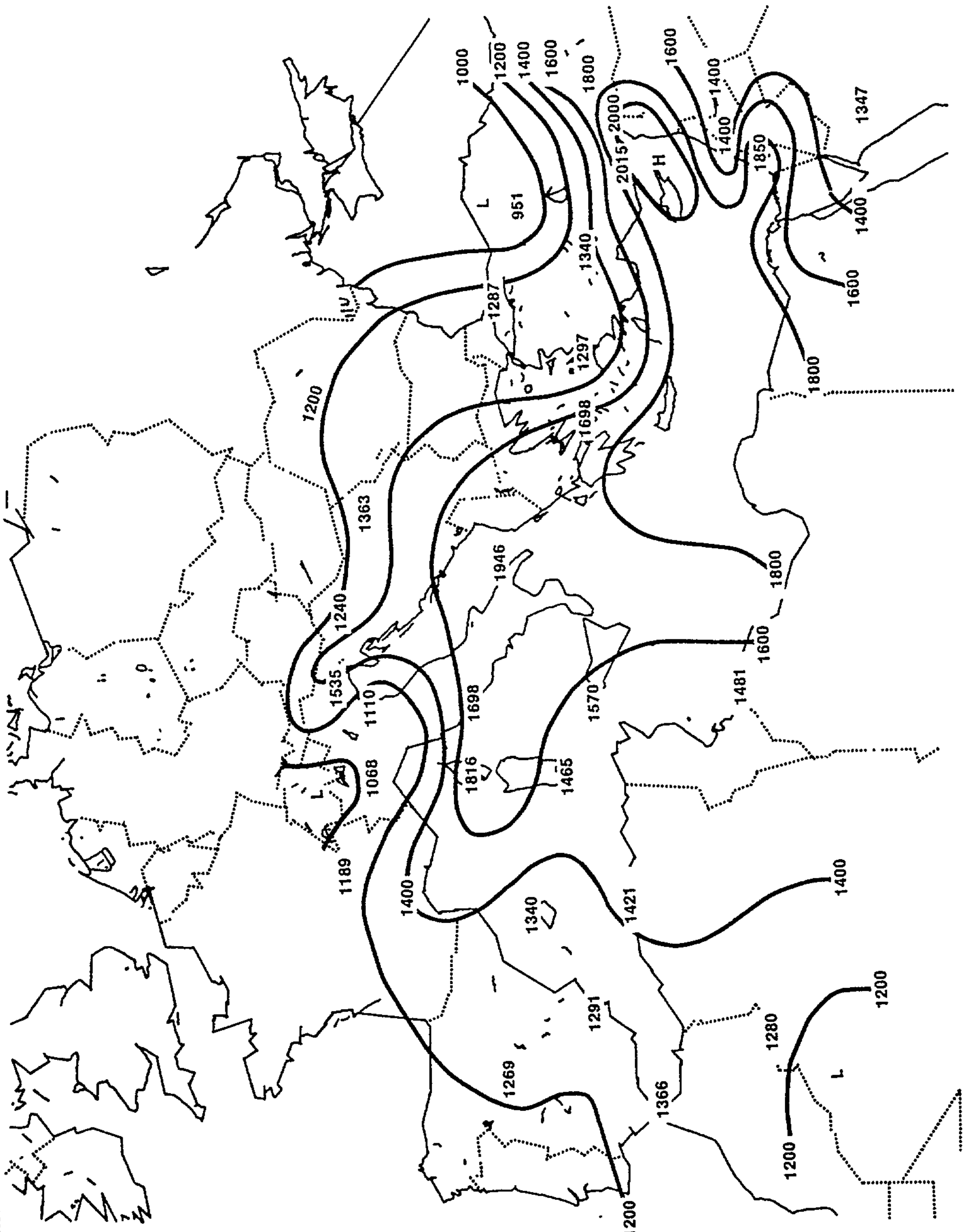

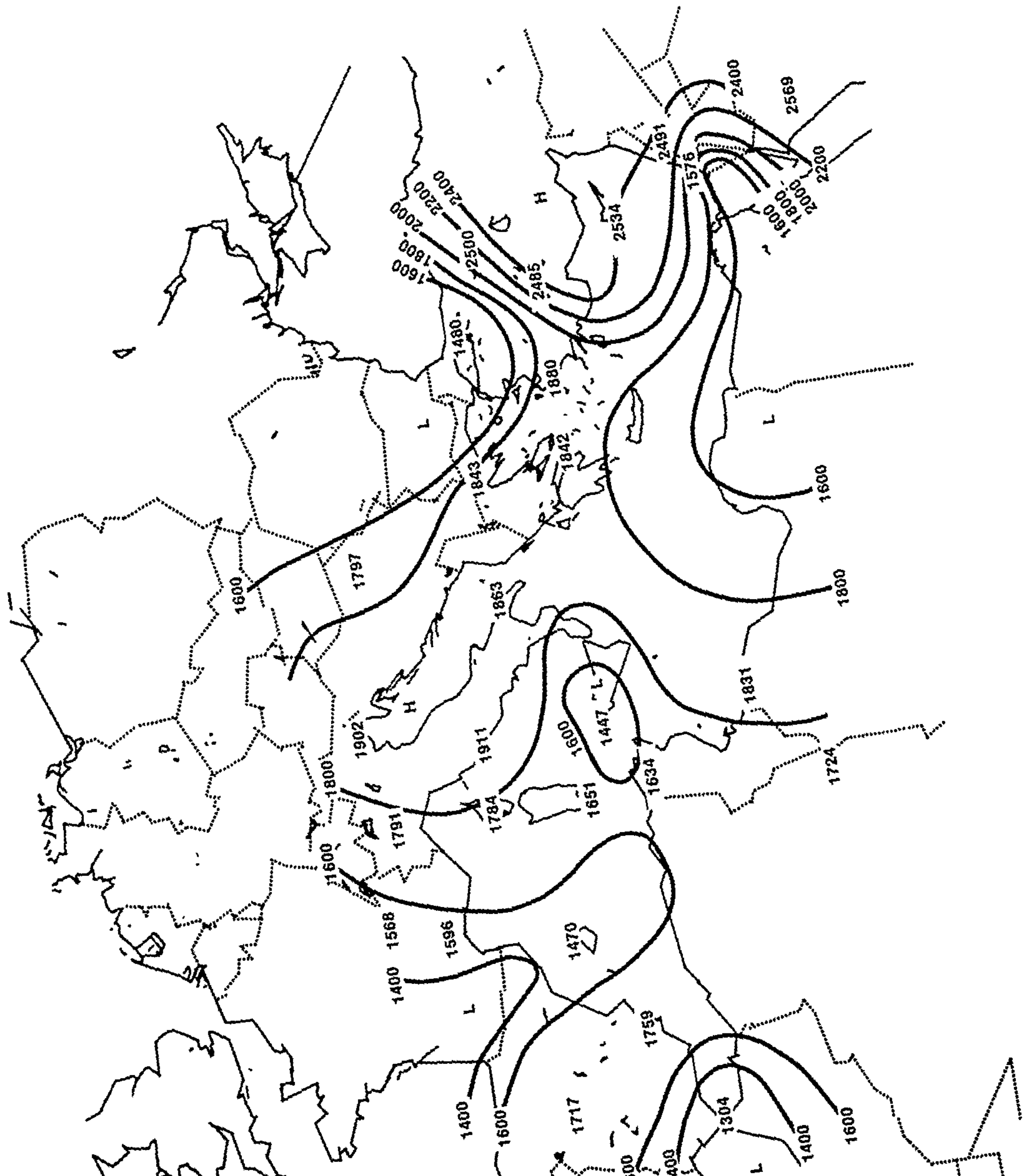

Map 9
SPRG86 12GMT

Map 10

SPRG87 12GMT

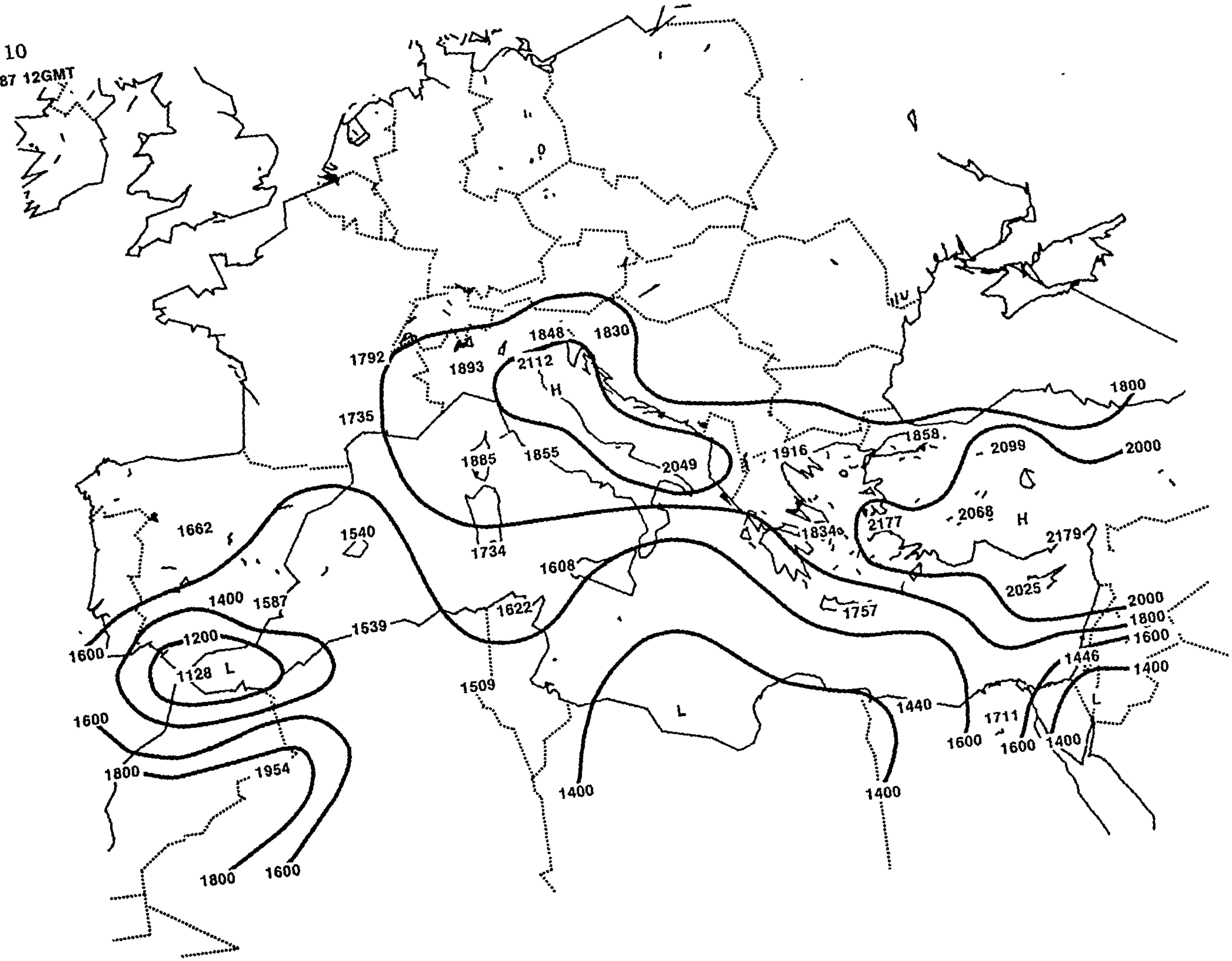

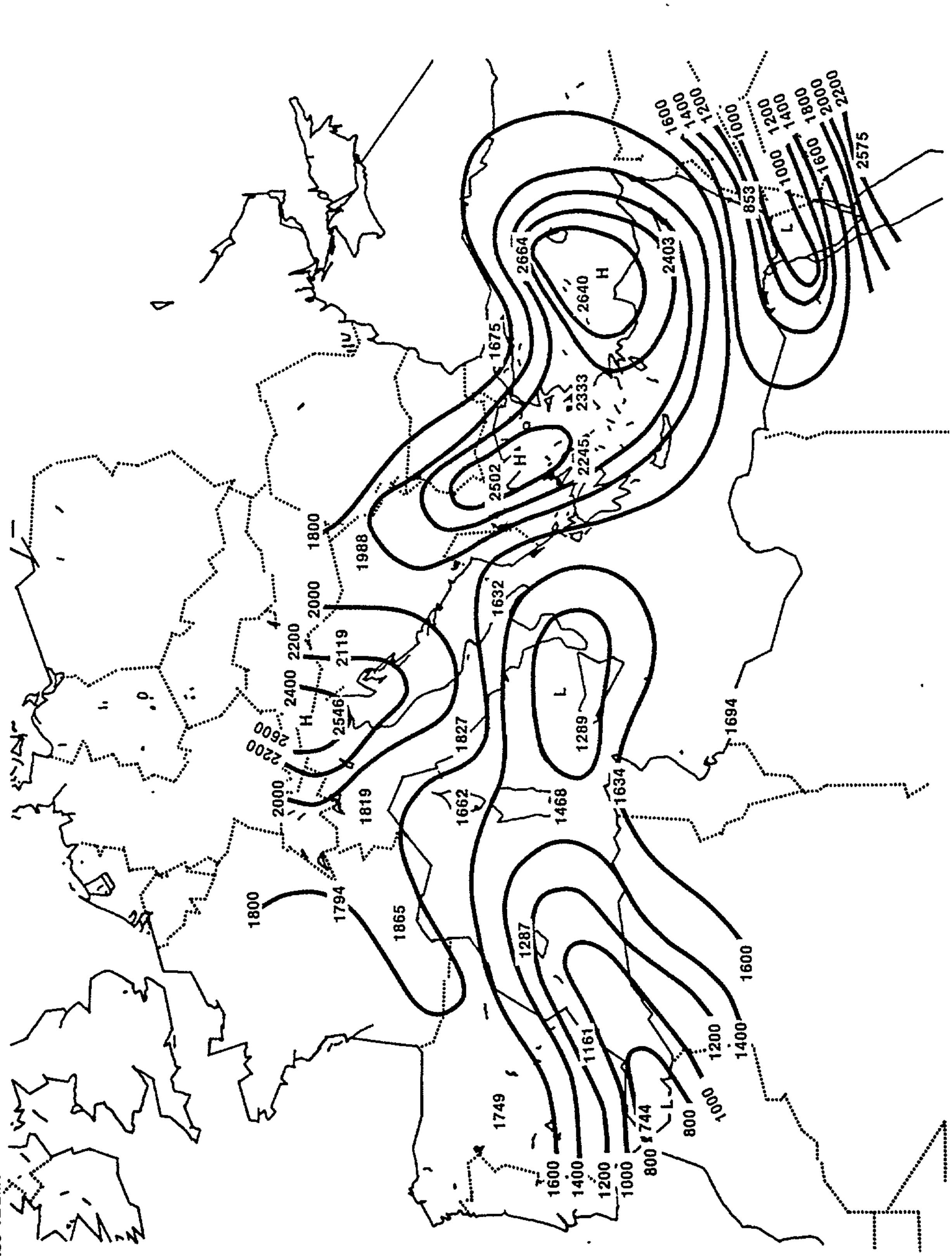

Map 11
SUMR86 12GMT

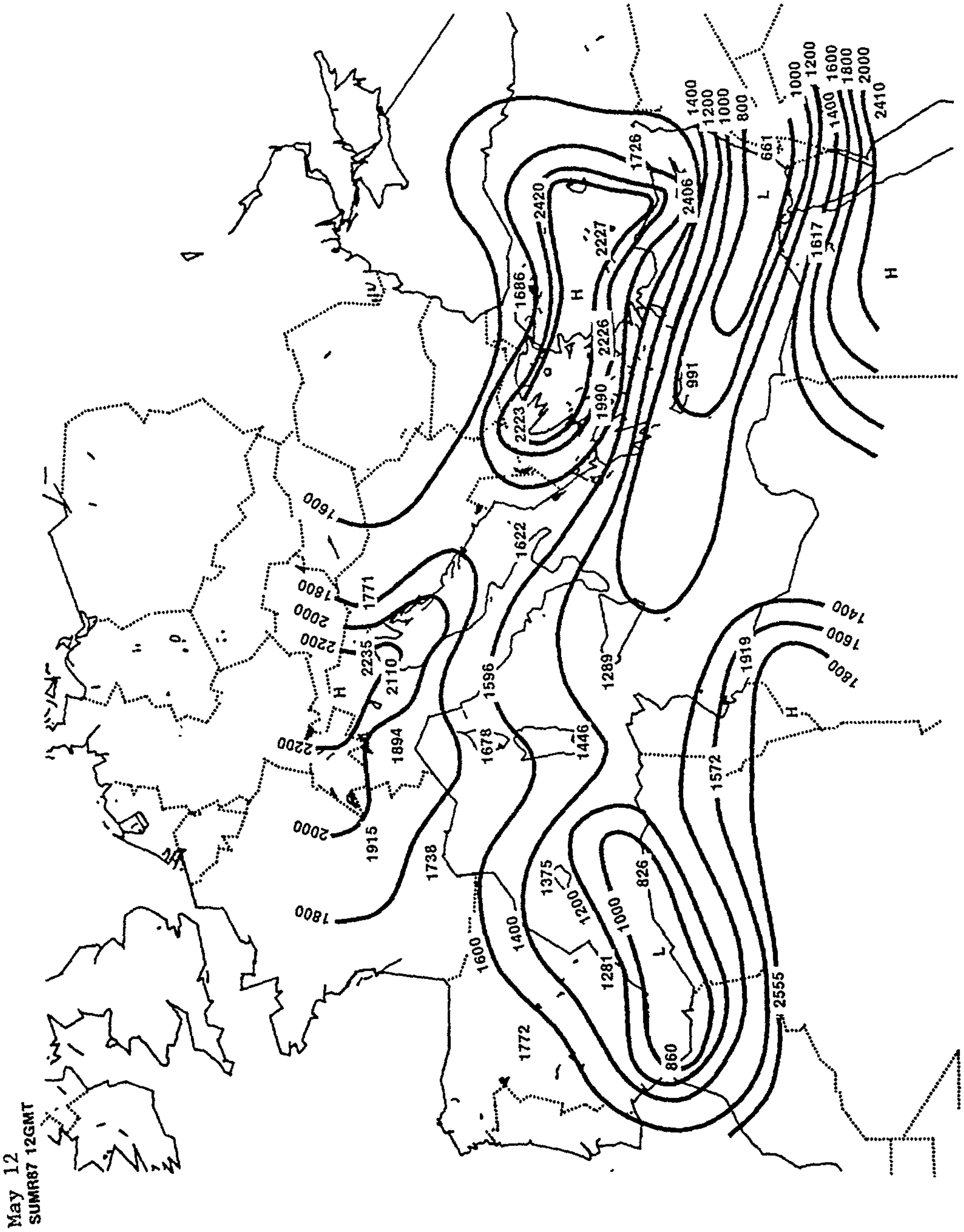
May 12
SUMR87 12GMT

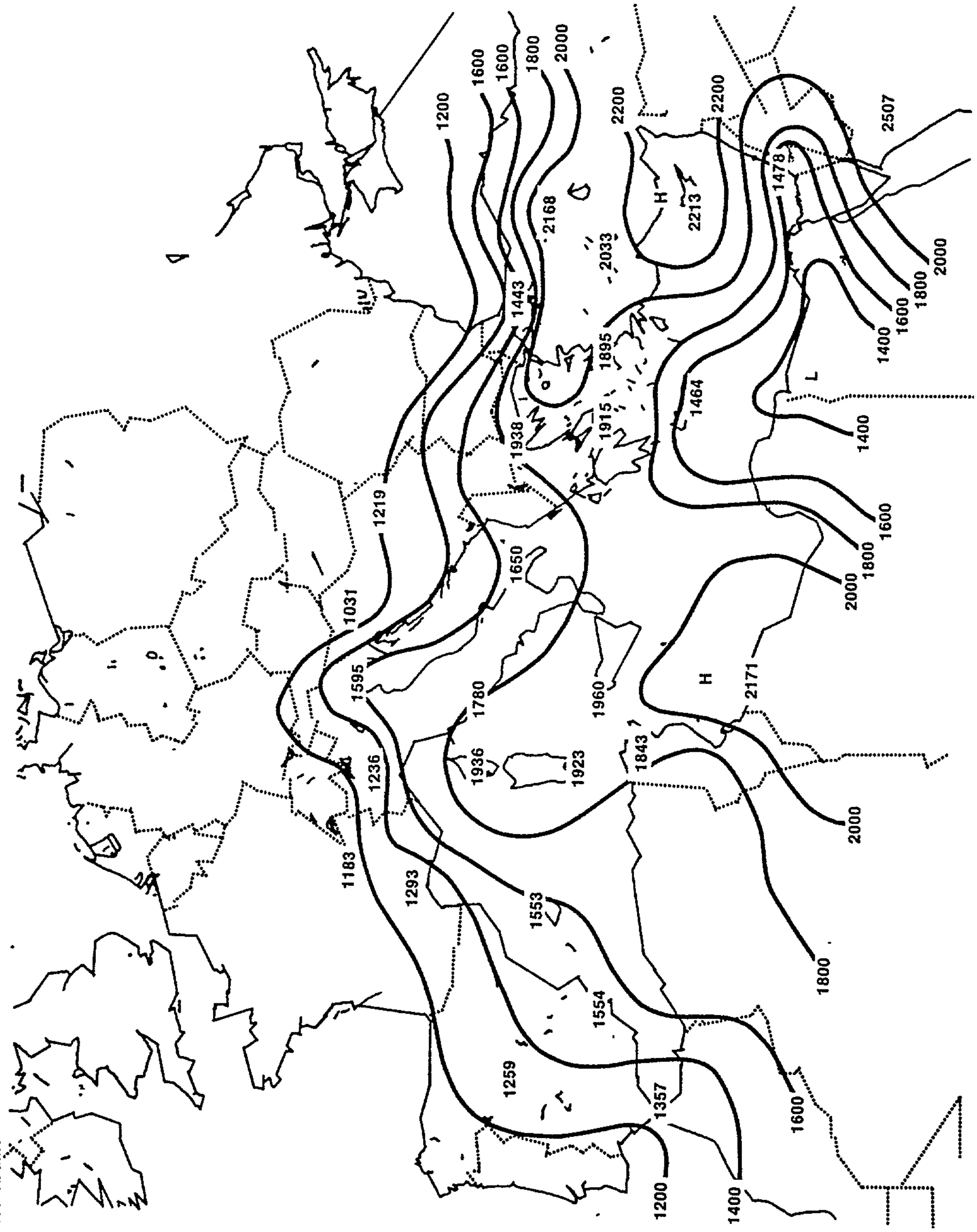

Map 13
FALL86 12GMT

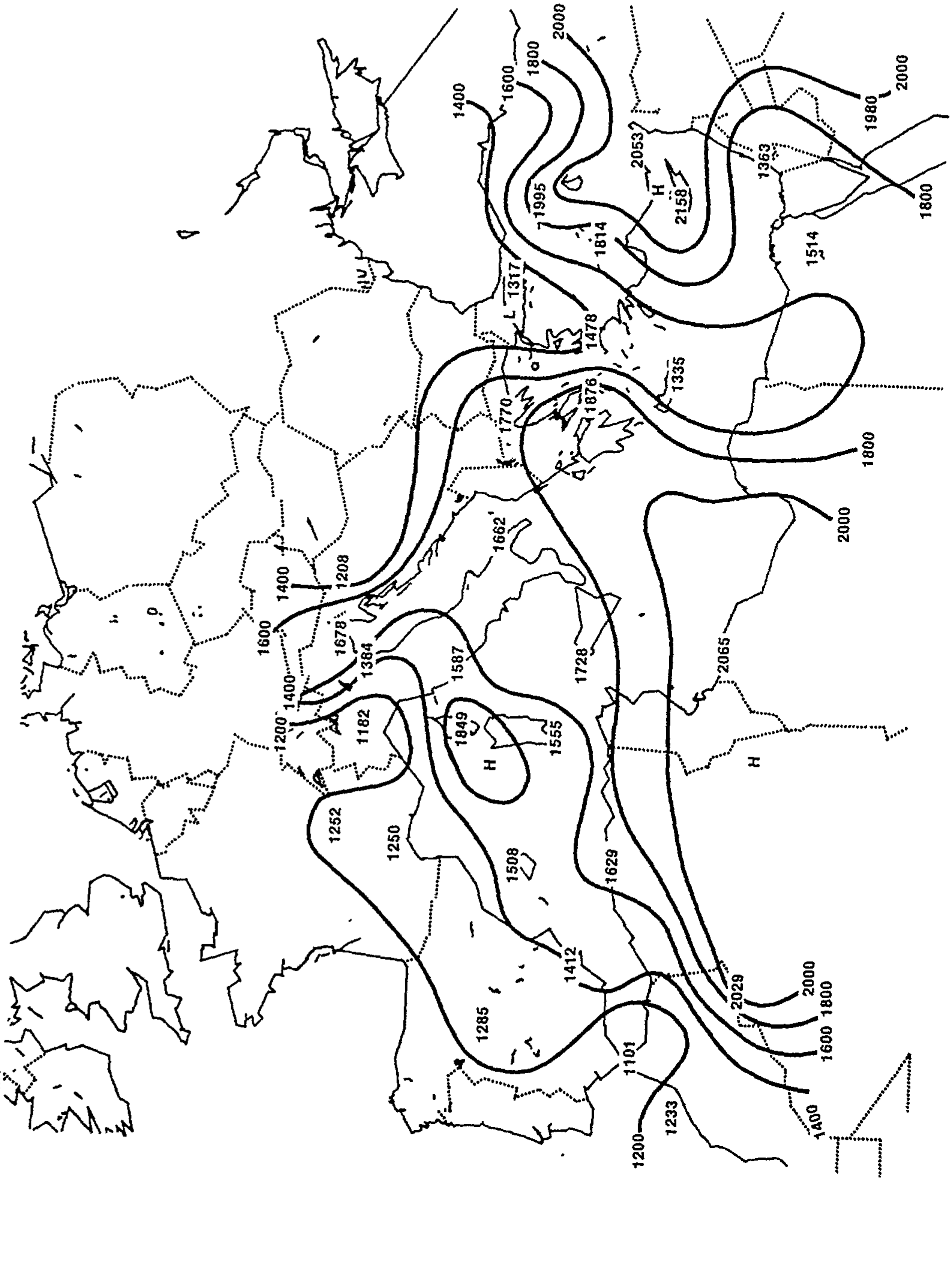

Map 14
FALL87 12GMT

Map 15
WNTR87 12GMT

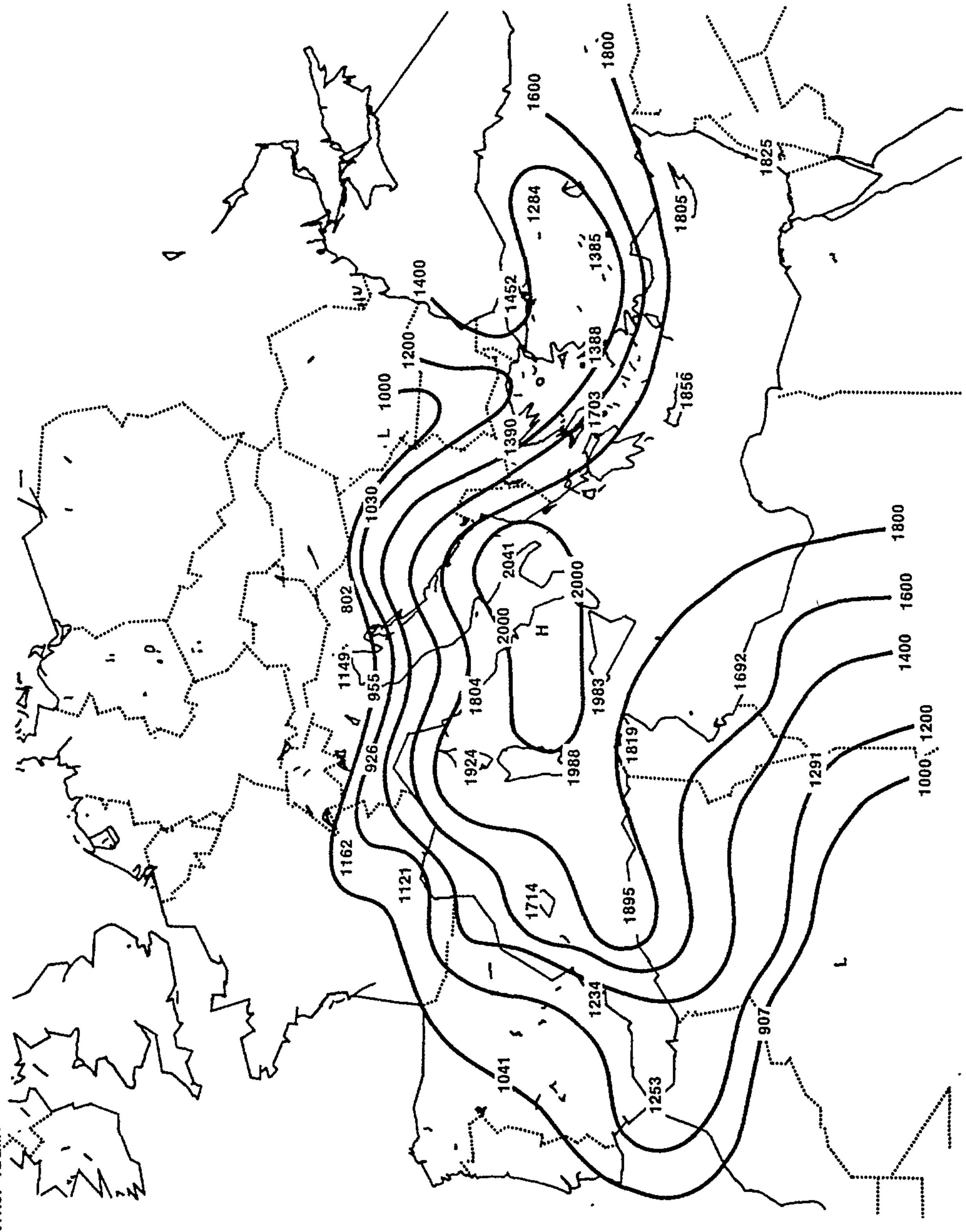

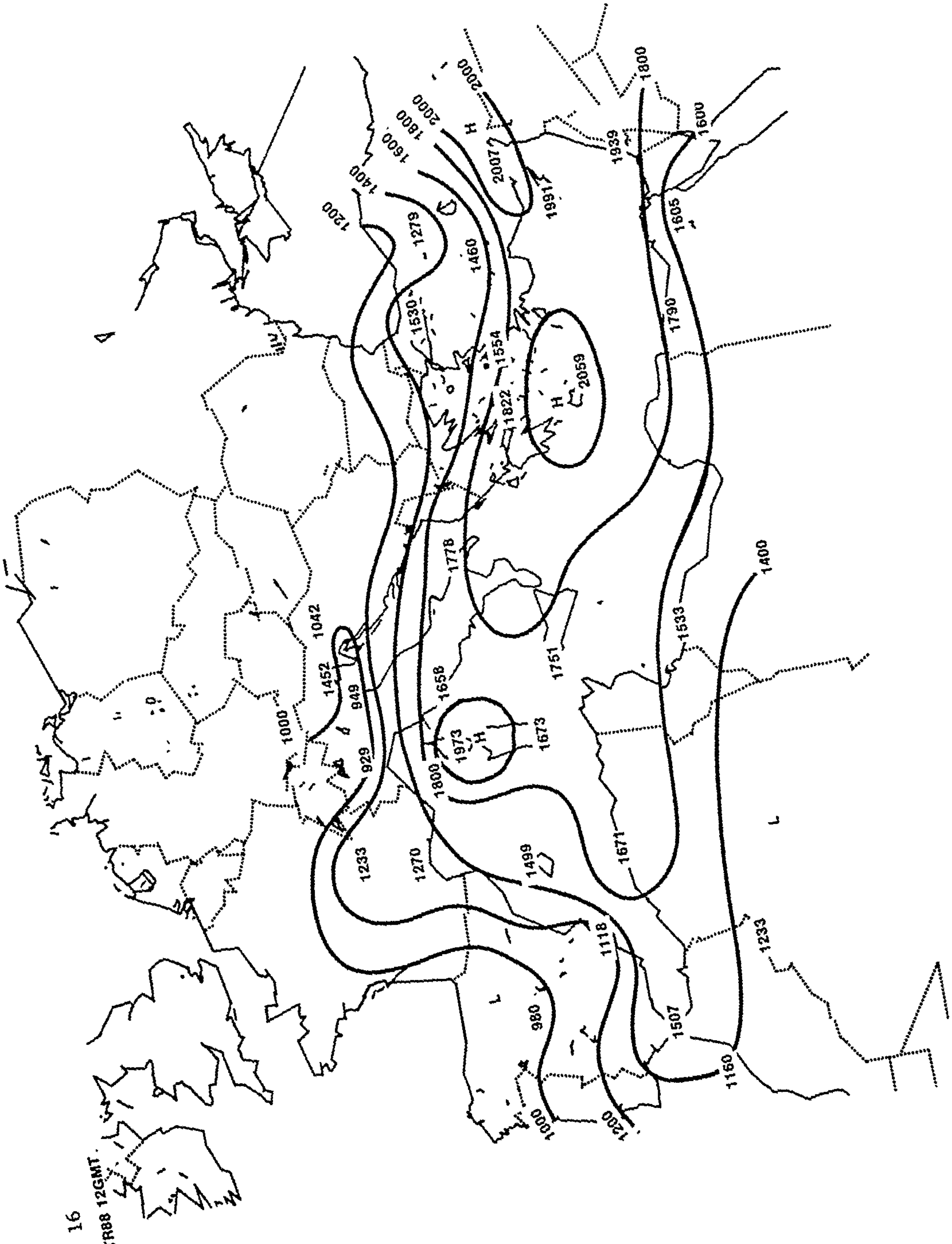

Map 16
WNTR88 12GMT

7.0 DISCUSSION ON THE SEASONAL PBLD DISTRIBUTIONS

The spatial and temporal behavior of the PBLD over the Mediterranean Basin were evaluated and are displayed as seasonal maps (Maps 1-16) and a summary table (Table 1). Two sets of maps were charted, for midnight (0000 GMT) and midday (1200 GMT), for eight consecutive seasons (spring 1986 through winter 1988). Seasonal averages are presented in order to give the potential user insight into the variation of the PBLD values from one year to the following for each season.

From analyses of calculated values and their distributions in the Mediterranean Basin, the most striking elements that seem to govern the patterns are the location of rawinsonde sites and the orientation of the sites with respect to the Mediterranean Sea (altitude, rate of exposure to sea breeze, etc.).

7.1 Altitudes of the Rawinsonde Sites

As defined in Section 5, the upper and lower values for depths of the PBL were set at 3000 and 300 m respectively (see Fig. 5). Therefore, the topographical height of the station was found to have a direct impact on characterization of the PBLD (aside from indirect effects caused by topographical features). This effect is especially evident in the eastern Mediterranean under subsiding conditions caused by the presence of a subtropical high barometric pressure, which dominates the southern part of the sea during certain seasons. Therefore, for example, the two elevated sites in Turkey (stations 17130 and 17240 in Fig. 3) might be above the PBLD of the Mediterranean Basin. This is especially the case during the summer, which is characterized by relatively low PBLD values (i.e. 800 to 1000 m) in the Eastern Mediterranean Basin (Table 1). This should therefore be noted when applying the PBLD values given on the maps in Section 6 or those given in summary Table 1.

7.2 Distances from the Mediterranean Shoreline

The significant variation observed in the PBLD values with inland penetration is mainly determined by the strength of the sea breeze. The sea breeze can act as a weak cold front, splitting the boundary layer into two distinctive layers: a shallow, cool, moist marine layer above ground and a relatively warm, dry subsiding layer aloft (Halevy and Steinberger, 1974). The PBLD seasonal means increase inland due to the disappearance, moving inland, of this shallow marine inversion intrusion. This effect is well illustrated for the eastern part of the Mediterranean in the summer PBLD distribution maps (Maps 3, 4, 11, 12), for which orientation of the PBLD isopleths follows the predominant onshore wind direction.

Table 1. Typical seasonal PBLD Values (m) for the Western (W), Central (C), and Eastern (E) Mediterranean Basin

Time	Spring PBLD W	C	E	Summer PBLD W	C	E	Fall PBLD W	C	E	Winter PBLD W	C	E
0000 GMT	1300	1500	1300	0800	1000	0800	1300	1500	1300	1500	1800	1700
1200 GMT	1600	1700	1600	1500	1500	1000	1600	1800	1400	1700	1900	1900

7.3 Diurnal Effects on the PBLD Distributions

Temporal behavior of the PBLD near the Mediterranean sea surface is governed mainly by two distinct features: (1) the diurnal cycle (nocturnal weak convection above relatively lukewarm water vs. daylight stability confined to the cooled surface layer above the water) and (2) the larger-scale synoptic weather systems. Heat capacity of the sea, being of greater value than that of the ground, causes a lag in heating and cooling of the water. This produces a difference in the sea-air temperature in the layer interface just above the sea vs. the temperature in this same layer above ground. These thermal differences reach extreme values for the central and western parts of the Mediterranean Basin during the spring and beginning of the summer (reflected by the PBLD in Table 1) when the northern coast of Africa is already warmer than its adjacent shores and close sea water. In general, as an overall average of the Mediterranean Sea, the largest day-night PBLD differences (approximately 500 m) are shown for the summer months (Maps 3, 4, 11, 12).

7.4 Seasonal/Synoptical Effects on the PBLD Distributions

Seasonal effects on the PBLD distribution above the Mediterranean Basin are mainly governed by the climatological positions of the most prevalent synoptical systems, which follow, on a seasonal basis, the latitudes of strongest solar radiation.

A way to emphasize these synoptical/climatological influences on the PBLD values is by observing the distribution of these values for the eastern part of the Mediterranean Sea for summer 1987, 1200 GMT (Map 12). The most outstanding feature is the gradient of the PBLD value along the Eastern Mediterranean Coast, showing a sharp decrease to the south. This phenomenon is explained by the increased distance from the cyclonic center of the Persian Trough to the northeast (which persists in summer) and the decreased distance from the North African anticyclonic high to the southwest (which persists during the whole year). This feature was confirmed in a recent study (Dayan et al., 1988) in which an analysis of the temporal and spatial behavior of the PBLD values above Israel was performed on the basis of intensive upper-air measurements.

In conclusion, this study shows that factors influencing spatial variations in the PBLD are, mainly, topography and the distance from shoreline, and to a lesser extent, synoptic weather systems and the distances to their centers. The most striking feature of the PBLD distributions is the predominant pattern in all the maps displayed (Section 6) in which the values at the center of the Mediterranean Sea are consistently higher than those at the eastern and western tips of this basin. Temporal behavior of the PBLD was found to be mainly governed by seasonal cycles, as determined by large-scale synoptic weather systems, rather than by diurnal effects (see Table 1).

The values given in this report (Maps 1-16 and Table 1) should be used with care, being aware of the assumptions, methods, and limitations mentioned in earlier sections. Of particular concern are the interpolated contours drawn between widely spaced rawinsonde stations, many of which may represent only local effects. Nevertheless, it is the authors' belief that the stringent quality assurance employed for decisions on how these data should be treated and which stations should be included (Section 5) together with the consistency of seasonal patterns from year to year should give confidence that the values presented here are appropriate for input to long-range transport models in the Mediterranean Sea region.

8.0 BIBLIOGRAPHY AND REFERENCES

8.1 Selected Bibliography on Transport and Dispersion Over Water

Collins, G.F., 1971: Predicting "Sea Breeze Fumigation" from Tall Stacks at Coastal Locations. Nuclear Safety 12: 110-114.

DiVecchio, R.A., D.B. Smith, and G. Martin, 1975: Performance of a Recent Formulation for Rate of Growth of Boundary Layers Near Shorelines. Preprints, Conf. on Coastal Meteorology, Virginia Beach, VA. Amer. Meteorol. Soc., Boston, 124-125.

Dooley, J.E., 1976: Fumigation from Power Plant Plumes in the Lakeshore Environment. M.Sc. Thesis, University of Wisconsin-Milwaukee, Milwaukee, Wisc.

Echols, W.T., and N.K. Wagner, 1972: Surface Roughness and Internal Boundary Layer Near a Coastline. J. Appl. Meteorol. 11: 658-662.

Edinger, J.G., 1973: Vertical Distribution of Photochemical Smog in Los Angeles Basin. Environ. Sci. Tech. 7: 247-252.

Edinger, J.G., M.H. McCutchan, P.R. Miller, B.C. Rhyan, M.J. Schroeder, and J.V. Behar, 1971: Penetration and Duration of Oxidant Air Pollution in the South Coast Air Basin of California. J. Air Poll. Control Assoc. 22: 882-886.

Garratt, J.R., 1977: Review of Drag Coefficients over Oceans and Continents. Mon. Wea. Rev. 105: 915-929.

Hoff, R.M., N.B.A. Trivett, N.M. Millan, P. Fellin, K.G. Anlauf, H.A. Weibe, and R. Bell, 1982: The Nanticoke Shoreline Diffusion Experiment, June 1978--III. Ground Based Air Quality Measurements. Atmos. Environ. 16: 439-454.

Kerman, B.R., R.E. Mickle, R.V. Portelli, N.B. Trivett, and P.K. Misra, 1983: The Nanticoke Shoreline Diffusion Experiment, June 1978--II. Internal Boundary Layer Structure. Atmos. Environ. 16: 423-437.

Knox, N.B., and W.A. Lyons, 1975: The Thermal Internal Boundary Layer in a Lakeshore Environment During Summer Fumigation Episodes. First Conf. on Regional and Mesoscale Modelling, Analysis, and Prediction, Las Vegas. Amer. Meteorol. Soc., Boston, MA.

Leteau, H., and J. Zabransky, 1968: Interrelated Changes of Wind and Profile Structure and Richardson Number in Air Flow from Land to Inland Lakes. J. Atmos. Sci. 25: 718-728.

Lyons, W.A., 1975: Turbulent Diffusion and Pollutant Transport in Shoreline Environments. In: Lectures in Air Pollution and Environmental Impact Analyses. Amer. Meteorol. Soc., Boston, MA.

Lyons, W.A., and H.S. Cole, 1973: Fumigation and Plume Trapping on the Shore of Lake Michigan During Stable Onshore Flow. J. Appl. Meteorol. 12: 494-510.

Lyons, W.A., and L.E. Olsson, 1972: Mesoscale Air Pollution Transport in the Chicago Lake Breeze. J. Air Poll. Control Assoc. 22: 876-881.

Lyons, W.A., and L.E. Olsson, 1973: Detailed Mesometeorological Studies of Air Pollution Dispersion in the Chicago Lake Breeze. Mon. Wea. Rev. 101: 387-403.

Lyons, W.A., and S.R. Pease, 1972: "Steam Devils" Over Lake Michigan During a January Arctic Outbreak. Mon. Wea. Rev. 100: 235-237.

Lyons, W.A., J.C. Dooley, C.S. Keen, J.A. Schuh, and H.R. Rizzo, 1974: Detailed Field Measurements and Numerical Models of SO2 from Power Plants in the Lake Michigan Shoreline Environment. Contract Report to Wisconsin Electric Power Co. by Air Pollution Analysis Laboratory, University of Wisconsin--Milwaukee, Milwaukee, Wisc.

Meroney, R.N., J.E. Cermak, and B.T. Yang, 1975: Modelling of Atmospheric Transport and Fumigation at Shoreline Sites. Bound.-Layer Meteorol. 9: 69-90.

Michael, P., G.S. Raynor, and R.M. Brown, 1973: Atmospheric Diffusion from an Off-Shore Site. Proc. IAEA/WMO Symp. on Physical Behaviour of Radioactive Contaminants in the Atmosphere, Vienna, Austria.

Miller, A., and C.D. Ahrens, 1969: Ozone Within and Below the West Coast Temperature Inversion. Rep. No. 6, San Jose State College, Dept. of Meteorol., San Jose, Calif.

Misra, P.K., 1980: Dispersion from Tall Stacks into a Shoreline Environment. Atmos. Environ. 14: 397-400.

Misra, P.K., and S. Onlock, 1982: Modelling Continuous Fumigation of Nanticoke Generating Station Plume. Atmos. Environ. 16: 497-489.

Naito, G., 1978: Direct Measurements of Momentum and Sensible Heat Fluxes at the Towers in the Open Sea. J. Meteorol. Soc. Japan 56:

Nixon, W., and A. Ghobadian, 1983: A Simulation Study of Atmospheric Turbulence Over the Southern Coast of Long Island During On-Shore Flow. SRD R268.

Ozoe, H., T. Shibata, H. Sayama, and H. Ueda, 1983: Characteristics of Air Pollution in the Presence of Land and Sea Breeze--A Numerical Simulation. Atmos. Environ. 17: 35-42.

Portelli, R.V., 1982: The Nanticoke Shoreline Diffusion Experiment, June 1978--I. Experimental Design and Program Overview. Atmos. Environ. 16: 413-421.

Prophet, D.T., 1961: Survey of the Available Information Pertaining to the Transport and Diffusion of Airborne Material Over Ocean and Shoreline Complexes. Tech. Rep. No. 89, Aerosol Lab., Stanford Univ., Stanford, Calif.

Raynor, G.S., P. Michael, R.M. Brown, and S. Sethuraman, 1974: A Research Program on Atmospheric Diffusion from an Oceanic Site. Preprints, Symp. on Atmospheric Diffusion and Air Pollution, Santa Barbara, Calif. Amer. Meteorol. Soc., Boston, 289-295.

Raynor, G.S., P. Michael, R.M. Brown, and S. Sethuraman, 1975: Studies of Atmospheric Diffusion from a Nearshore Oceanic Site. J. Appl. Meteorol. 14: 1080-1094.

Raynor, G.S., S. Sethuraman, and R.M. Brown, 1979: Formation and Characteristics of Coastal Internal Boundary Layers During Onshore Flows. Bound.-Layer. Meteorol. 16: 487-514.

Raynor, G.S., P. Michael, and S. Sethuraman, 1980: Meteorological Measurement Methods and Diffusion Models for Use at Coastal Nuclear Reactor Sites. Nuclear Safety 21: 749-765.

Slade, D.H., 1962: Atmospheric Dispersion over Chesapeake Bay. Mon. Wea. Rev. 90: 217-224.

Super, A.B., 1965: A Study of Small Scale Air Mass Modification over Lake Mendota. Ph.D. Thesis, University of Wisconsin, Madison, Wisc.

8.2 References

Benaries, M.M., 1980: Urban Air Pollution Modelling. Mac Millan, London, 9-17.

Dayan, U., and J. Koch, 1988: Analysis of Upper Air Meteorological Data in the Northern Coast of Israel for the Assessment of Critical Transport and Dispersion Conditions from Elevated Point Sources. I.A.E.C. SNRC Tech. Rep. (in press) (in Hebrew).

Dayan, U., R. Shenhav, and M. Graber, 1988: The Spatial and Temporal Behavior of the Mixed Layer in Israel. J. Clim. Appl. Meteorol. (in press).

Graber, M., U. Dayan, and J. Laznow, 1984: Development of a Dispersion Model for Power Plant Siting: Applications in Coastal Israel. Preprints, Fourth Joint Conf. on Applications of Air Pollution Meteorology, Portland, Ore. Amer. Meteorol. Soc., Boston, 268-270.

Halevy, G., and E.H. Steinberger, 1974: Inland Penetration of the Summer Inversion from the Mediterranean Coast in Israel. Isr. J. Earth Sci. 23: 47-54.

Hanna, S.R., 1969: The Thickness of the Planetary Boundary Layer. Atmos. Environ. 3: 519-536.

Hanna, S.R., R.T. Paine, and L.L. Schulman, 1984: Overwater Dispersion in Coastal Regions. Bound.-Layer Meteorol. 30: 389-411.

Hanna, S.R., L.L. Schulman, R.J. Paine, J.E. Pleim, and M. Baer, 1985: Development and Evaluation of the Offshore and Coastal Dispersion Model. J. Air Pollut. Control Assoc. 35: 1039-1047.

Holzworth, G.C., 1967: Mixing Depth, Wind Speeds and Air Pollution Potential for Selected Locations in the United States. J. Appl. Meteorol. 6: 1039-1044.

Lyons, W.A., and L.E. Olsson, 1973: Detailed Mesometeorological Studies of Air Pollution Dispersion in the Chicago Lake Breeze. Mon. Wea. Rev. 101: 387-403.

McRae, G.J., F.H. Shain, and J.H. Seinfeld, 1981: Convective Downmixing of Plumes in a Coastal Environment. J. Appl. Meteorol. 20: 1312-1324.

Mahrer, Y., 1985: A Numerical Study of the Effects of Sea Surface Temperature on the Sea and Land Breeze Circulation. Isr. J. Earth Sci. 34: 91-95.

Neumann, J., 1977: On the Rotation of the Direction of Sea and Land Breezes. J. Atmos. Sci. 34: 1913-1917.

Nieuwstadt, F.T.M., 1980: Application of Mixed Layer Similarity to the Observed Dispersion from a Ground Level Source. J. Appl. Meteorol. 19: 157-162.

Nieuwstadt, F.T.M., and A.P. Van Ulden, 1978: A Numerical Study on the Vertical Dispersion of Passive Contaminants from a Continuous Source in the Atmospheric Surface Layer. Atmos. Environ. 12: 2119-2124.

Prophet, D.T., 1961: Survey of the Available Information Pertaining to the Transport and Diffusion of Airborne Material Over Ocean and Shoreline Complexes. Tech. Rep. No. 89, Aerosol Lab., Stanford Univ., Stanford, Calif.

Rindsberger, M., 1976: Air Pollution Potential in Greater Tel-Aviv Area. Isr. J. Earth Sci. 25: 127-132.

Segal, M., R.A. Pielke, and Y. Mahrer, 1982: Evaluation of Onshore Pollutant Recirculation over the Mediterranean Coastal Area. Isr. J. Earth Sci. 31: 39-46.

Tadmor, J., and A. Manes, 1973: Photochemical Smog Potential of Urban Areas in Israel. Isr. J. Earth Sci. 22: 93-105.

Van Dop, H., 1986: The CCMS Air Pollution Model Intercomparison Study. Atmos. Environ. 20: 1261-1271.

Van Ulden, A.P., and A.A.M. Holtslag, 1985: Estimation of Atmospheric Boundary Layer Parameters for Diffusion Applications. J. Clim. Appl. Meteorol. 24: 1196-1207.

WMO, 1986: International Meteorological Vocabulary, World Meteorological Organization, No. 182:77

PUBLICATIONS OF THE MAP TECHNICAL REPORTS SERIES

No. 1 UNEP/IOC/WMO: Baseline studies and monitoring of oil and petroleum hydrocarbons in marine waters (MED POL I). MAP Technical Reports Series No. 1. UNEP, Athens 1986 (96 pages) (parts in English, French or Spanish only).

No. 2 UNEP/FAO: Baseline studies and monitoring of metals, particularly mercury and cadmium, in marine organisms (MED POL II). MAP Technical Reports Series No. 2. UNEP, Athens 1986 (220 pages) (parts in English, French or Spanish only).

No. 3 UNEP/FAO: Baseline studies and monitoring of DDT, PCBs and other chlorinated hydrocarbons in marine organisms (MED POL III). MAP Technical Reports Series No. 3. UNEP, Athens 1986 (128 pages) (parts in English, French or Spanish only).

No. 4 UNEP/FAO: Research on the effects of pollutants on marine organisms and their populations (MED POL IV). MAP Technical Reports Series No. 4. UNEP, Athens 1986 (118 pages) (parts in English, French or Spanish only).

No. 5 UNEP/FAO: Research on the effects of pollutants on marine communities and ecosystems (MED POL V). MAP Technical Reports Series No. 5. UNEP, Athens 1986 (146 pages) (parts in English or French only).

No. 6 UNEP/IOC: Problems of coastal transport of pollutants (MED POL VI). MAP Technical Reports Series No. 6. UNEP, Athens 1986 (100 pages) (English only).

No. 7 UNEP/WHO: Coastal water quality control (MED POL VII). MAP Technical Reports Series No. 7. UNEP, Athens 1986 (426 pages) (parts in English or French only).

No. 8 UNEP/IAEA/IOC: Biogeochemical studies of selected pollutants in the open waters of the Mediterranean (MED POL VIII). MAP Technical Reports Series No. 8. UNEP, Athens 1986 (42 pages) (parts in English or French only).

No. 8 Add. UNEP: Biogeochemical studies of selected pollutants in the open waters of the Mediterranean (MED POL VIII). Addendum, Greek Oceanographic Cruise 1980. MAP Technical Reports Series No. 8, Addendum. UNEP, Athens 1986 (66 pages) (English only).

No. 9 UNEP: Co-ordinated Mediterranean pollution monitoring and research programme (MED POL - PHASE I). Final report. 1975-1980. MAP Technical Reports Series No. 9. UNEP, Athens 1986 (276 pages) (English only).

No. 10 UNEP: Research on the toxicity, persistence, bioaccumulation, carcinogenicity and mutagenicity of selected substances (Activity G). Final reports on projects dealing with toxicity (1983-85). MAP Technical Reports Series No. 10. UNEP, Athens 1987 (118 pages) (English only).

No. 11 UNEP: Rehabilitation and reconstruction of Mediterranean historic settlements. Documents produced in the first stage of the Priority Action (1984-1985). MAP Technical Reports Series No. 11. UNEP, Priority Actions Programme, Regional Activity Centre, Split 1986 (158 pages) (parts in English or French only).

No. 12 UNEP: Water resources development of small Mediterranean islands and isolated coastal areas. Documents produced in the first stage of the Priority Action (1984-1985). MAP Technical Reports Series No. 12. UNEP, Priority Actions Programme, Regional Activity Centre, Split 1987 (162 pages) (parts in English or French only).

No. 13 UNEP: Specific topics related to water resources development of large Mediterranean islands. Documents produced in the second phase of the Priority Action (1985-1986). MAP Technical Reports Series No. 13. UNEP, Priority Actions Programme, Regional Activity Centre, Split 1987 (162 pages) (parts in English or French only).

No. 14 UNEP: Experience of Mediterranean historic towns in the integrated process of rehabilitation of urban and architectural heritage. Documents produced in the second phase of the Priority Action (1986). MAP Technical Reports Series No. 14. UNEP, Priority Actions Programme, Regional Activity Centre, Split 1987 (500 pages) (parts in English of French only).

No. 15 UNEP: Environmental aspects of aquaculture development in the Mediterranean region. Documents produced in the period 1985-1987. MAP Technical Reports Series No. 15. UNEP, Priority Actions Programme, Regional Activity Centre, Split 1987 (101 pages) (English only).

No. 16 UNEP: Promotion of soil protection as an essential component of environmental protection in Mediterranean coastal zones. Selected documents (1985-1987). MAP Technical Reports Series No. 16. UNEP, Priority Actions Programme, Regional Activity Centre, Split 1987 (424 pages) (parts in English or French only).

No. 17 UNEP: Seismic risk reduction in the Mediterranean region. Selected studies and documents (1985-1987). MAP Technical Reports Series No. 17. UNEP, Priority Actions Programme, Regional Activity Centre, Split 1987 (247 pages) (parts in English or French only).

No. 18 UNEP/FAO/WHO: Assessment of the state of pollution of the Mediterranean Sea by mercury and mercury compounds. MAP Technical Reports Series No. 18. UNEP, Athens 1987 (354 pages) English and French).

No. 19 UNEP/IOC: Assessment of the state of pollution of the Mediterranean Sea by petroleum hydrocarbons. MAP Technical Reports Series No. 19. UNEP, Athens 1988 (130 pages) (English and French).

No. 20 UNEP/WHO: Epidemiological studies related to Environmental Quality Criteria for bathing waters, shellfish-growing waters and edible marine organisms (Activity D). Final report on project on relationship between microbial quality of coastal seawater and health effects (1983-86). MAP Technical Reports Series No. 20. UNEP, Athens 1988 (156 pages) (English only).

No. 21 UNEP/UNESCO/FAO: Eutrophication in the Mediterranean Sea: Receiving Capacity and Monitoring of Long term Effects. MAP Technical Reports Series No. 21. UNEP, Athens 1988 (200 pages) parts in English or French only).

No. 22 UNEP/FAO: Study of ecosystem modifications in areas influenced by pollutants (Activity I). MAP Technical Reports Series No. 22. UNEP, Athens 1988 (146 pages) (parts in English or French only).

No. 23 UNEP: National Monitoring programme of Yugoslavia, Report for 1983-1986. MAP Technical Reports Series No. 23. UNEP, Athens 1988 (223 pages) (English only).

No. 24 UNEP/FAO: Toxicity, persistence and bioaccumulation of selected substances to marine organisms (Activity G). MAP Technical Reports Series No. 24. UNEP, Athens 1988 (122 pages) (parts in English or French only).

No. 25 UNEP: The Mediterranean Action plan in a Functional Perspective: A Quest for Law and Policy. MAP Technical Reports Series No. 25. UNEP, Athens 1988 (105 pages) (English only).

No. 26 UNEP/IUCN: Directory of Marine and Coastal Protected Areas in the Mediterranean Region - part I Sites of biological and ecological value. MAP Technical Reports Series No. 26. UNEP, Athens 1989 (195 pages) (English only).

No. 27 UNEP: Implications of Expected Climate Changes in the Mediterranean Region: An Overview. MAP Technical Reports Series No. 27. UNEP, Athens 1989 (52 pages) (English only).

No. 28 UNEP: State of the Mediterranean Marine Environment. MAP Technical Reports Series No. 28. UNEP, Athens 1989 (221 pages) (English only).

No. 29 UNEP: Bibliography on Effects of Climatic Change and related topics. MAP Technical Reports Series No. 29. UNEP, Athens 1989 (143 pages) (English only).

Issued and printed by:

Mediterranean Action Plan
United Nations Environment Programme

Additional copies of this and other publications issued by the Mediterranean Action Plan of UNEP can be obtained from:

Co-ordinating Unit for the Mediterranean Action Plan
United Nations Environment Programme
Leoforos Vassileos Konstantinou, 48
P.O. Box 18019
11610 Athens
GREECE

Publié et imprimé par:

Plan d'action pour la Méditerranée
Programme des Nations Unies pour l' Environnement

Des exemplaires de ce document ainsi que d'autres publications du Plan d'action pour la Méditerranée du PNUE peuvent être obtenus de:

Unité de coordination du Plan d'action pour la Méditerranée
Programme des Nations Unies pour l' Environnement
Leoforos Vassileos Konstantinou, 48
B.P. 18019
11610 Athénes
GRECE